THE EFFECT OF POST WELD HEAT TREATMENT AND DISTRIBUTION OF RESIDUAL STRESS IN WELD REPAIRED HIGH CHROMIUM STEEL [AISI 410] COMPONENTS.

BY

ABDUL GHANI OLABI

This thesis is submitted as the fulfilment of the requirement for the award of Master of Engineering (M.Eng) by research to :

DUBLIN CITY UNIVERSITY

Sponsoring Establishment :

Scientific Studies & Research Centre
DAMASCUS - SYRIA

Collaborating Establisment :

Airmotive Ireland (Dublin)

November 1990

DECLARATION

I here by declare that all the work reported in this thesis was carried out by me at Dublin City University during the period of January 1989 to November 1990.

To the best of my knowledge, the results presented in this thesis originated from the present study, except where references have been made. No part of this thesis has been submitted for a degree at any other institution.

Signature of Candidate

ABDUL GHANI OLABI

CONTENTS

CONTENTS

CONTENTS

CONTENTS

ABSTRACT

THE EFFECT OF POST WELD HEAT TREATMENT AND DISTRIBUTION OF RESIDUAL STRESS IN WELD REPAIRED HIGH CHROMIUM STEEL[AISI 410] COMPONENTS.

A.G.OLABI

The aim of this work is to study the effect of Post Weld Heat Treatment on the micostructural and strength properties of high chromium steel [AISI 410] components. This work also aims to estimate the magnitude and distribution of the residual stress on the above type of welded components.

In introducing this work an extensive literature survey on the historical development and the advantages and disadvantages of welding process has been presented. A review of the different technique which are used to determine the residual stress is also presented.

In this work two types of Post Weld Heat Treatment were used. In the first type of heat treatment, the specimen was kept at 316°C for 30 min, then at 427°C for 30 min, and finally, at 546°C for 2 hrs. In the second type of heat treatment the specimen was kept at 760°C for 2 hrs. Two types of specimens were used to simulate build-up welding and crack repair conditions, each type of these specimens have different parameters (thickness, bead length and width).

Stress relaxation technique was used to detemine the magnitude and distribution of the residual stresses for the above specimens.

The results show that the first type of heat treatment reduces the hardness in the welding zone by about 15% of the hardness of the as welded specimen and improves the tensile strength. The second type of heat treatment decreases the hardness in the welding zone by about 40% but decreases the tensile strength by about 10%.

The residual stress measurements show that there is a tensile stress around the welded zone, and that the greatest value recorded is about 72 N/mm^2. These residual stresses decrease as the distance from the welding zone increases.

ACKNOWLEDGEMENT

I would like to express my appreciation to **Prof. M.S.J. Hashmi**, Head of the School of Mechanical and Manufacturing Engineering for his helpful supervision and guidance during the course of this project.

I would like to express my gratitude to **Dr. A.W. Shahid** Director Of Scientific Studies & Research Centre, DAMASCUS, SYRIA, for his kind support and encouragement.

I would also like to acknowledge the technical collaboration and help of the following: **Mr. L. MaCarthy, Mr. J. Walsh** and **Mr. G. Toyrrell** in Airmotive Ireland; **Mr. G. Dardes** and **Mr. M. Fleming** of EOLAS; **Mr. T. Walsh, Mr. J. Treacy** and **Mr. I. Hooper** the workshop technicians in the School.

Finally, I would like to thank all my friends who lent support and encouragement while the thesis was being prepared.

LIST OF FIGURES

LIST OF FIGURES

LIST OF FIGURES

LIST OF FIGURES

LIST OF FIGURES

LIST OF FIGURES

LIST OF FIGURES

LIST OF FIGURES

LIST OF PLATES

CHAPTER 1

INTRODUCTION

1.1 WELDING (HISTORICAL AND TYPES)

More than 2000 years ago, welding was used to join small gold boxes which were made by pressure welding lap joints. During the iron age it appears that the Egyptians and other people in the Eastern Mediterranean area learned to weld pieces of iron together. During the middle ages different works have been seen which were welded by hammering. However, it was not until the early 19th century that welding as we know it today was discovered and used. During this period, two types of welding were discovered, the first was by acetylene and the second was by the production of an arc between two carbon electrodes using a battery. The period of 1877 to 1903 provided a great number of discoveries pertaining to welding. During this period gas welding and cutting and arc welding with the carbon arc were developed and resistance welding became a practical joining process.

IN 1892 the arc metal process using a metal electrode was discovered and in 1900 Strohmeyer introduced a coated metal electrode in Great Britain. Meanwhile, the resistance welding process was developed including seam welding and spot welding. During the period from about 1900 to 1918 the oxyacetylene welding and cutting process together with the carbon arc welding and metal arc welding process with lightly covered electrodes were used primarily for repair and maintenance work. In 1920 Automatic welding was introduced, during the 1920s various different types of welding electrodes were developed and used for different kinds of metals.

During 1930s the tungsten inert gas welding was discovered using atmospheres of argon and helium. Submerged arc welding was used in the late 1930s and early 1940s. In 1948 gas shielded metal arc welding was successfully developed. In 1950s the Co2 was used as an inert gas. Electroslag welding process was used in 1958 and electro-moulding process was used in 1959 for the fabrication of welded diesel engine blocks. The plasma arc welding process, which is very similar to gas tungsten arc welding was invented by Robert Gage in 1957. The electron beam welding process, which uses a

focused beam of electrons as a heat source in a vacuum chamber, was developed in the late 1940s. In the last few years the process has gained widespread acceptance for welding, its popularity is increasing since recent developments have allowed it to be used without any need for the vacuum chamber. The newest of welding processes is laser welding, it has been used for cutting metals also. Additional welding processes and methods will be developed and as the need arises they will be adapted to metalworking requirements.

The AMERICAN WELDING SOCIETY (AWS) [1 - 4] recognizes 12 major headings for welding and allied processes. Fig. 1 shows a block diagram for these welding processes. Figs. 2 to 13 show different types of welding processes which are used to weld different kinds of metals.

1.2 ADVANTAGES AND DISADVANTAGES OF WELDED STRUCTURES

The advantages of welded structures are:

1 - High joint efficiency: The joint efficiency is defined as the percentage of the fracture strength of a

joint to the fracture strength of the base plate. The values of joint efficiency of welded joints are higher than riveted joints, it can be as high as 100%.

2 - Water and air tightness: A welded structure is ideal for situation which require water and air tightness such as submarine hulls and storage tanks.

3 - Weight saving: The weight of a hull structure can be reduced as much as 10 - 20% if welding is used.

4 - No limit on thickness: It is very difficult to rivet plates that are more than 2 inches thick. In welded structures there is virtually no limit to thickness that may be employed.

5 - Simple structure design: In welded structures, members can be simply butted together or fillet welded. In riveted structures, complex joints are required.

6 - Reduction in the fabrication time: A welded structure can be fabricated in a short period of time and be less costly than riveted structures.

The problems with welded structures are:

1 - Difficult to arrest fracture: Since the crack starts to propagate in a welded structure, it is very difficult to arrest it.

2 - Possibility of defects: Welds are often plagued with various types of defects including porosity, cracks, slag inclusion,etc.

3 - Sensitive to materials: Some materials are more difficult to weld than others.

4 - Lack of reliable NDT techniques: Although many non-destructive testing methods have been developed and are in use today, some are completely satisfactory in terms of cost and reliability for specific application only.

5 - Residual stress and distortion: Because of the non-uniform heating during welding, residual stress and distortion result after welding, which may lead to cracking and mismatching.

1.3 CRACK IN WELDED COMPONENTS

Residual stresses contribute to weld cracking. The restrained contraction of welded structures during cooling sets up tensile stresses in the joint and may cause one of the most serious of weld defects, which is crack. Weld cracking will occur during manufacturing operation of the weldment or shortly after the weldment is completed. Cracking may occur in the weld deposit, in the heat affected zone, or in both of these regions. It is either of the gross type, which is visible to the naked eye and is termed macrocracking, or is visible only under the microscope, in which case it is termed microcracking or microfissuring. Cracking that occurs during the solidification of the weld metal is known as solidification cracking or hot cracking. Cracks may form in the heat affected zone due to liquidation of low melting components, this is known as liquidation cracking. Embrittlement of the parent metal or heat affected zone may result in subsolidus or cold cracking. In solidification cracking there are two necessary preconditions for the occurence of cracking during the weld thermal cycle; the metal must lack ductility, and the tensile stress developed as a result of contraction

must exceed the corresponding fracture stress. The mechanical properties of the metal in the region of the solidus are therefore important in relation to solidification cracking. In general, cracking may occur for many reasons and may occur years after the weldment is completed. Restraint and residual stresses are the main reasons for weld cracking during the fabrication of a weldment. Weld restraint can come from several factors one of the most important is the stiffness and rigidity of the weldment itself. Another factor involved is the rapid cooling of the weld deposit, if the base metals being joined are cold and the weld is relatively small it will cool extremely rapidly. So shrinkage will occur quickly and cracking can occur. Another reason for cracking is the content of carbon and other elements in the base metal, when the weld is made with higher carbon or high alloy base metal. During welding the base metal is melted and mixed with the electrode to produce the weld metal. The resulting weld metal have a higher carbon and alloy content, giving it a higher strength but low ductility and as it shrinks it may not have sufficient ductility to cause plastic deformation and therefore cracking may occur. Another factor is the hydrogen pickup in the weld metal. In the heat affected zone of the base

metal, the presence of hydrogen in the arc atmosphere will cause it to be absorbed in the molten metal. As the metal cools it will reject the hydrogen and if there is sufficient restraint, cracking will occur.

1.4 RESIDUAL STRESS IN WELDING COMPONENT

Due to local heating during welding, complex thermal stresses occur during welding and residual stress is developed after welding. Thermal stress and residual stresses cause cracking and mismatching. High tensile residual stresses in areas near the weld cause fracture under certain condition.

Many techniques have been used for measuring residual stresses in metal. The most widely used method for measuring residual stresses in weldments is the stress relaxation technique in which the residual stress is determined by measuring the elastic strain when a specimen is cut into pieces or a piece is removed.

In most cases electrical or mechanical strain gages are used for measuring this strain relaxation. There are many ways to section the specimen to determine

residual stresses. Some techniques are employed to determine the stress in plates, while others are used in cylinders, tubs,...etc.

The main disadvantage of the stress relaxation technique is that it is destructive testing.

1.5 MEASUREMENT OF RESIDUAL STRESS IN WELDED COMPONENTS

Many techniques have been used for measuring residual stresses in metal. There are different available techniques for measuring residual stress which can be classified in four main groups.

1 - Stress relaxation techniques.

2 - X - Ray diffraction techniques.

3 - Techniques by use of stress - sensitive properties.

4 - Cracking techniques.

The stress relaxation techniques are based on the principle that strains created during unloading are elastic even when the material has undergone plastic deformation. It is therefore possible to determine residual stress without knowing the history of the material.

In X - Ray diffraction technique the elastic strains in the metals that have crystalline structures can be determined by measuring the lattice parameter by X - Ray diffraction. Because the lattice parameter of a metal in the unstressed state is known or can be determined separately, elastic strains in the metal can be determined non-destructively without machining. X-Ray diffraction techniques are applicable only to crystalline materials having randomly oriented small grains. Most metals fall into this category.

The technique for determining the residual stresses by stress sensitive technique is based on the principle that when stresses exist in the metals some of the physical or mechanical properties, such as the

propagation speed of shear waves and hardness, are changed. However, none of this techniques have been developed beyond the laboratory stage.

The cracking technique developed to determine the stress involves close observation of cracks caused in the specimen due to the stress, the crack being induced by Hydrogen or stress corrosion.

1.6 POST WELD HEAT TREATMENT

Stress relief heat treatment is defined as the uniform heating of a structure at a suitable temperature, holding at this temperature for a predetermined period of time, followed by uniform cooling. Stress relief heat treatment is usually performed below the critical temperature range.

The temperature and time for post weld heat treatment depend on the type of material. The percentage relief of internal stresses is dependent on the material type, composition, or yield strength. The temperature reached during the stress relief heat treatment has a greater effect in relieving stresses than the length of

time the specimen is held at that temperature. The temperature near the critical temperature is more effective in the removal of residual stress.

When a thermal stress relief treatment is employed to reduce residual stresses, other important properties must be taken into consideration such as the microstructure, tensile and impact strength. Thus, it is necessary to select a temperature that will develop the desirable properties in the material, while at the same time providing the maximum stress relief.

1.7 STRAIN GAUGES

The electrical resistance strain gauge was developed in the late 1930s, by two researchers in the USA. Working independently of each other, Simmons at Caltec and Ruge at MIT developed a strain gauge consisting of a length of wire glued to the test object so that changes in lengths on the surface were transferred to the wire. These length changes caused alterations in the resistance of the wire which could be measured by comparatively simple electrical circuitry.

Modern strain gauge works exactly in the same way with strain being detected by measuring the resistance variations caused by changes in the gauge length of the wire. The strain gauge can be very small and compact having negligible mass to exert a minimum of influence on the measuring object. They can be easily mounted on the test specimen, usually by cementing the electrical detection circuits required to measure the very small changes in the gauge resistance. Measurement of such changes is comparatively uncomplicated by using the familiar Wheatstone bridge, when suitable compensation circuits are employed or self - compensating gauges used. The resistance strain gauge allows a very economically priced measuring system to be made, where the actual cost per gauge is often so low as to be virtually of no consequence. Gauge costs are no longer a hindrance to the use of strain gauges, cemented in their hundreds on a structure, to solve any particular stress analysis task by actual multiple measurements, instead of the laborious calculation procedures, based on extrapolation from a few measurements, that had been used previously.

Typical well known application for strain gauges include experimental strain and stress measurement on aircraft, boats, cars, and other form of transportation vehicles. Strain gauges are also used for the measurement of stress in larger structures, for example apartment buildings and office blocks, pressurized containers, bridges, dams, etc. The strain gauge is an important laboratory implement used for pure research and as a design tool in the development stages of many machines and structures.

Modern strain gauges are often made by etching a thin metal foil rather than using a wire. In recent years semiconductor strain gauges have become available, which are more sensitive than the wire and foil gauges. Fig. 14 shows different types of strain gauges.

1.8 REVIEW OF PREVIOUS WORKS

Different studies and investigations have been carried out to evaluate the effect of various parameters on the residual stress, and the effect of stress relief

on the metal composition and properties. A number of papers reported the effect of vibrational treatment on the residual stress as a new method which has some advantage.

In reference [5] the results of a study towards the application of vibratory stress relief process instead of the heat treatment. The author described it as a method of applying controlled low amplitude, low frequency vibrations in metal components to obtain dimensional stability and control machining tolerances. This process has many advantages. It is an economical, fast and convenient method of reducing stress and is used during processing without causing metallurgical changes, movements, oxidation or scaling.

A vibratory relief system consists of a small electrically operated vibrator, an accelerometer to transmit the degree of vibration to a resonance readout, a motor control to speed up or slow down the rate of vibration, and r.p.m readout and an ammeter. The author mentioned the advantages and limitations of this process of treatment, and reported that most applications which

require vibration take 10 to 20 min and use an average of 1/2 kW of power and the typical frequency range is 20 to 90 Hz.

The application of the vibratory process has eliminated 68 percent of the thermal stresses developed during welding, assuring dimensional stability with the same degree of accuracy.

Olenin et al [6] have studied the effect of vibration treatment on reducing the residual stresses especially when the heat treatment can not be used or when the work piece is too large. In this paper the residual stress relief was determined on specimens of St3 steel in the form of sheets 300 mm long, 20-40 mm wide, and 2 mm thick. The reduction in residual stress was 50-55% and the duration of vibrational treatment in the optimum conditions was 20-25 min.

Thomas [7] gave a general idea about using vibration method for stress relieving. He called this method as Meta Lax. In this paper he described this method and how it works. This process is applicable to most kinds of the metals except copper and copper

alloys. He also outlined the advantages of this process. Keller [8] also described the vibration method and their advantages.

Another work has been carried out by Merun and Olenin [9] to show that electrohydraulic treatment makes it possible to reduce the residual welding stresses by 50 - 70% for specimens produced from low carbon steels.

A Paper has been written by Candeland [10] to report the two most common types of heat treatment undertaken in the fabrication of welded structures, preheat and post weld heat treatment .He discussed both of these heat treatments and the various techniques used throughout the world.

Bmankirski [11] has investigated the mechanical properties for welded joint on 20K sheet plate [GOST 5520-69] 40 mm thick. He has compared this properties under three conditions, (1) initial condition, (2) tempering [heating temperature 625+10°C, holding time 2 hrs, cooling in air], and (3) after vibration treatment [which was carried out at the resonance frequency of 24-32 Hz for a time of 20-25 min]. Welding was carried out by manually. The result detected that tempering

reduced yield strength and hardness but increased impact toughness. Vibration loading resulted in slight increase of strength and reduced ductility.

In reference [12] the author investigated the mechanical strength and fracture mechanics of [Crack Tip Opening Displacement] of welded joints. He used Submerged Arc Welding, the base metal was a modified steel TT St E36, the initial plate thickness was 60 mm and a wire electrode of type S3 was used. The welds were examined in the as welded state and after stress relief annealing (570°C for 2.5 hr). The investigation involved comparison between the tensile strength, yield strength, hardness, and impact energy for the plates and pipes before and after heat treatment. The paper also has discussed the characteristic of the heat affected zone in the welded component.

Another investigation has been done by Suzuki,et al [13] for evaluating the effect of weld residual stresses on fracture toughness in heat affected zone (HAZ), and the effect of notch acuity on HAZ toughness of the reactor pressure vessel steel [Sa 533 Grade B, class1]. The investigator used three sizes of specimens

and two different types of post - weld heat treatment (1/4 hrs at 600°C and 40 hrs at 600°C). He studied the fracture toughness for all the above situation.

Adoyan,et al [14] used a new form of specimen to assess the effect of welding technology and all types of external loading on the distortion of the structure. The author used a ring shape element which was made of St3 steel for many different range of heat treatment temperatures as 250 °C to 600°C for 3 hrs. The efficiency of stabilisation of dimensions by low temperature heat treatment (250°C) in distortion caused by the relaxation of the residual stresses is almost identical with that achieved in high temperature tempering (600°C).

Research at the University of Tennessee [15] has dealt with the weldability of Cr-Mo steels and determined the stress relief cracking susceptibility of Cr-Mo alloys ranging in composition from 2.25Cr, 1Mo to 12Cr, 2Mo, using 51 mm thick plate. The author investigated the effect of the material composition [Si,P,C,] and the temperatures of post welding heat treatment on the stress relief cracking susceptibility.

In reference [16] the results of investigation on post weld treatments of steel pressure vessels were reported. The author described the conditions of applied heat treatment according to different regulations [Dutch, French, U.S, Japan]. He also mentioned all other kinds of treatments which are possible to affect stress relief in pressure vessels.

Another study has been undertaken by Bosansky,et al [17] to investigate the effect of Niobium (Nb) and the influence of Molybdenum (Mo) on weld toughness as a function of stress relieving heat treatment. Different percentage of Niobium with and without Molybdenum with different conditions of stress relief heat treatment (different temperature and coaling time) were looked at, and good result was obtained for heat treatment at 580°C for 1 hr. Hardness measurements and Electron microscopy were used to define the difference between all the above conditions.

Zubchenko,et al [18] investigated the effect of temperature and time conditions on hardening welded joints in 15Kh2MFA and 15Kh2NMFA steels and of their relaxation resistance. The author also investigated the

effect of temperature and heating time on the relaxation process of residual stresses in heat treatment. Different reheating temperatures were used, and the investigator looked into the relation between the chemical composition and the time duration.

Nedjeljko [19, 20] investigated the effect of preheating and stress relieving heat treatments on the micro alloyed steel. The preheating temperatures were 150 °C and 300°C, and the stress relieving temperatures were 450°C, 550°C, and 650 °C. The results of the tests show that better mechanical characteristics are not achieved with preheating and annealing process. Another investigation [21] has been carried out to study the effect of stress relieving heat treatment on the metallurgical structure for low alloy steel used for pressure vessels.

Evans [22] investigated the effect of stress relieving on the microstructure and properties of C-Mn as welded metal deposits using different content of C and Mn. 16 different metal deposits have been used, all specimens were stress relieved at 580°C for 2 hrs. To evaluate the effect of stress relief heat treatment

the investigator examined the metallographic and mechanical properties [hardness, tensile strength, impact].

Evans [23, 24] also studied the effects of Silicon, Sulphur and Phosphorus on the microstructure and properties of C-Mn steels. Different kinds of testing have been done to evaluate the effects of Si,P,S on [hardness, tensile strength, impact and metallography structure] by changing the content of those elements Si [0.20 - 0.90%], S [0.007 - 0.046%], and P [0.007 - 0.040%]. Heat treatments have been applied and all the above testing was carried out on specimens before and after heat treatment.

An investigation has been done by Glover,et al [25] to assess reheat cracking for low alloy steels using Vinckier test. Test specimens were made from a range of different materials, all about 50 mm thick, and different length of specimens were used to evaluate the length of crack with different heat input and composition. A microscope was used to define the structures and evaluate the grain size.

Lieurade [26] summarized in his paper the effects of residual stresses and stress ratio after welding on the fatigue strength. He also mentioned the effect of heat treatment on the fatigue strength.

An investigation [27] has been undertaken to study the effect of stress relieving on the fatigue property for cruciform welded joint. Two welded plate cruciforms were produced from Grade 250 steel. In the treatment the specimens were slowly heated to approximately 580°C and were held at that temperature for 8 hrs. The results indicated that stress relieving influence the fatigue performance of fillet welded cruciform joints. Another investigation [28] has been carried out to study the effect of stress relief on the fatigue strength of high strength steel. The specimens are box sections welded from 15 mm thick plates and groove welds were applied with the Submerged - Arc process. An improvement has been noted as a result of the stress relief.

Vachav,et al [29] investigated the correlations

between the structural characteristics of welded joints in the Ferritic/Austenitic steels and their mechanical properties after thermal and mechanical loading.

Lamb,et al [30] have studied the residual stresses in two stainless steel surfaces melted by laser.* The stresses were measured by X-Ray diffractometry over a range of depths and they defined the stresses after heat treatment. Higuchi,et al [31] studied the weld repair through half bead method and they compared it with the conventional repair method. An investigation has been done by Karjalainen,et al [32] to evaluate the residual stresses in welding from Barkhousen noise measurement. It seams possible to evaluate the distribution of residual stress using this method. But the determination of exact magnitudes of residual stress seems difficult. Debabrata and Bhattacharya [33] have investigated the effect of normalising time on the hardness for steel but-welded joints under identical welding condition. Another investigation has been done by Watkins,et al [34] to determine Sulfide Stress Cracking (SSC) resistance of welded repairs to wellhead equipment. They studied the effect of hardness and stress relief heat treatment on (SSC).

* The results show that there is a tensile stress at a specimen surface and by applying the heat treatment (500°C for 1 hr) the residual stress is minimized to about 50 $MN.m^{-2}$ without any adverse metallurgical effects.

In reference [35] investigation was undertaken to study the residual stress relieving in reclaimed and built-up welding of steel castings by hammer peening. The author investigated three types of steel and evaluated the distribution of residual stresses on the surface and across the thickness before and after peening. They also described the effect of peening on the hardness. Fick and Rogerson [36] studied the variations in toughness between the root and sub-surface regions of some multipass welds. Their study shows the effect of the electrode composition and the thermal ranges on the toughness; they also described the effect of stress relief heat treatment. Farrar,et al [37] have studied the effect of stress relieving on fracture properties. The steel weld metals containing 1.0% Mn and 0.08% C, the post weld heat treatments were at 625°C for 4 hrs. The investigation revealed the effect of stress relieving on the redistribution of the carbon. Another investigation [38] has been done to study the effect of stress relieving on the rupture strengths of dissimilar metal welds (Ferritic and Austenitic).

1.9 PRESENT WORK AND ITS OBJECTIVES

The objective of this project is to study the effect of post weld heat treatment on the metal microstructure and properties for high Chromium Steel AISI 410 welded component. Another object, is to determine the magnitude and distribution of the residual stress for the same kind of welded components.

To reach these objectives, two types of post weld heat treatment was carried out. Stress relaxation technique also was employed for measuring the residual stress, as described fully in Chapter 2.

In Chapter 3 results of these studies. Chapter 4 discuss these results. The final Chapter gives a conclusion of the present work and recommendations for further work.

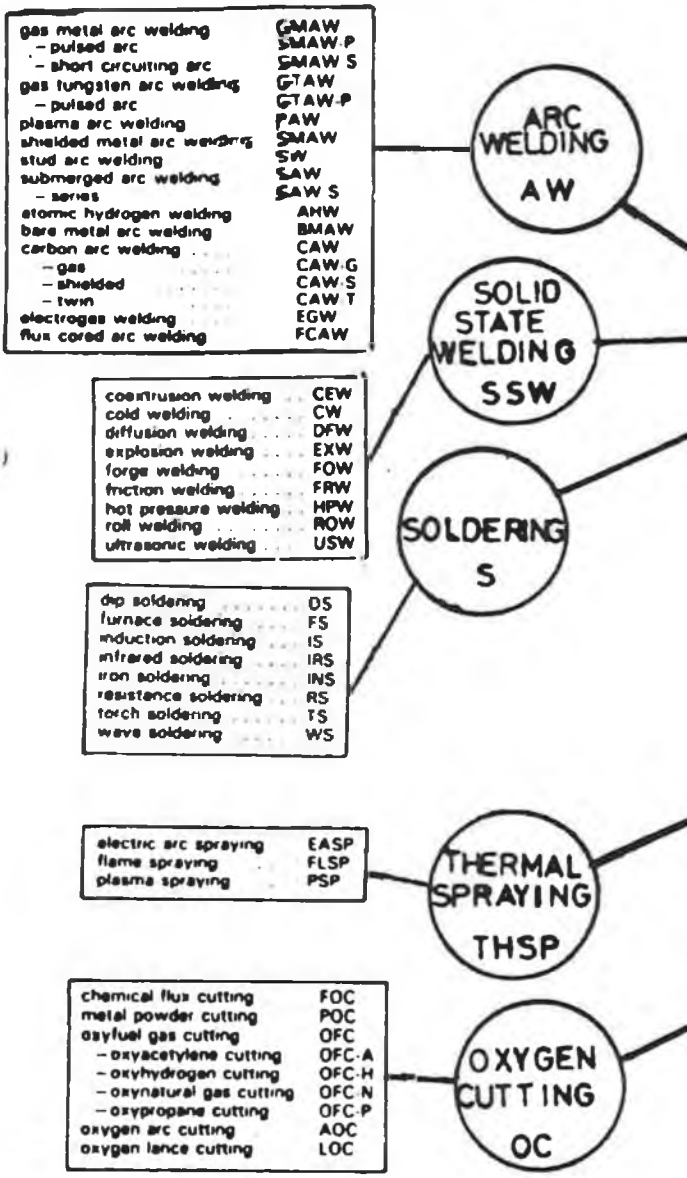

Fig. 1 Welding Society

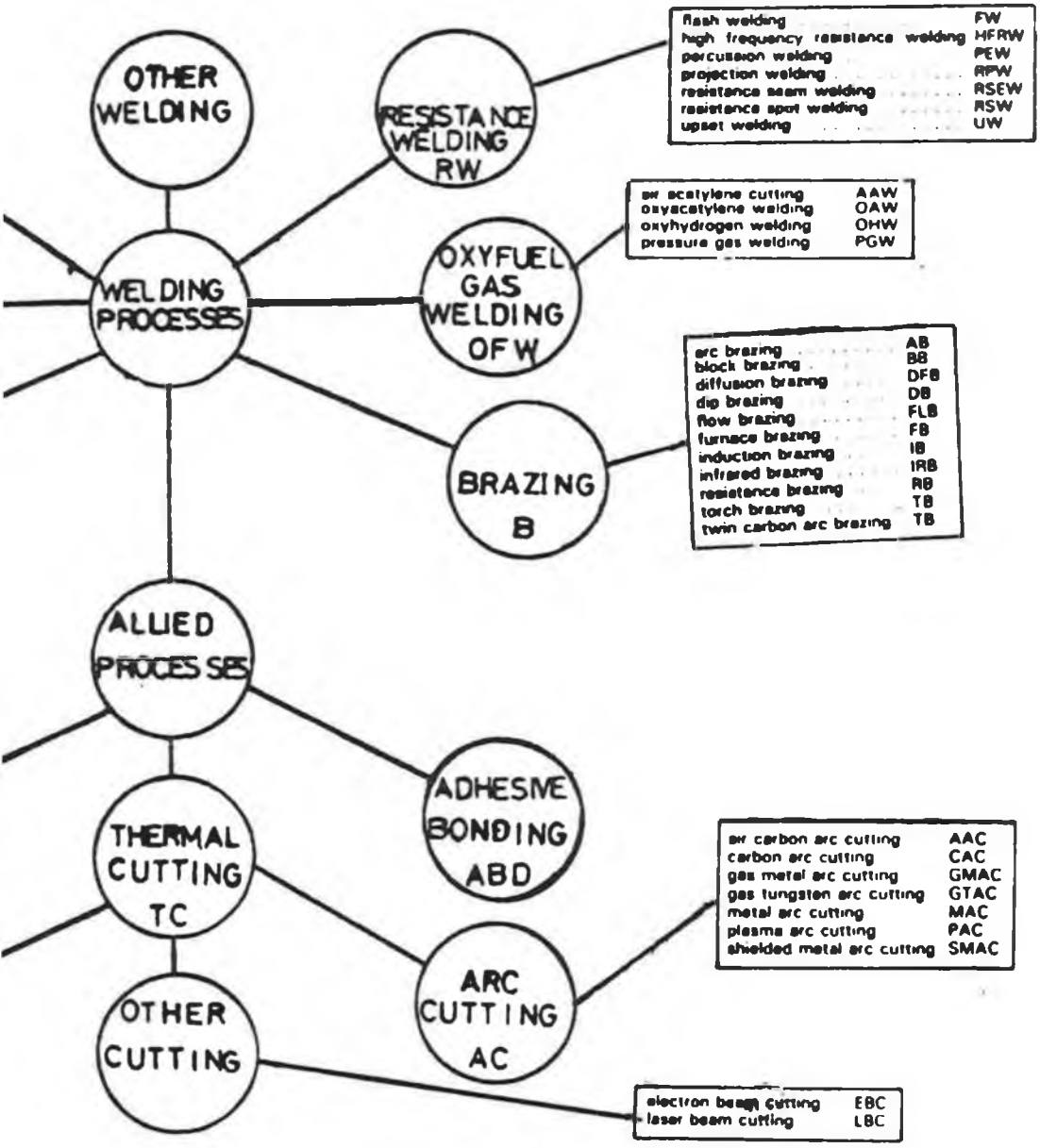

processes defined by American Welding (AWS).

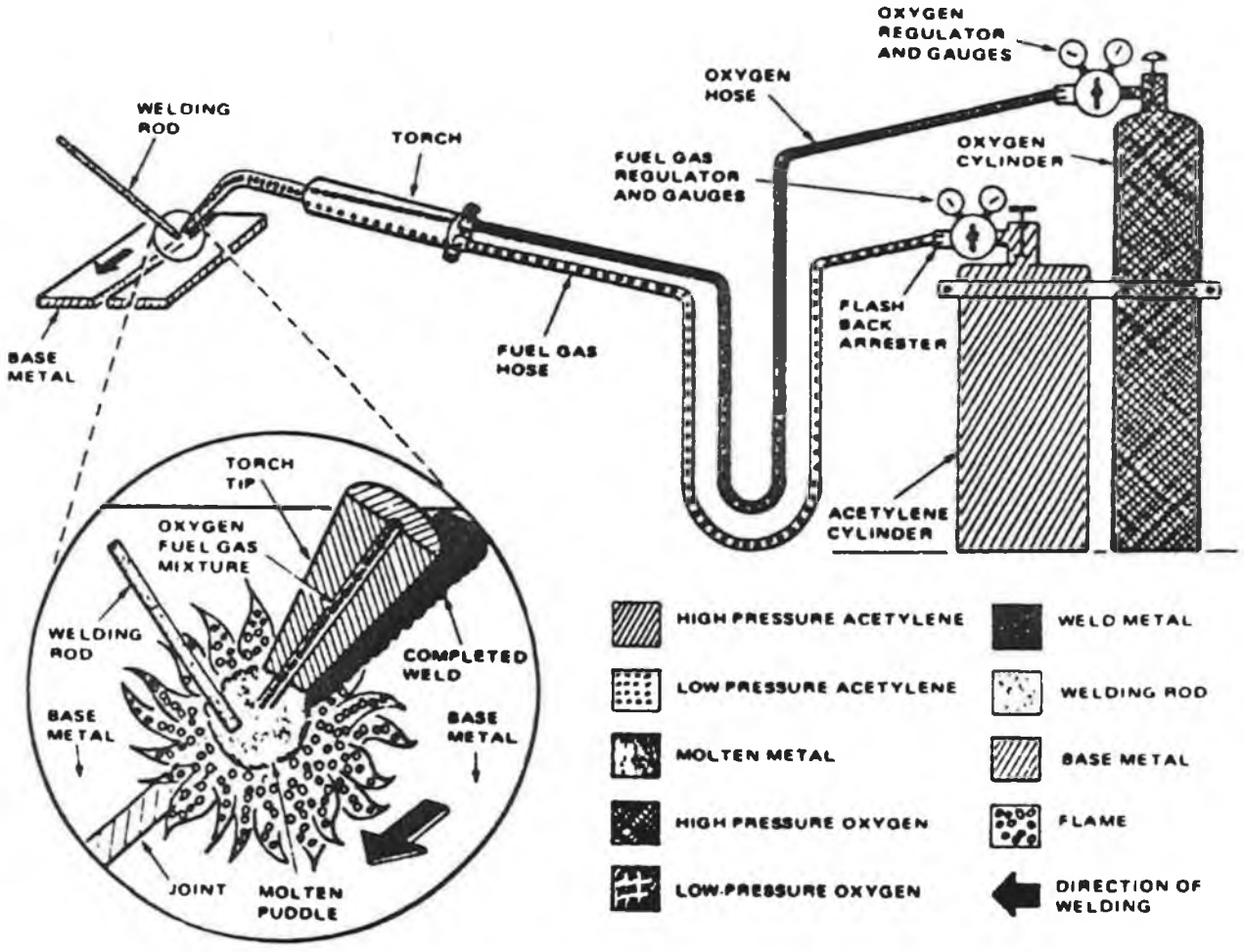

Fig. 2 Oxyacetylene welding (OAW).

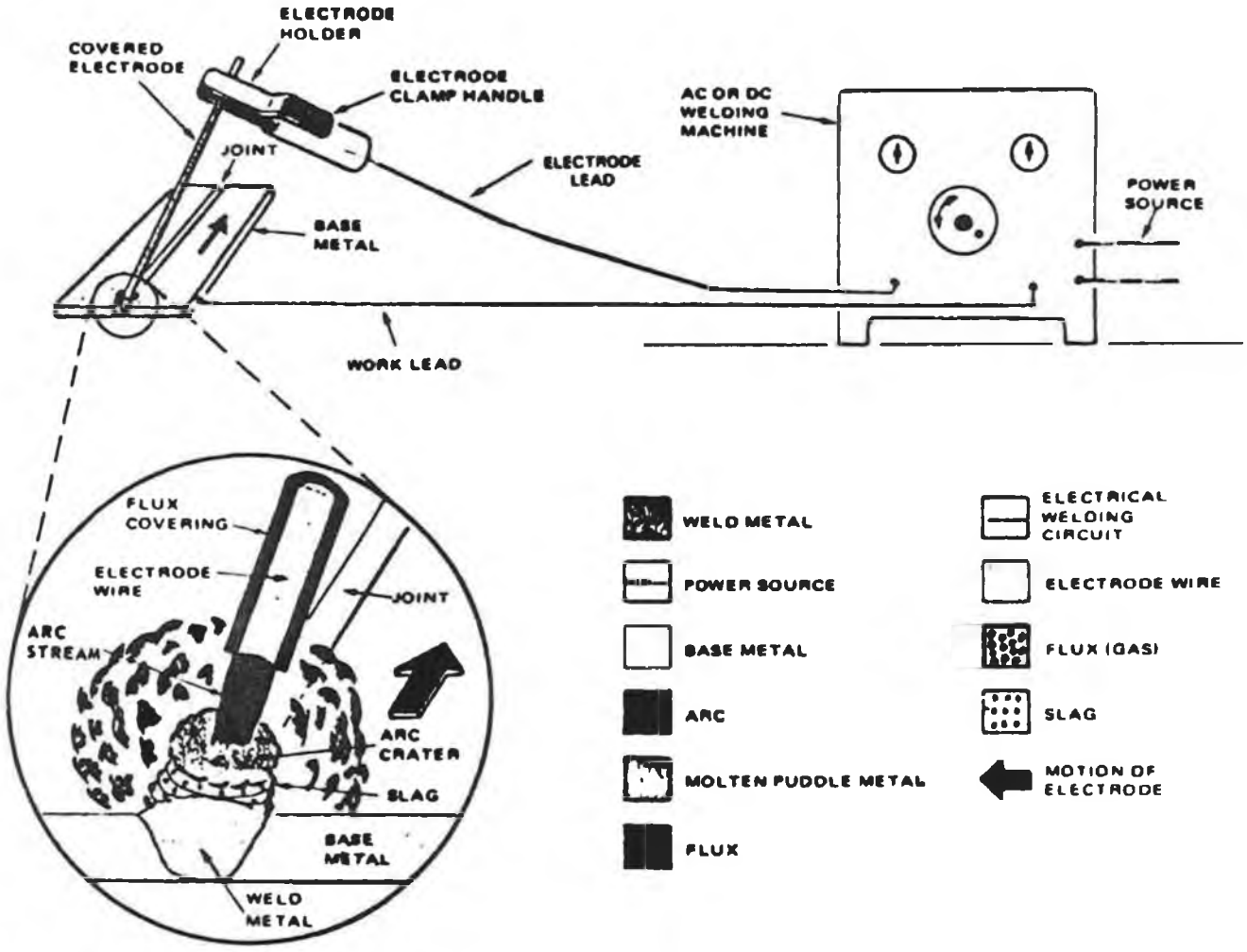

Fig. 3 Shielded metal arc welding (SMAW).

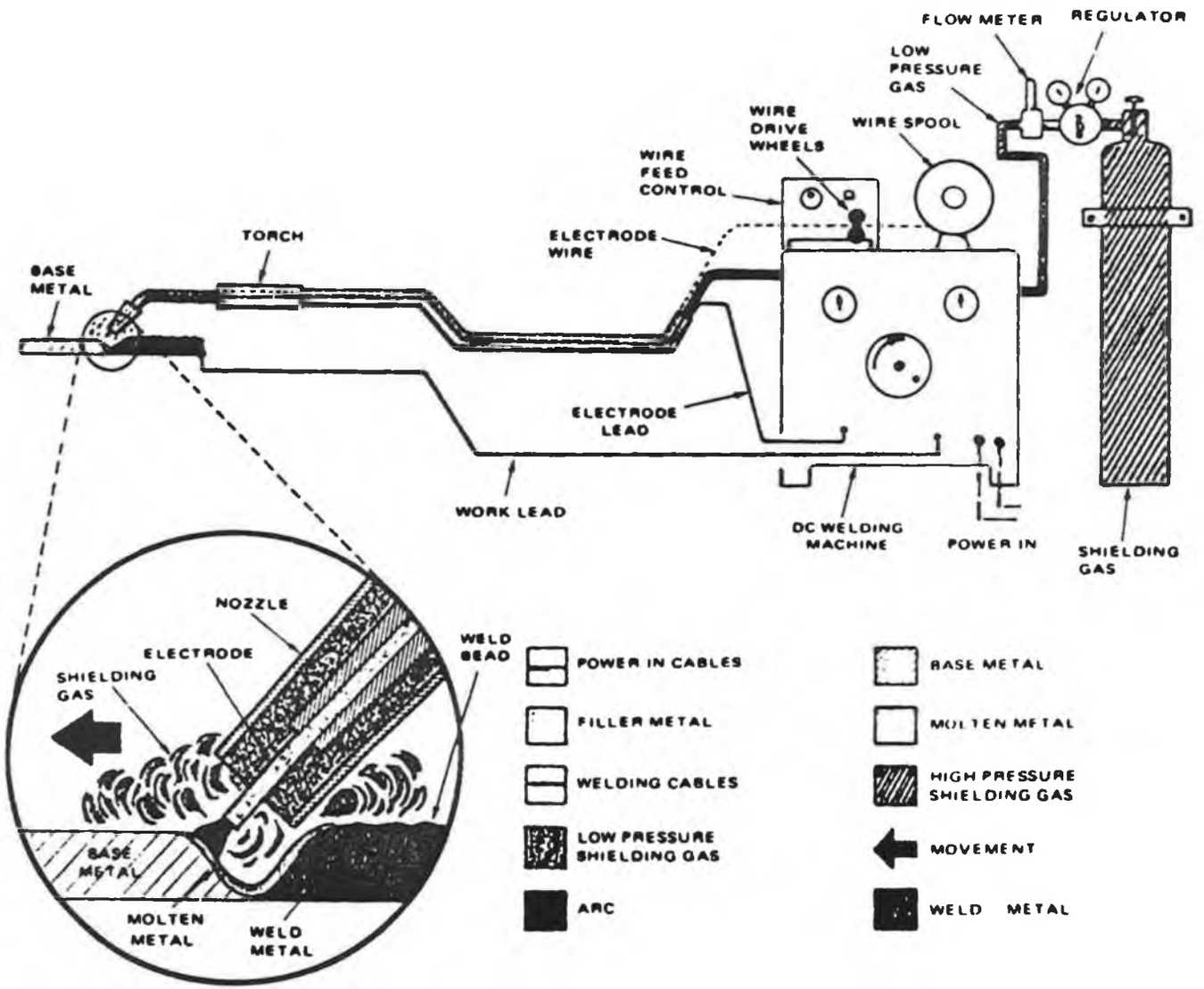

Fig. 4 Gas metal arc welding (GMAW).

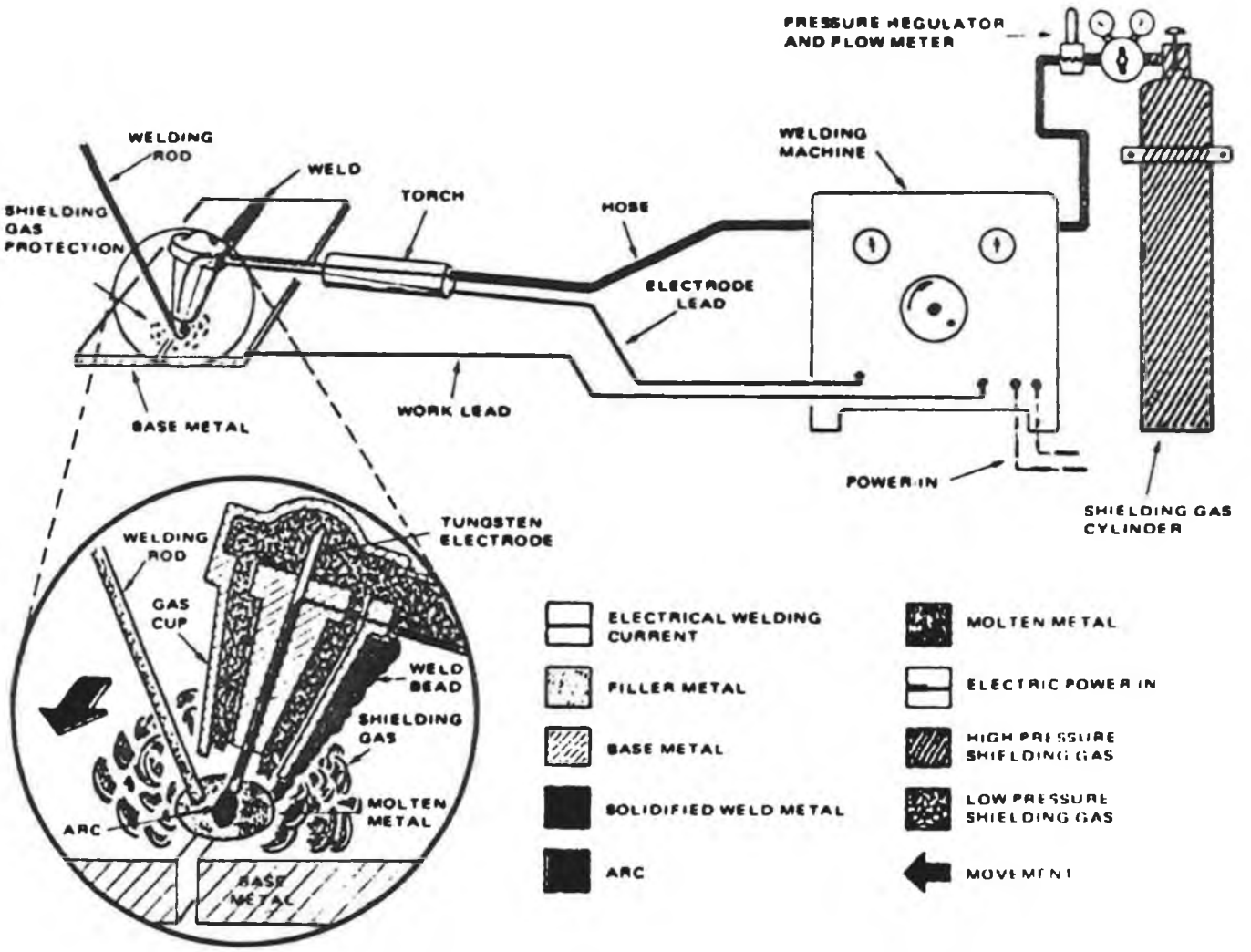

Fig. 5 Gas tungsten arc welding (GTAW).

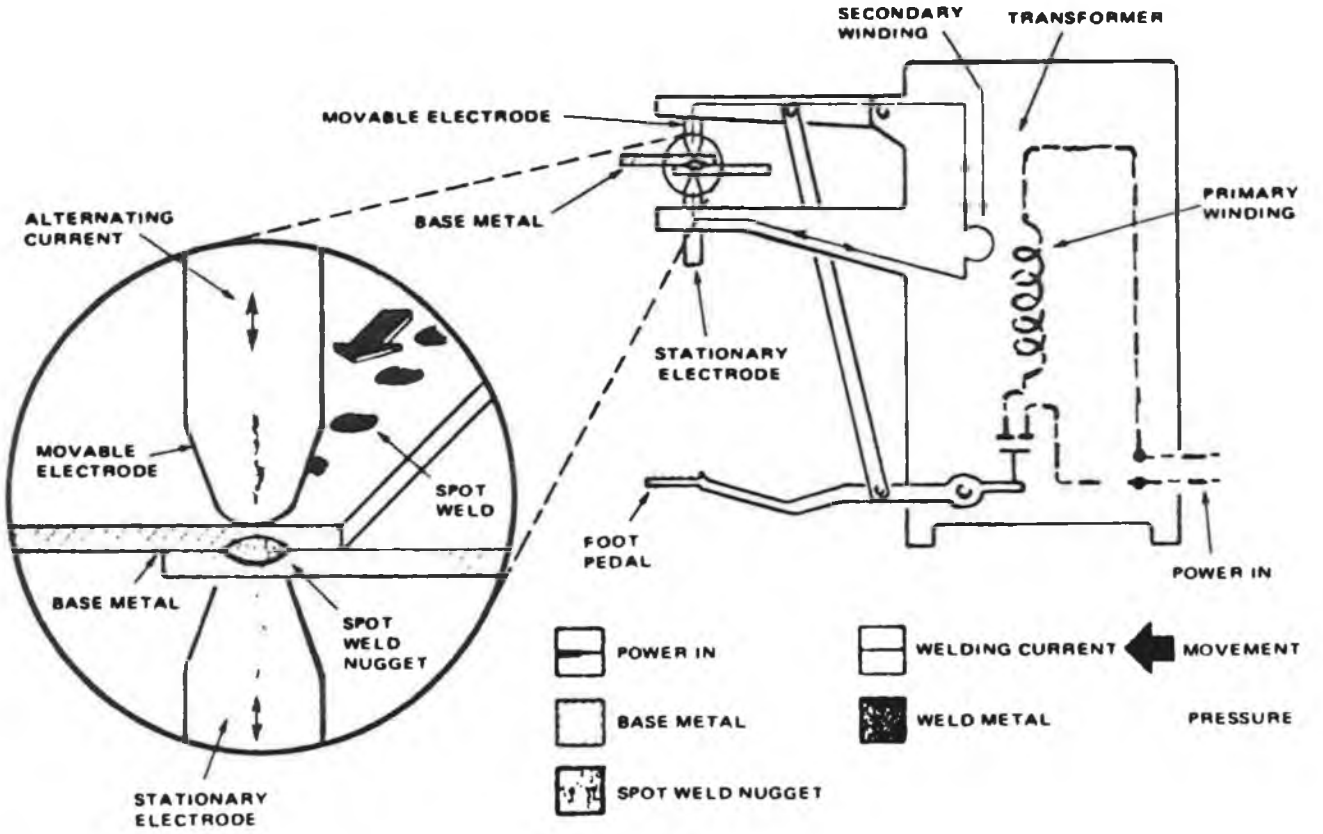

Fig. 6 Resistance spot welding (RSW).

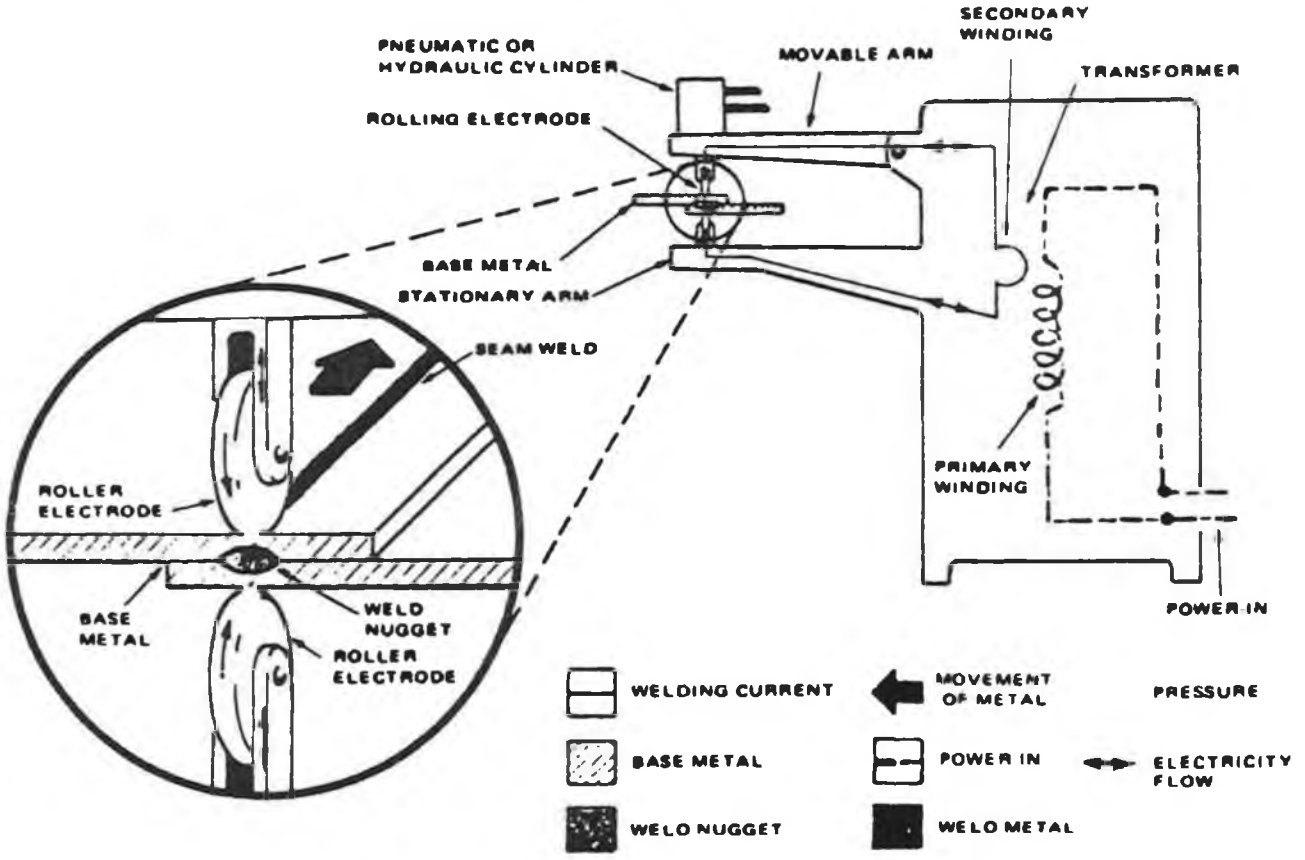

Fig. 7 Resistance seam welding (RSEW).

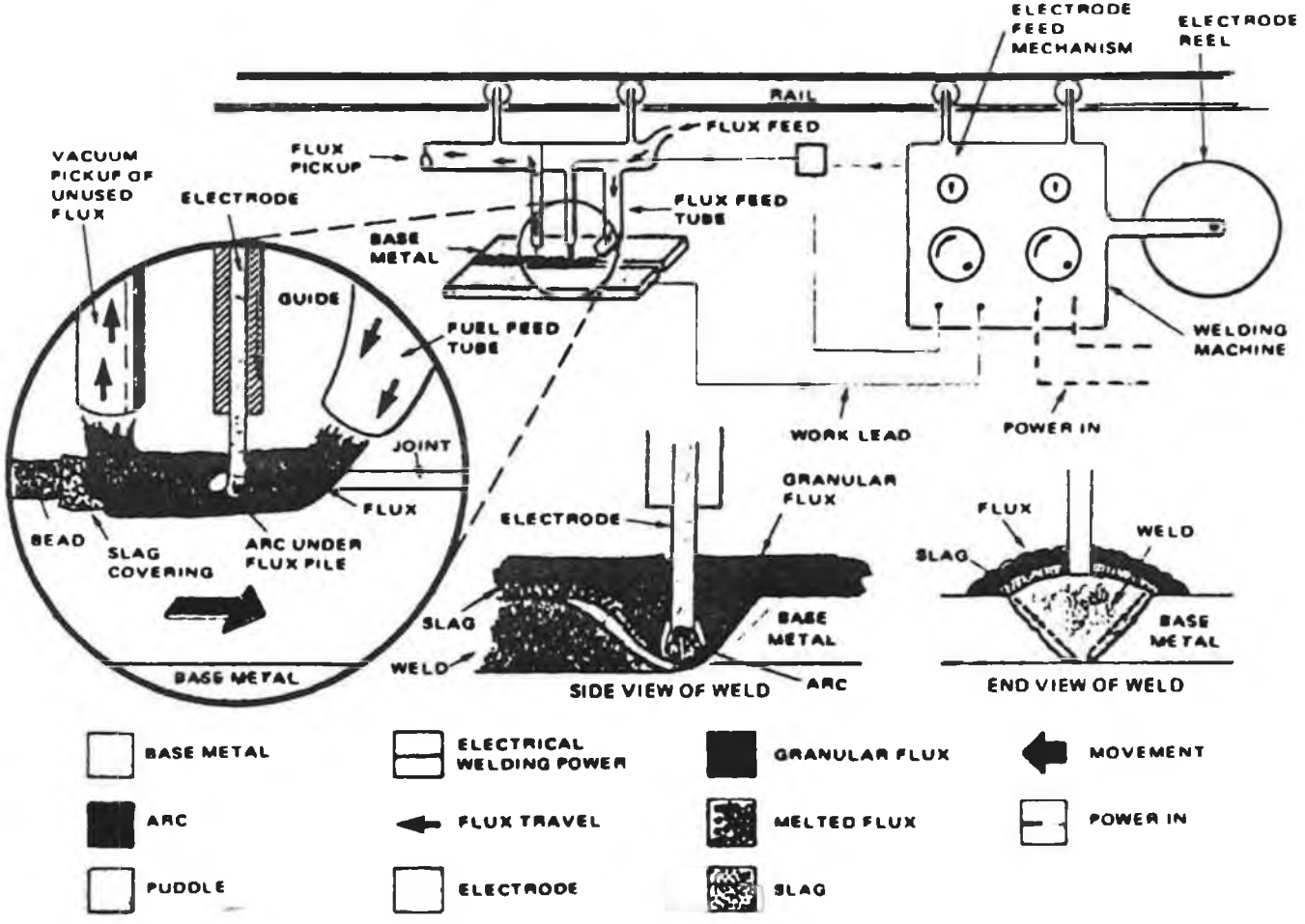

Fig. 8 Submerged arc welding (SAW).

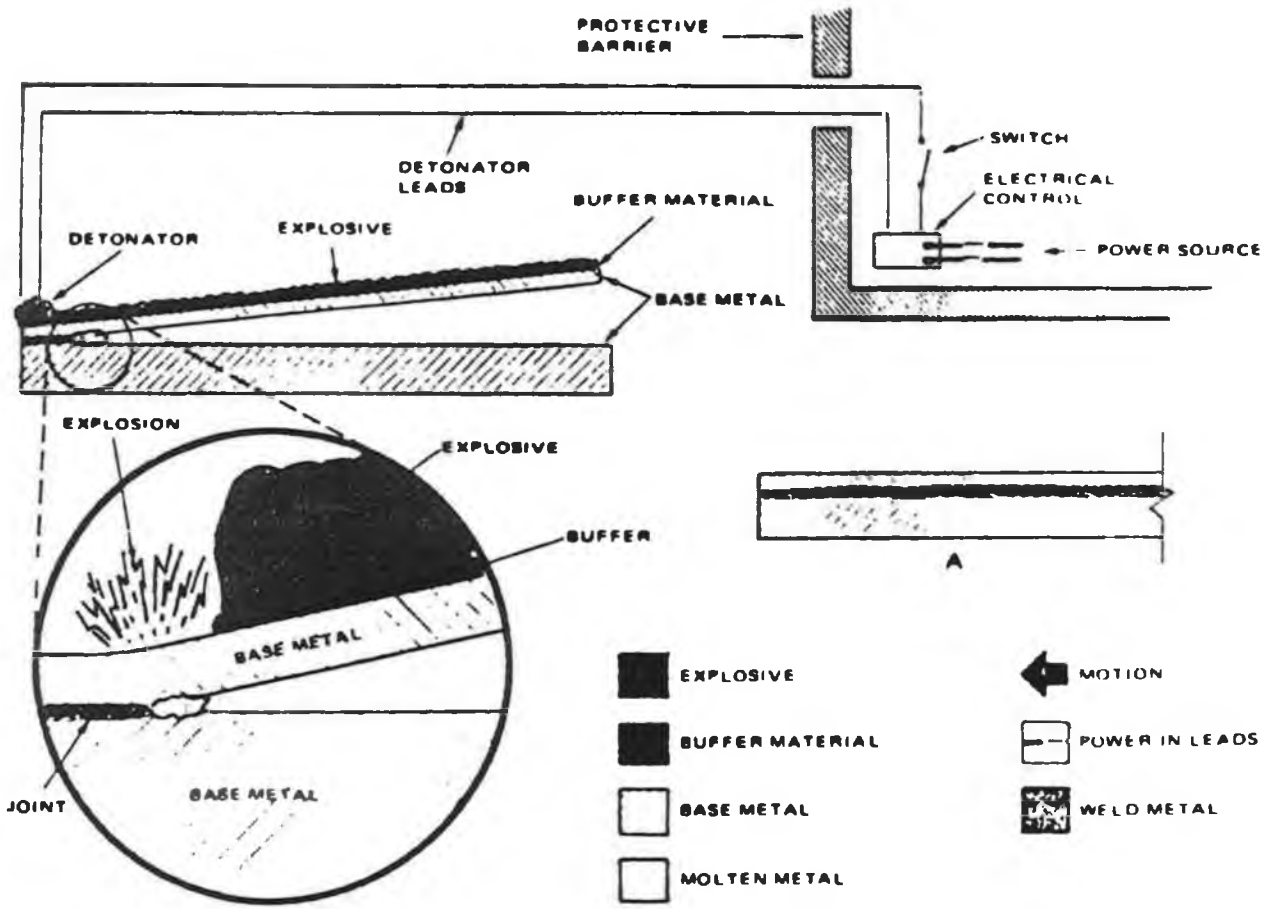

Fig. 9 Explosion welding (EXW).

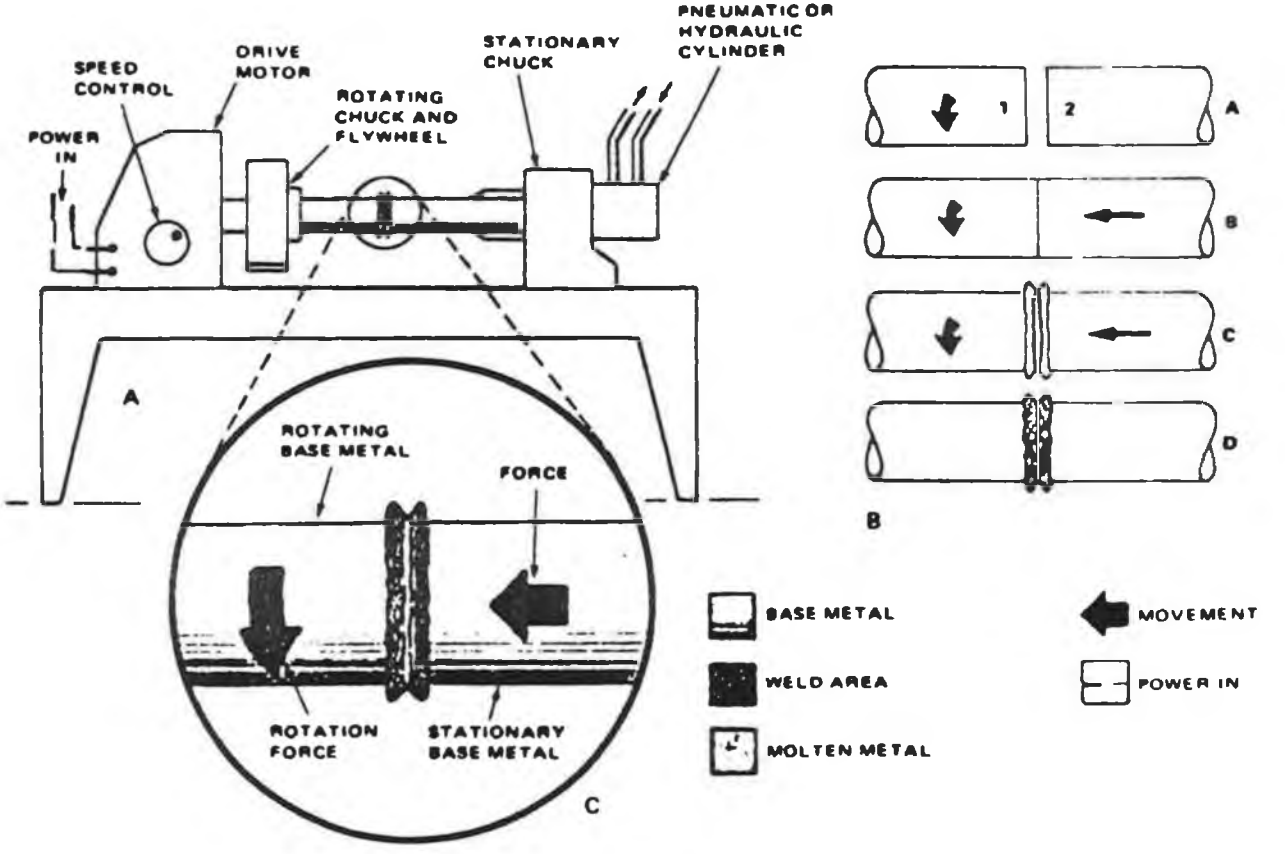

Fig. 10 Friction welding (FRW).

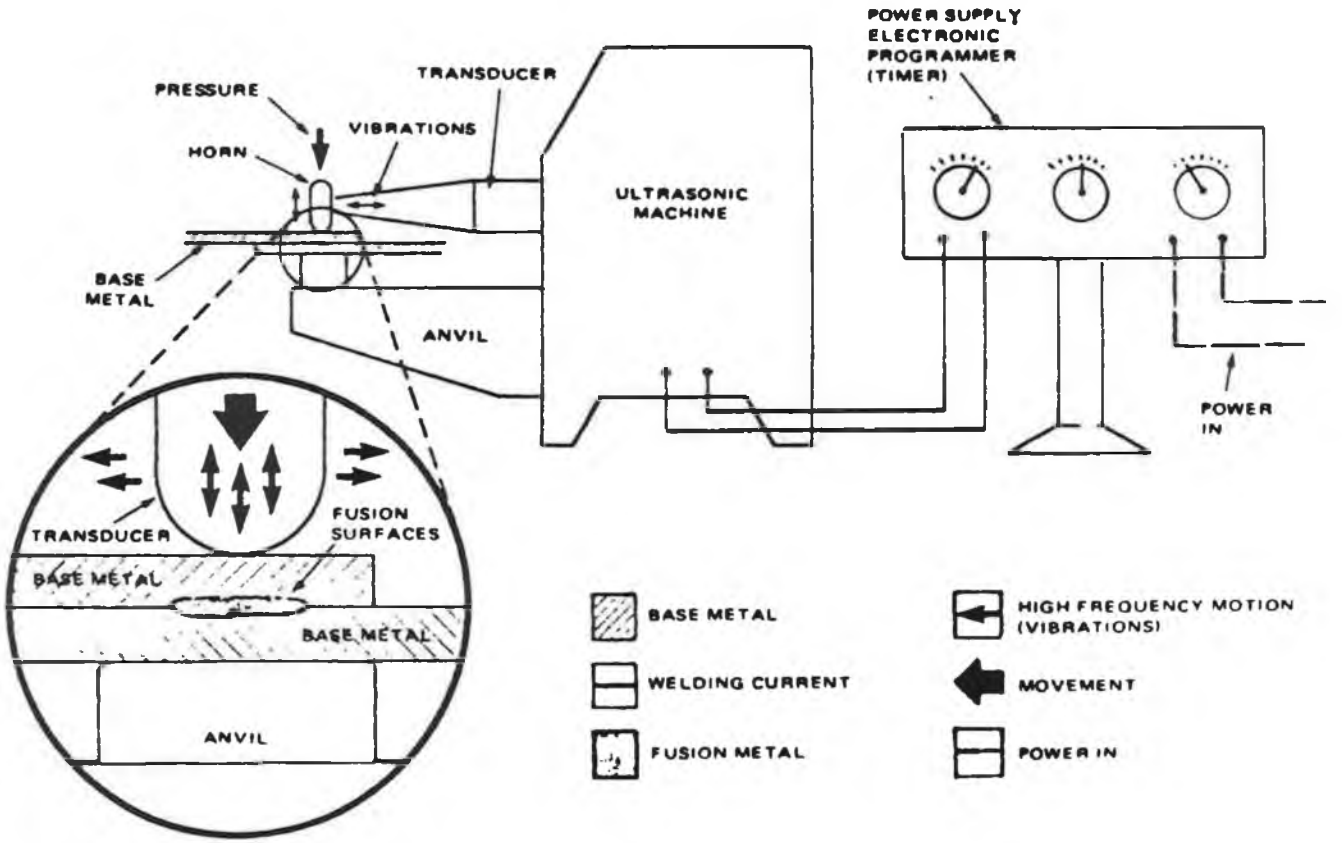

Fig. 11 Ultrasonic welding (USW).

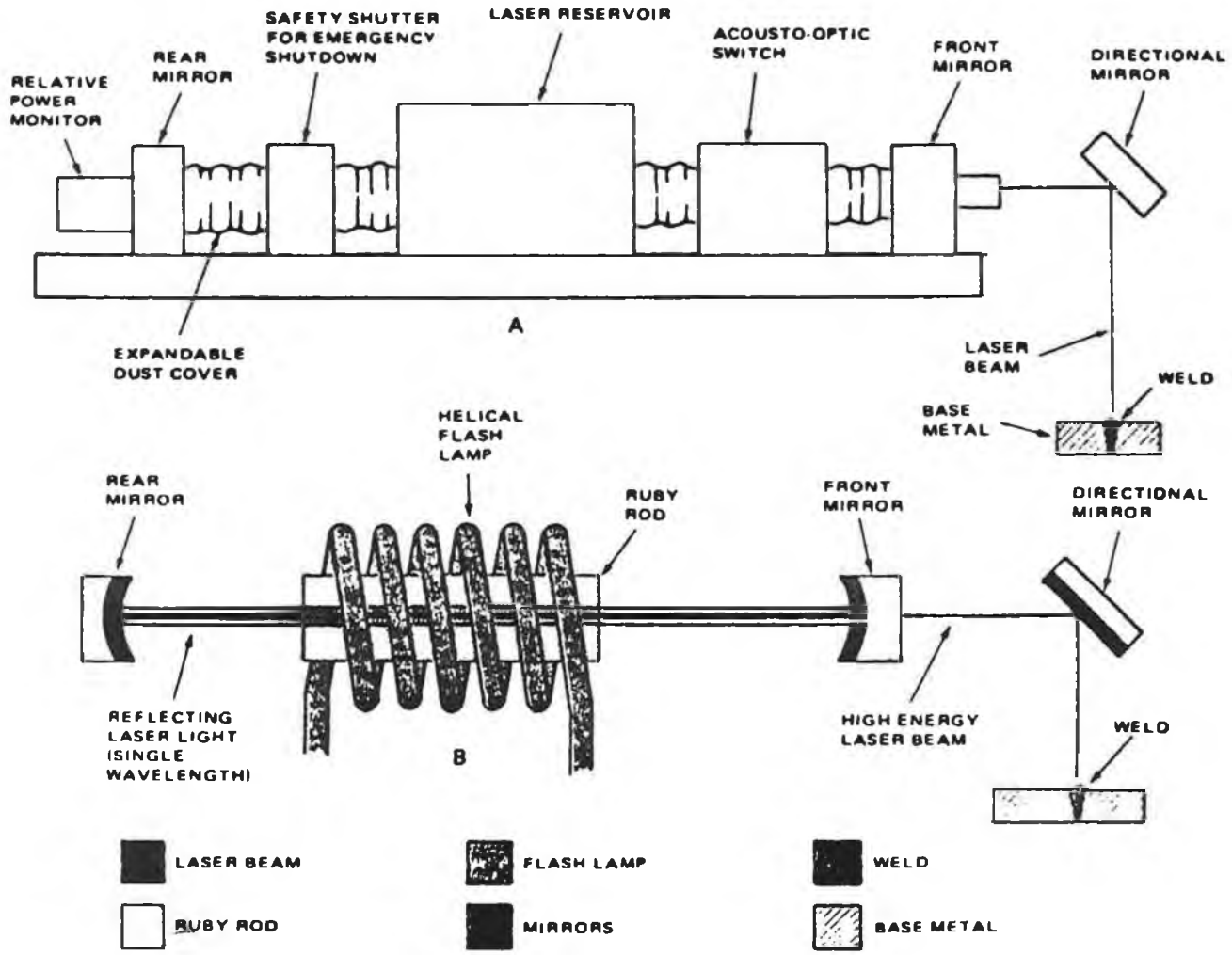

Fig. 12 Laser beam welding (LBW).

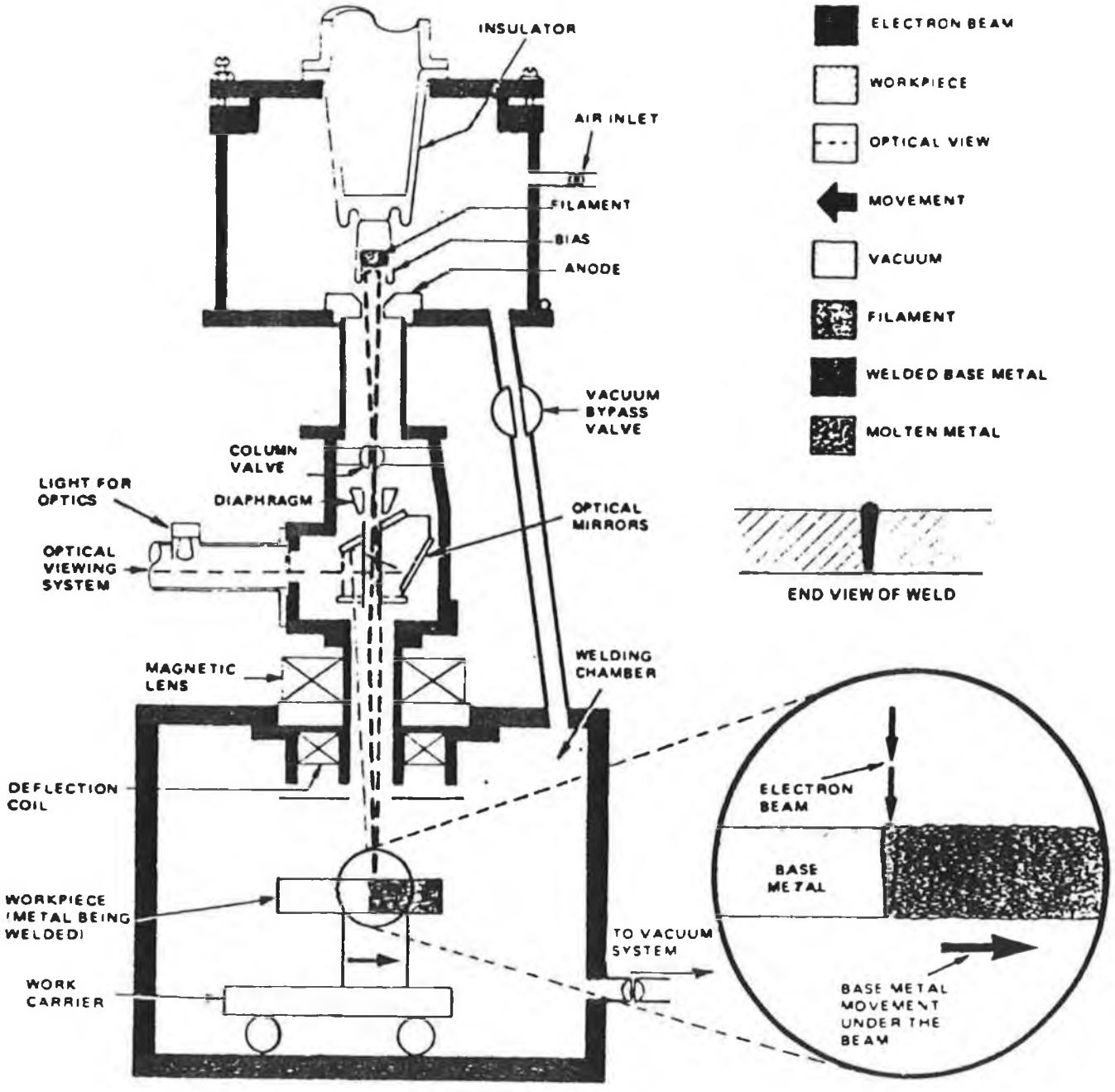

Fig. 13 Electron beam welding (EBW).

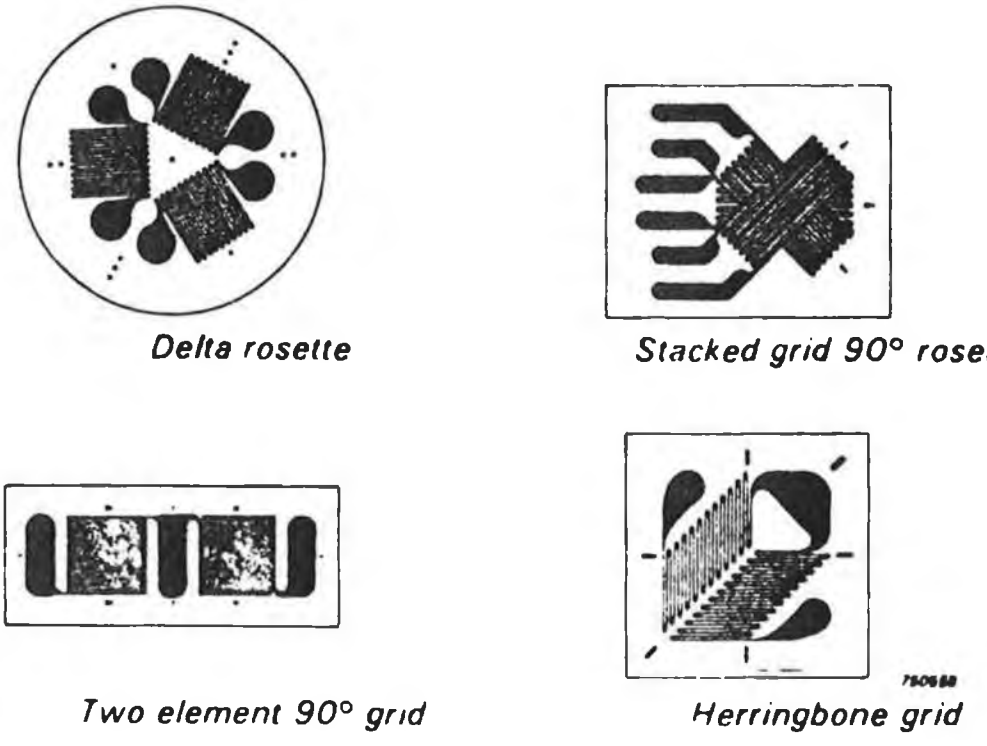

Fig. 14 Different types of strain gauges.

CHAPTER 2

EXPERIMENTAL EQUIPMENT
&
TEST PIECE PREPARATION

2.1 EQUIPMENT

2.1.1 ELECTRIC FURNACE

In this work a Lenton Laboratory Electric Chamber Furnace, series ECF1200, was used. The working temperature is up to 1200°C. It is operated from a 13 amp, 230 - 250 volt, single phase A.C. power supply.

The chamber size is 101 mm high, 127 mm wide, 203 mm deep. Maximum power rating is 2.0 kW. Plate 1 shows this electric furnace.

2.1.2 TENSILE TESTING MACHINE

The tensile testing machine was an Instron Universal Testing instrument model 4204, which consists of a loading frame and a control console as separate assemblies. The frame has a load capacity of up to 50 kN and is designed for testing materials in either tension or compression.

The basic operation of the instrument consists of selecting a load cell for a particular testing application, mounting the load cell in the moving cross head within the loading frame, then setting the specimen in position so that an applied load can be measured. The specimen is held by grips for tension testing, or is table - mounted for compression testing. plate 2 shows a photograph of the machine and its accessories.

During a test, results are displayed as tracked values of load, extension and strain or, after a test,as stored break and peak values of these parameters. The action of the moving cross head during a test (stop, return, cycle) may be controlled manually by push button switches or automatically by the functions provided by limits panel. These functions may be based on the applied load extension or strain, or to a specimen break detection.

2.1.3 HARDNESS TESTER

A micro hardness tester was used to measure the hardness of the specimens. This tester is capable of measuring three kinds of hardness - vickers, knoop and

scratch hardness - by changing the diamond indenter. However, for this project only vickers hardness method was employed. The tester is accompanied by a hardness test plate for calibration and a set of loads varying from 5g to 300g. These loads are chosen according to the thickness of the test piece; the tester type being LEITZ MINILOAD 2. Plate 3 shows a photograph of the hardness tester.

In this work a load of 100 g have been used.

2.1.4 OPTICAL MICROSCOPE

An entirely new metallograph Reichert MeF3 was used, which had the following facilities. It has a convenient position of binocular body with inclination angle of 32 and viewing height of 420 mm. It provides 6 nosepieces to make it suitable for all types of objectives. There are four step magnetic changers. It has reticule insert. The MeF3 has low coaxial coarse and fine controls which are easily accessible and a rotatable mechanical stage with coaxial controls.

A 4x5 Camera is built-in into the MeF3 Microscope and an additional 35 mm camera with automatic film transport is also provided. The Microscope is also supplied with an automatic control system for changing

from one camera to the other with display of exposure time. The MeF3 is provided with an illuminated frame projection for focussing purpose using the binocular tube with automatic brightness regulator. It is supplied with a Rotoscope projection device with a high resolution screen. A 100 Watt Halogen lamp and mirror house for use with high power lamps of up to 450 Watt are built into it. A Macrodual zoom system for large specimens (22 to 175 mm) imaging for both visual observation and photography is provided. It is also supplied with a Varicode projection system for luminous measuring bars with numbers or reticules for both visual observation and photography. A photograph of this device can be found on plate 4.

2.1.5 TIG WELDING MACHINE

A FILARC TIG 350D was used to execute all welding needed in this work. The current for this machine ranges from 4 - 350 A. This machine has water hoses for providing proper cooling for the welding torch. The FILARC TIG welding machine is also supplied with a gas cable to provide the protective inert gas environment.

This welding machine is fitted to carry the gas bottle and optional water cooler, comprising plastic tank with a pump, well able to cool a torch employed at high welding temperatures. Water cooling lines pass under the power source, away from any circuitry.

In this work the current range was about 65 to 75 A, and Argon gas was employed to protect the welding.

2.1.6 DIGITAL STRAIN INDICATOR

Digital Strain Indicator V/E -20A was used in this work. The V/E -20A Digital Strain Indicator is designed primarily for use with resistive type of strain gauges or strain gauge devices to determine the strain in the structure. The V/E -20A has a high accuracy and is an automatic instrument capable of measuring -+19999 microstrain in two ranges of -+1999 and -+19999 with 10 channels.

When the strain gauge and the resistor are connected to this instrument, direct reading appears on the digital board of this instrument. Plate 5 shows a photograph of the Digital Strain Indicator.

2.2 TOOLS AND MATERIALS

2.2.1 CLAMPING DIES

Clamping dies were used for two purposes; first, to clamp the second type of specimens to execute the welding, the second purpose was to hold the specimen during machining process to measure the residual stresses. This clamping die consists of two pieces and the specimen were mounted between them to provide a good matching during welding and machining. Fig. 15 shows the assembly drawings for this die.

The bottom piece of this die has a circular groove as a pilot for mounting the specimen on it. Fig. 16 shows the bottom piece of the die.

The top piece is quite similar to the bottom piece. The specimen (which was clamped by four bolts) was fixed between those two pieces. Fig. 17 shows the top piece of this die. Plate 6 shows a photograph of the top and bottom pieces.

2.2.2 STRAIN GAUGES

CEA - 06 - 125 UR - 120 Rosette strain gauges and CEA - 06 - 125 UN - 120 single strain gauges have been used to determine the residual stresses in this work. These strain gauges are a general purpose family of constant strain gauges widely used in experimental stress analysis. The gauges are supplied with a fully encapsulated grid and exposed copper coated integral solder tabs to which heavy lead wires may be soldered directly. The resistance of this gauge is 120 +- 0.4 % Ohms. Normal gauge factor is 2.04 - 0.5 % .

2.3 SPECIMEN PREPARATION

Two main types of specimens were used. The first type was for weld build-up with different lengths, widths, and thicknesses. The second type is for the welding of simulated cracks of different thicknesses. The chemical composition of this steel is : 0.15% C, 1.00% Mn, 0.040% P, 0.030% S, 1.00% Si, and 11.5-13.5% Cr.

2.3.1 BUILD-UP WELDING SPECIMEN PREPARATION

In preparing a specimen it was first machined to produce a circular shape of diameter 75 mm. In the central location of this specimen a slot has been made

of different lengths (20, and 40 mm) and different widths (10, and 20mm). The depth of this slot is 3 mm for 6 mm thick specimen's, and 1.5 mm for 3 mm thick specimen's. Fig. 18 shows the drawing of this specimen.

After machining, build-up welding was done by filling the deposit metal into this slot in the middle of this specimen. Plate 7 shows a photograph of this specimen before and after build-up welding.

2.3.2 CRACK REPAIRING SPECIMEN PREPARATION

This specimen consists of two similar parts, each part having a semi-circular shape, which when placed together produce a circular shape of 75 mm diameter. Between those two parts there is a very thin gap, about 0.2 mm, to simulate the crack. Fig. 19 shows the drawing of this specimen.

After machining, welding passes have been done to fill the deposit metal into and around this gap between the two parts of this specimen. Plate 8 shows a photograph of this specimen before and after welding.

2.3.3 STRAIN GAUGE PREPARATION

In order to obtain the best results from a strain gauge, it is important to prepare the gauge and the surface of the specimen to which the gauge is to be attached.

To prepare the specimen surface, an area larger than the installation was smoothed with fine grade emery paper of a fine sand blasting to provide a sound bonding surface. Then the area was degreased with a solvant cleaner; for this purpose a PCB solvant cleaner was used. Finally the specimen surface was neutralised with a weak detergent solution. Tissues were used for this operation. The final cleaning was immediately prior to the installation of the gauge.

After preparing the specimen surface a desired location for the strain gauge was determined. After that a short length of adhesive tape was placed over about half of the gauge tabs. Then the gauge backing and the specimen surface was coated with a thin layer of Cyanoacrylate adhesive. The adhesive was held for about 1 minute to dry. Then the strain gauge was placed in its desired location and reasonable pressure was applied

to ensure that the assembly was firmly in place. Then the gauge was covered with Polyethylene to prevent any external effect which might happen to the strain gauge.

2.4 TEST PROCEDURE

In addition to preparing those specimen, other approaches have been followed to establish the proper procedure for this series of experiments.

2.4.1 WELDING PROCEDURE

After the specimen has been machined as mentioned before, a TIG welding method has been used to produce the welding which was required in this work. For both these types of specimens (build up welding and crack repairing specimens), Argon gas has been used as a shielding gas to protect the welding zone from any harm during the welding. The Amperage was 65 to 75 Ampere. Electrode E410 was used, which has the same composition as the specimen material.

The build-up welding specimen has been produced by filling the slots of different widths, lengths and depths, which have been machined in the specimens.

Different passes and layers have been employed to fill this slot; 4 and 8 passes have been used for 10 and 20 mm width, 2 and 4 layers have been used for 3 and 6 mm depth. The crack repairing specimen has been produced by filling the slit between those two halves. Photographs 7 and 8 show different specimens before and after welding.

2.4.2 MICROSTRUCTURE AND HARDNESS TESTING PROCEDURE

To evaluate the microstructure and the hardness of these specimens, slices of 5 mm width have been cut from the middle of the specimen. Then the perpendicular face of the surface has been ground. After that a metallurgy lab has been used to polish this face. At first, however, before polishing this face, the specimen was surrounded by BAKELITE by using the thermoplastic instrument. After that, different grades of polishing was employed. Then the surface of this specimen was treated with acid. Finally it was washed and dried. At this stage the microstructure and the hardness testing have been started. Photograph 9 shows the specimen after machining encapsulated in the BAKELITE.

2.4.3 TENSILE TESTING PROCEDURE

For determining the tensile strength of these different specimens, before and after applying the post weld heat treatment, a special standard shape of tensile specimen was machined by following the guideline in German Standard (DIN) [39]. Fig. 20 shows a drawing for the tensile test specimen.

2.4.4 THE STRAIN MEASURING PROCEDURE

As mentioned above, strain gauges were used to evaluate the magnitude and the distribution of the residual stresses. To ensure a good result, the surface of the specimen was cleaned with solvant cleaner. Then the strain gauge was fixed at the correct place, by spreading the adhesive on the back of the strain gauge and on the surface of the specimen. After that a Silicone rubber was used to cover the strain gauge to protect it.

After the strain gauge was fixed, the first or the initial reading has been taken by connecting it to the digital strain indicator. Then the piece of the

specimen containing the strain gauge was machined to get the second reading. Photograph 10 shows the specimen after the strain gauges have been fixed and after machining the pieces of specimen containing the strain gauge.

2.4.5 POST WELD HEAT TREATMENT PROCEDURE

Two different types of Post weld heat treatment have been applied to evaluate the effect of heat treatment on the hardness and tensile strength and also to study their effect on the microstructure.

The specimens have been sectioned and machined as described above, then the heat treatment was applied. In the first type of heat treatment the specimen was left for 30 min at 316°C, then for 30 min at 427°C, and 2 hrs at 546°C and kept to coal in the furnace, (as prescribed in the industrial recommendations). In the second type of heat treatment, the specimen was kept for 2 hrs at 760°C and kept to coal in the furnace (AWS recommendation) [40].

PLATE 1 ELECTRIC FURNACE

PLATE 2 TENSILE TESTING MACHINE

PLATE 3 HARDNESS TESTER

PLATE 4 OPTICAL MICROSCOPE


Metallography of Weld Metal in Carbon-Manganese Steels

PLATE 5 DIGITAL STRAIN INDICATOR

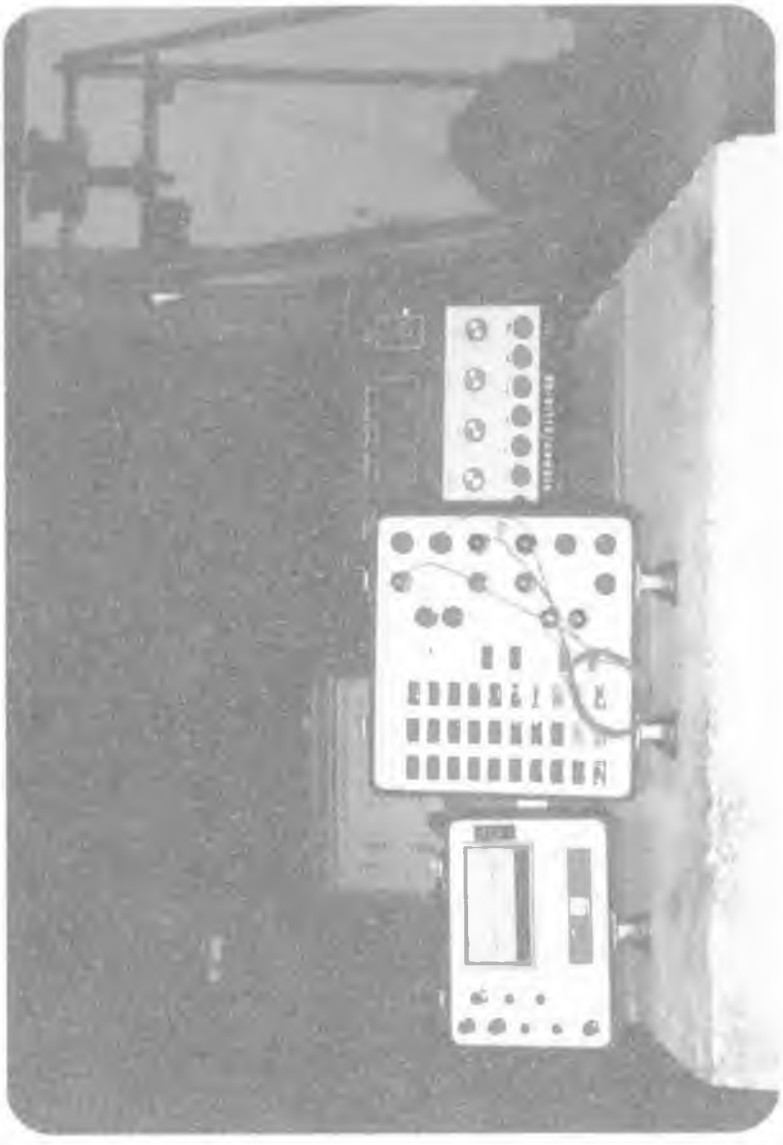

PLATE 6 CLAMPING DIE

PLATE 7 BIULD-UP WELDING SPECIMEN

PLATE 8 CRACK REPAIRING SPECIMEN

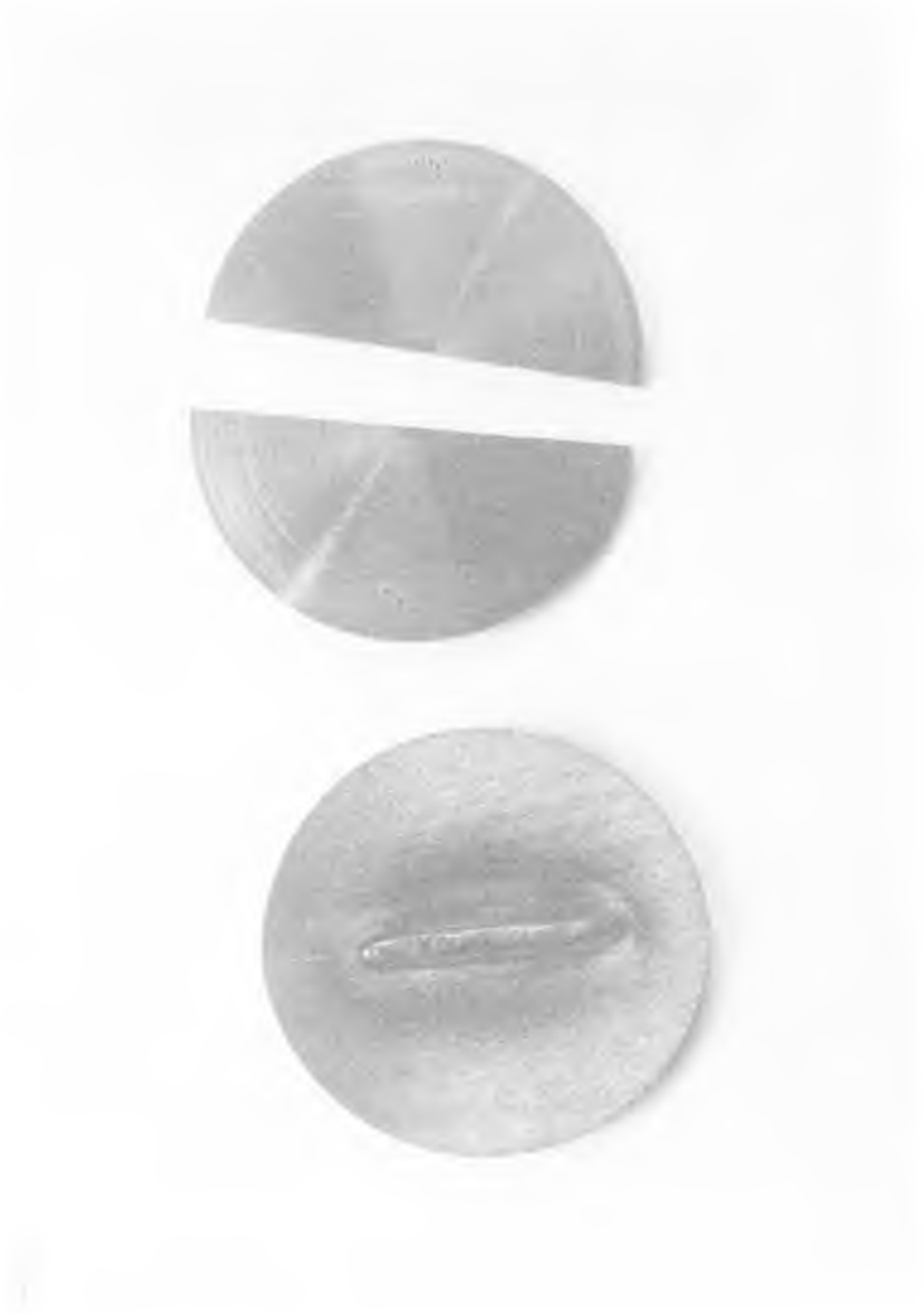

PLATE 9 METALLURGY SPECIMEN

PLATE 10 AFTER MACHINING TO MEASURE THE RESIDUAL STRESS

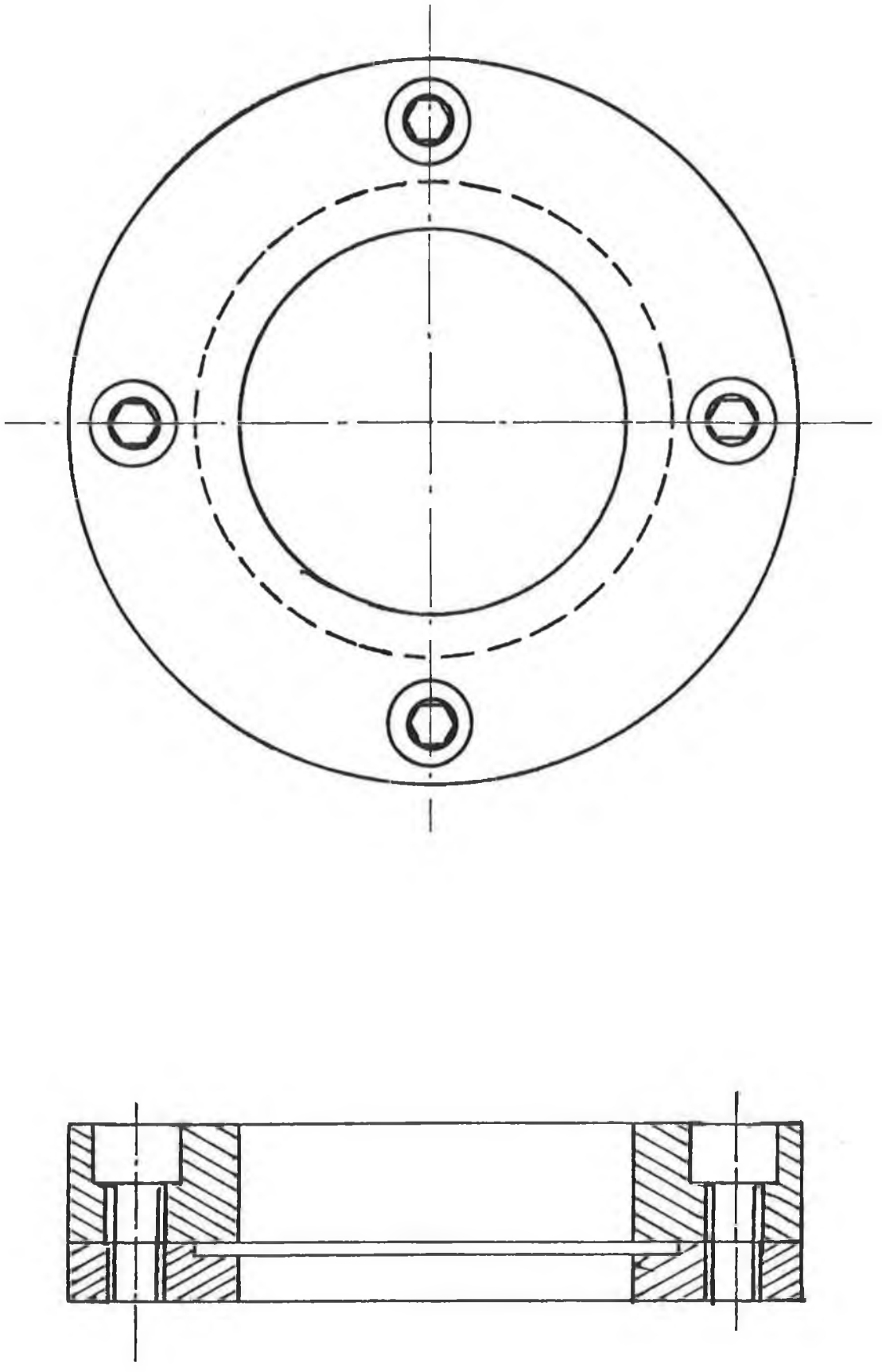

Fig. 15 The assembly drawings of the clamping dies.

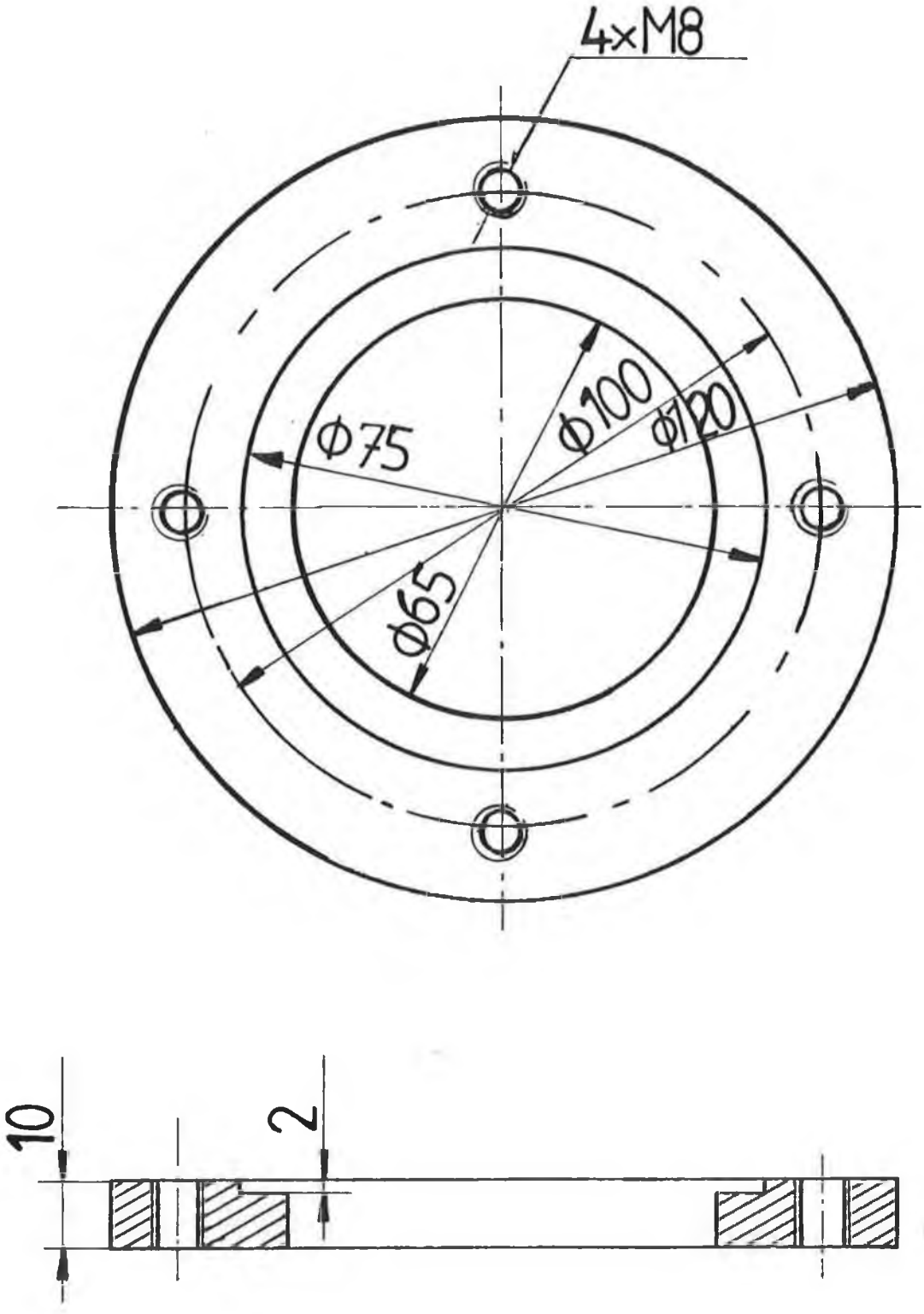

ALL DIMENSION IN [m.m].

Fig. 16 The bottom piece of the die.

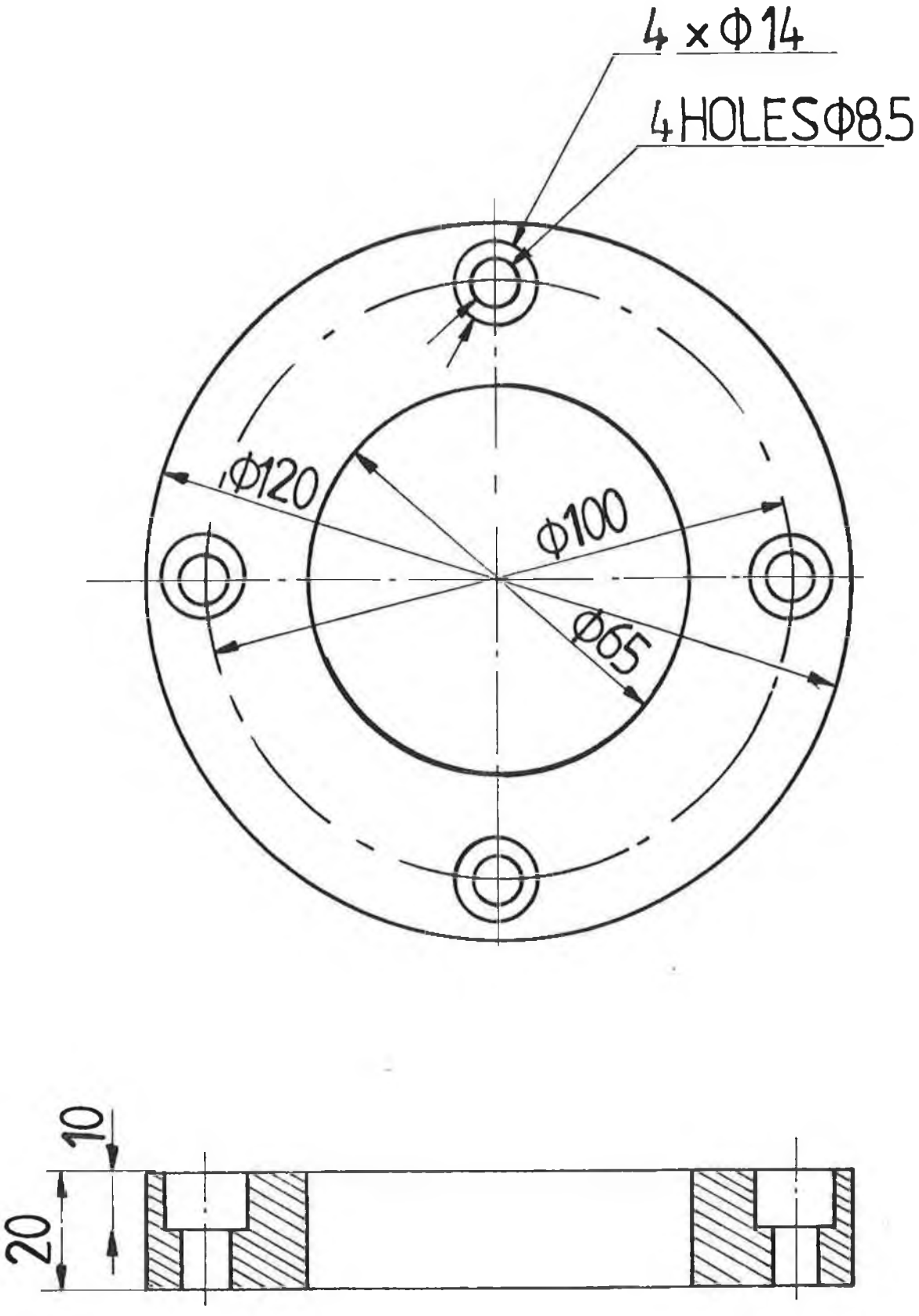

ALL DIMENSION IN [m.m].

Fig. 17 The top piece of the die.

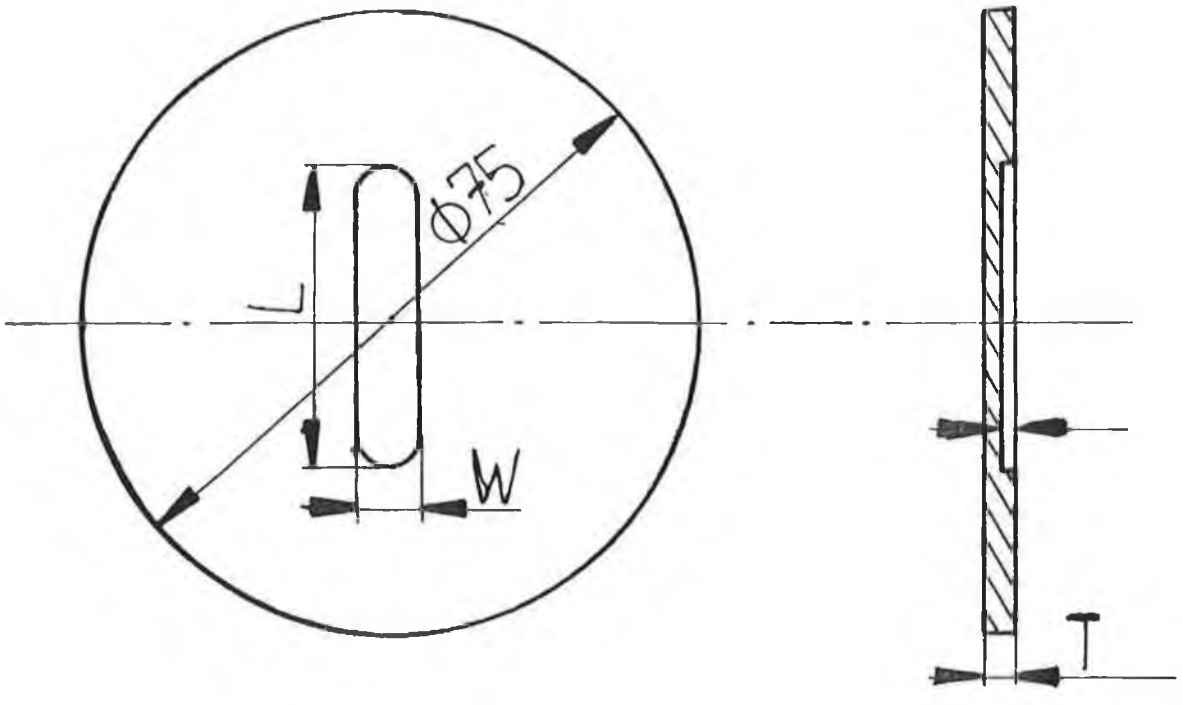

ALL DIMENSION IN [m.m].

Fig. 18 The drawing for build_up welding specimen.

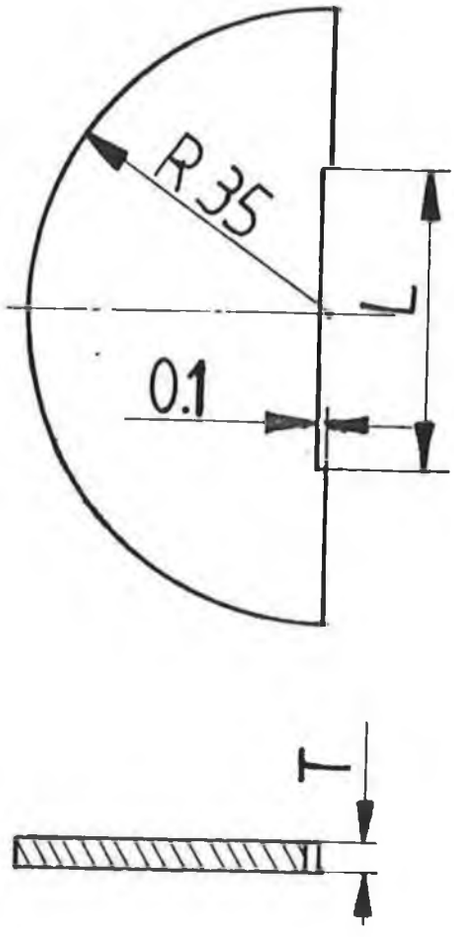

ALL DIMENSION IN [m.m].

Fig. 19 The drawing for crack repairing specimen.

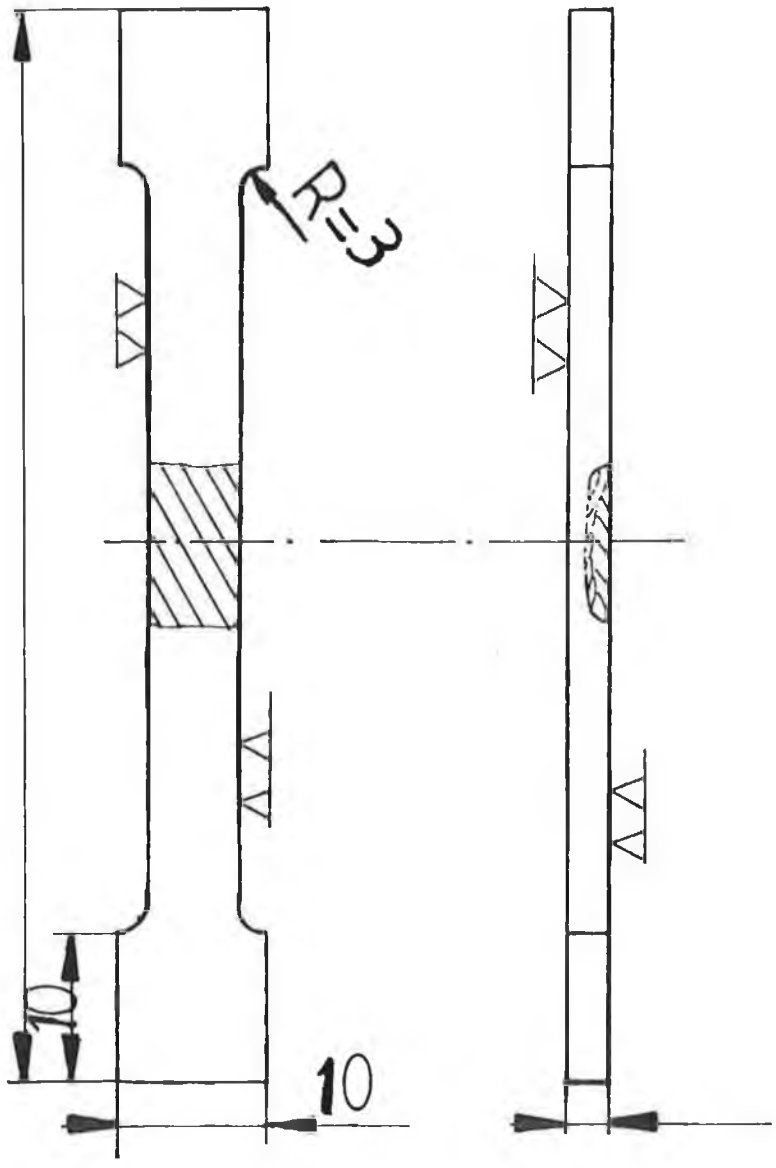

ALL DIMENSION IN [m.m].

Fig. 20 The drawing for tensile testing specimen.

CHAPTER 3

ANALYSIS OF RESULTS

3.1 EFFECT OF STRESS RELIEF HEAT TREATMENT

3.1.1 INTRODUCTION

In order to study the effect of stress relief heat treatment on metal microstructure and properties, two types of post weld heat treatments have been applied. Comparisons of results for different conditions both before and after heat treatment have been made, for both build-up welding and crack repair specimen.

As described before, in the first kind of heat treatment the specimens were left for 30 min at 316°C, 30 min at 427°C, and 2 hrs at 546°C; this will be referred to as heat treatment (1). In the second type of heat treatment, the specimens were kept for 2 hrs at 760 °C, which will be referred to as heat treatment (2).

3.1.2 METAL MICROSTRUCTURE

In order to study the effect of stress relief heat treatment a number of specimens have been prepared to provide a good microstructural examination.

Both types of specimens (build -up welding specimen, and crack repair specimen) have been investigated and comparisons of results for a number of conditions [after welding and before applying any kind of heat treatment; after heat treatment (1) and after heat treatment (2)] have been carried out. The results reveal that the microstructure in the welding zone for all types of specimens [A1 - A8] and [B1 and B2] have the same microstructure for the same condition (before or after heat treatment).

In the first condition, after welding and before applying any kind of heat treatment, the metal microstructure consists of almost completely martensite. Plates 11 and 12 show photographs of the metal microstructure in the welding zone, before applying any kind of heat treatment.

In the second condition, after applying heat treatment (1), the metal microstructure becomes completely tempered martensite with low percentage of ferrite . Plates 13 and 14 show photographs of the metal microstructure in the welding zone, after heat treatment (1).

Finally, after applying heat treatment (2), the metal microstructure consists of tempered martensite, precipitated carbide and ferrite. Plates 15 and 16 show photographs of the metal microstructure in the welding zone after heat treatment (2).
The photograph's magnification is X500 and X1000 as it appears at the plates.

3.1.3 HARDNESS TESTING

A large number of readings have been taken to determine the variation of the hardness across the specimen's section at different depths from the specimen's surface, and along the specimen's axis. The different axes where the readings have been taken are shown in Fig. 21.

The initial results for the build-up welding specimens before heat treatment, reveal that the hardness increases to the range of 490 - 510 HV in the

welding zone and the surrounding area, and outside this zone it decreases to about 260 - 270 HV. However after applying heat treatment (1) for the same type of specimens, the results indicate that the hardness becomes about 430 - 450 HV in and near the welding zone and outside the welding zone it decreases to about 250 - 270 HV. Similarly the variations in hardness have been measured for the same type of specimens after heat treatment (2). The results point out that the hardness decreases to about 300 - 330 HV in and near the welding zone and outside the zone it decreases to about 250 - 265 HV.

Different diagrams have been plotted to demonstrate the effect of different variables for build-up welding specimens [A1 - A8], and crack repair specimens [B1 and B2]. See table. 1 and 2.

In Figs. 22 - 55 the hardness variation across the specimen are presented for different depths from the surface and along the specimen's axis for the above three conditions (as welded specimen and after stress relief heat treatment) for both build-up welding and crack repair specimens.

Figs. 22 and 23 show the hardness variation for specimen A1, for two different depths: 0.5 mm from the specimen's surface (Fig. 22), and 2 mm from the specimen's surface (Fig. 23).

Fig. 22 shows that the hardness for as welded specimen reaches about 510 HV over about 9 mm of the welded zone from the specimen's axis, then it reduces to about 265 HV over the next 6 mm. After employing the first type of heat treatment, the hardness becomes about 440 HV over about 7.5 mm of the welded zone from the specimen's axis, then it decreases to about 260 HV over the next 8 mm. The second type of heat treatment shows that the hardness decreases to about 320 HV over about 3 mm of the welded zone from the specimen's axis, after that, it drops to about 255 - 260 HV.

Fig. 23 shows that the hardness for the first condition [before heat treatment], is about 510 HV for about 7 mm from the specimen's axis, then it decreases to about 265 HV. After applying heat treatment (1), the hardness decreases to about 440 HV for about 6 mm then it reduces to about 260 HV. In the third

condition, the hardness becomes between 280 and 290 HV for about 5 mm from the specimen's axis, then it decreases to about 250 HV.

Fig. 24 shows the hardness variation along the specimen's axis in the thickness direction. For the as welded specimen, the hardness varied between 490 and 520 HV, and between 425 and 440 HV after the first type of heat treatment, and between 290 and 315 HV after the second type of heat treatment.

Figs. 25 and 26 reveal the hardness variation for specimen A2, for two different depths: 0.5 mm from the specimen's surface, (Fig. 25), and 2 mm from the specimen's surface, (Fig. 26).

Fig. 25 shows that the hardness before any kind of heat treatment is about 505 HV for about 15 mm, then it decreases to about 260 HV. After heat treatment (1) the hardness is decreased to 440 HV for about 13.5 mm, then it becomes about 255 HV. In the third condition, the hardness decreases to 320 HV for about 11 mm then it reduces to about 250 HV.

Fig. 26 reveals that the hardness is about 505 HV for about 13 mm before heat treatment and it decreases to about 260 HV. After heat treatment (1) the hardness decreases to about 440 HV for about 11.5 mm, then it reduces to about 255 HV. The hardness becomes between 300 and 320 HV after heat treatment (2), then it decreases to about 250 HV.

Fig. 27 shows the hardness variation along the specimen axis in the thickness direction, for the same specimen [A2]. Before heat treatment the hardness is between 480 and 520 HV. After heat treatment (1) it becomes between 415 and 440 HV. Finally after heat treatment (2) it is decreased to the range of 300 - 325 HV.

Figs. 28 and 29 show the hardness variation across specimen A3, for two different depths: 0.5 mm from the specimen's surface, (Fig. 28), and 2 mm from the specimen's surface, (Fig. 29).

Fig. 28 reveals that the hardness before heat treatment is increased to about 500 HV for about 9 mm from the specimen's axis, then it reduces to about 265

HV. After first kind of heat treatment the hardness becomes about 455 HV for about 8 mm, after that it decreases to about 260 HV. After heat treatment (2), the hardness is diminished to about 310 HV for about 6 mm, then it decreases to about 250 HV.

Fig. 29 reveals that the hardness, in the first condition is increased to about 500 HV for about 8.5 mm, after that it decreases to about 265 HV. After heat treatment (1) the hardness is decreased to about 450 HV to about 7.5 mm, then it reduces to about 260 HV. In the third condition, the hardness decreases to the range of 300 - 310 Hv for about 6 mm, after that it becomes about 250 HV.

Fig. 30 shows the hardness variation along the specimen's axis in the thickness direction, for specimen A3. In the first condition the hardness is between 490 and 505 HV. And it is decreased to the range of 445 - 455 HV after heat treatment (1). Finally, after heat treatment (2) the hardness is decreased to become between 300 and 310 HV.

Figs. 31 and 32 show the hardness variation across specimen A4, for two different depths: 0.5 mm from the specimen's surface, (Fig. 31), and 2 mm from the specimen's surface, (Fig. 32).

Fig. 31 reveals that the hardness before any kind of heat treatment is 505 HV for about 16 mm, then it becomes about 265 HV. After heat treatment (1) it is decreased to about 440 HV for about 14 mm, after that it diminishes to about 260 HV. In the third condition the hardness decreases to become about 310 HV for 10 mm, then it drops to about 250 HV.

Fig. 32 shows that the hardness for the first condition is about 495 HV for about 15 mm, then it reduces to about 265 HV. After heat treatment (1), the hardness is decreased to about 435 HV for about 13 mm, after that it drops to about 260 HV. After the second type of heat treatment, the hardness decreases to become about 310 HV for about 10 mm, then it is decreased to about 250 HV.

Fig. 33 reveals the hardness variation along the specimen axis in the thickness direction, for specimen A4. Before any kind of heat treatment the hardness is between 495 and 505 HV. It becomes between 435 and 445 HV after heat treatment (1). In the third condition the hardness is decreased to the range of 300 - 310 HV.

Figs. 34 - 36 show the hardness variation across specimen A5, for different depths: 0.5 mm from the specimen's surface, (Fig. 34), 2.5 mm from the specimen's surface, (Fig. 35), and 4.5 mm from the specimen's surface, (Fig. 36).

Fig. 34 reveals that the hardness before any kind of heat treatment is about 490 HV for about 10 mm from the specimen's axis, after that it decreases to about 265 HV. After heat treatment (1) the hardness is decreased to about 440 HV for about 8 mm from the specimen's axis, then it diminishes to about 260 HV. After heat treatment (2), the hardness becomes between 290 and 310 HV for about 10 mm, after that it decreases to about 255 HV.

Fig. 35 shows that the hardness before employing the heat treatment is about 490 HV for about 8.5 mm from the specimen's axis, after that it reduces to about 265 HV. In the second condition, the hardness is decreased to about 435 HV for about 7.5 mm from the specimen's axis, then it becomes about 260 HV. After heat treatment (2), the hardness diminishes to become about 300 HV for about 6 mm from the specimen's axis, then it is decreased to about 255 HV.

Fig. 36 shows that the hardness before heat treatment is increased to about 490 HV for about 8.5 mm, after that it decreases to about 265 HV. After heat treatment (1) the hardness becomes about 435 HV for about 7.5 mm, then it drops to 260 HV. Finally, after the second kind of heat treatment the hardness is decreased to the range of 295 - 300 HV for about 6 mm, then it reduces to about 255 HV.

Fig. 37 shows that the hardness variation along the specimen axis in the thickness direction, for specimen A5. The hardness is between 490 and 510 HV before employing any kind of heat treatment. After heat

treatment (1), the hardness is decreased to become between 435 and 445 HV. Finally, after heat treatment (2), it is decreased to the range of 300 - 310 HV.

Figs. 38 - 40 show the hardness variation across specimen A6, for depths 0.5, 2.5, and 4.5 mm from the specimen's surface.

Fig. 38 reveals that the hardness before heat treatment is about 500 HV for about 17.5 mm from the specimen's axis, after that it decreases to become about 265 HV. After heat treatment (1), the hardness is decreased to about 450 HV for about 15.5 mm, then it reduces to about 260 HV. After heat treatment (2), the hardness decreases to the range of 310 - 320 HV for about 13 mm, after that it becomes about 255 HV.

Fig. 39 shows that the hardness, in the first condition, is increased to about 500 HV for about 14 mm, after that it decreases to become about 265 HV. After heat treatment (1), the hardness is decreased to about 450 HV for about 13 mm, then it drops to about 260 HV.

After heat treatment (2), the hardness is diminished to about 310 HV for about 11 mm, after that it decreases to about 255 HV.

Fig. 40 reveals that the hardness, before employing any kind of heat treatment is about 500 HV for about 13 mm, then it reduces to about 265 HV. After heat treatment (1), the hardness is decreased to about 445 HV for about 11 mm, after that it becomes about 260 HV. Finally, after heat treatment (2), the hardness is decreased to become about 310 HV for about 10 mm, then it reduces to about 255 HV.

Fig. 41 shows the hardness variation along the specimen axis in the thickness direction, for the same specimen, A6. The results reveal that the hardness is between 495 and 505 HV before employing any kind of heat treatment. After heat treatment (1), the hardness is decreased to become between 440 and 450 HV. And after heat treatment (2), it is decreased to the range of 305 - 315 HV.

The hardness variation across specimen A7, for three different depths, 0.5, 2.5, and 4.5 mm from the specimen's surface, are plotted in Figs. 42 to 44.

Fig. 42 shows that the hardness, before applying any kind of heat treatment is about 505 HV for about 10 mm, after that it is decreased to to about 270 HV. After heat treatment (1), the hardness is diminished to about 450 HV for about 8 mm, then it decreases to about 260 HV. After the second type of heat treatment, the hardness reduces to the range of 300 - 315 HV for about 7 mm, after that it becomes about 255 HV.

Fig. 43 reveals that the hardness, before any kind of heat treatment is about 505 HV for about 8 mm, after that it decreases to become about 270 HV. After heat treatment (1), the hardness is decreased to about 450 HV for about 7 mm, then it reduces to about 265 HV. Finally, after the second type of heat treatment, the hardness becomes about 300 - 310 HV for about 5 mm, after that it decreases to about 260 HV.

Fig. 44 shows that the hardness, before employing any kind of heat treatment, is increased to about 505 HV for about 7.5 mm. after that it drops to about 270 HV. After heat treatment (1), the hardness is decreased to about 450 HV for about 7 mm, after that it

reduces to about 265 HV. In the third condition, the hardness becomes about 300 HV for about 5 mm, then it decreases to about 255 HV.

Fig. 45 reveals the hardness variation along the specimen axis in the thickness direction, for the same specimen, A7. The results point out that the hardness in the first condition is between 490 and 510 HV. It is decreased to the range of 440 - 455 HV after heat treatment (1). After heat treatment (2), the hardness is decreased to become between 300 and 320 HV.

Figs. 46 - 48 show the hardness variation across specimen A8, for three different depths from the specimen's surface, 0.5, 2.5, and 4.5 mm.

Fig. 46 reveals that the hardness, before heat treatment, is increased to about 510 HV for about 18 mm, after that it decreases to about 265 HV. After heat treatment (1), the hardness is decreased to about 450 HV for about 17 mm, then it reduces to about 260 HV. After heat treatment (2), the hardness is also decreased to about 310 HV for about 12 mm, then it diminishes to about 255 HV.

Fig. 47 shows that the hardness in the first condition, is about 510 HV for about 15.5 mm, after that it decreases to about 265HV. After heat treatment (1), the hardness is decreased to about 440 HV for about 13 mm, then it drops to about 260 HV. Finally, after heat treatment (2), the hardness is diminished to about 305 HV for about 11 mm, after that it reduces to about 255 HV.

Fig. 48 shows that the hardness is increased to about 510 HV for about 15 mm, after that it reduces to about 265 HV. After heat treatment (1), the hardness is decreased to about 440 HV for about 12 mm, then it diminishes to about 260 HV. After heat treatment (2), the hardness is decreased to the range of 300 - 310 HV for about 10 mm, after that it drops to about 255 HV.

Fig. 49 reveals the hardness variation along the specimen axis in the thickness direction, for the same specimen, A8. The results show that the hardness, in the first condition is between 495 and 515 HV. After heat treatment (1), it is decreased to the range of 430 - 445 HV. Finally, after heat treatment (2), it becomes between 295 and 310 HV.

The following figures results for crack repair welding. Figs. 50 and 51 reveal the hardness variation across specimen B1, for two different depths from the specimen's surface, 0.5 mm from the specimen's surface (Fig. 50), and 1.5 mm from the specimen's surface (Fig. 51).

Fig. 50 and 51 show very similar results, which reveal that the hardness, after welding and before applying any kind of heat treatment is increased to about 525 HV for about 4 mm, then it decreases to about 265 HV. After heat treatment (1), the hardness is reduced to about 460 HV for about 3.5 mm, after that it decreases to about 260 HV. After heat treatment (2), the hardness is diminished to about 290 HV for about 3 mm, then it becomes about 250 HV.

Fig. 52 reveals the hardness variation along the specimen axis in the thickness direction, for the same kind of specimen B1. The results show that the hardness is between 525 and 530 HV before applying any kind of heat treatment. After heat treatment (1), the hardness

is decreased to the range of 460 - 465 HV. Finally, after heat treatment (2), the hardness is diminished to become between 295 and 300 HV.

Figs. 53 and 54 reveal the hardness variation across specimen B2, for two different depths from the specimen's surface. 0.5 mm from the specimen's surface (Fig. 53), and 2.5 mm from the specimen's surface (Fig. 54).

Fig. 53 shows that the hardness, before applying any kind of heat treatment is about 520 HV for about 6 mm, after that it decreases to about 265 HV. After heat treatment (1), the hardness is reduced to about 465 HV for about 5 mm, then it decreases to about 260 HV. After heat treatment (2), the hardness is diminished to about 295 HV for about 3 mm, then it reduces to about 250 HV.

Fig. 54 reveals that the hardness, before heat treatment is about 525 HV for about 5 mm, after that it decreases to about 265 HV. After heat treatment (1), the hardness is reduced to about 465 HV for about 5 mm, then it decreases to about 260 HV. Finally, after heat treatment (2), the hardness is diminished to about 300 HV for about 3 mm, after that it becomes about 250 HV.

Fig. 55 shows the hardness variation along the specimen axis in the thickness direction, for the same specimen B2. The results reveal that the hardness is between 515 and 520 HV, before applying any kind of heat treatment. After heat treatment (1), the hardness is decreased to the range of 460 - 465 HV. Finally, after heat treatment (2), the hardness reduces to become between 295 and 305 HV.

In order to study the effect of the different variables in the specimen (thickness, length, and width), and to compare between the results of the hardness variation for the same kind of specimen, for different depths from the specimen's surface, a number of graphs have been plotted for both types of specimens (build-up welding specimen, and crack repair specimen). The first condition (after welding and before applying any kind of heat treatment) has been chosen for these comparisons.

Figs. 56 to 65 show different curves which represent the hardness variation across the specimens. Each of these curves has been produced for a particular depth, 0.5 and 2 mm for specimens A1 - A4; 0.5, 2.5,

and 4.5 mm for specimens A5 - A8; 0.5 and 1.5 mm for specimen B1; and 0.5 and 2.5 mm for specimen B2. Each of these figures compares the hardness variations at different depths of the same specimen.

Figs. 66 to 70 have been plotted to demonstrate the effect of the thickness on the hardness variation. Comparisons between similar specimens which differ only in thickness, (A1 and A5, A2 and A6, A3 and A7, A4 and A8, B1 and B2) have been made at the depth of 0.5 mm from the specimen surface.

Different curves have been plotted to study the effect of the bead lengths on the hardness variation. Comparisons have been made between similar specimens which differ only in bead lengths, (A1 and A3, A2 and A4, A5 and A7, A6 and A8). The hardness variation measured at the depth of 0.5 mm from the specimen surface. The results of this comparison are shown in Figs. 71 to 74.

In order to study the effect of the bead width on the hardness variation, different curves have been plotted. Comparison has been made between similar specimens which differ only in bead widths, (A1 and A2,

A3 and A4, A5 and A6, A7 and A8). The hardness variation measured at the depth of 0.5 mm from the specimen surface. The results of these comparisons are shown in Figs. 75 to 78.

3.1.4 TENSILE TESTING RESULTS

As described in section 2.4.3, after the specimens have been welded, these have been machined to produce standard tensile testing specimens. These tests have been carried out for the above three conditions, before applying any kind of heat treatment and after heat treatment (1) and (2).

This testing has been done to determine the ultimate tensile strength for both types of specimens, (build-up welding specimens and crack repair specimens).

The results reveal that the magnitude of the ultimate tensile strength, for the first type of specimens (build-up welding specimen), before applying any kind of heat treatment is between 686 and 762 N/mm^2. After heat treatment (1), the ultimate tensile tensile strength is between 686 and 756 N/mm^2. After heat

treatment (2), the ultimate tensile strength decreases to the range of 649 - 706 N/mm^2. These results are shown in Table 3.

In the second type of specimens (crack repair specimen). The ultimate tensile strength, before applying any kind of heat treatment is between 728 and 732 N/mm^2. After heat treatment (1), it becomes between 733 and 735 N/mm^2. After heat treatment (2), the ultimate tensile strength reduces to the range of 678 - 683 N/mm^2. These results are shown in Table 4.

In this testing, all the specimens were loaded to fracture and the fracture has occured outside the welding zone. Moreover, there is no significant reduction in the area of the section in or near the welding zone.

This area extends to about 20 mm for specimens A1, A3, A5, and A7; to about 30 mm for specimens A2, A4, A6, and A8; and to about 10 mm for specimens B1 and B2. Plate 17 shows a photograph of two different specimens, after they have been fractured.

3.2 THE MAGNITUDE AND DISTRIBUTION OF RESIDUAL STRESSES

3.2.1 INTRODUCTION

Stress relaxation technique has been used to determine the magnitude and the distribution of the residual stress in both types of specimens (build-up welding specimens, and crack repair specimens).

The strain gauges have been mounted on three different positions on the specimen's surface along X axis as shown in Fig. 79 which shows a sketch illustrating the positions of strain gauges on the specimen's surface.

Some difficulties have been experienced in attaching the gauges due to the small surface of the specimen around the welding zone. For this reason, the testings have been made for only those specimens which have narrow welding zone (A1, A3, A5, A7, B1, and B2).

To determine the strain in different orientations, strain gauge rosettes have been used and three different readings have been recorded from each

strain gauge rosette. After that, the residual stresses have been computed by using [stress, strain] formula given in the next section.

3.2.2 COMPUTING THE RESIDUAL STRESSES

From the theoretical approach [41], stress at specimen's surface cannot act perpendicular to the surface plane, so that effectively the gauge is measuring a two dimensional strain system. The stresses in the X and Y directions can be expressed [42] as follows:

$$\sigma_x = \frac{E}{1 - v^2} (\epsilon_x + v.\epsilon_y)$$

$$\sigma_y = \frac{E}{1 - v^2} (\epsilon_y + v.\epsilon_x) \quad \} \quad (1)$$

Where:

σ_x = The stress in X direction.

σ_y = The stress in Y direction.

ϵ_x = The strain in X direction.

ϵ_y = The strain in Y direction.

E = The elastic modulus.

v = Poisson's ratio.

Often the directions of the principal stresses are not known in the practical measurement situation, so that it it advantageous to have expressions for the principal strains that refer to arbitrarily positioned axes as used in equation (2):

$$\epsilon_\alpha = \epsilon_x.\cos^2\alpha + \epsilon_y.\sin^2\alpha + \Gamma_{xy}.\sin\alpha.\cos\alpha \qquad (2)$$

The equation defines the strain ϵ_α at a point, where α is the angle that the strain makes with the X axis in arbitrary X - Y axes, and Γ_{xy} is the shearing strain present at the point (see Fig. 80). The strain $\epsilon\alpha$ can be measured at three different angles to obtain three values for $\epsilon\alpha$. Thus, three equations can be solved simultaneously to give ϵ_x, ϵ_y, and Γ_{xy}.

In this work, the measurements have been carried out by employing strain gauge rosettes, which give three values ϵ_1, ϵ_2, and ϵ_3 to three different directions. Fig. 79 shows the three different directions of the strain gauges.

ϵ_1 is measured by gauge 1 at $\alpha = 0°$

ϵ_2 is measured by gauge 2 at $\alpha = 45°$

ϵ_3 is measured by gauge 3 at $\alpha = -45°$

These measured levels can be substituted into equation (2) to give ϵ_x, ϵ_y and their direction referred to arbitrary axes, and Γ_{xy} in terms of measured levels so that

$$\epsilon_1 = \epsilon_x \cos^2(0°) + \epsilon_y \sin^2(0°) + \Gamma_{xy} \sin(0°)\cos(0°)$$

$$\epsilon_2 = \epsilon_x \cos^2(45°) + \epsilon_y \sin^2(45°) + \Gamma_{xy} \sin(45°)\cos(45°) \quad (3)$$

$$\epsilon_3 = \epsilon_x \cos^2(-45°) + \epsilon_y \sin^2(-45°) + \Gamma_{xy} \sin(-45°)\cos(-45°)$$

Further, to determine the principal strains (ϵ_{max} and ϵ_{min}) and the principal stresses (σ_{max} and σ_{min}). The principal strains can be determined by substituting (ϵ_x, ϵ_y, and Γ_{xy}) in the following equation:

$$\epsilon_{max} = \epsilon_x \cos^2\alpha_p + \epsilon_y \sin^2\alpha_p + \Gamma_{xy} \sin\alpha_p \cos\alpha_p \quad (4)$$

$$\epsilon_{min} = \epsilon_x \cos^2\alpha_{p1} + \epsilon_y \sin^2\alpha_{p1} + \Gamma_{xy} \sin\alpha_{p1} \cos\alpha_{p1}$$

Where:

α_p = the angle that the principal planes make with arbitrary axes, and $\alpha_{pl} = \alpha_p +- 90°$. This angle can be determined by the following equation:

$$\tan 2\alpha_p = \frac{\Gamma_{xy}}{\epsilon_x - \epsilon_y} \qquad (5)$$

The principal stresses can be determined by substituting ϵ_{max} and ϵ_{min} in the following equation:

$$\sigma_{max} = \frac{E}{1 - v^2} (\epsilon_{max} + v.\epsilon_{min})$$

$$\sigma_{min} = \frac{E}{1 - v^2} (\epsilon_{min} + v.\epsilon_{max}) \qquad (6)$$

3.2.3 THE RESULTS

As described above, three readings (ϵ_1, ϵ_2, ϵ_3) are obtained from each strain gauge rosette. Then the magnitudes of σ_x and σ_y, and the principal stresses have been computed at this location by using the above equations.

As mentioned before, three points have been tested to determine the distribution of the residual stresses along the X axis. Before demonstrating all the results an example will be described to show how the results have been computed.

In this example the residual stresses have been measured for specimen A3, at point 1, see Fig. 79. The results were as follows:

ϵ_1 = 292 microstrain.

ϵ_2 = 173 microstrain.

ϵ_3 = 247 microstrain.

By substituting these values in equation (3):

ϵ_x = 292 microstrain.

ϵ_y = 128 microstrain.

Γ_{xy} = 74 microstrain.

By substituting ϵ_x and ϵ_y in equation (1):

σ_x = 71.146 N/mm^2.

σ_y = 45.521 N/mm^2.

By substituting ϵ_x, ϵ_y, and Γ_{xy} in equation (5):

α_p = 9.3 °

By substituting ϵ_x, ϵ_y, Γ_{xy}, and α_p in equation (4):

ϵ_{max} = 289.3 microstrain.

ϵ_{min} = 120.4 microstrain.

Finally, by substituting ϵ_{max} and ϵ_{min} in equation (6):

$$\sigma_{max} = 72 \text{ N/mm}^2$$

$$\sigma_{min} = 44.2 \text{ N/mm}^2$$

Fig. 81 shows a diagram for the distribution of the residual stress σ_x along X axis, for specimen A3. This figure shows that at about 25 mm from the central axis of the welded zone, there is negligible residual stress. At a distance of 10 mm residual stress of 71 N/mm^2 is obtained in the X direction.

Fig. 82 shows a diagram for the distribution of the residual stress σ_y along X axis, for specimen A3. Similar trend is observed as in Fig. 81.

Fig. 83 shows a diagram for the distribution of the principal residual stresses σ_{max} and σ_{min} along X axis, for specimen A3. this figure shows a similar results which obtained in Figs. 81 and 82.

Figs. 84 and 85 show diagrams for the distribution of the residual stresses σ_x and σ_y along X axis, for specimen B1 and again the maximum magnitude of the residual stress in the X direction was obtained to be about 70 N/mm^2. Outside the 25 mm distance the residual stress was negligible.

Fig. 86 shows a diagram for the distribution of the principal residual stresses σ_{max} and σ_{min} along X axis, for specimen B1. Similar trend is obtained in Figs 84 and 85.

Due to the small size of the specimens and the high cost of the strain gauge rosette, a single strain gauge has been used instead of the strain gauge rosette to measure the residual strain in one direction only to make comparison between different specimens which have different variables.

In this situation $\epsilon_1 = \epsilon_x$ and the distribution of this parameter along the X axis has been compared for different specimens. Diagrams have been plotted to

illustrate these results, for specimens A1, A3, A5, A7, B1, and B2. Those diagrams are shown in Fig. 87 to 92.

Different curves have been plotted in Figs. 93 and 94 which represent a comparison between the above results, for specimens A1, A3, A5, and A7 (Fig. 93), and for specimens B1 and B2 (Fig. 94).

Specimen No	L [m.m]	W [m.m]	T [m.m]	D [m.m]
A1	20	10	3	1.5
A2	20	20	3	1.5
A3	40	10	3	1.5
A4	40	20	3	1.5
A5	20	10	6	3
A6	20	20	6	3
A7	40	10	6	3
A8	40	20	6	3

Table. 1 The different dimensions for build-up welding specimen.

Specimen No	T [m.m]
B1	3
B2	5

Table. 2 The different thickness for crack repairing specimen.

Specimen	Tensile strength [N/mm²]		
	before heat treatment	after heat treatment (1)	after heat treatment(2)
A1	686	688	657
A2	689	686	652
A3	694	695	653
A4	696	700	649
A5	709	724	688
A6	725	747	698
A7	739	751	713
A8	762	756	706

Tabel. 3 shows the tensile testing results for build-up welding specimen.

Specimen	Tensile Strength [N/mm²]		
	before heat treatment	after heat treatment (1)	after heat treatment(2)
B1	732	735	683
B2	728	733	678

Tabel. 4 shows the tensile testing results for crack repair specimen.

PLATE 11 THE MICROSTRUCTURAL BEFORE HEAT TREATMENT, FOR A8 (x500)

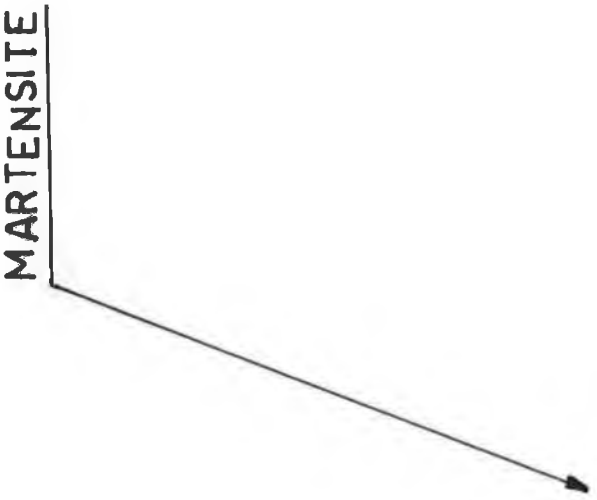

PLATE 12 THE MICROSTRUCTURAL BEFORE HEAT TREATMENT, FOR B2 (x500)

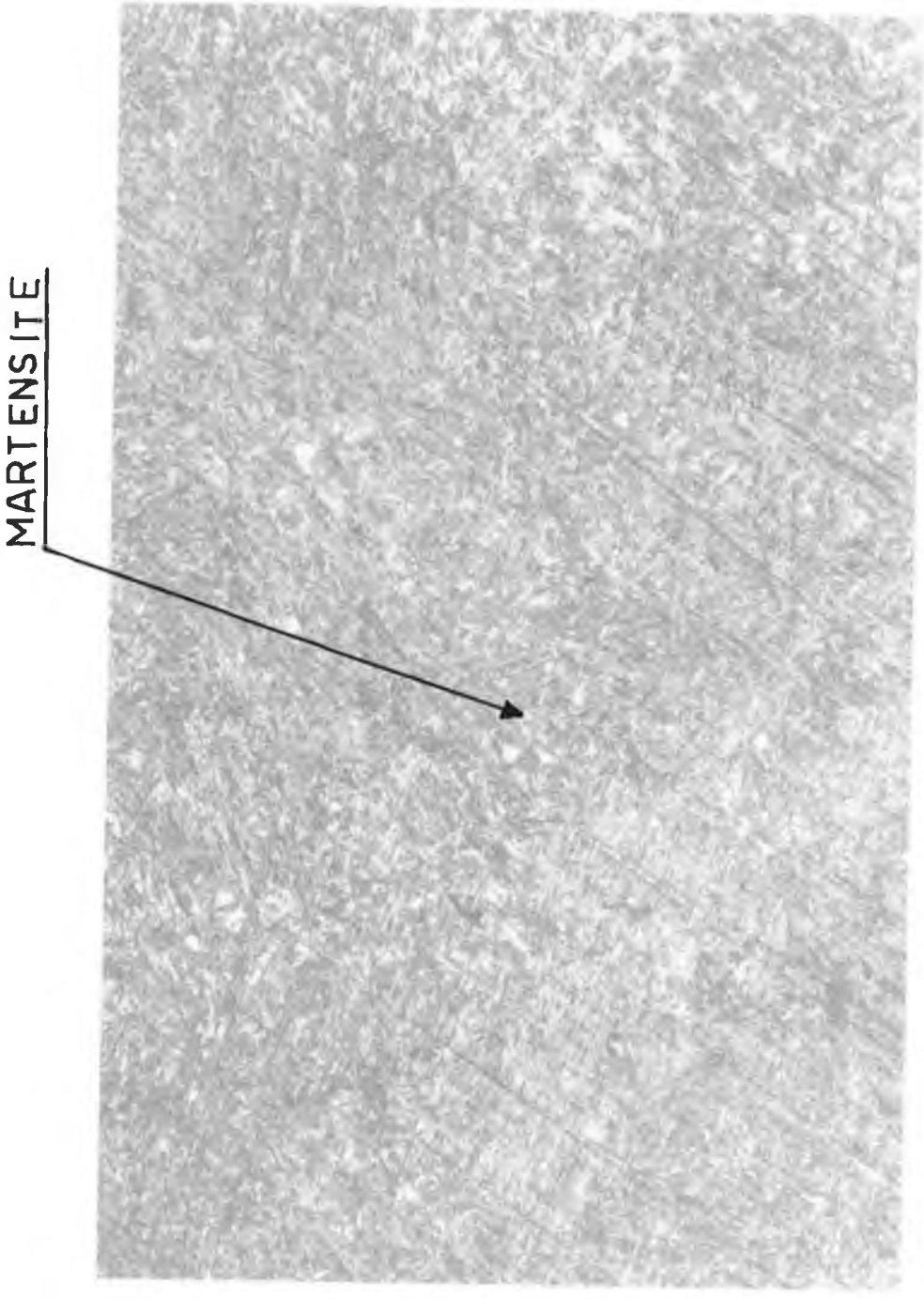

PLATE 13 THE MICROSTRUCTURAL AFTER HEAT TREATMENT(1), FOR A8 (x500)

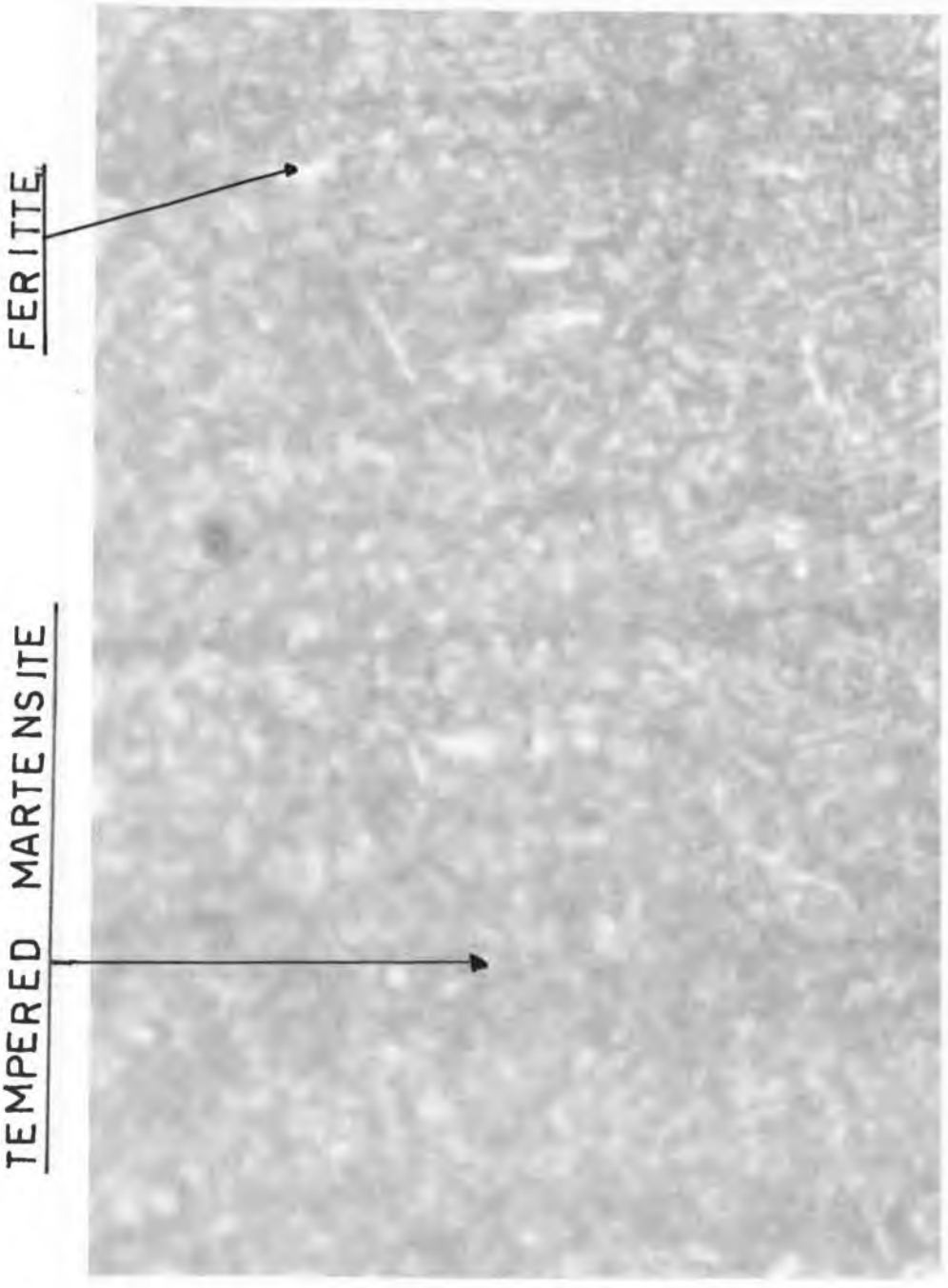

PLATE 14 THE MICROSTRUCTURAL AFTER HEAT TREATMENT(1), FOR B2 (x500)

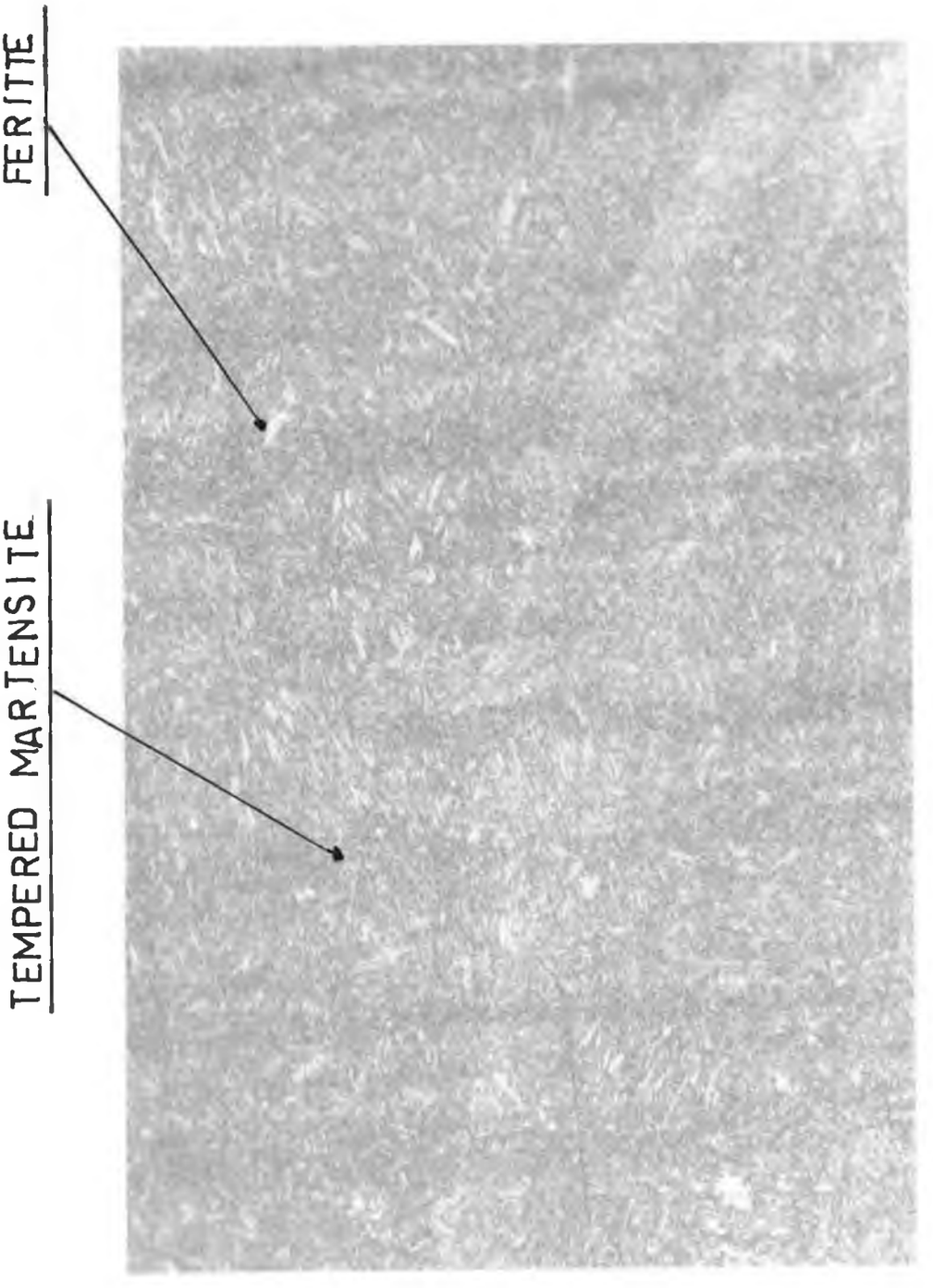

TEMPERED

PRECIPITATED CARBIDE

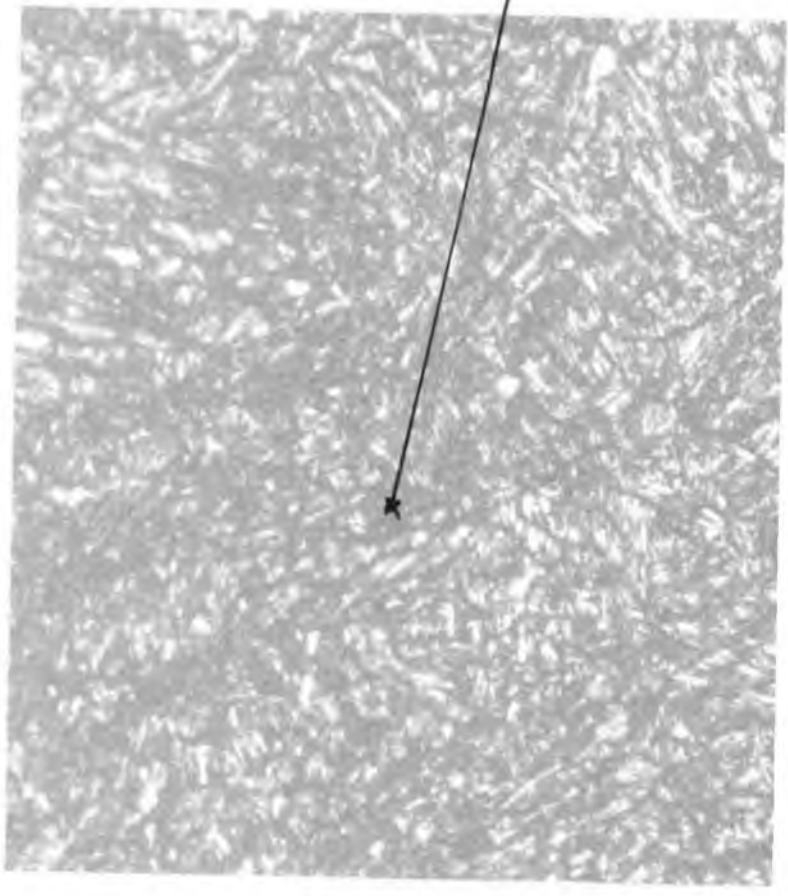

PLATE 15 THE MICROSTRUCTURAL AFTER HEAT TREATMENT(2), FOR A8 (x1000)

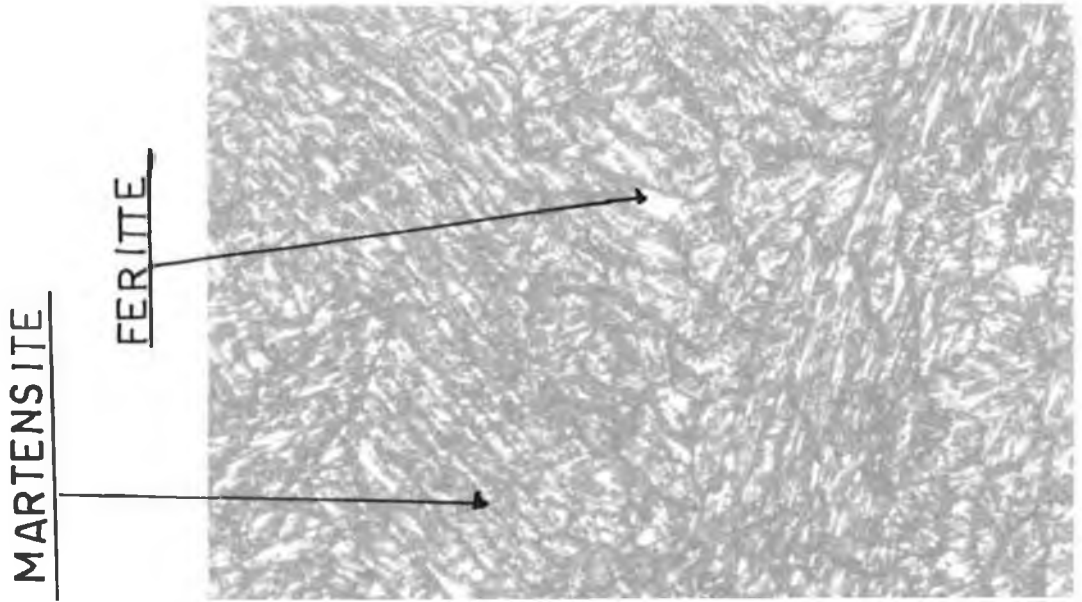

PLATE 16 THE MICROSTRUCTURAL AFTER HEAT TREATMENT(2), FOR B2 (x500)

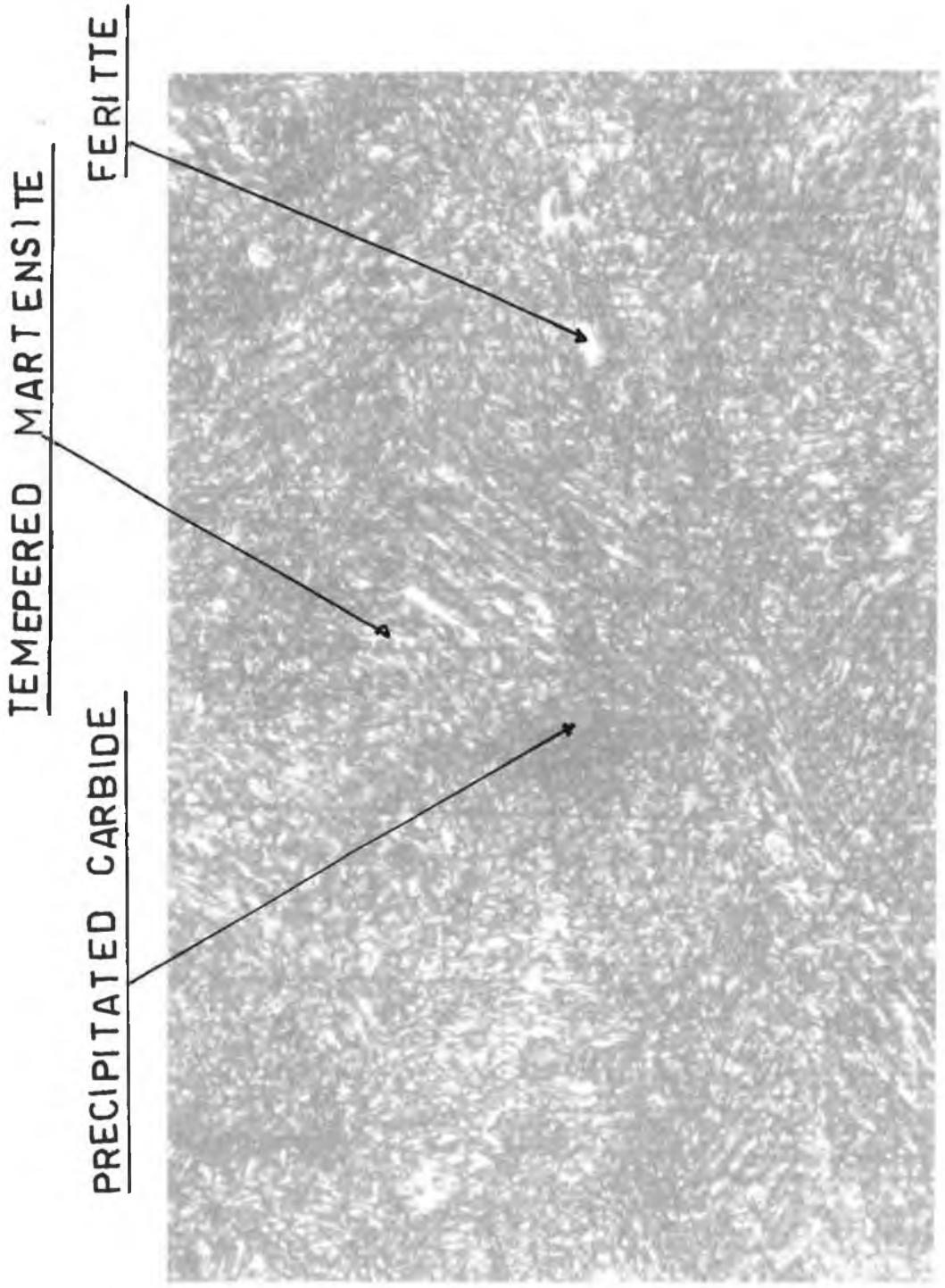

PLATE 17 TENSILE SPECIMEN

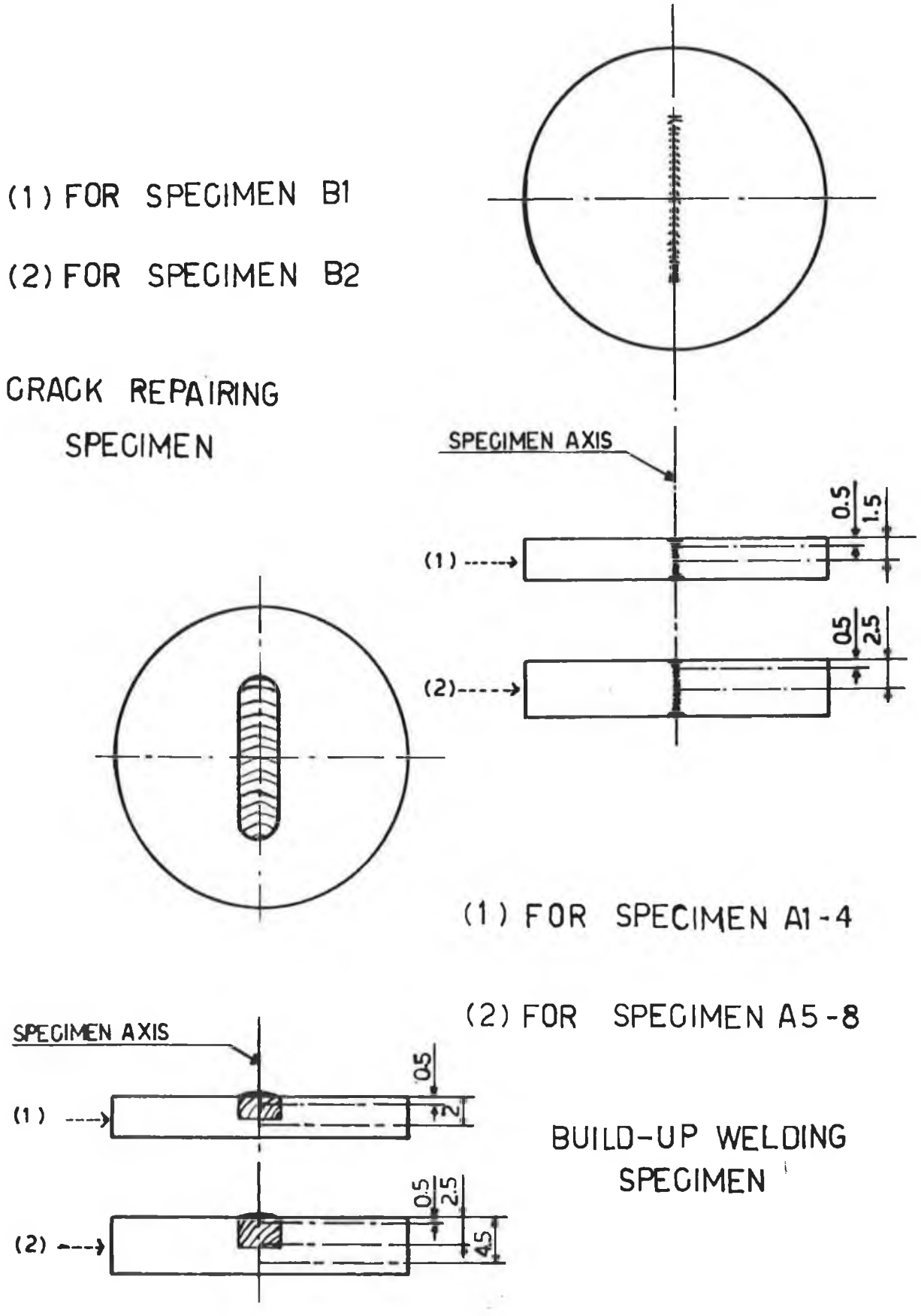

Fig. 21 Illustration sketch for the specimen's axis.

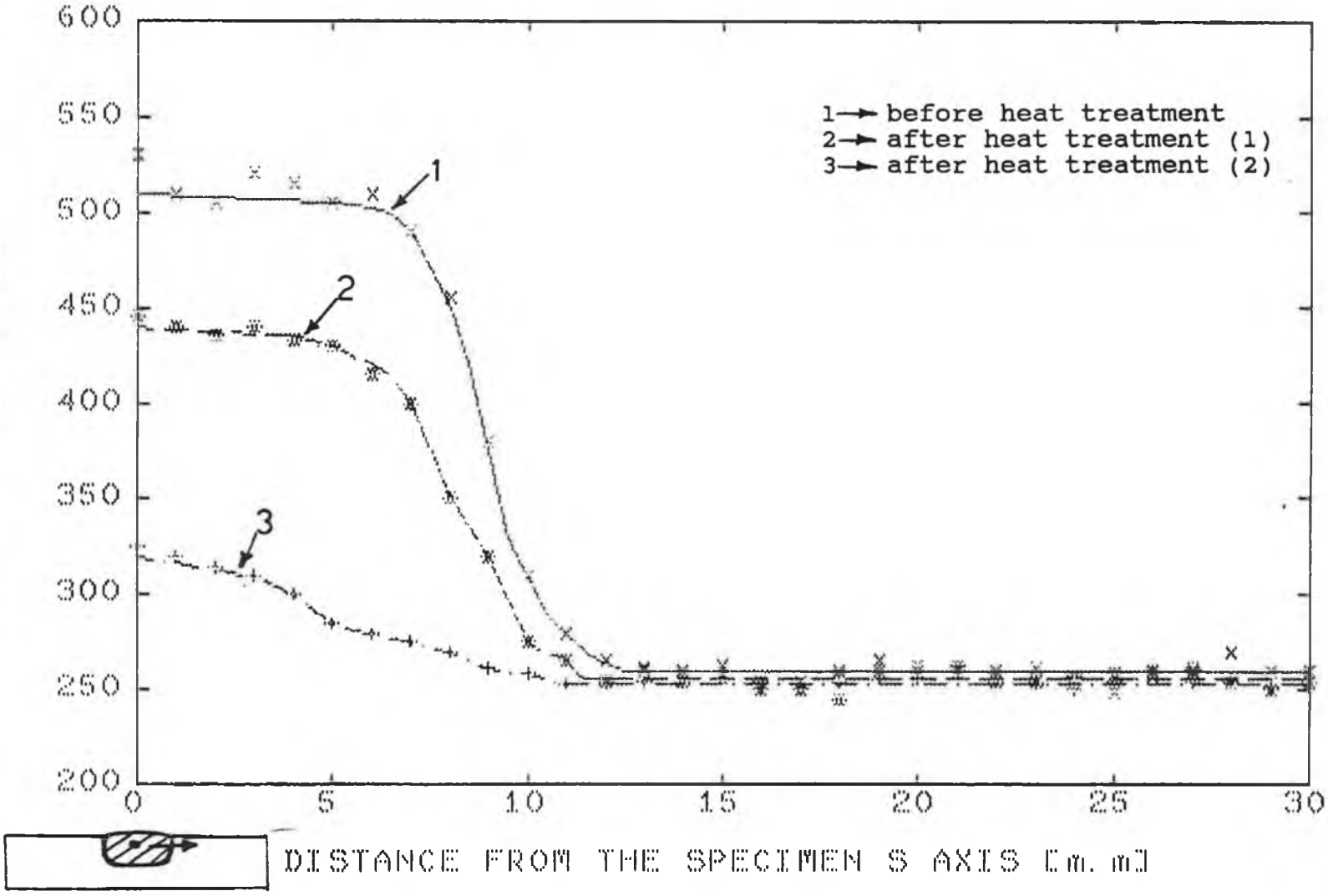

Fig. 22 The hardness variation across specimen A1, 0.5m.m from the surface.

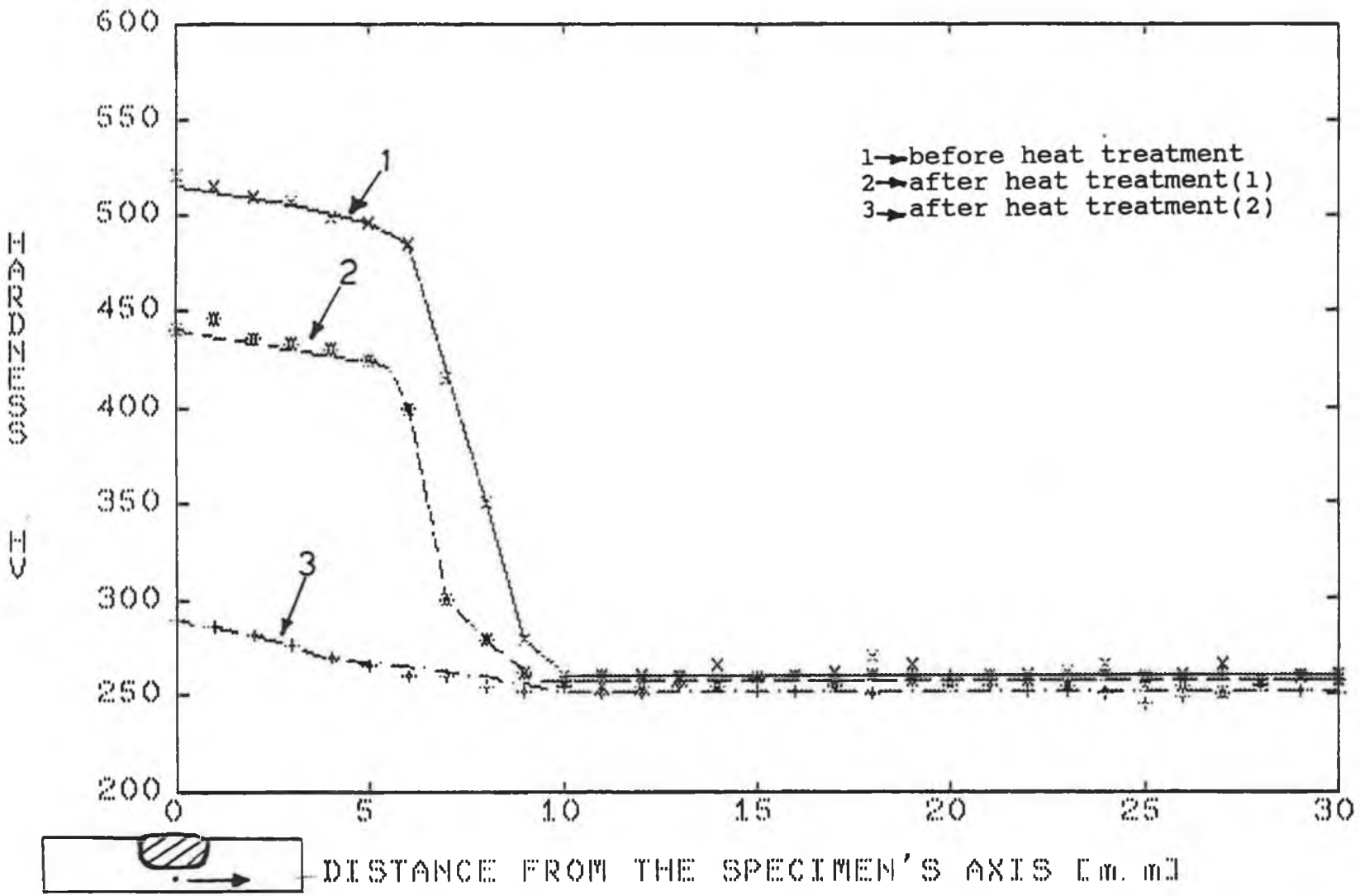

Fig. 23 The hardness variation across specimen A1, 2m.m from the surface.

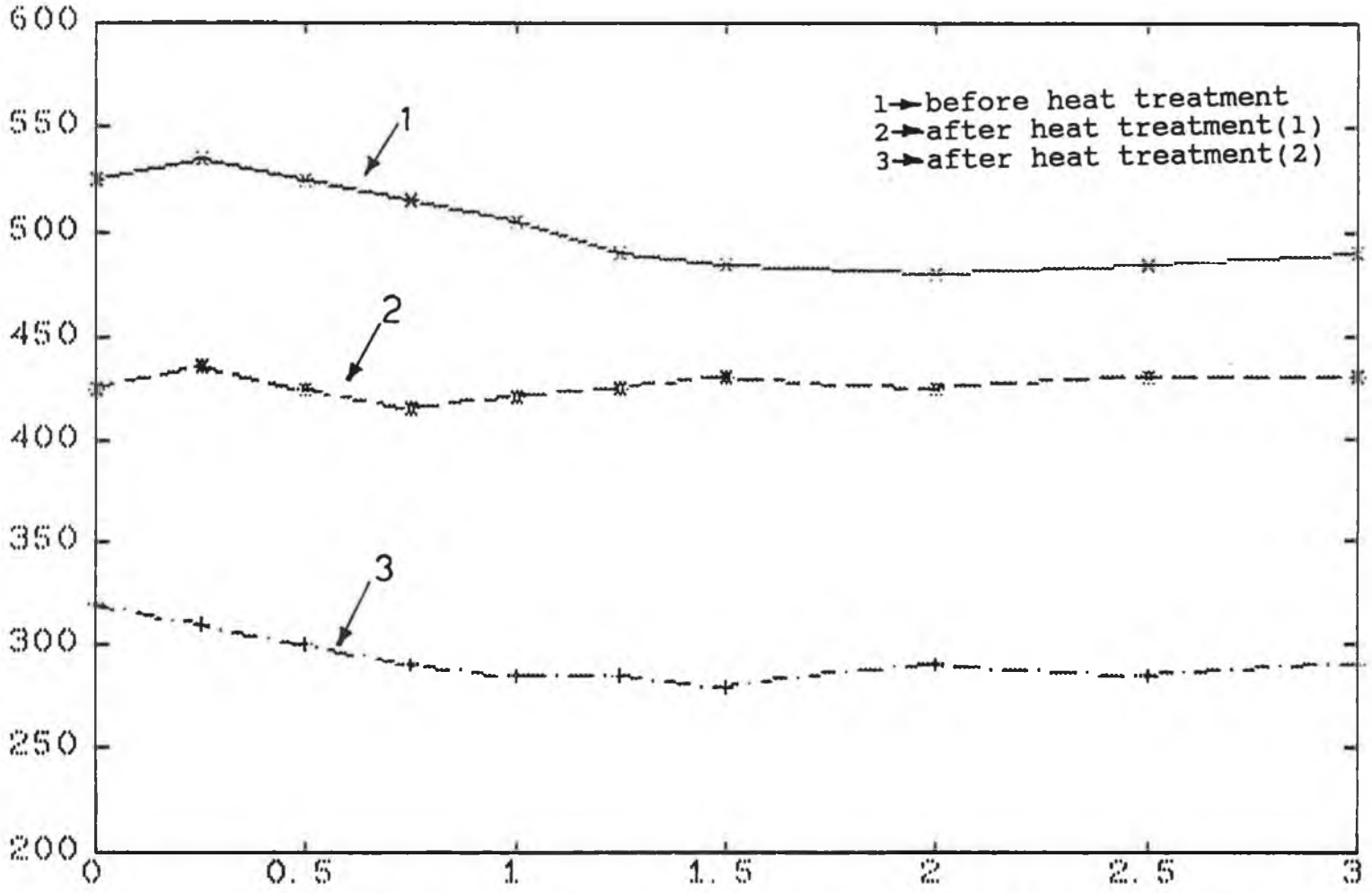

Fig. 24 The hardness variation along the specimen axis, for specimen A1.

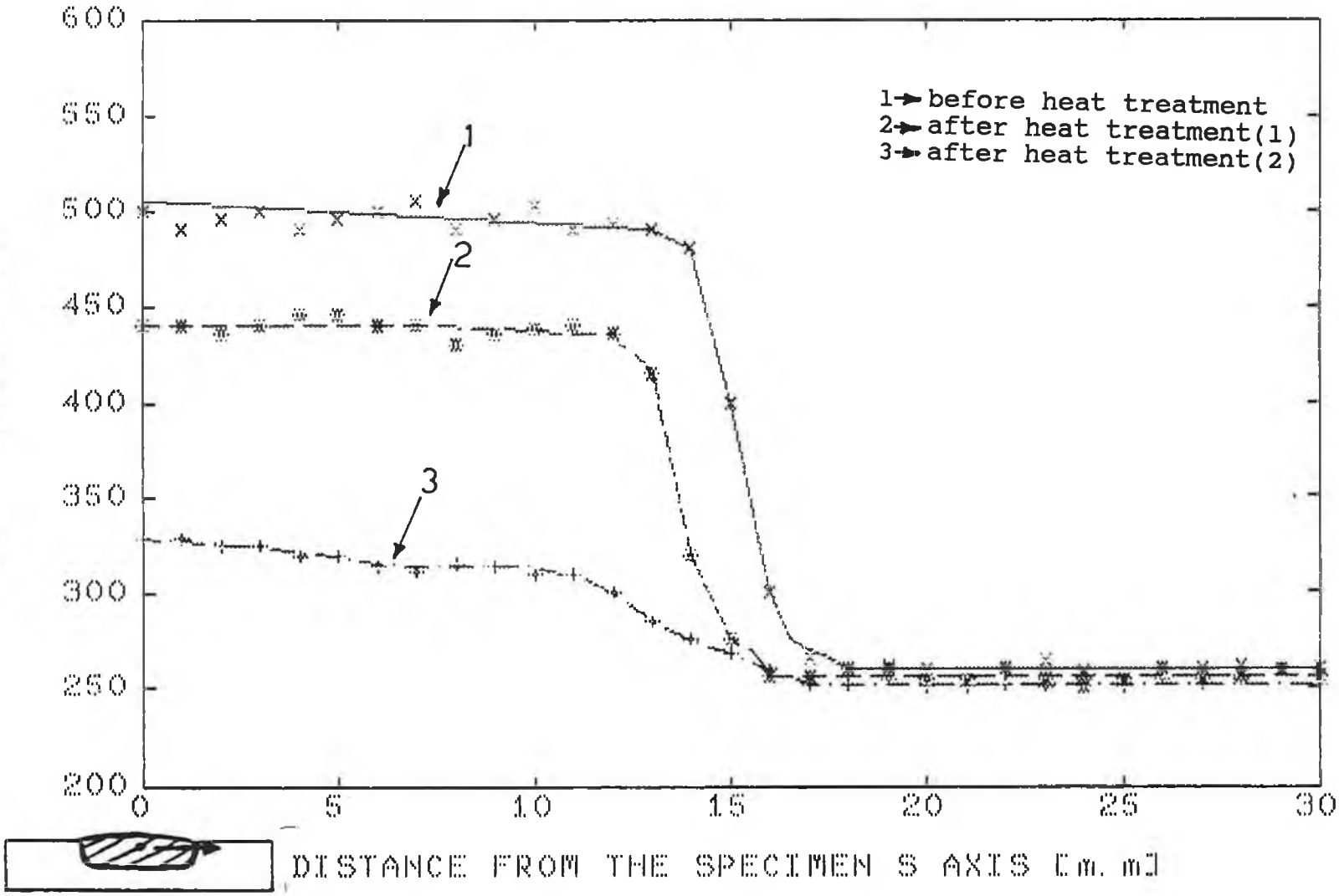

Fig. 25 The hardness variation across specimen A2, 0.5m.m from the surface.

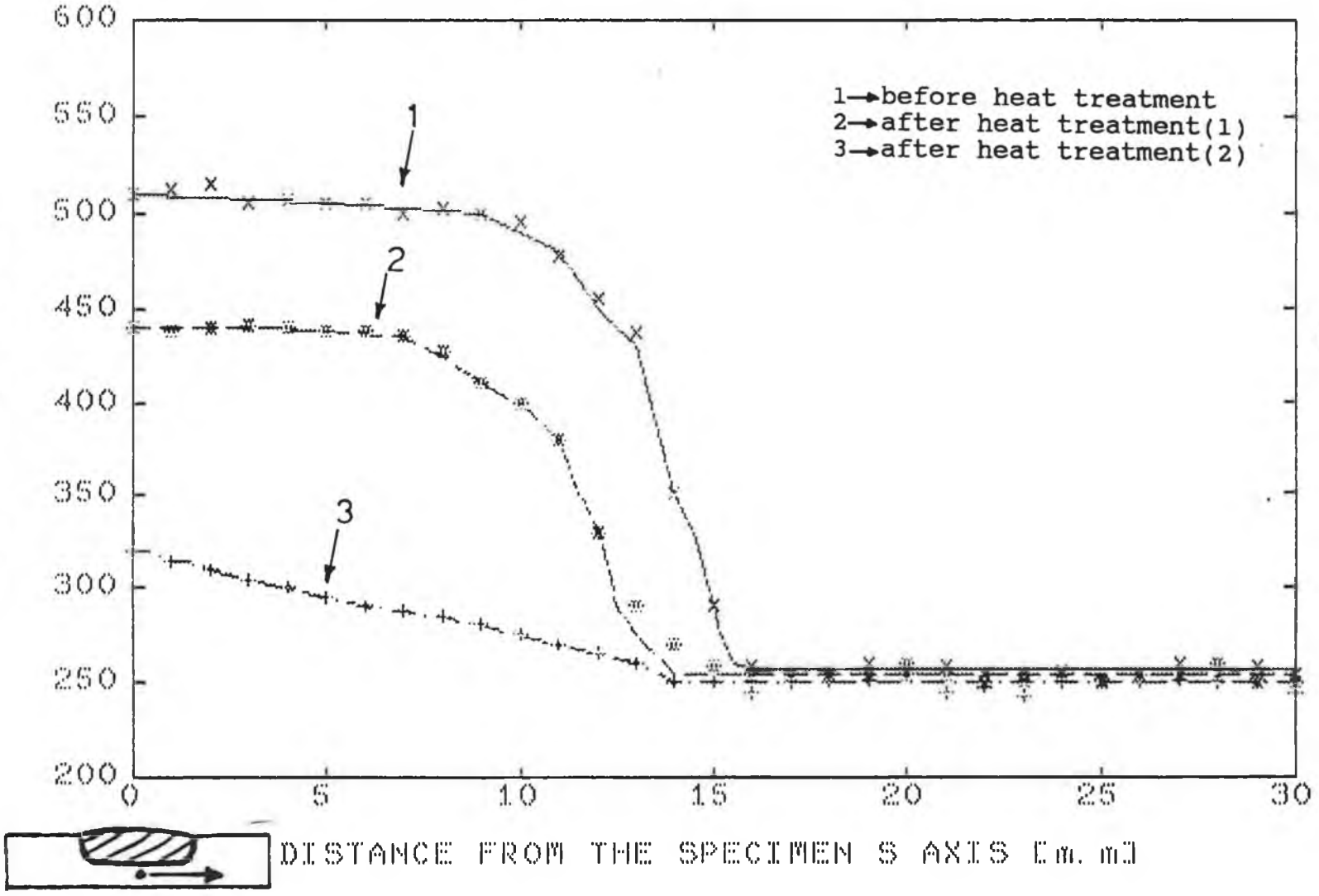

Fig. 26 The hardness variation across specimen A2, 2m.m from the surface.

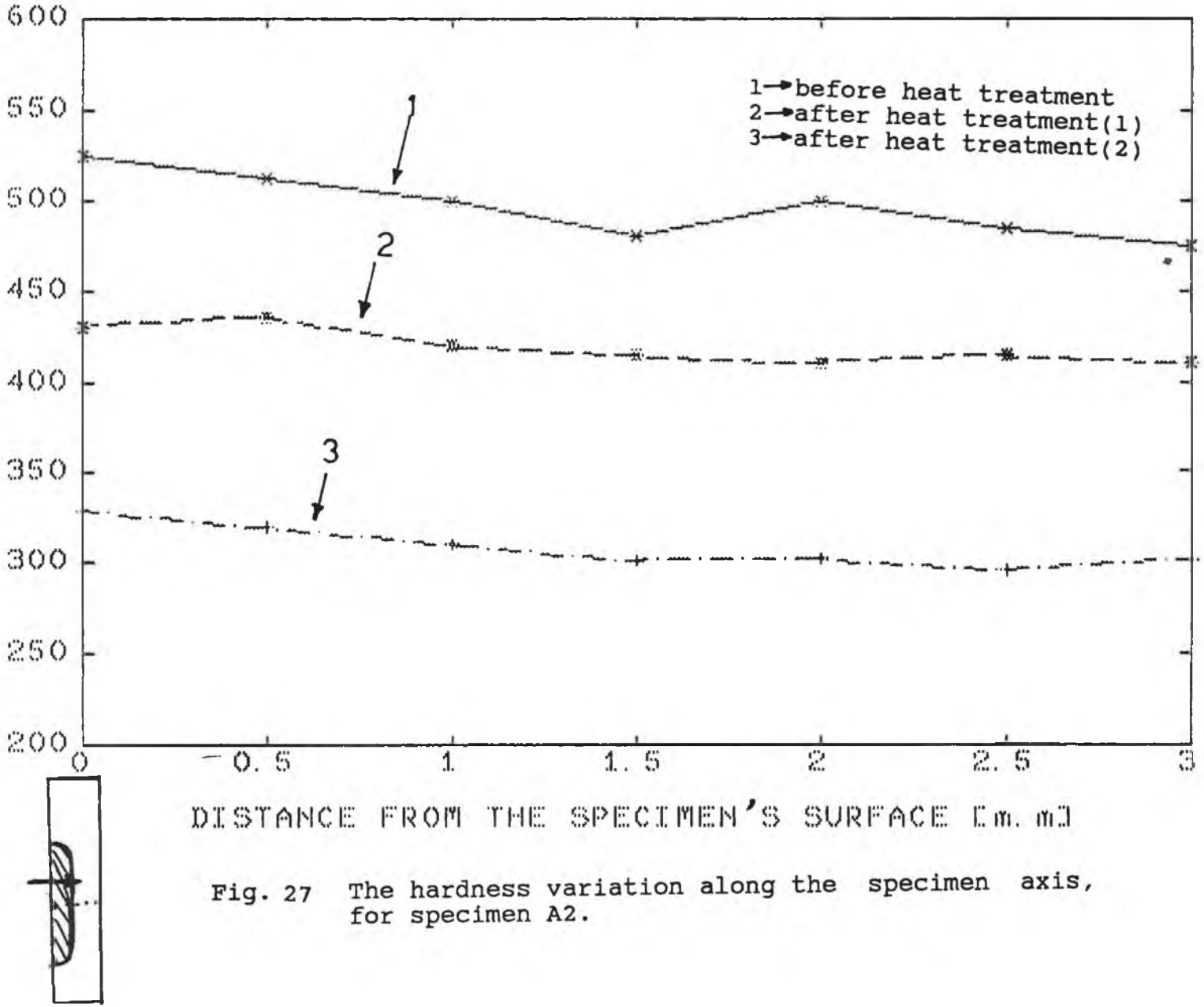

Fig. 27 The hardness variation along the specimen axis, for specimen A2.

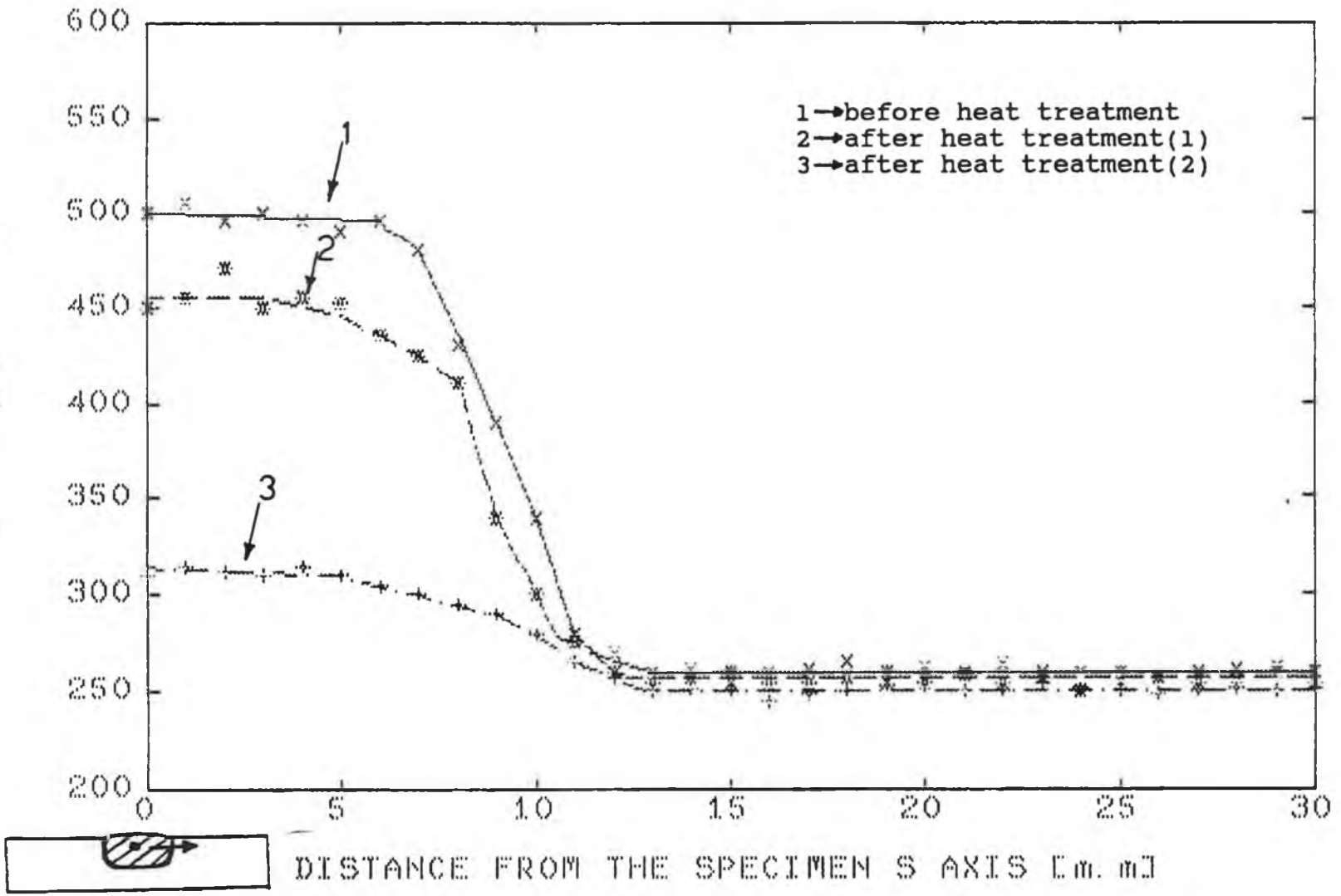

Fig. 28 The hardness variation across specimen A3, 0.5m.m from the surface.

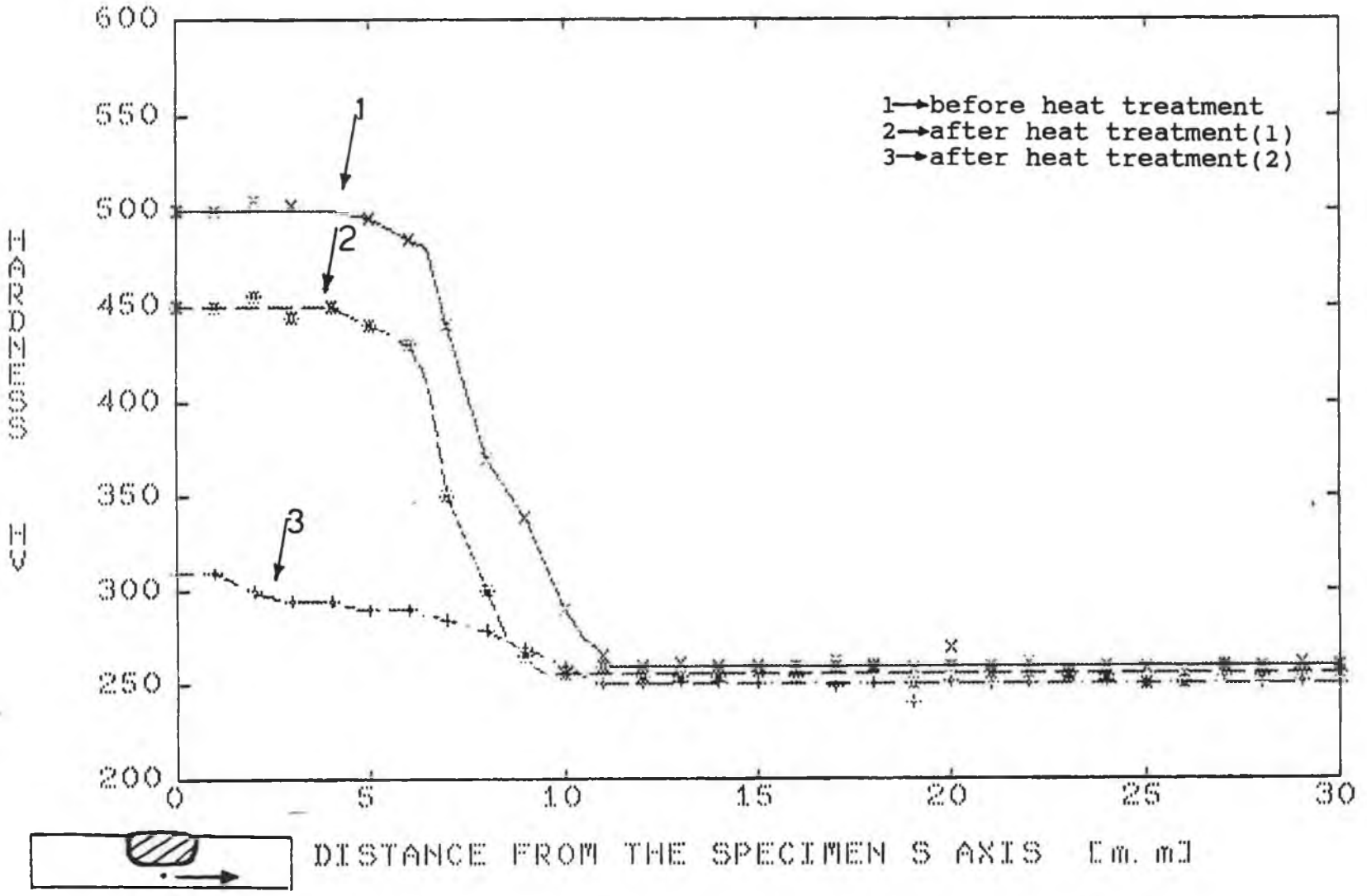

Fig. 29 The hardness variation across specimen A3, 2m.m from the surface.

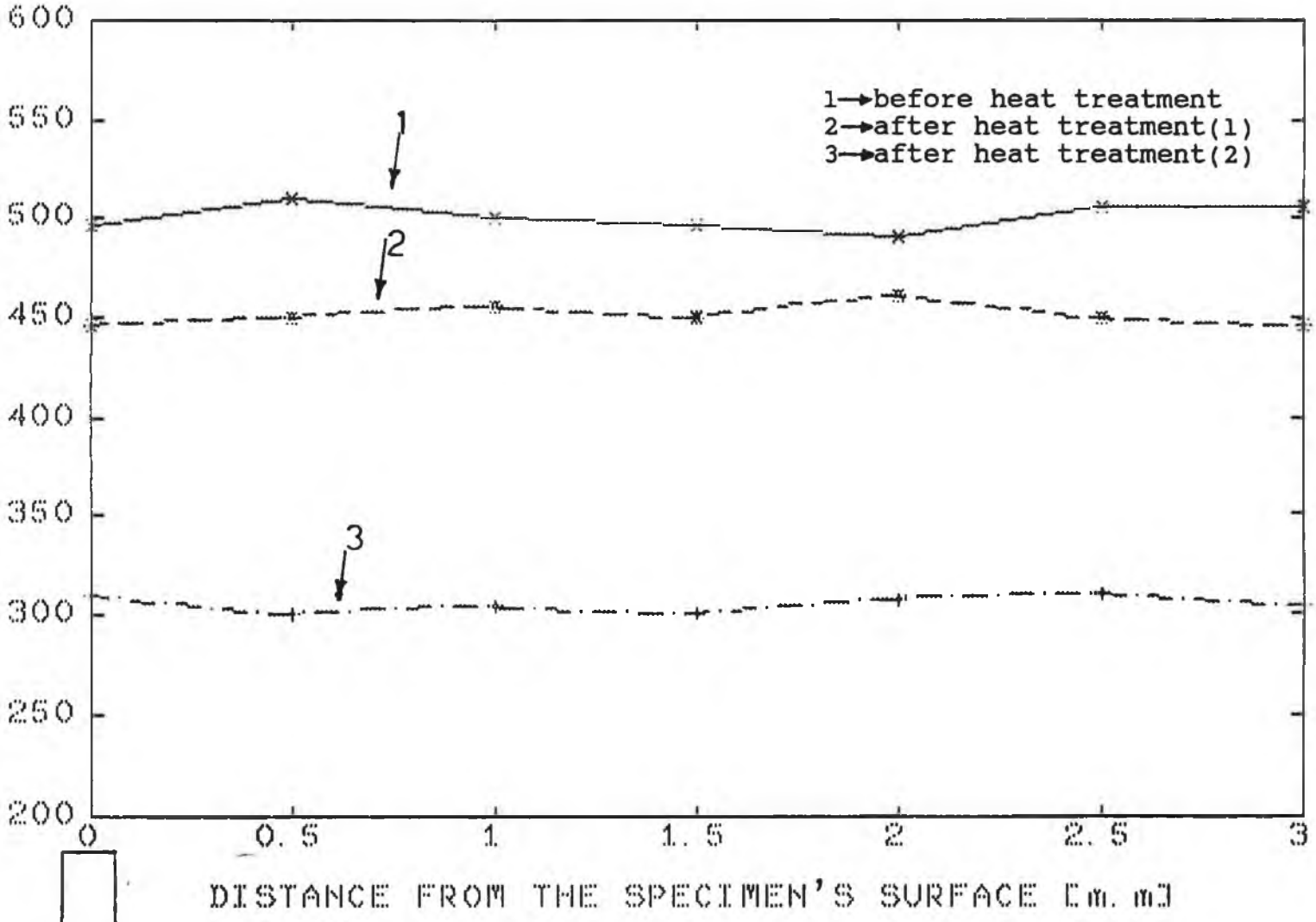

Fig. 30 The hardness variation along the specimen axis, for specimen A3.

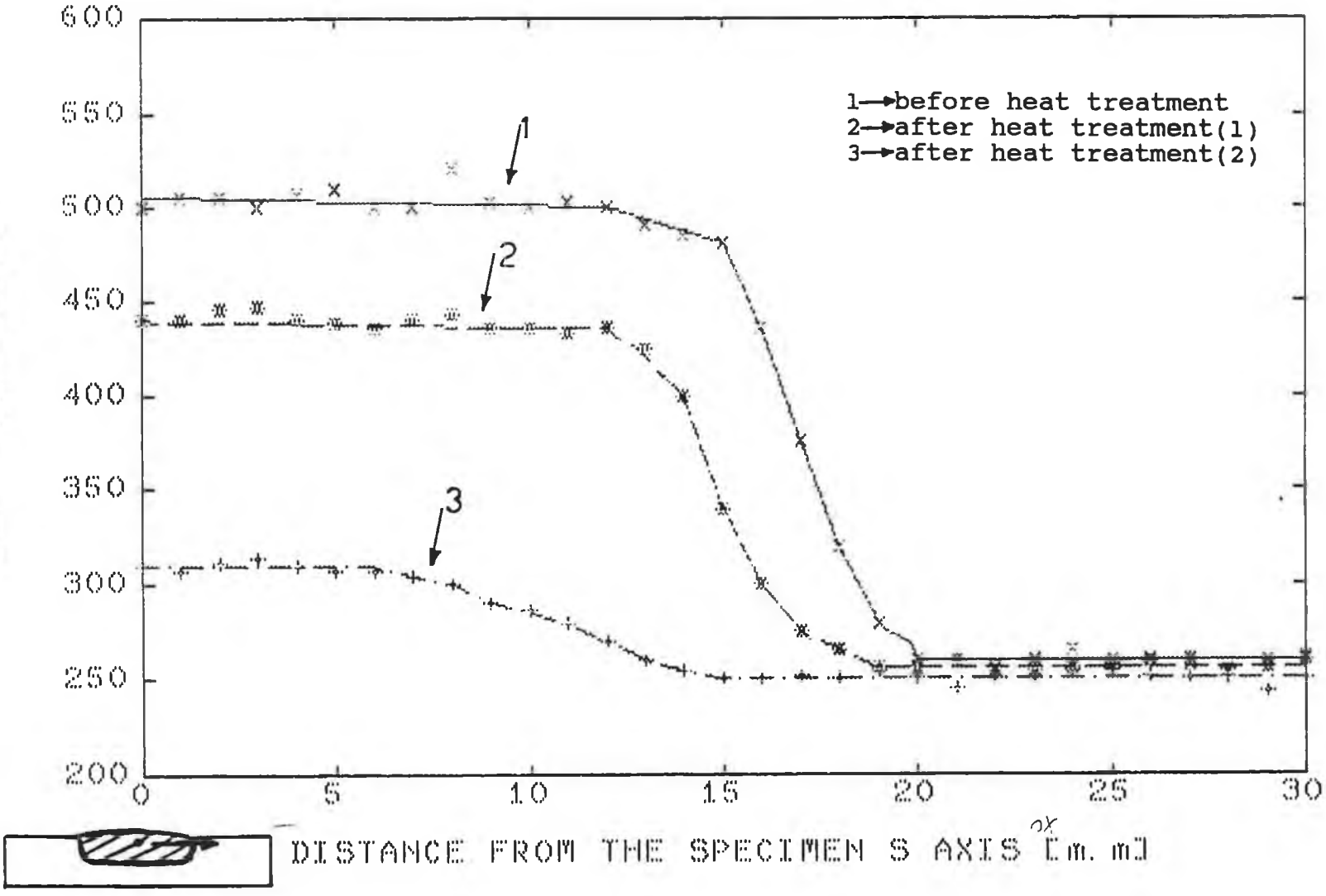

Fig. 31 The hardness variation across specimen A4, 0.5m.m from the surface.

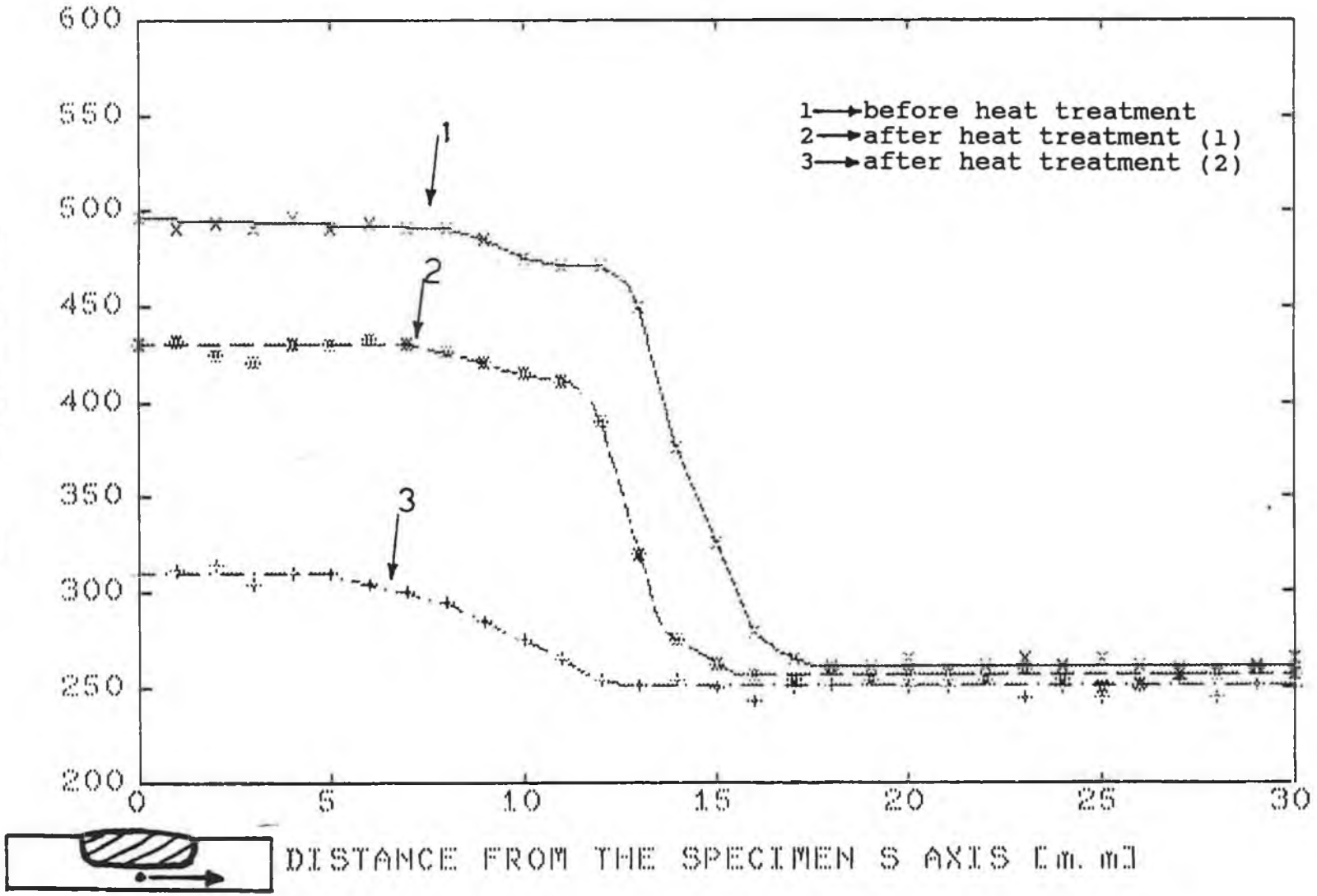

Fig. 32 The hardness variation across specimen A4, 2m.m from the surface.

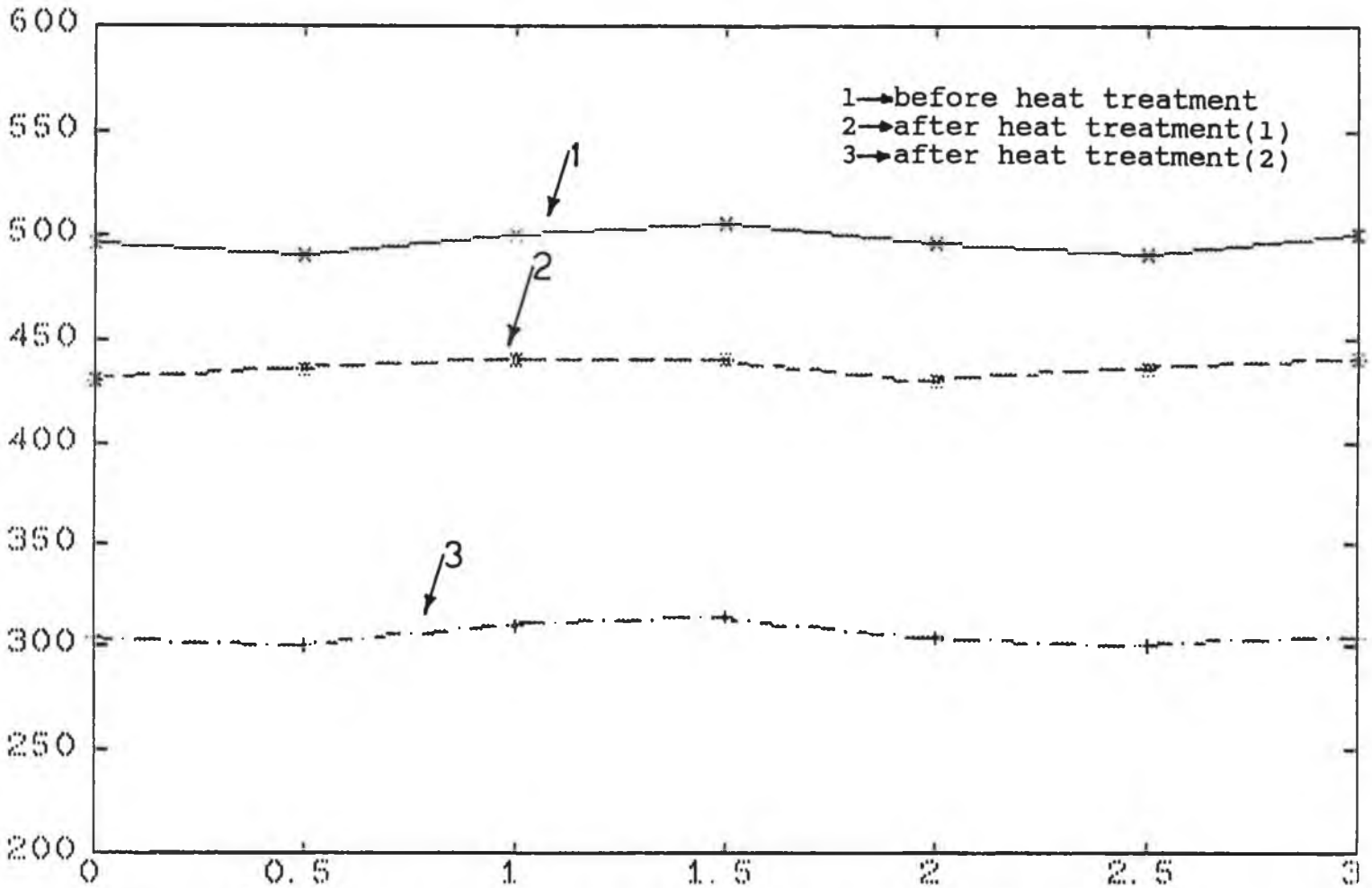

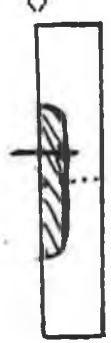

Fig. 33 The hardness variation along the specimen axis, for specimen A4.

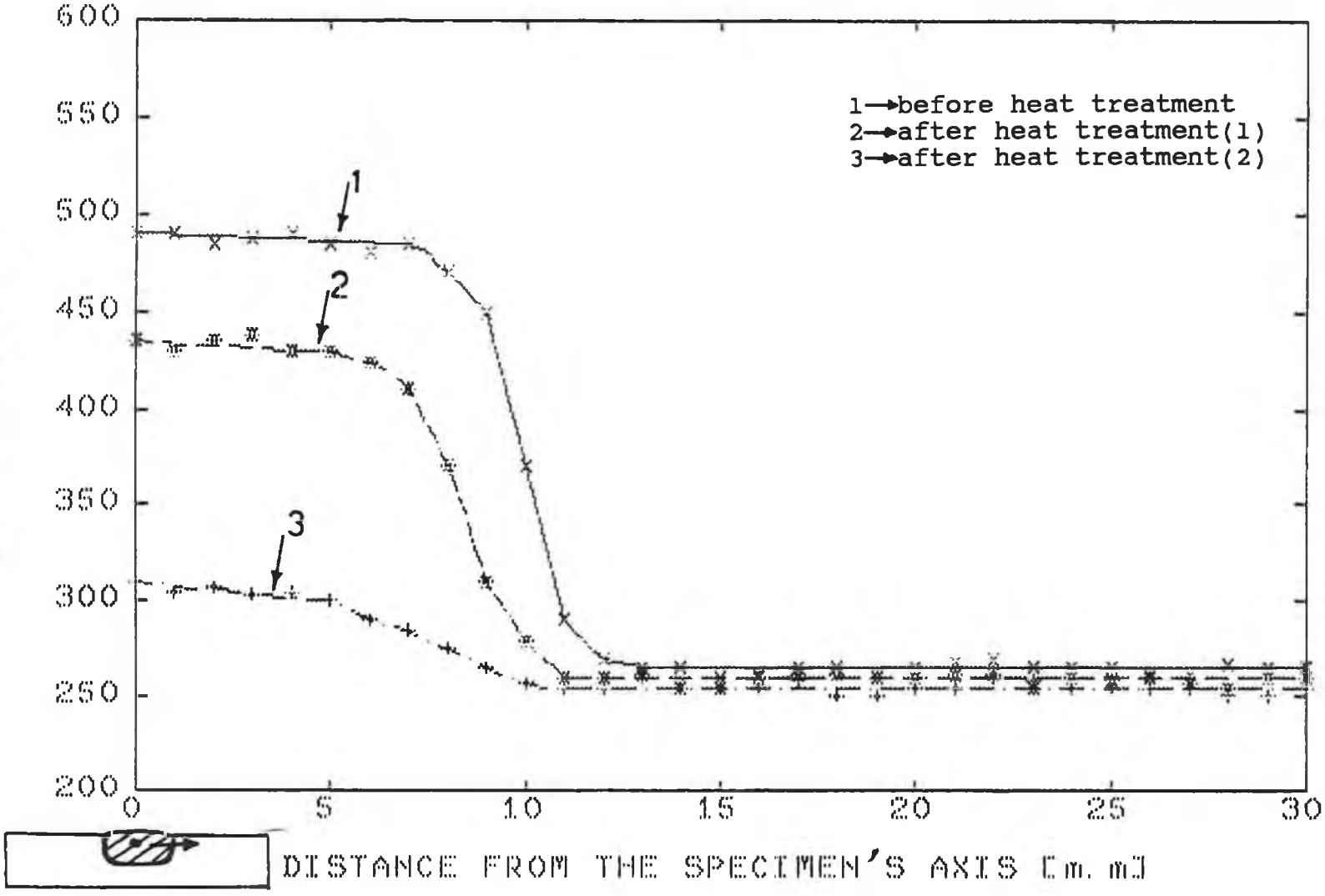

Fig. 34 The hardness variation across specimen A5, 0.5m.m from the surface.

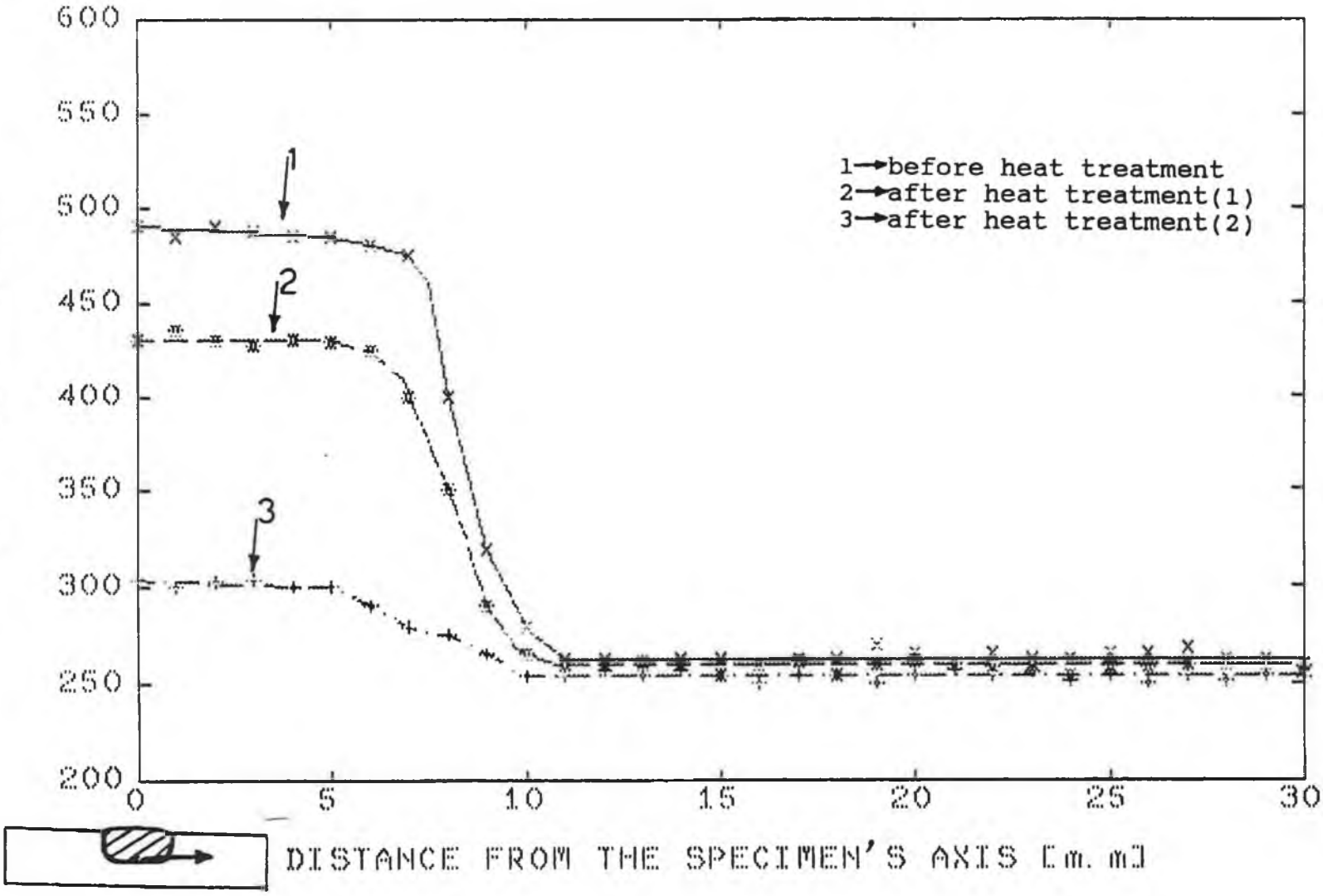

Fig. 35 The hardness variation across specimen A5, 2.5m.m from the surface.

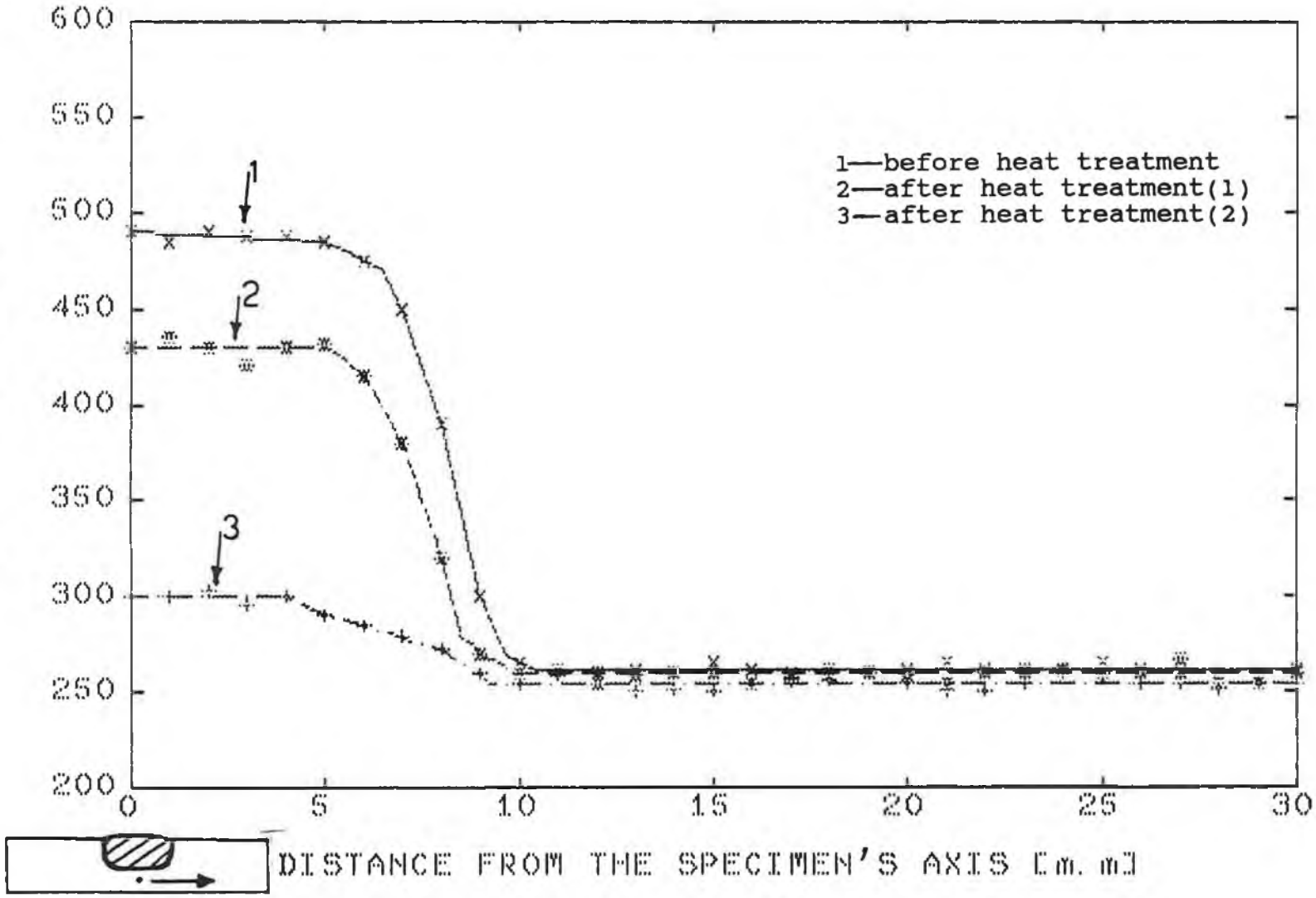

Fig. 36 The hardness variation across specimen A5, 4.5m.m from the surface.

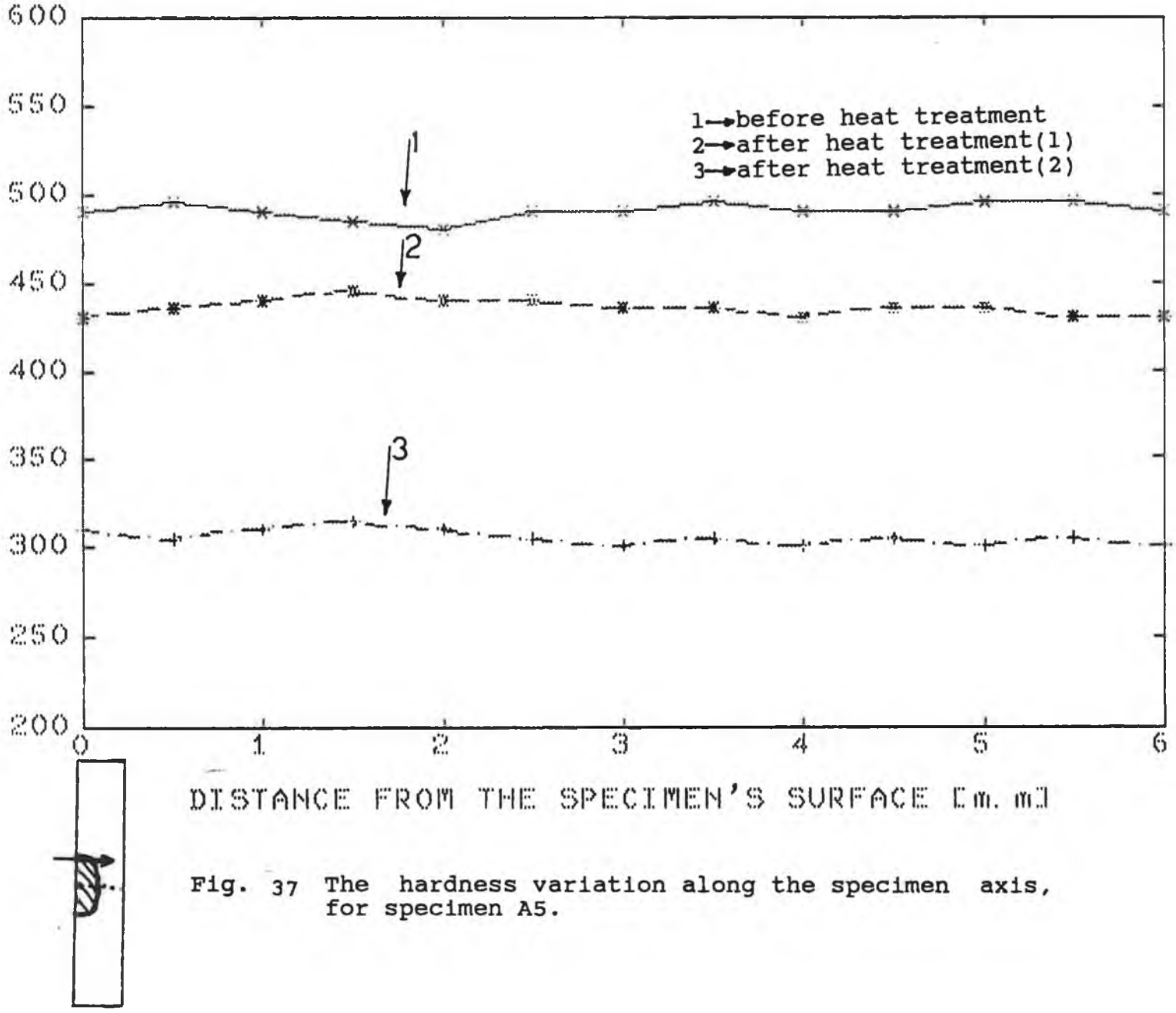

Fig. 37 The hardness variation along the specimen axis, for specimen A5.

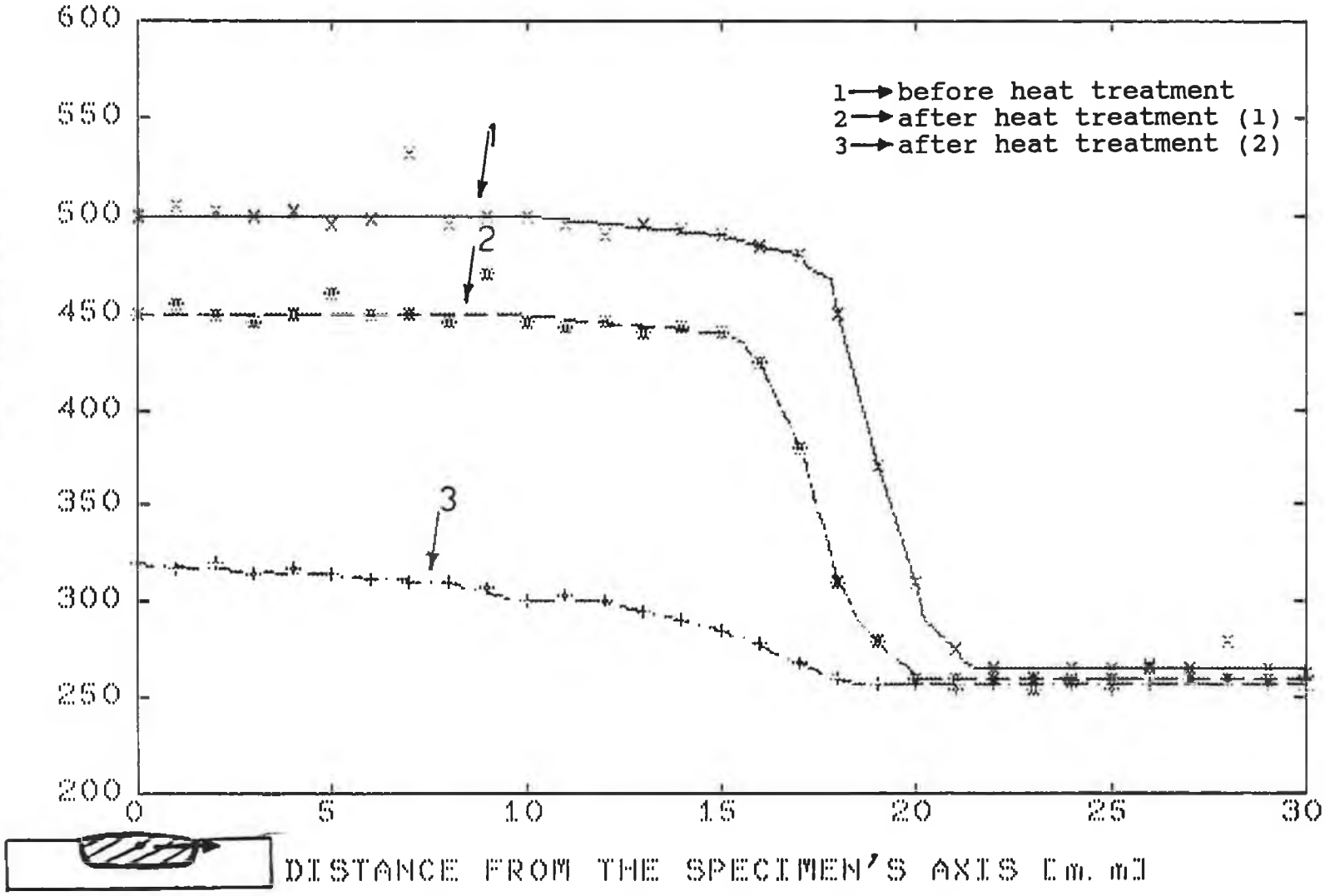

Fig. 38 The hardness variation across specimen A6, 0.5m.m from the surface.

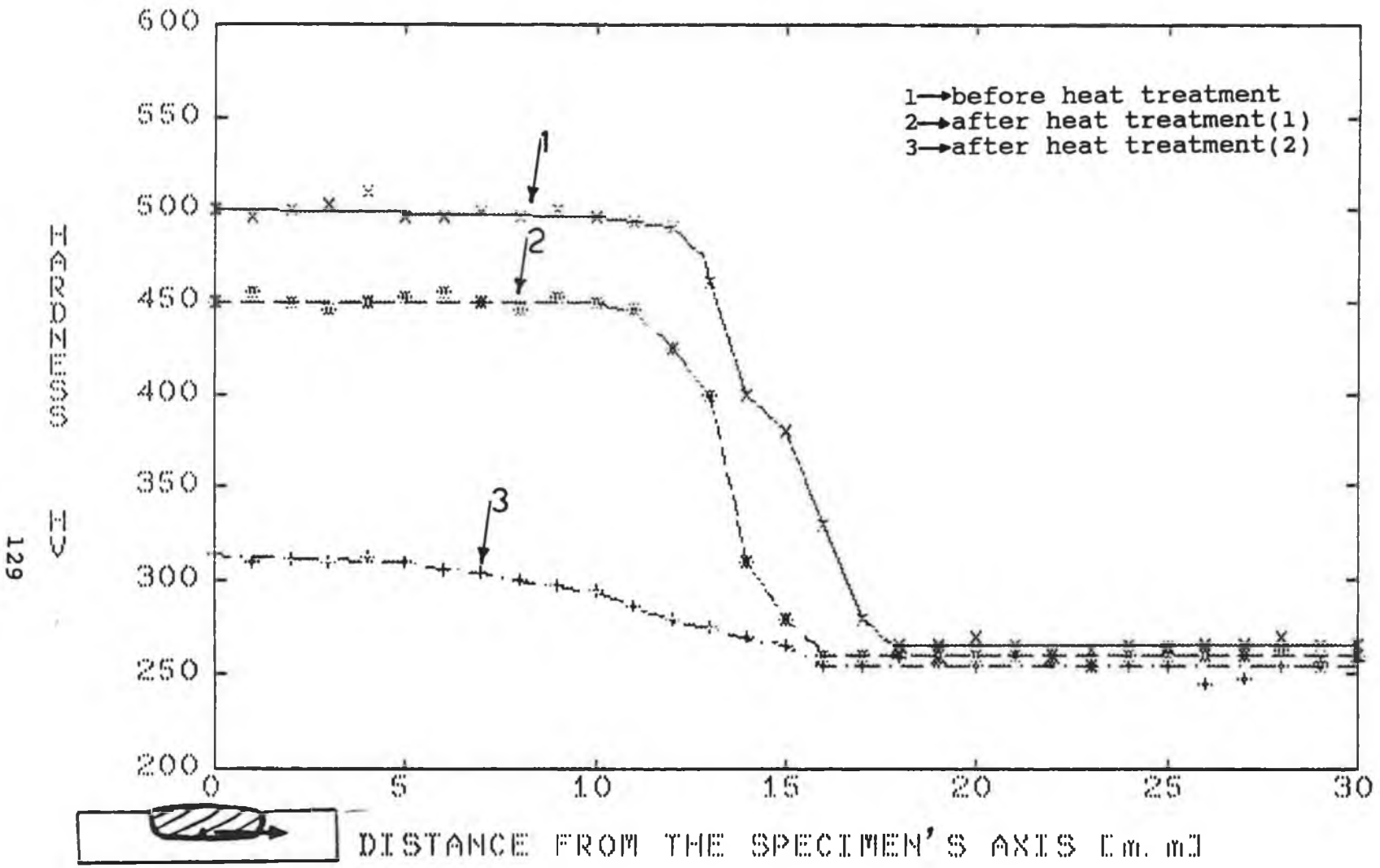

Fig. 39 The hardness variation across specimen A6, 2.5m.m from the surface.

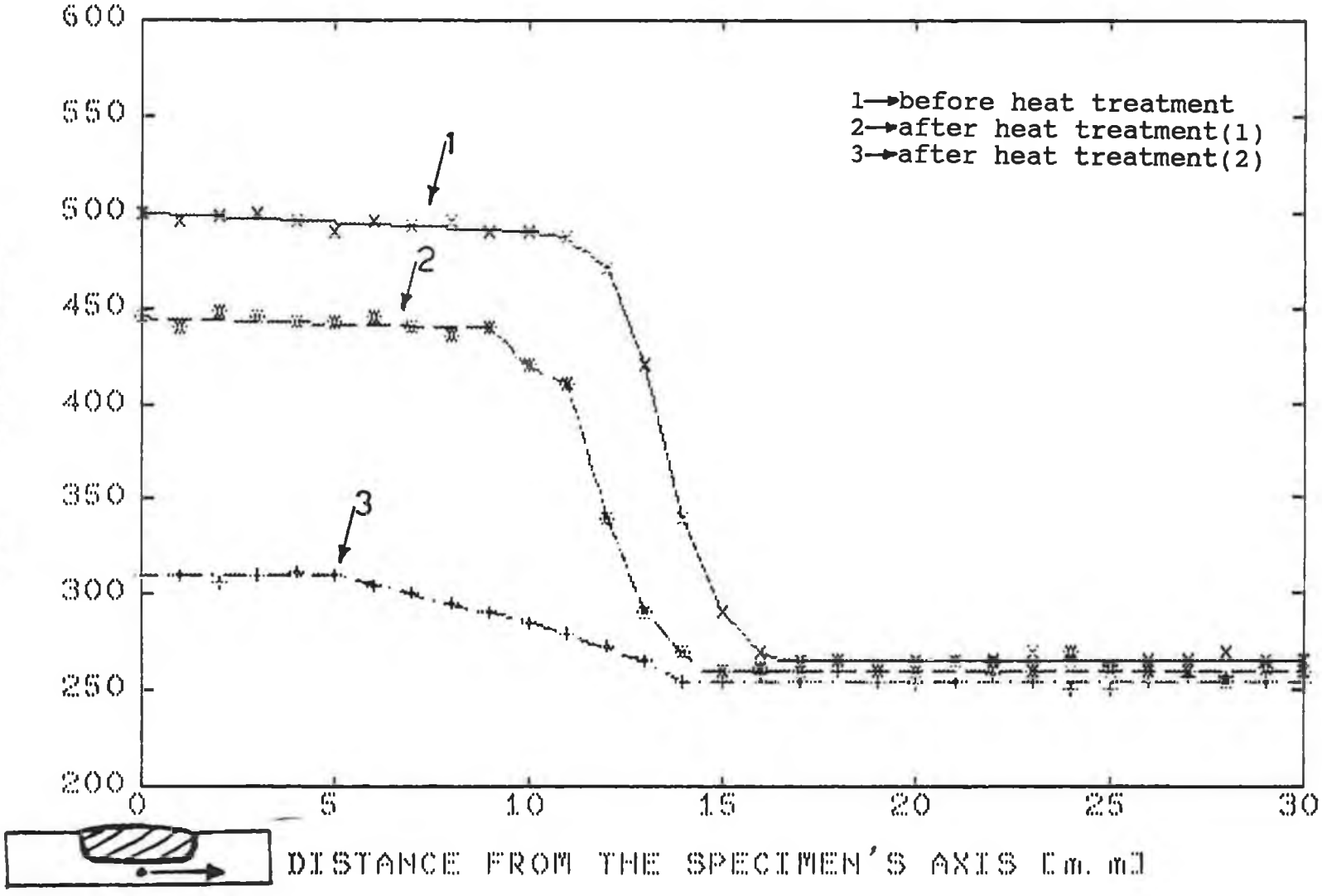

Fig. 40 The hardness variation across specimen A6, 4.5m.m from the surface.

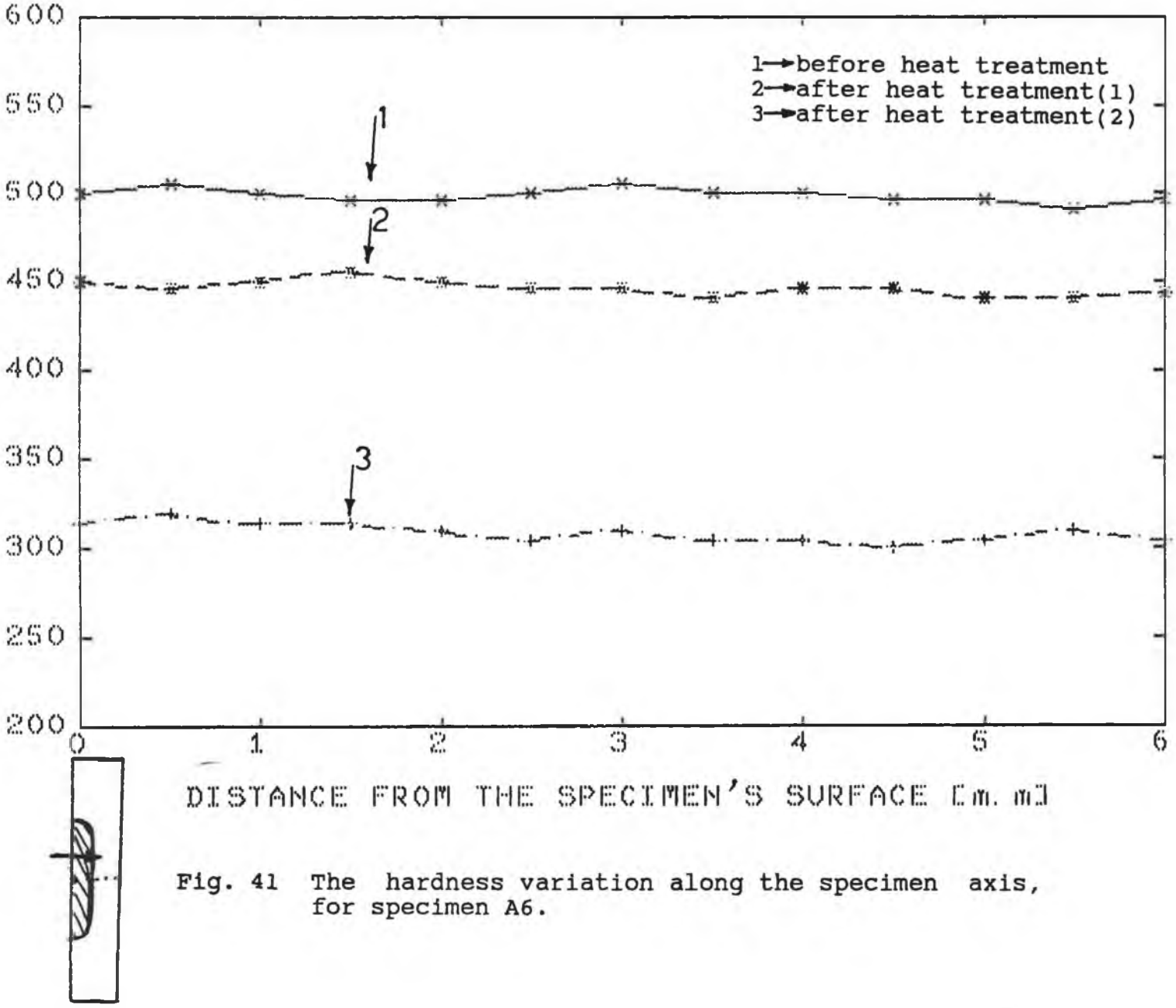

Fig. 41 The hardness variation along the specimen axis, for specimen A6.

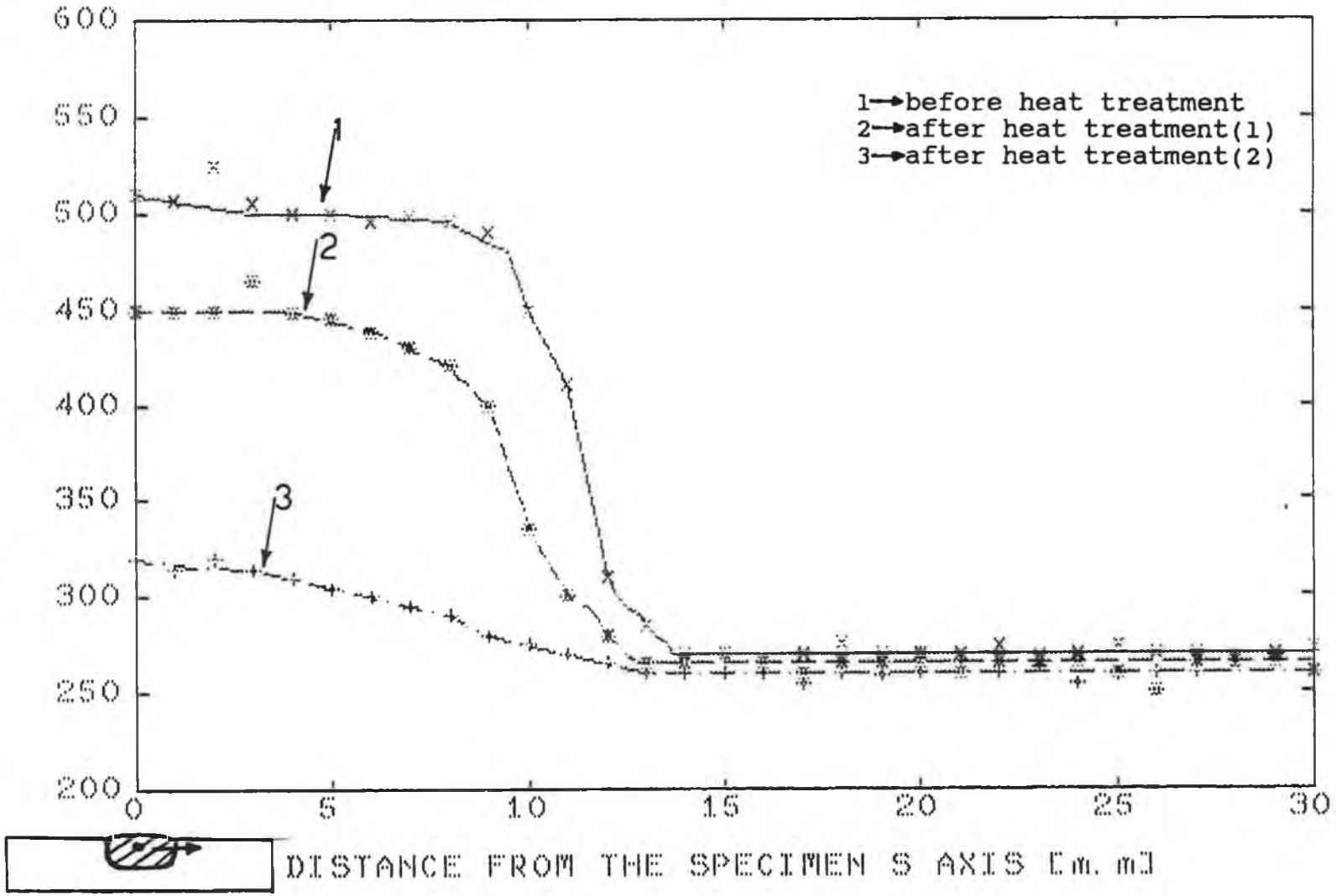

Fig. 42 The hardness variation across specimen A7, 0.5m.m from the surface.

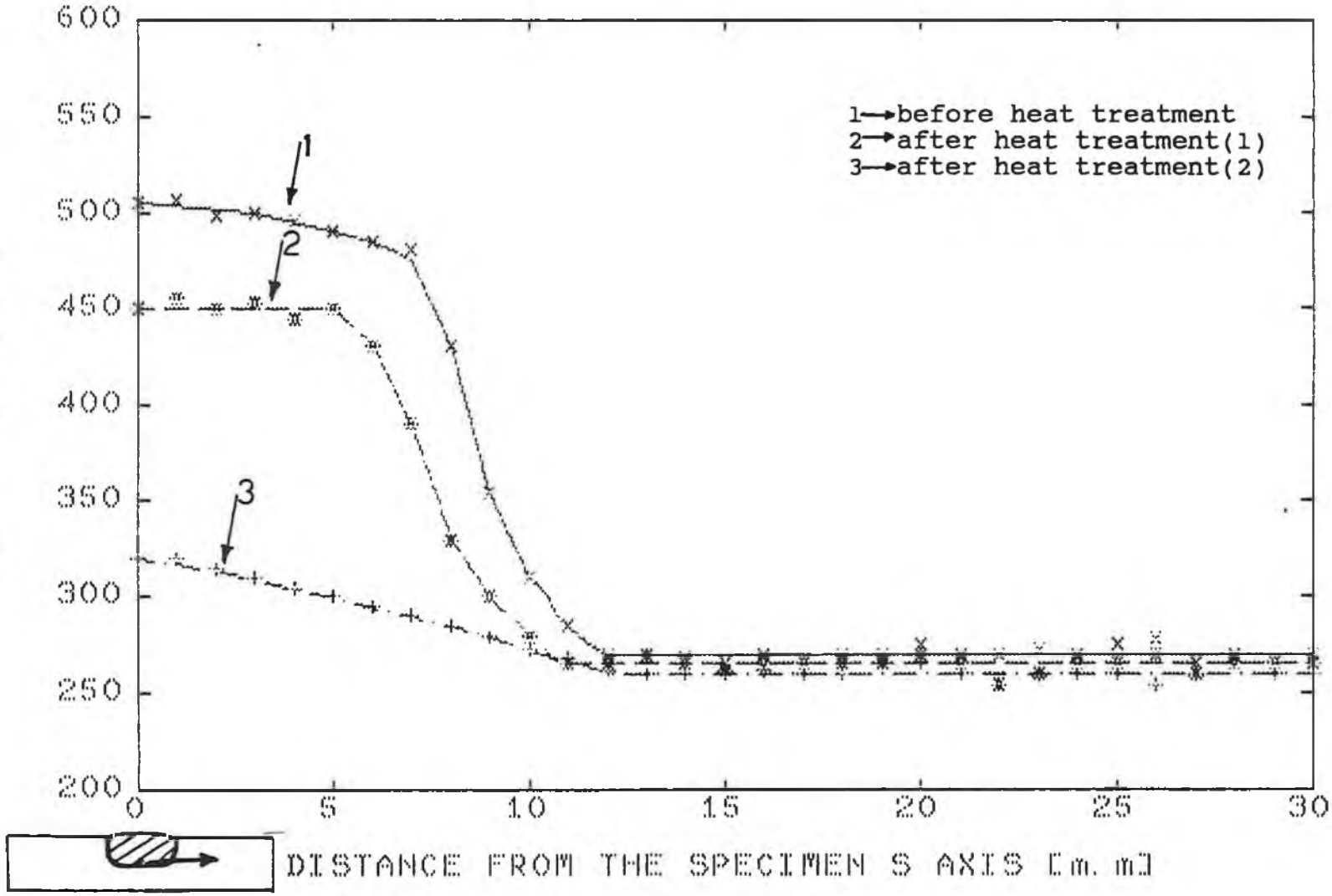

Fig. 43 The hardness variation across specimen A7, 2.5m.m from the surface.

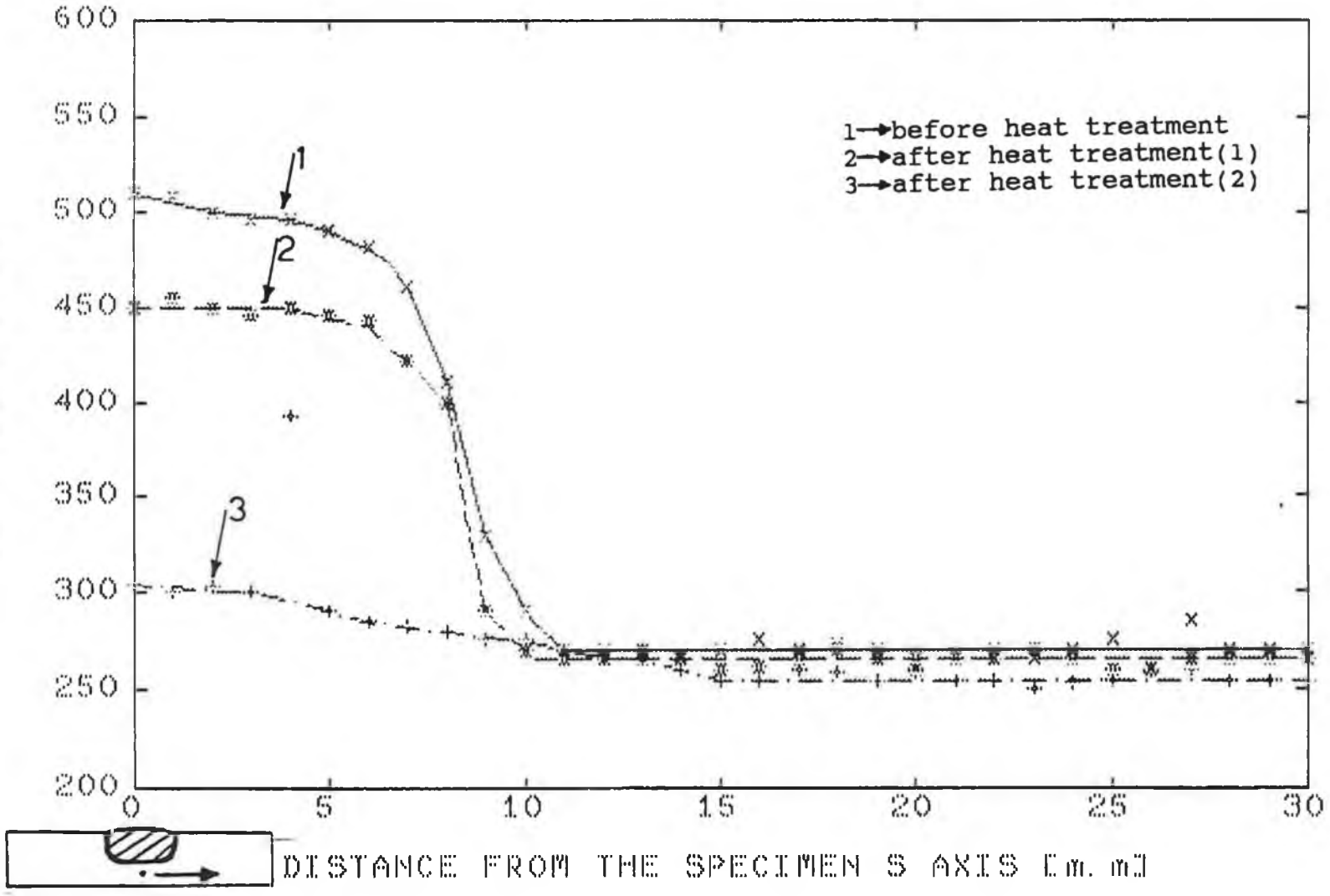

Fig. 44 The hardness variation across specimen A7, 4.5m.m from the surface.

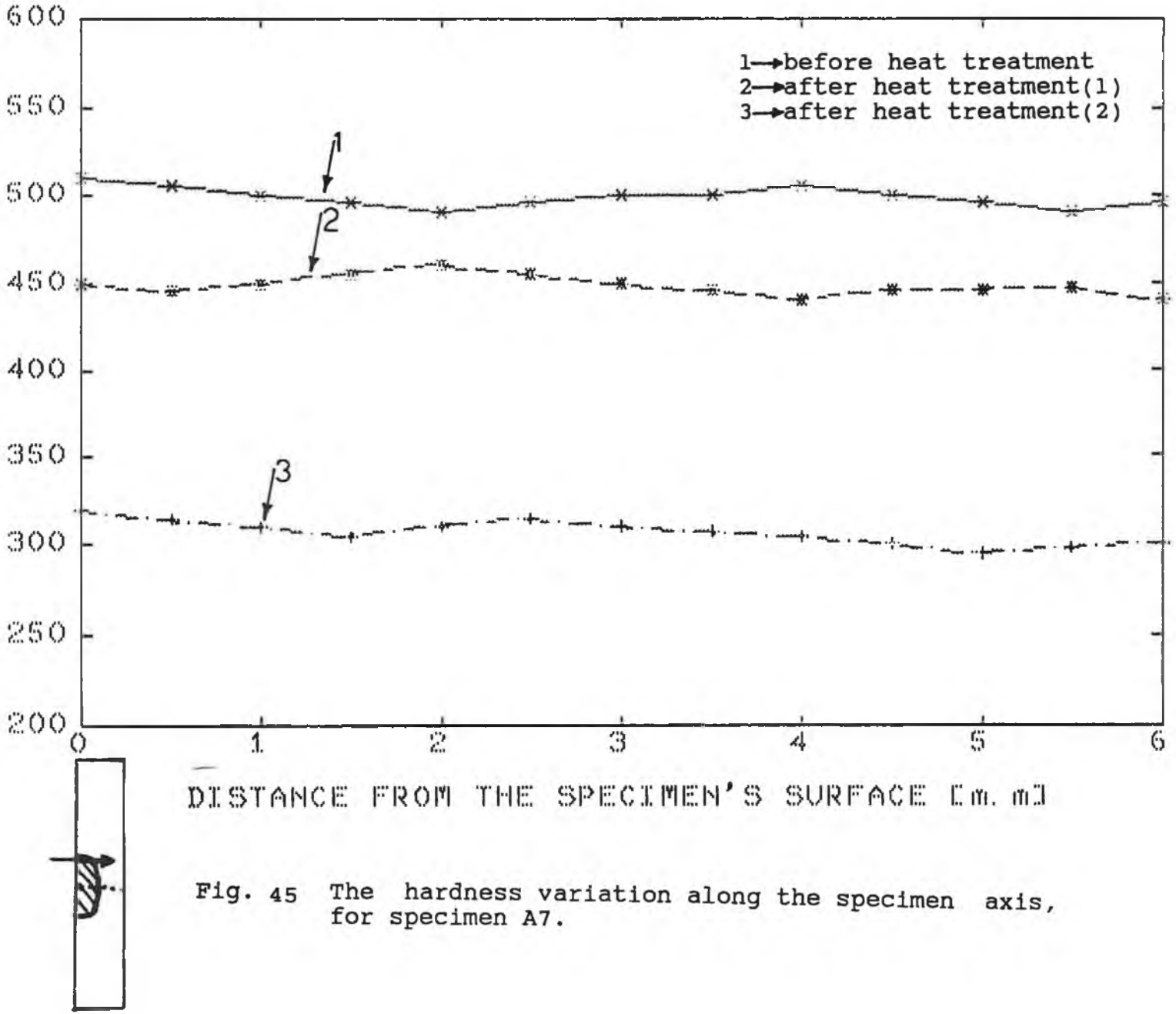

Fig. 45 The hardness variation along the specimen axis, for specimen A7.

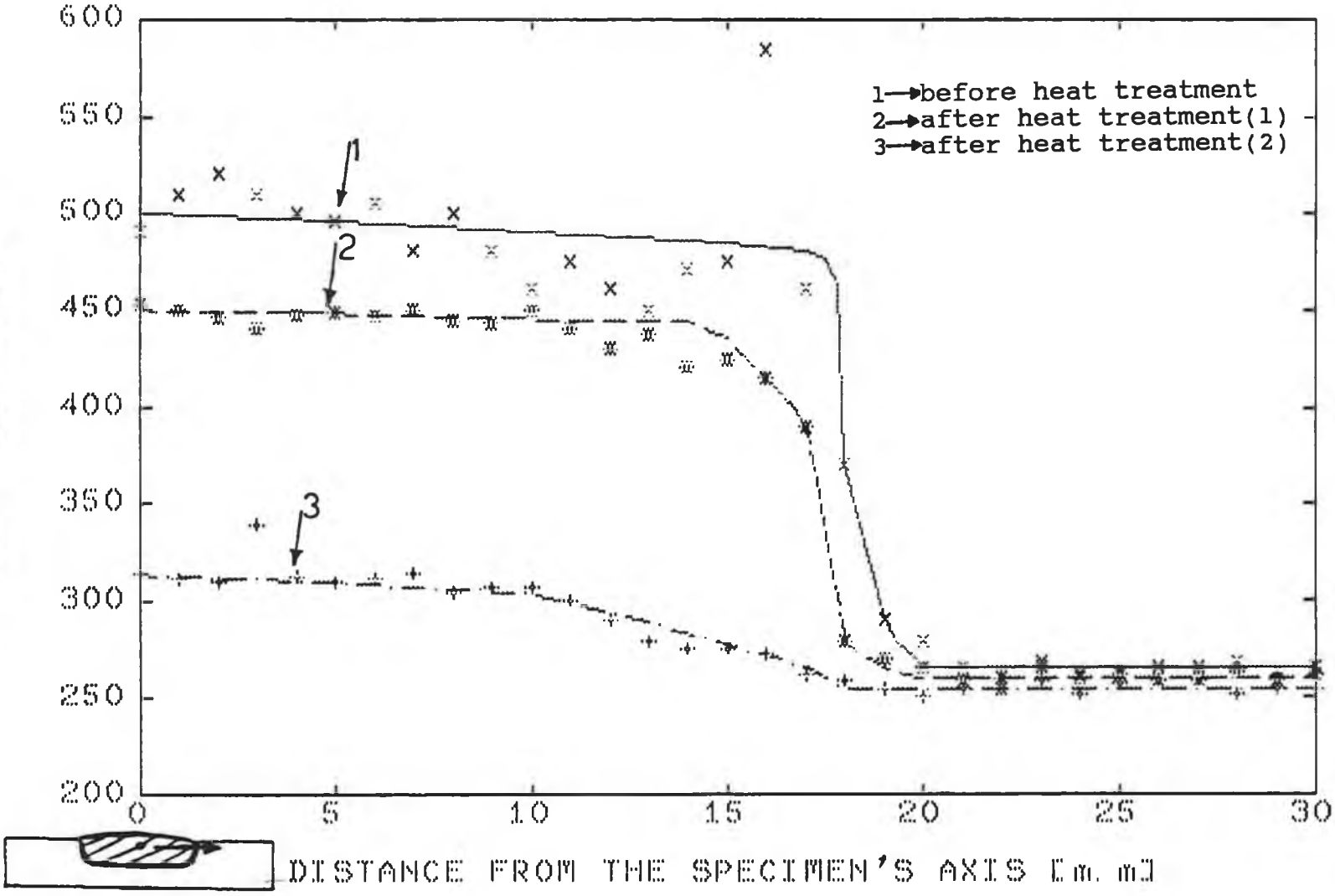

Fig. 46 The hardness variation across specimen A8, 0.5m.m from the surface.

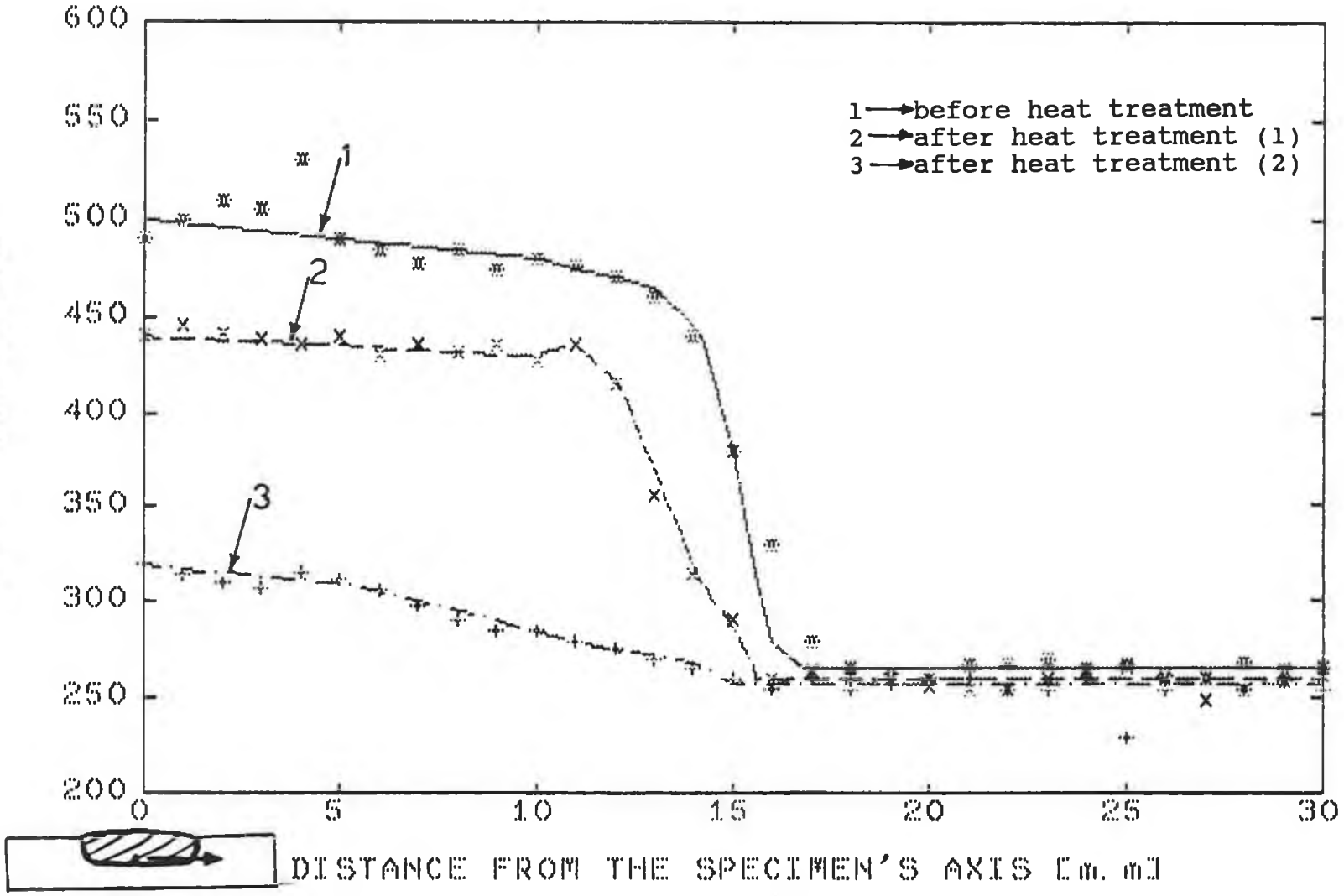

Fig. 47 The hardness variation across specimen A8, 2.5m.m from the surface.

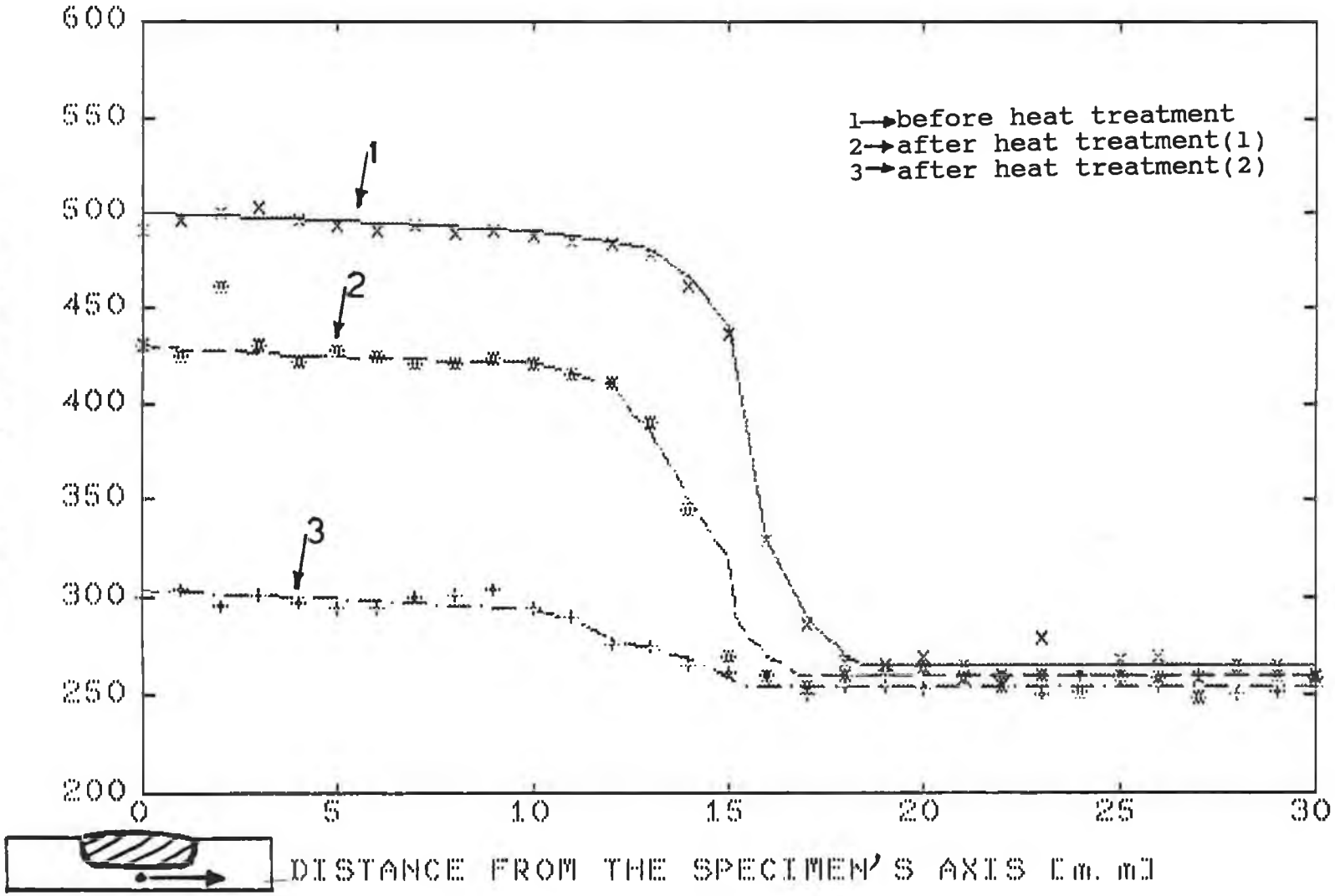

Fig. 48 The hardness variation across specimen A8, 4.5m.m from the surface.

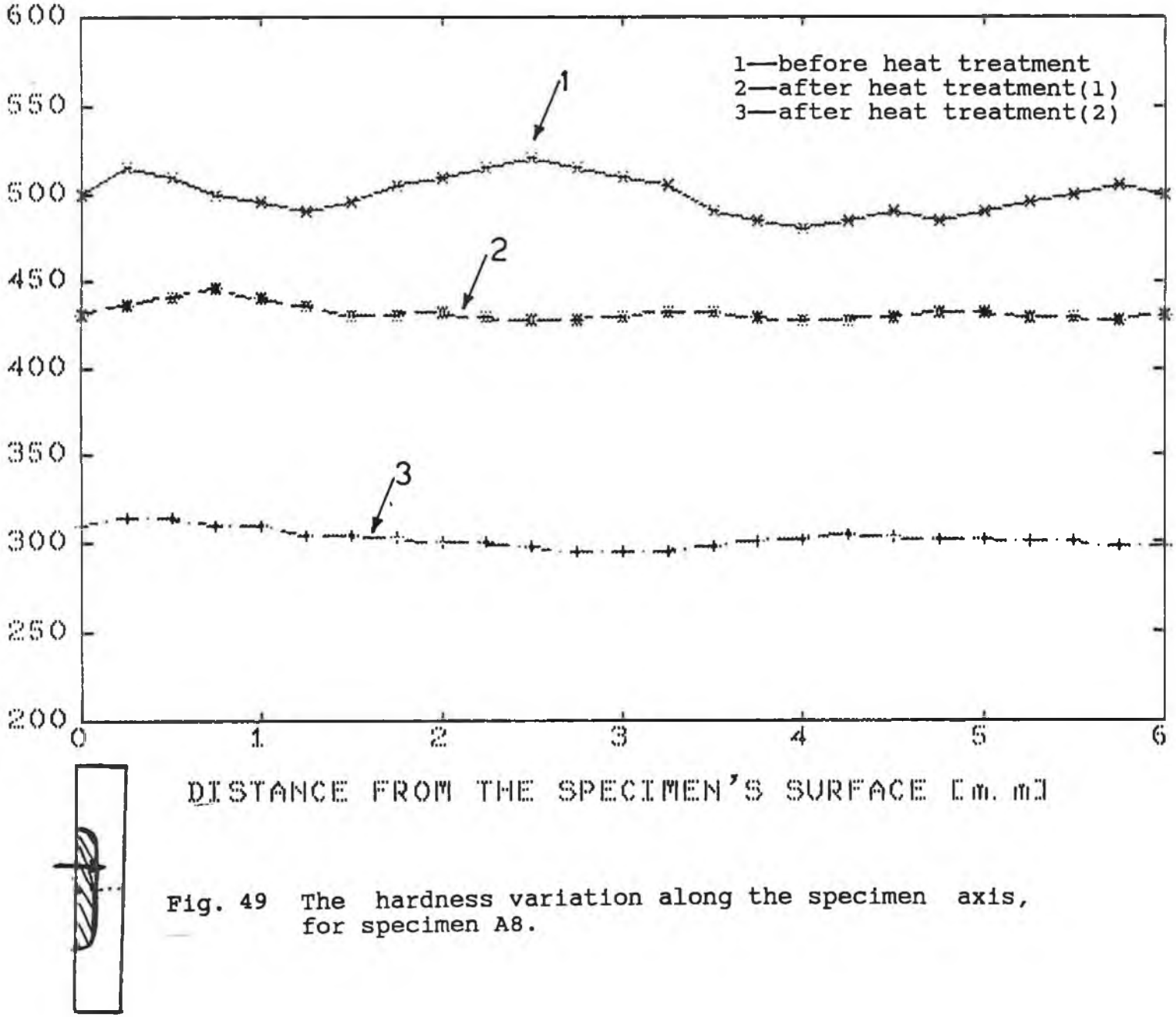

Fig. 49 The hardness variation along the specimen axis, for specimen A8.

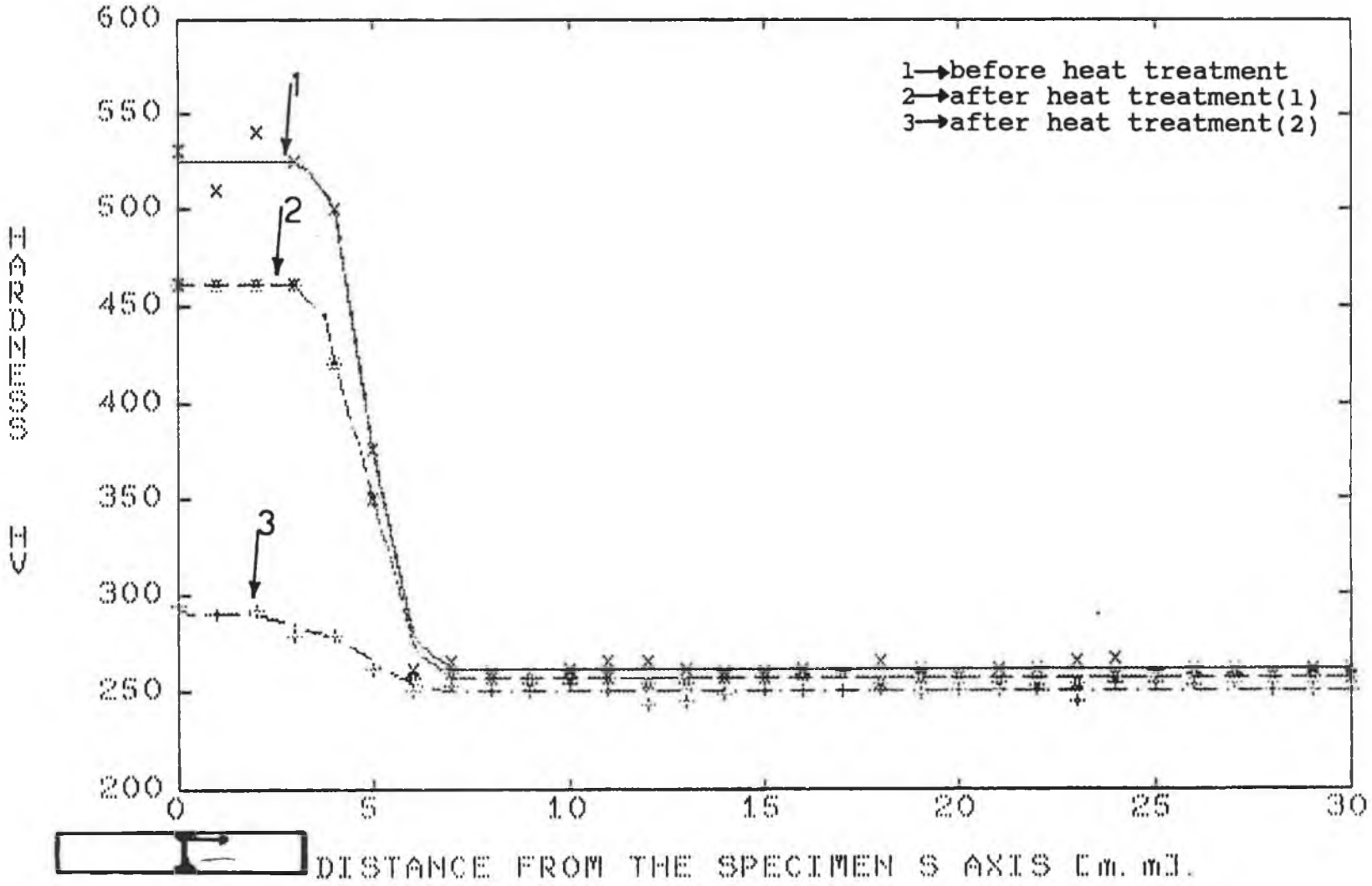

Fig. 50 The hardness variation across specimen B1, 0.5 mm from the surface.

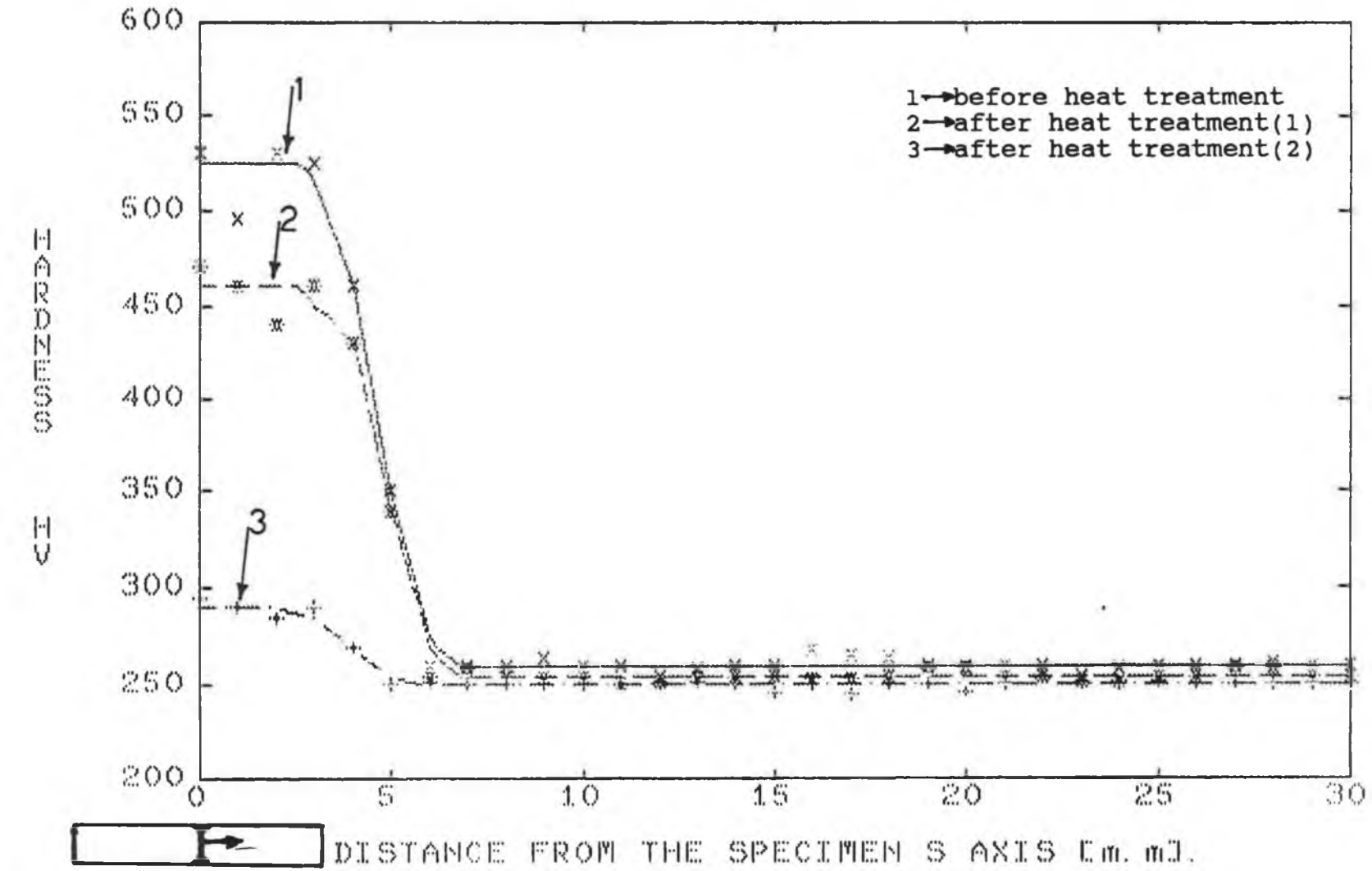

Fig. 51 The hardness variation across specimen B2, 1.5 mm from the surface.

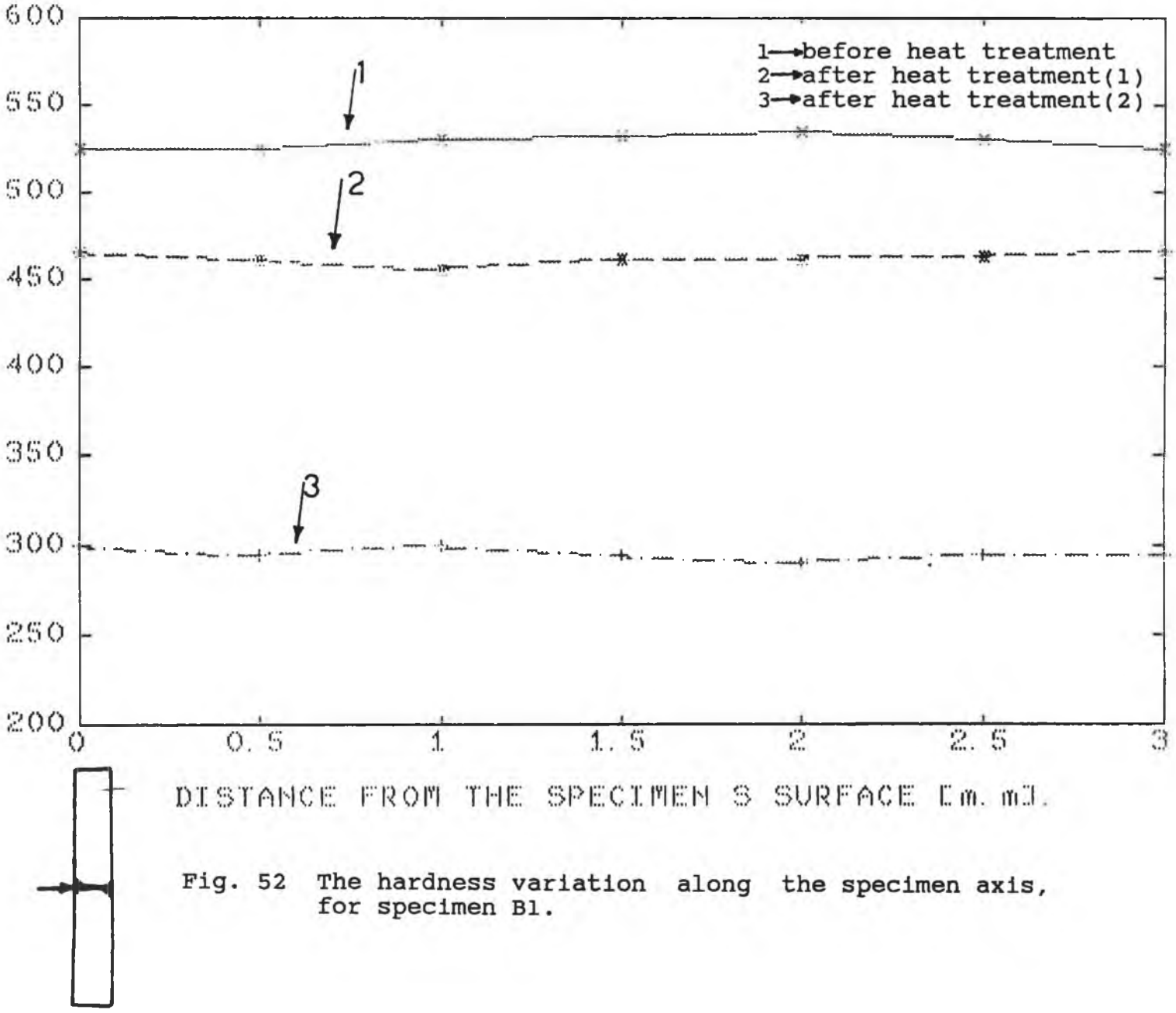

Fig. 52 The hardness variation along the specimen axis, for specimen B1.

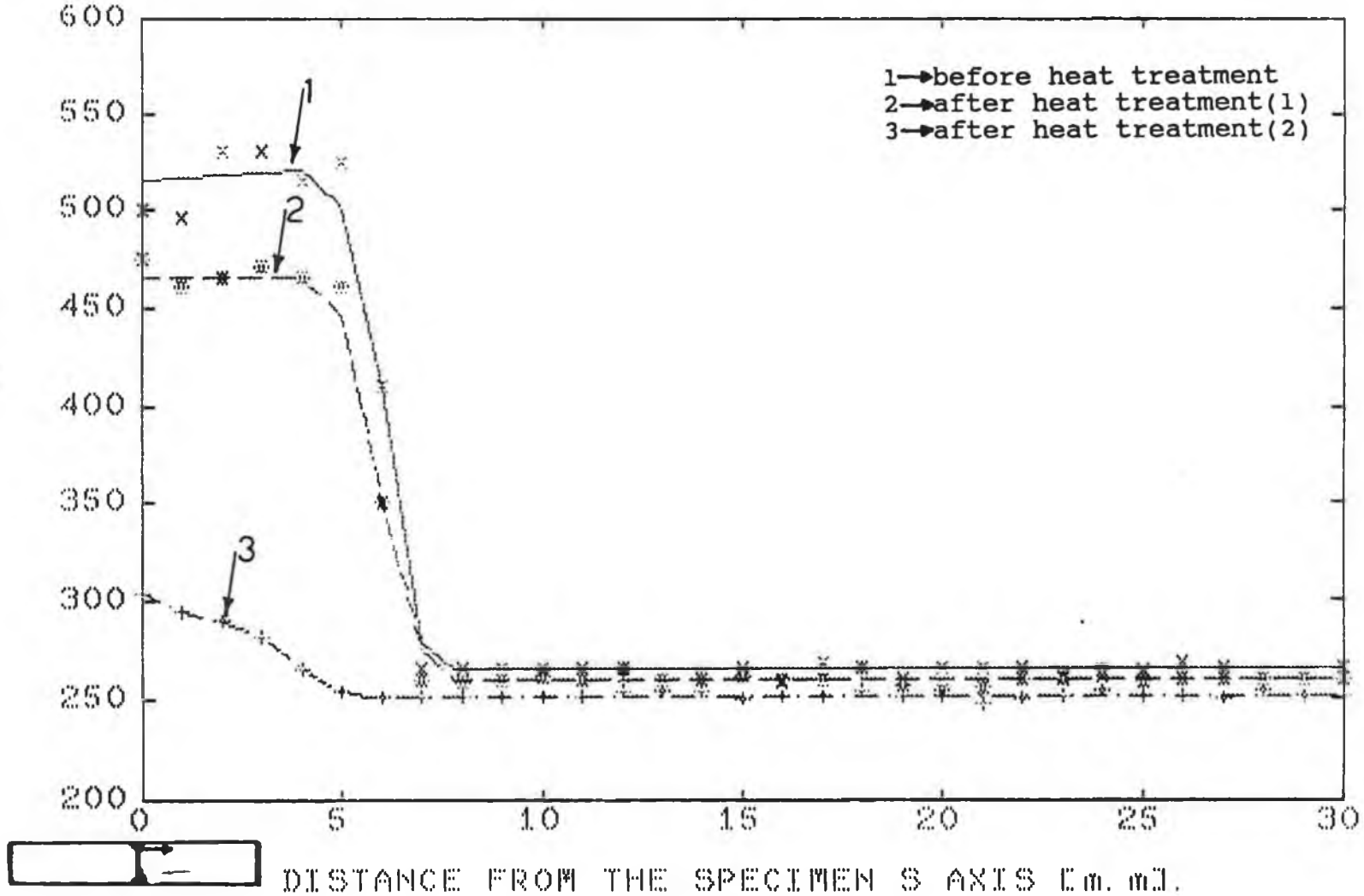

Fig. 53 The hardness variation across specimen B2, 0.5 mm from the surface.

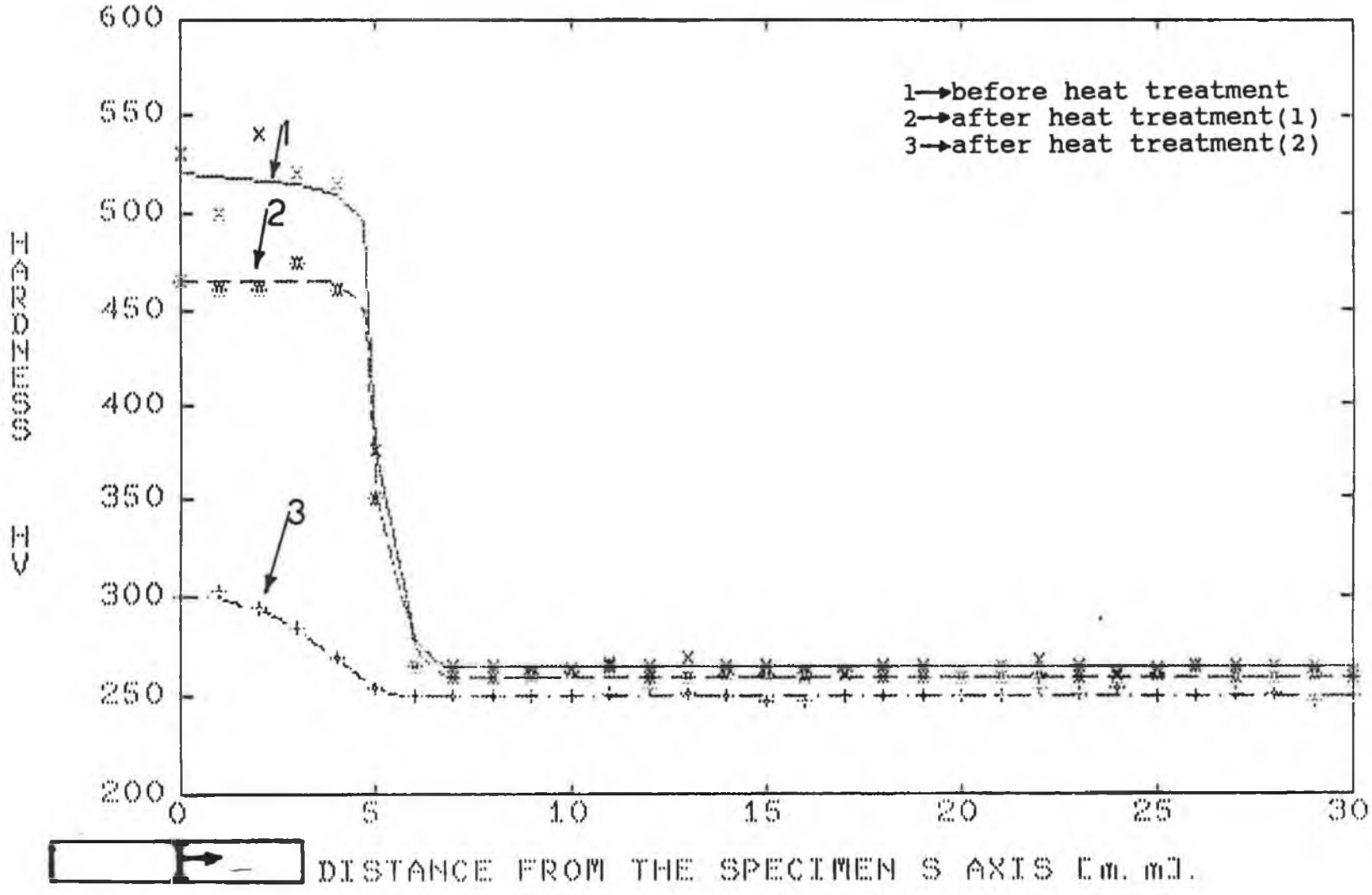

Fig. 54 The hardness variation across specimen B2, 2.5 mm from the surface.

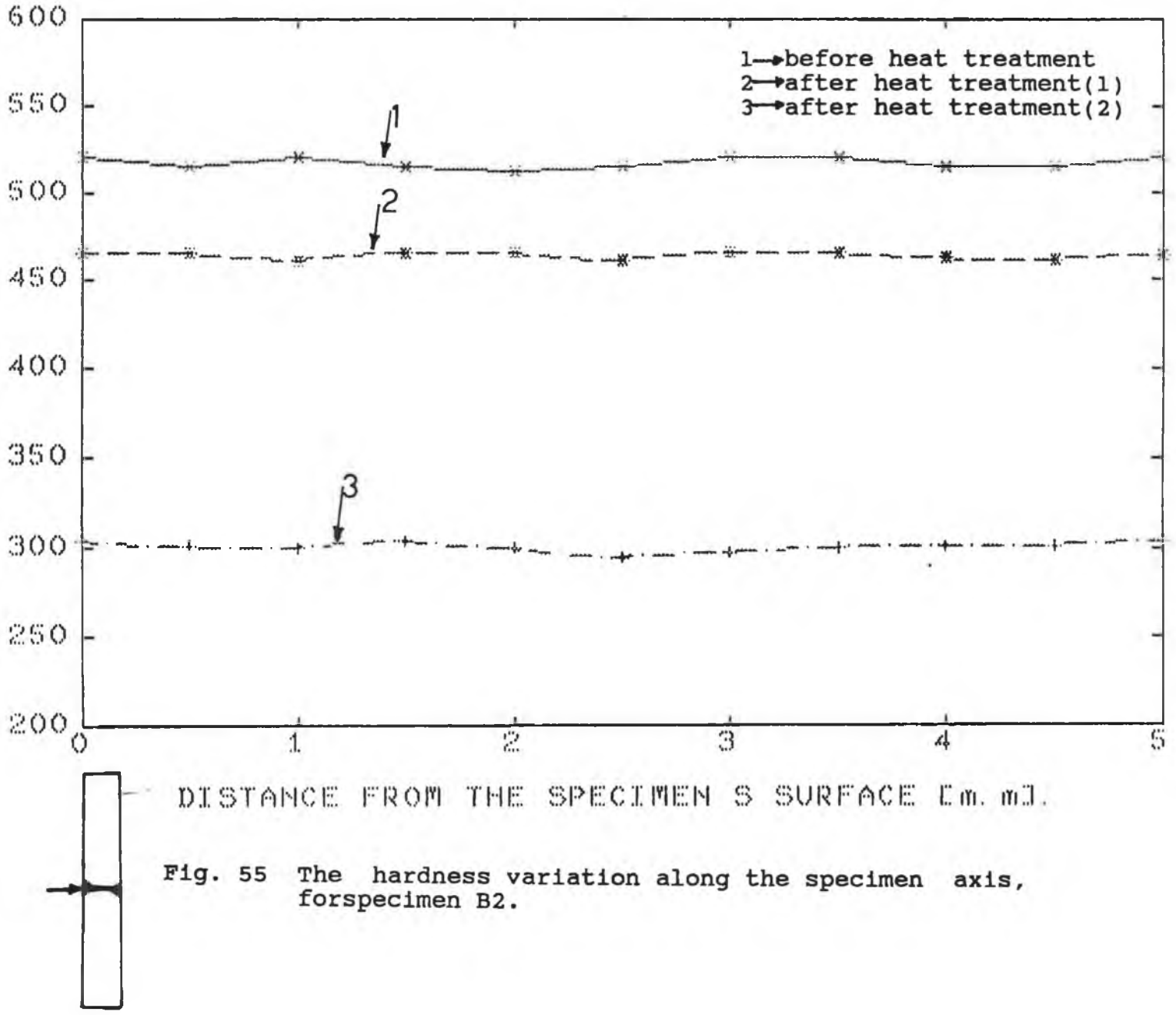

Fig. 55 The hardness variation along the specimen axis, forspecimen B2.

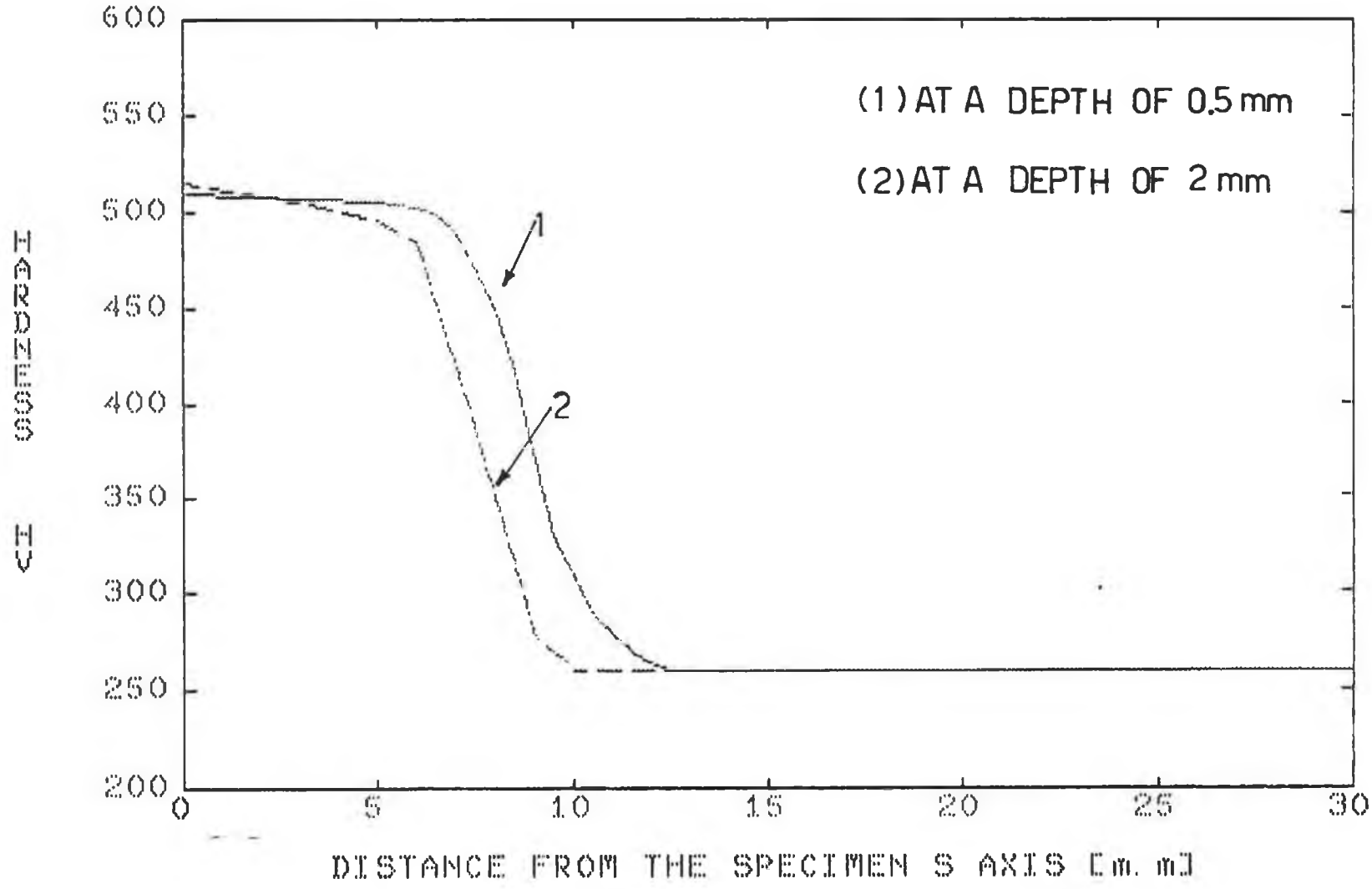

Fig. 56 Coparison between the hardness variation for the two different depths, for specimen A1.

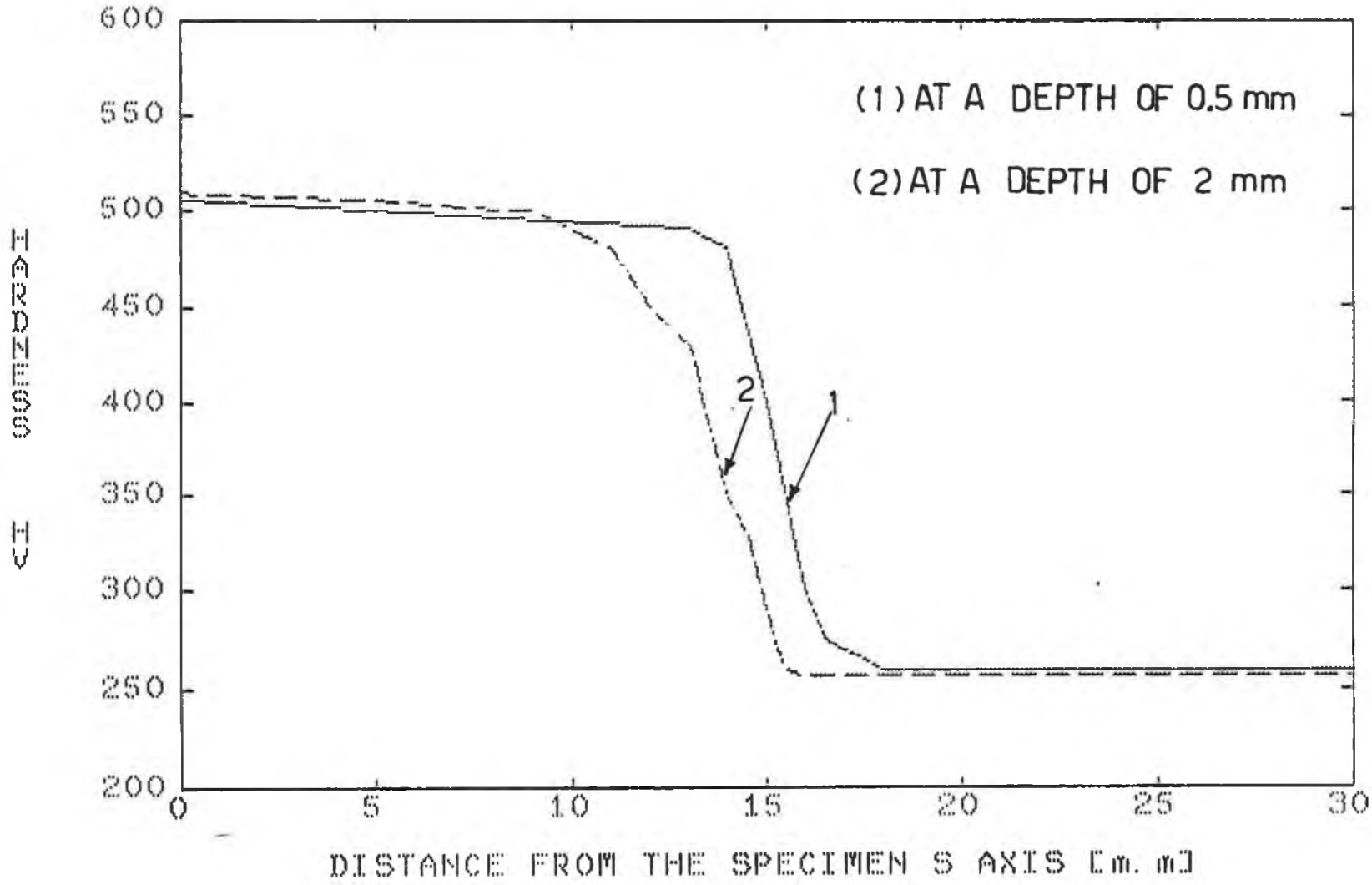

Fig. 57 Comparison between the hardness variation for the two different depths, for specimen A2.

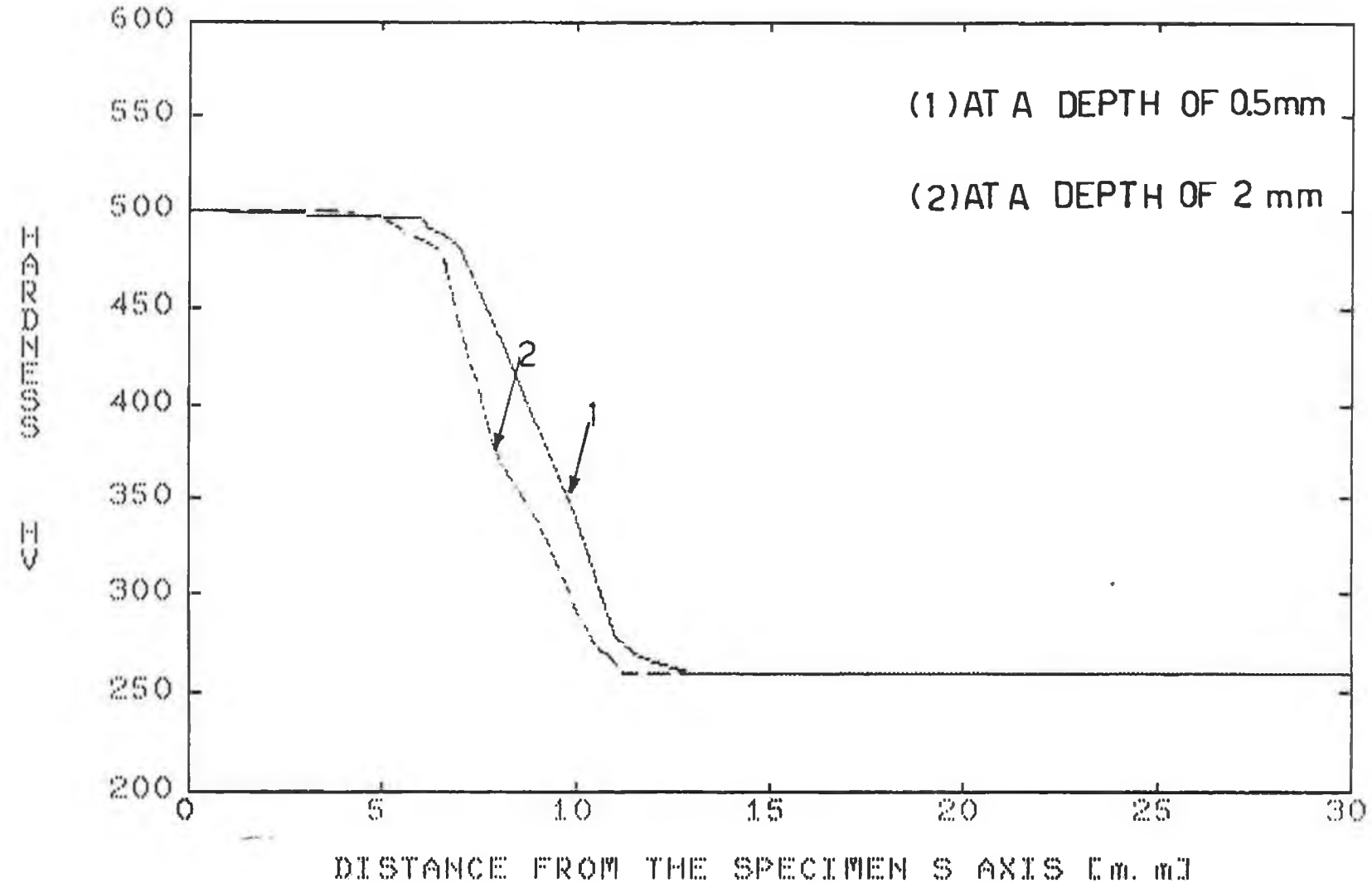

Fig. 58 Comarison between the hardness variation for the two different depths, for specimen A3.

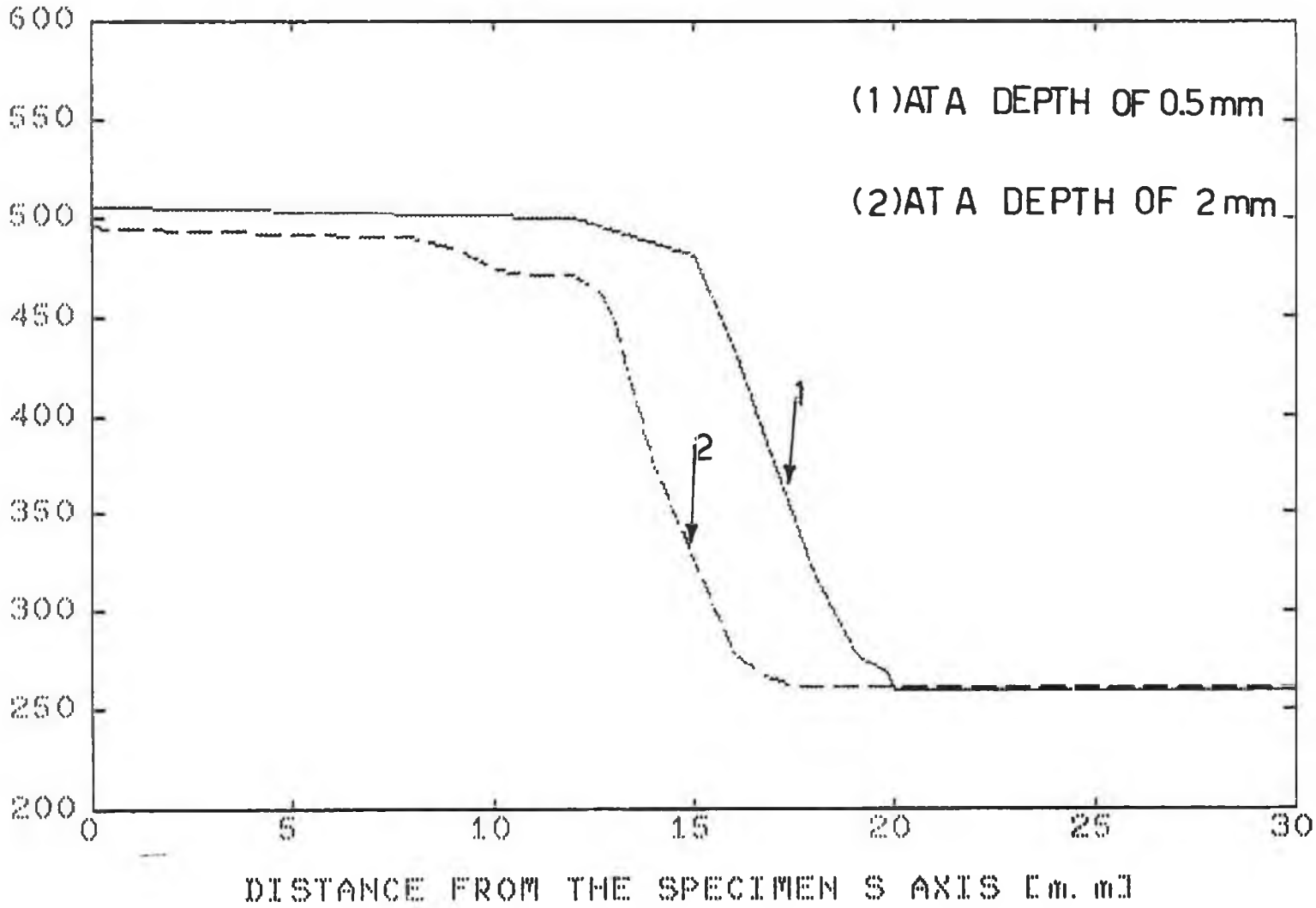

Fig. 59 Comparison between the hardness variation for the two different depths, for specimen A4.

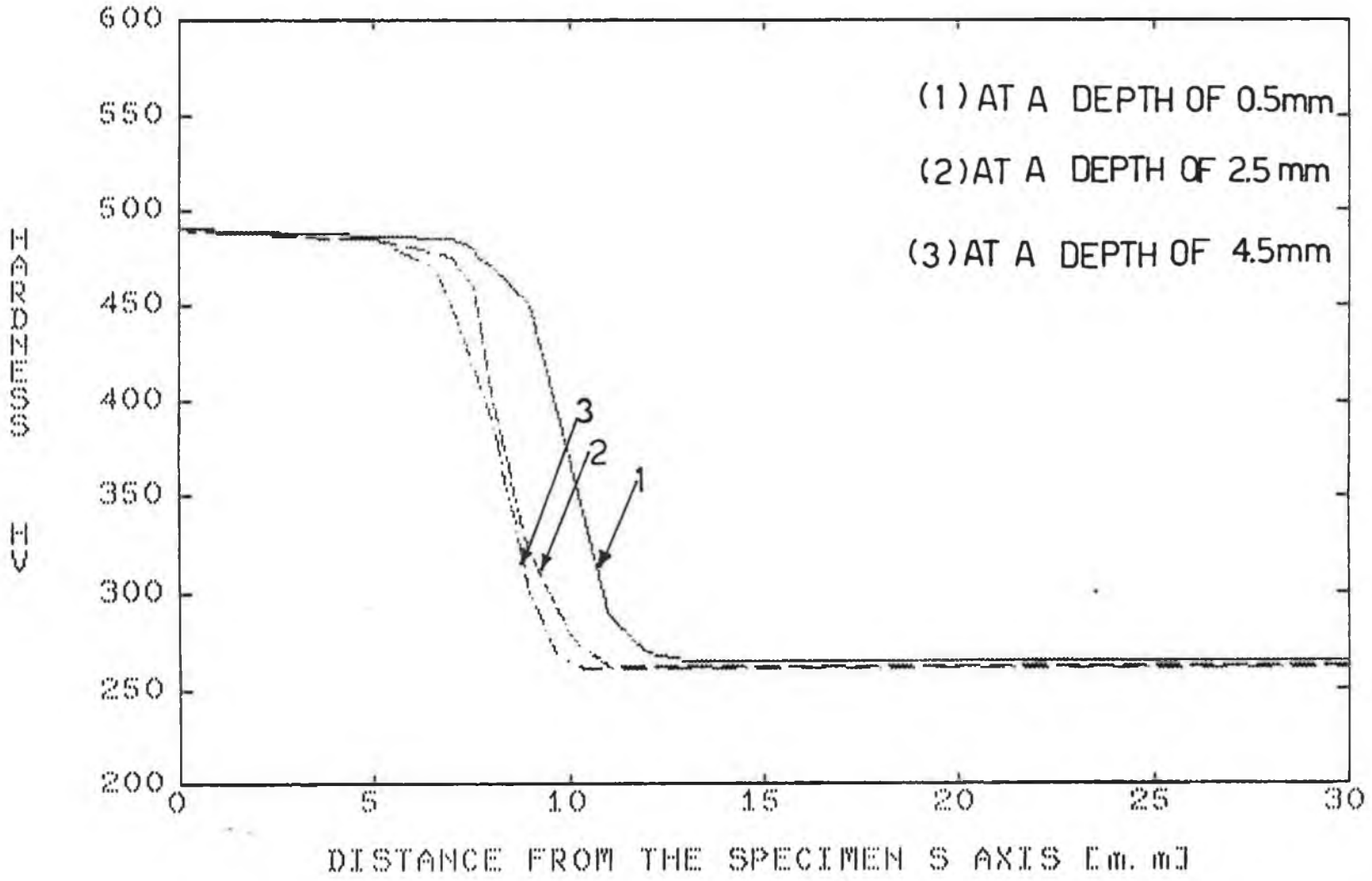

Fig. 60 Comparison between the hardness variation for the three different depths, for specimen A5.

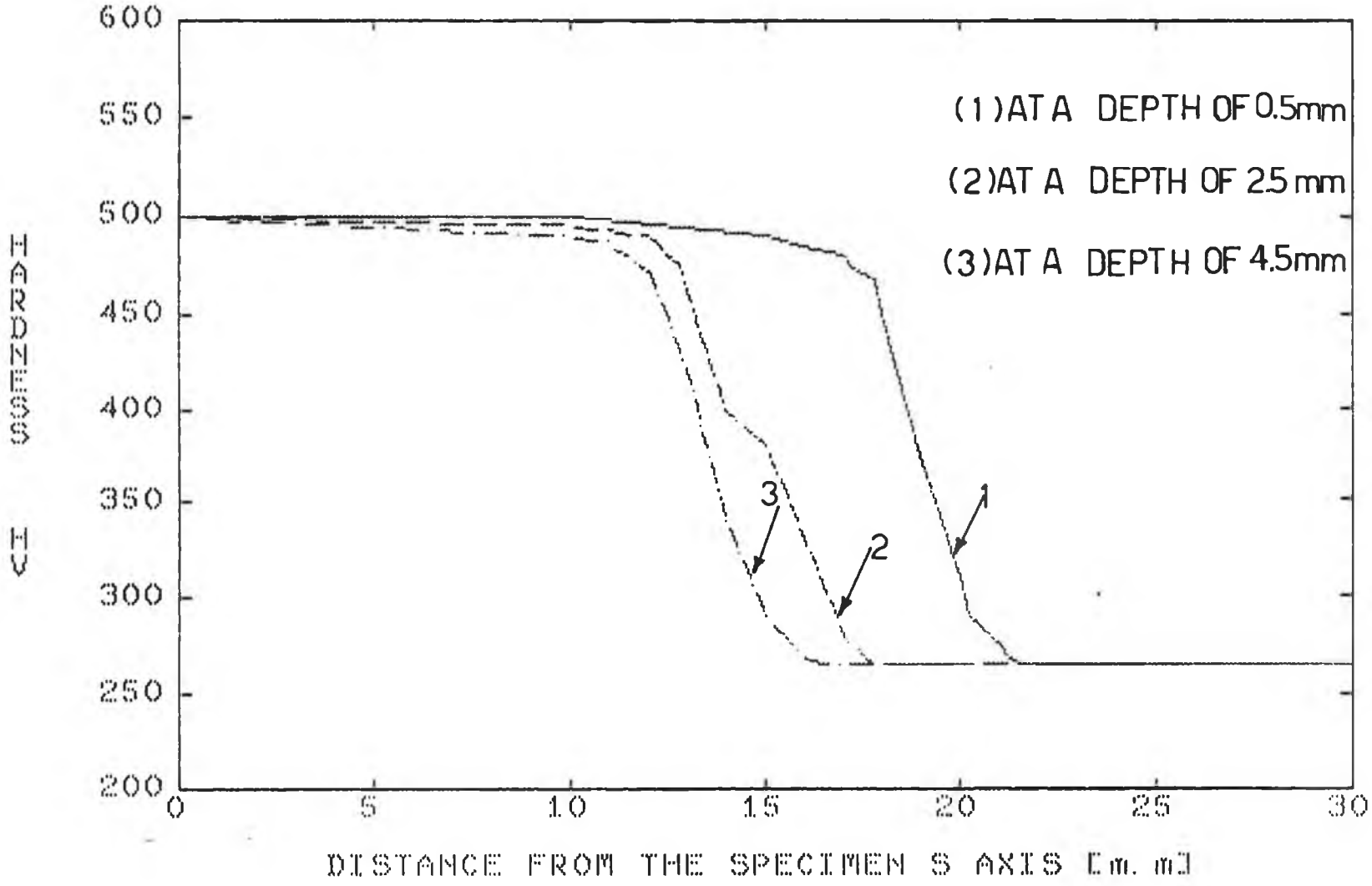

Fig. 61 Comparison between the hardness variation for the three different depths, for specimen A6.

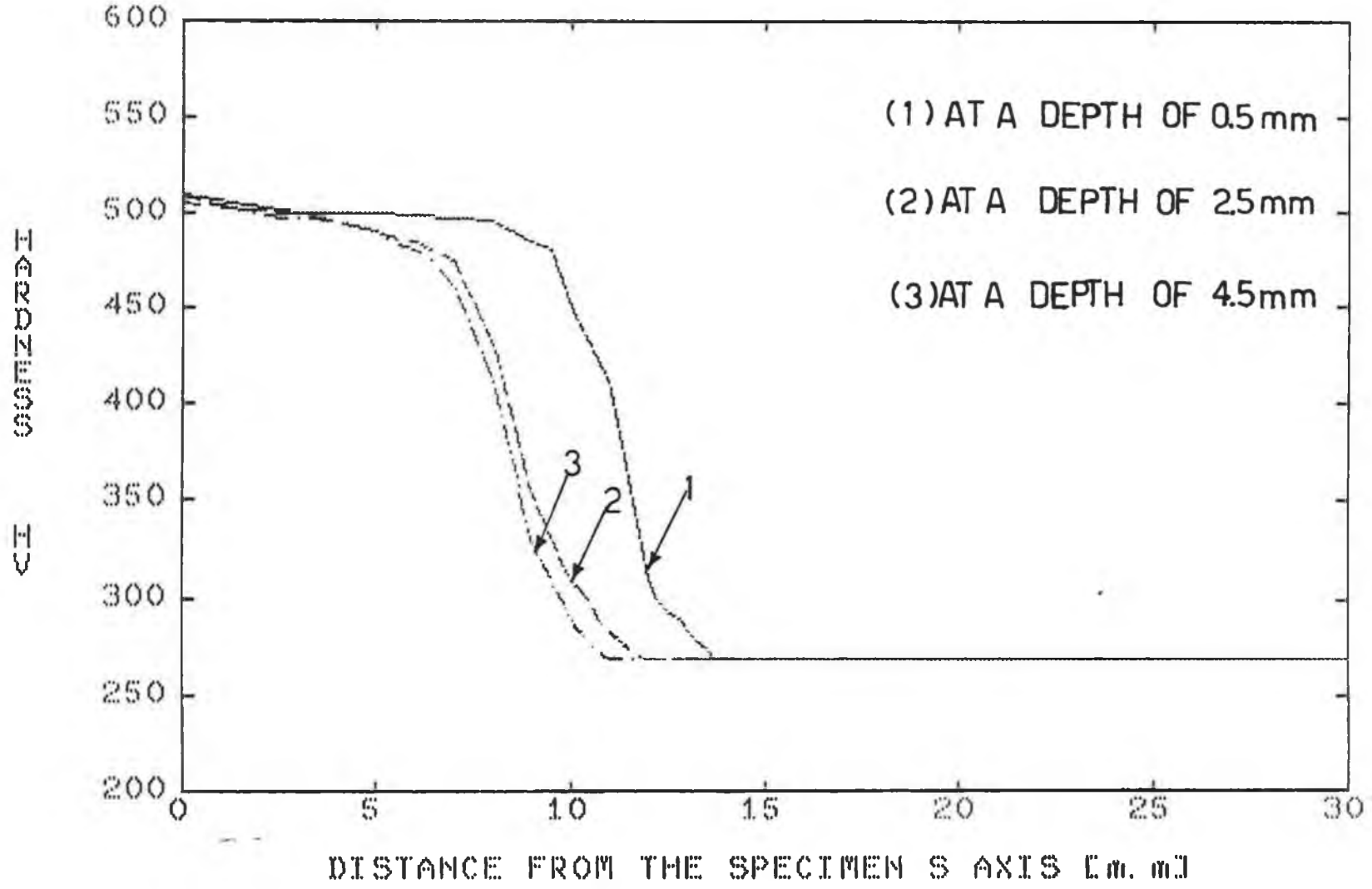

Fig. 62 Comparison between the hardness variation for the three different depths, for specimen A7.

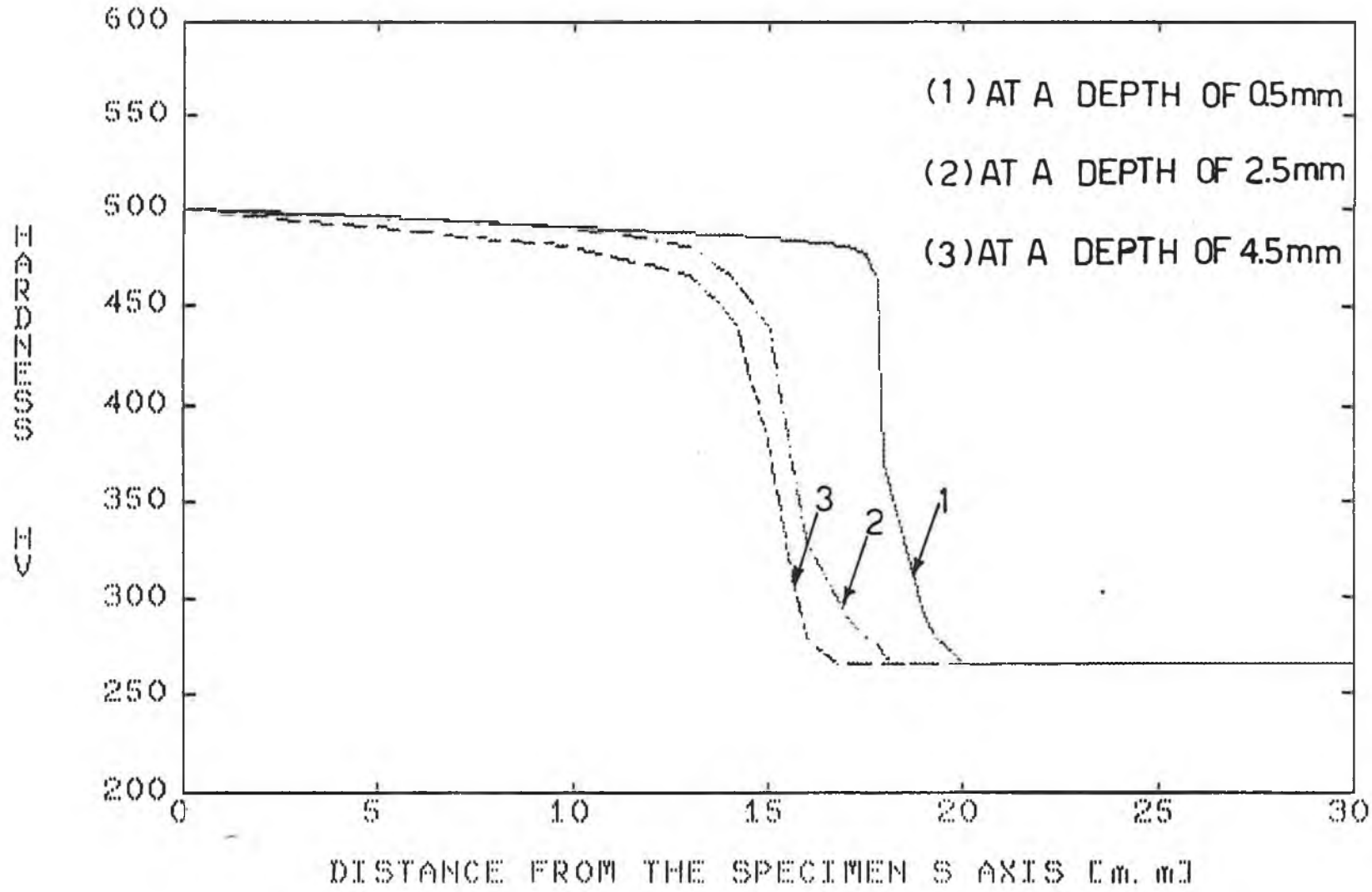

Fig. 63 Comparison between the hardness variation for the three different depths, for specimen A8.

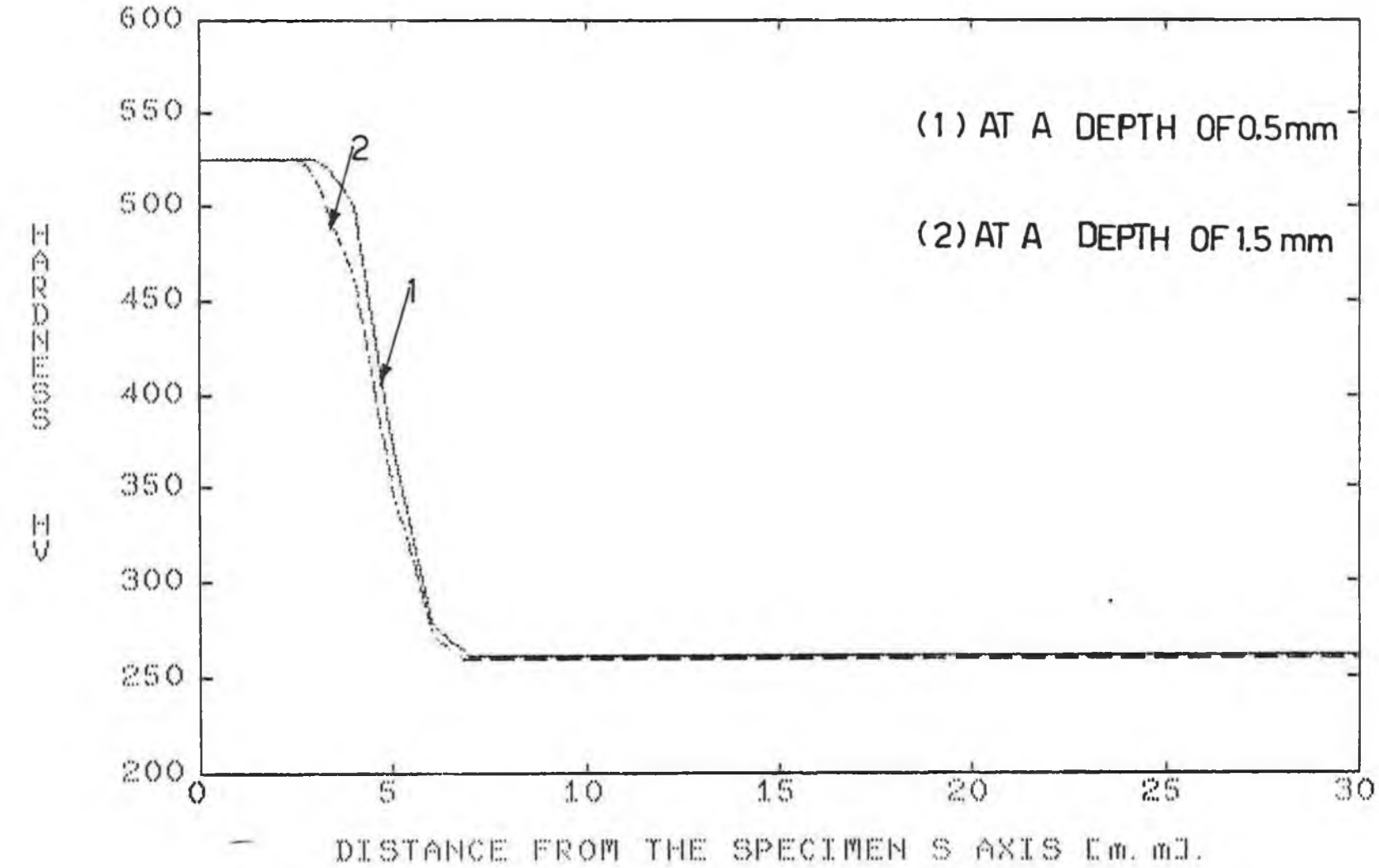

Fig. 64 Comparison between the hardness variation for the two different depths, for specimen B1.

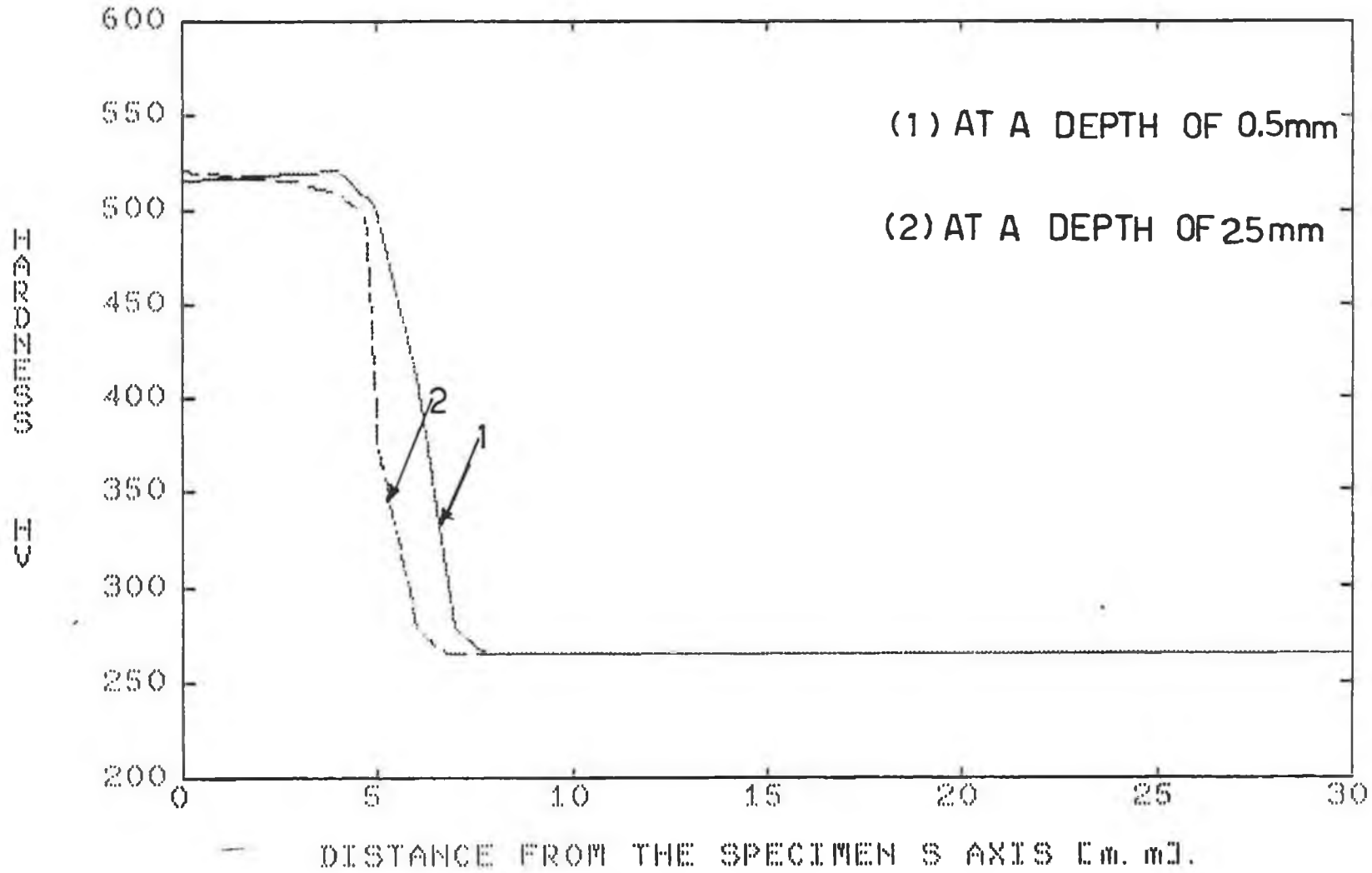

Fig. 65 Comparison between the hardness variation for the two different depths, for specimen B2.

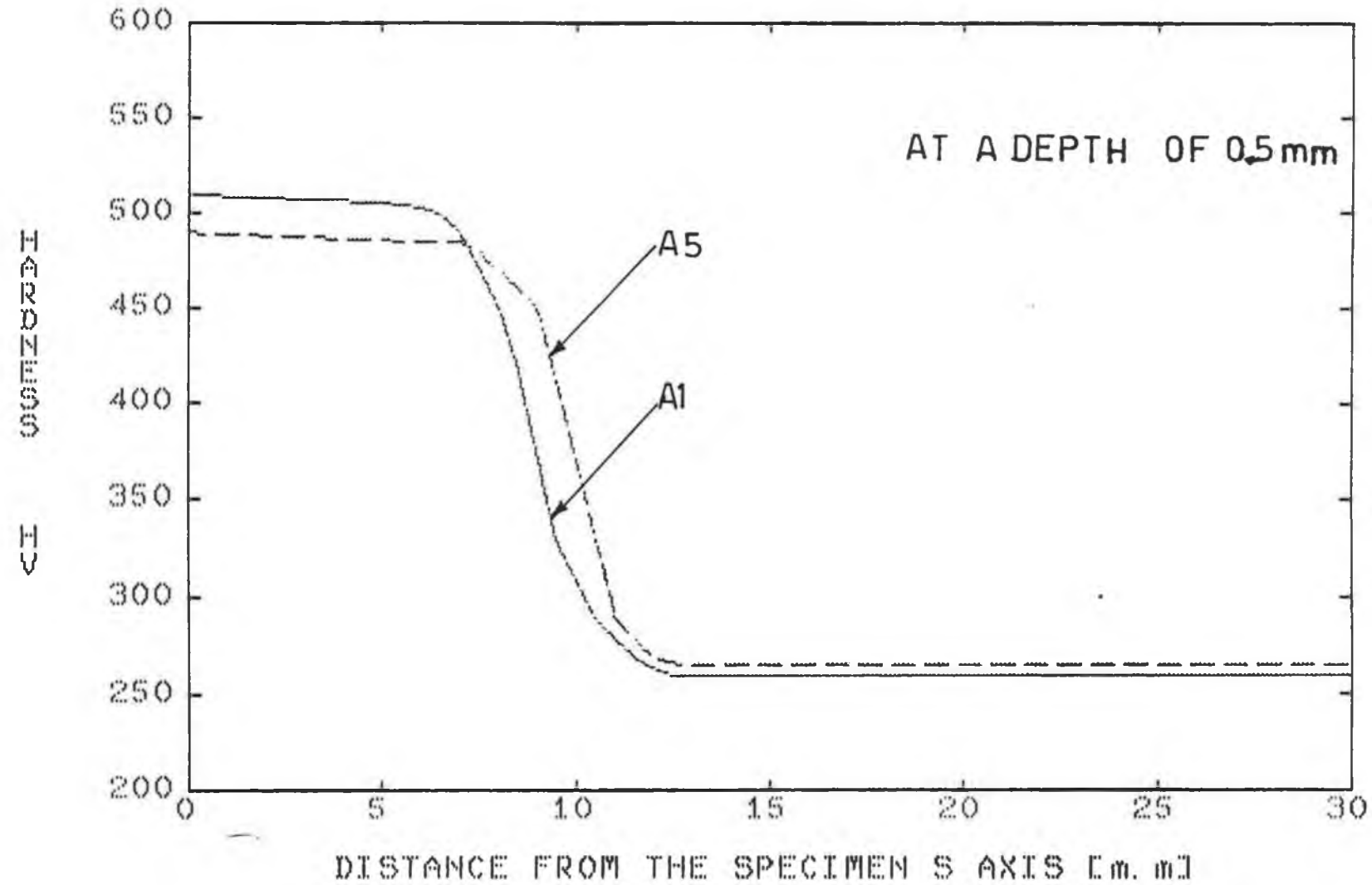

Fig. 66 Comparison between the hardness variation for specimens A1 and A5 which have different thickness.

Fig. 67 Comparison
specimens
thickness.

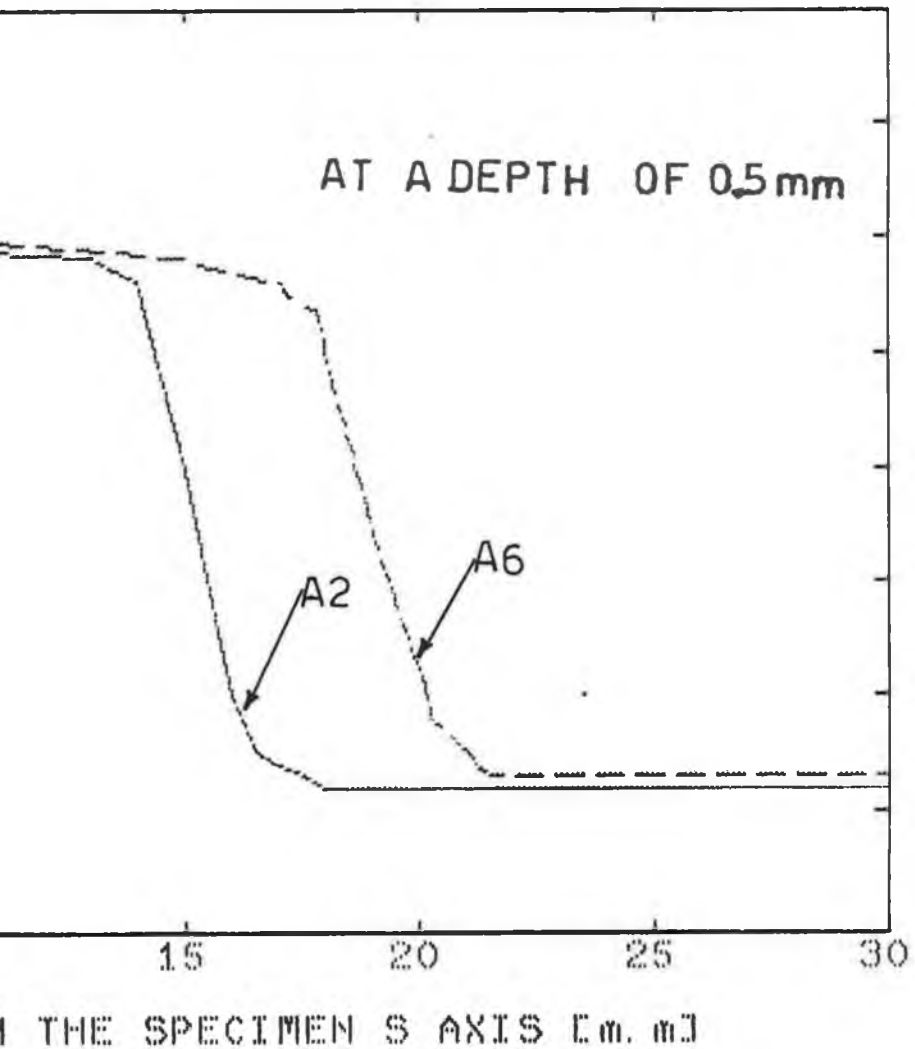

between the hardness variation for A2 and A6 which have different

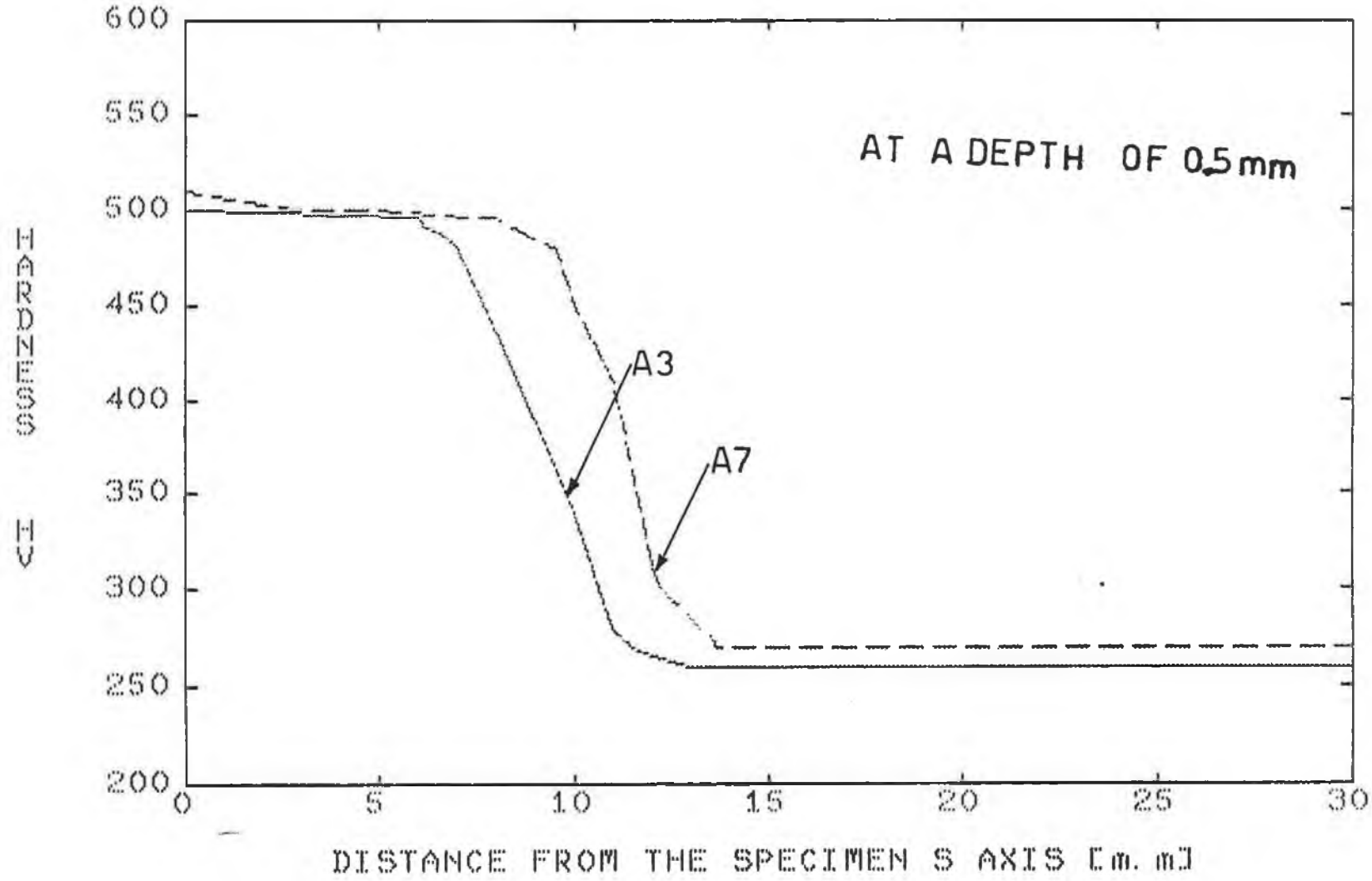

Fig. 68 Comparison between the hardness variation for specimens A3 and A7 which have different thickness.

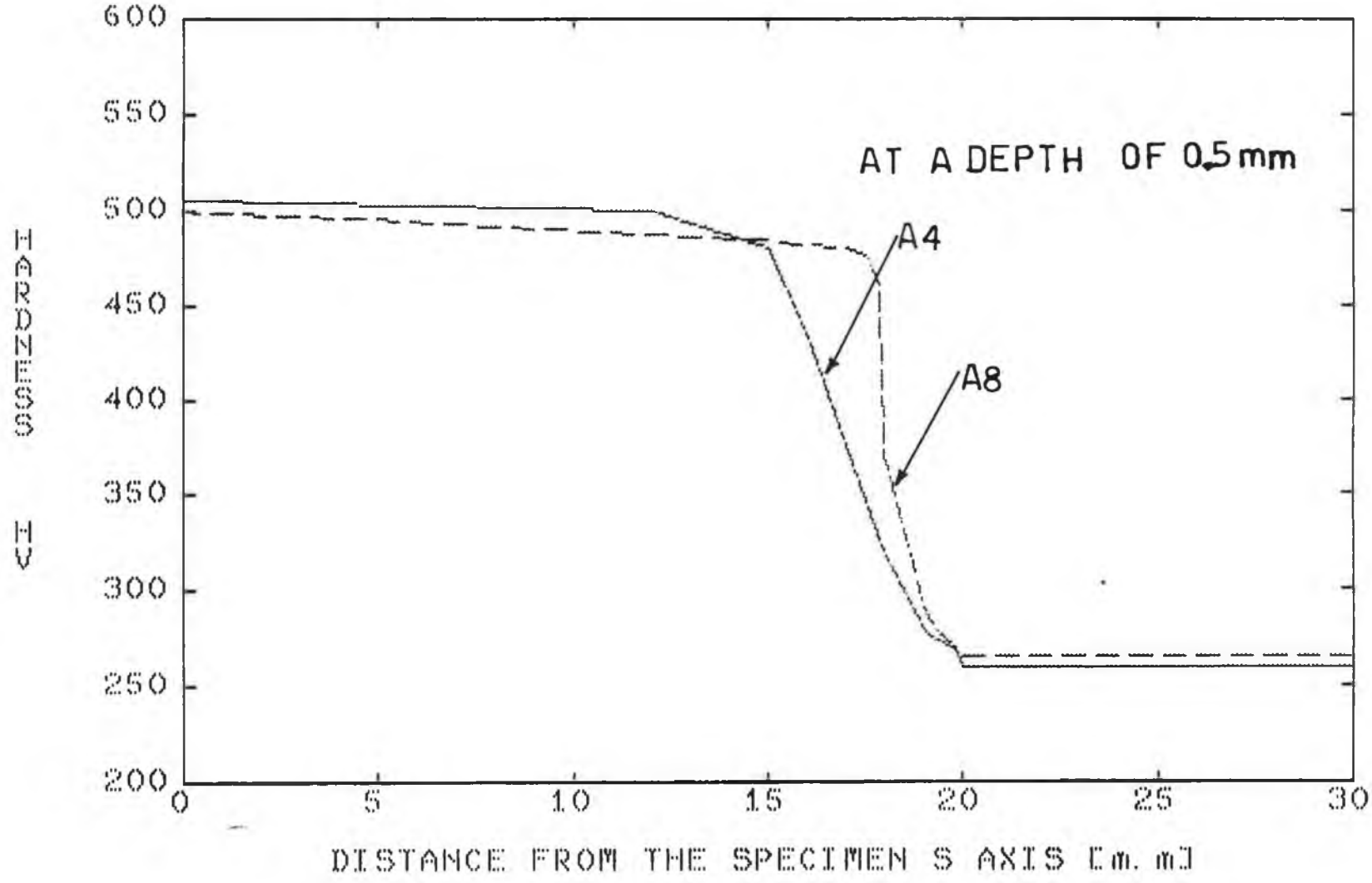

Fig. 69 Comparison between the hardness variation for specimens A4 and A8 which have different thickness.

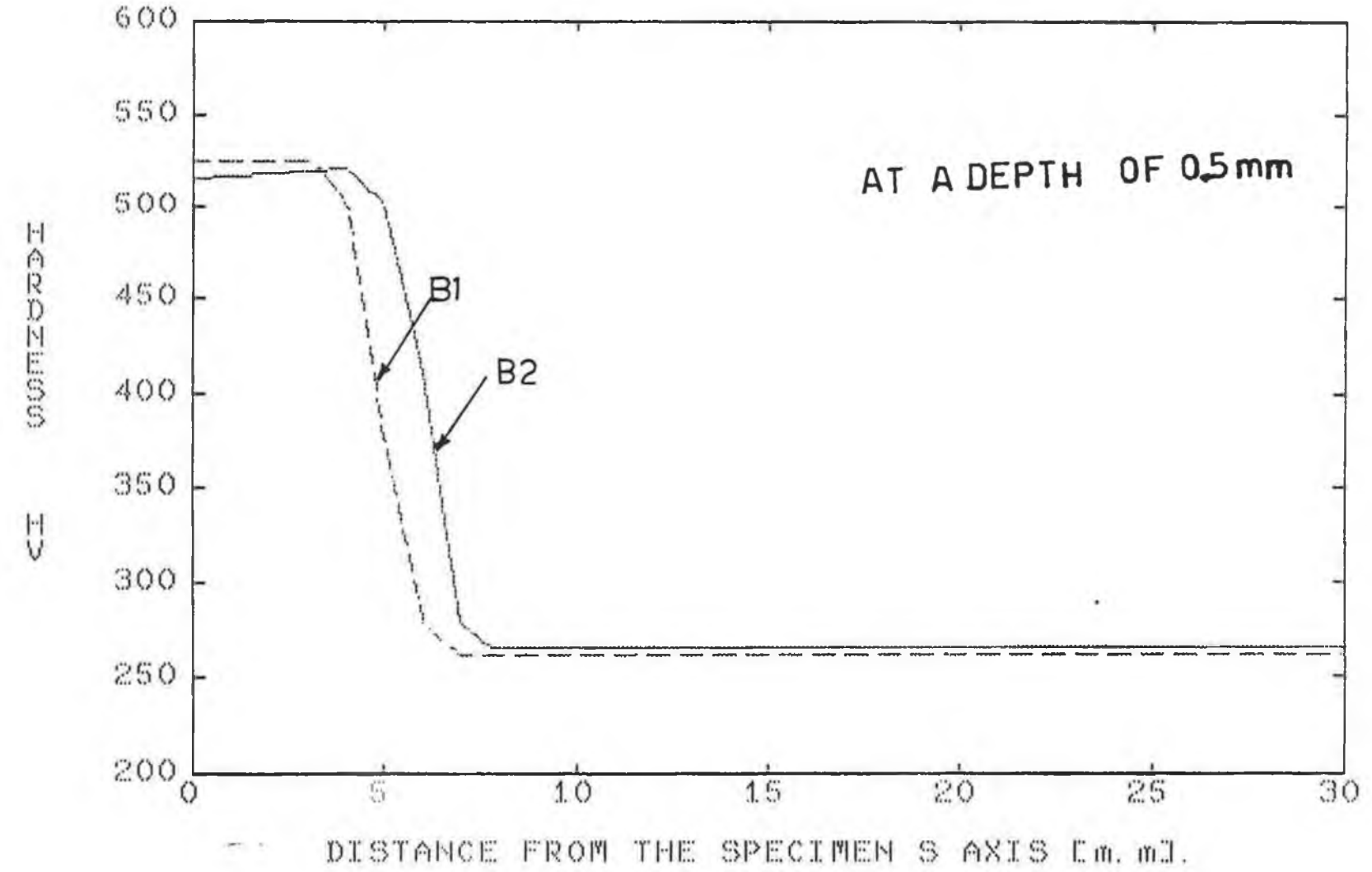

Fig. 70 Comparison between the hardness variation for specimens B1 and B2 which have different thickness.

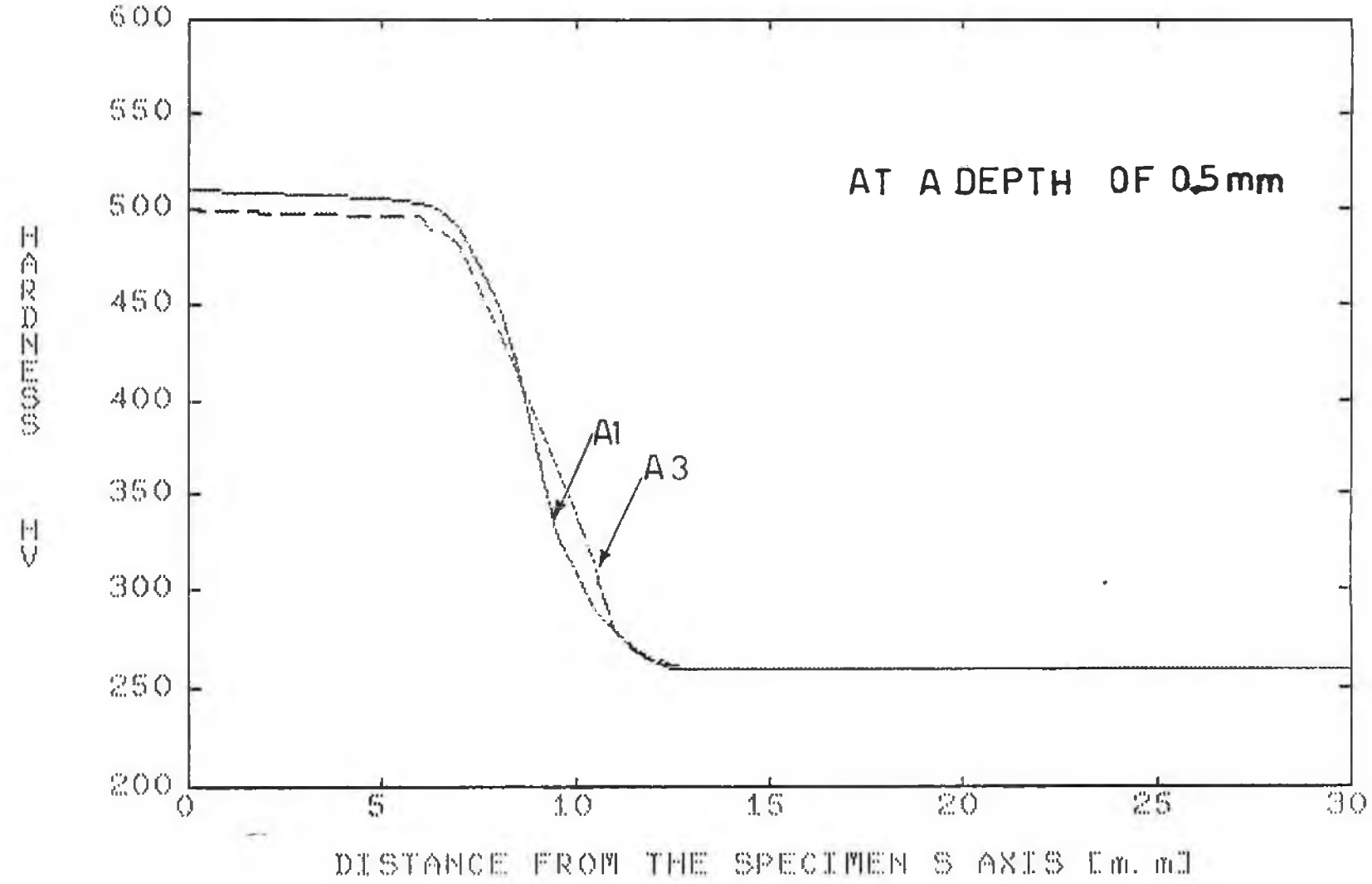

Fig. 71 Comparison between the hardness variation for specimens A1 and A3 which have different bead length.

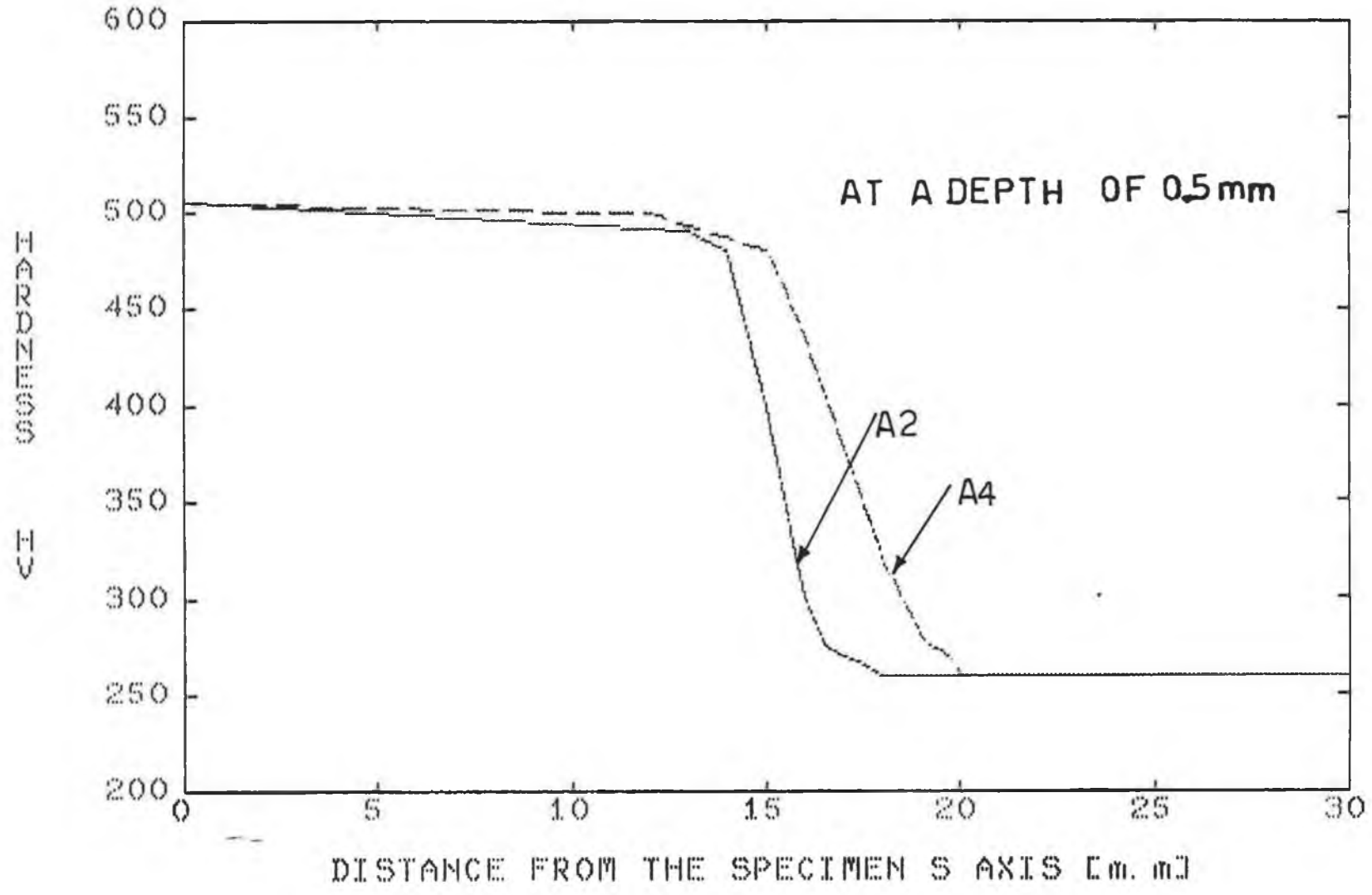

Fig. 72 comparison between the hardness variation for specimens A2 and A4 which have different bead length.

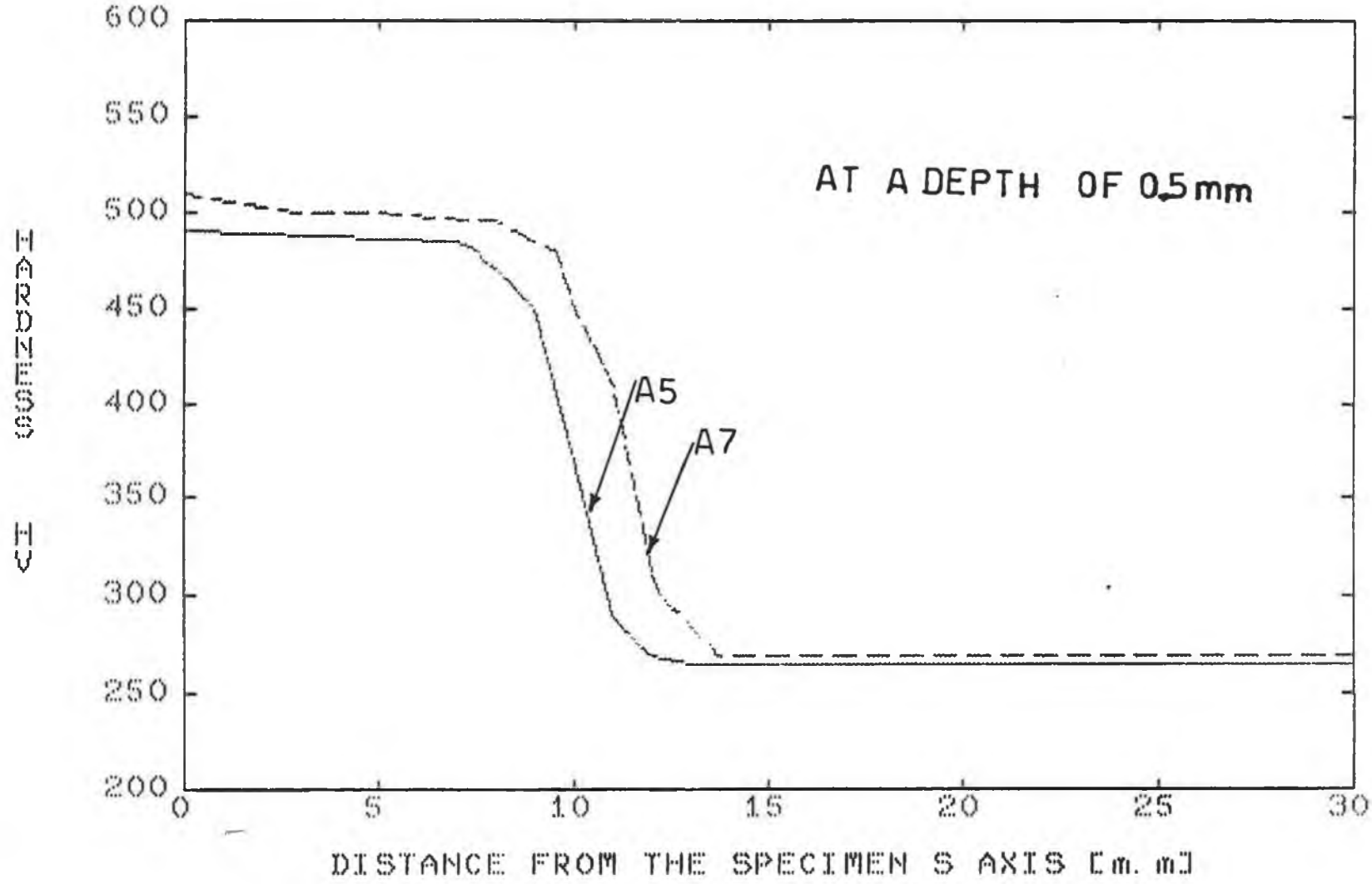

Fig. 73 Comparison between the hardness variation for specimens A5 and A7 which have different bead length.

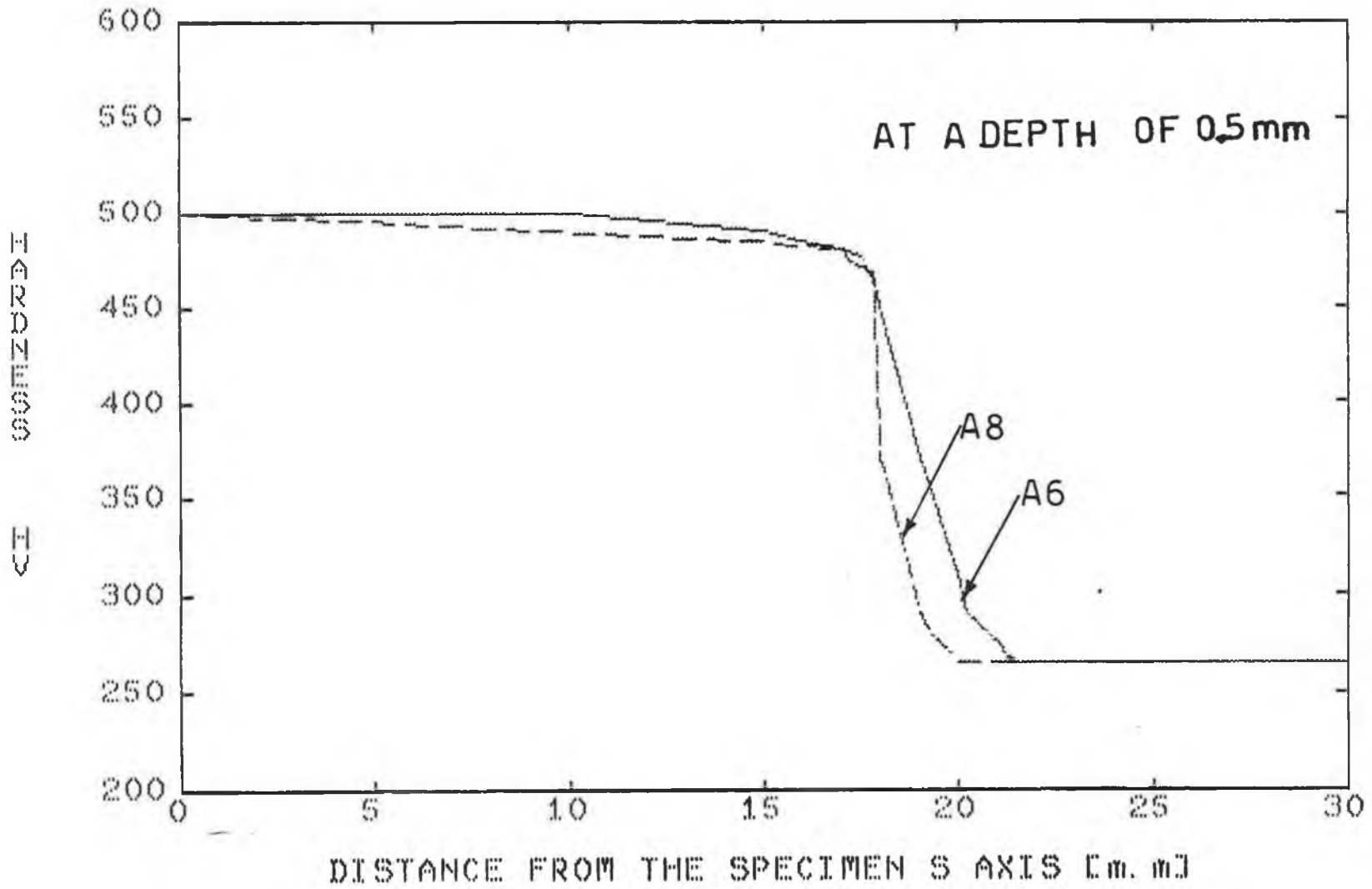

Fig.74 Comparison between the hardness variation for specimens A6 and A8 which have different bead length.

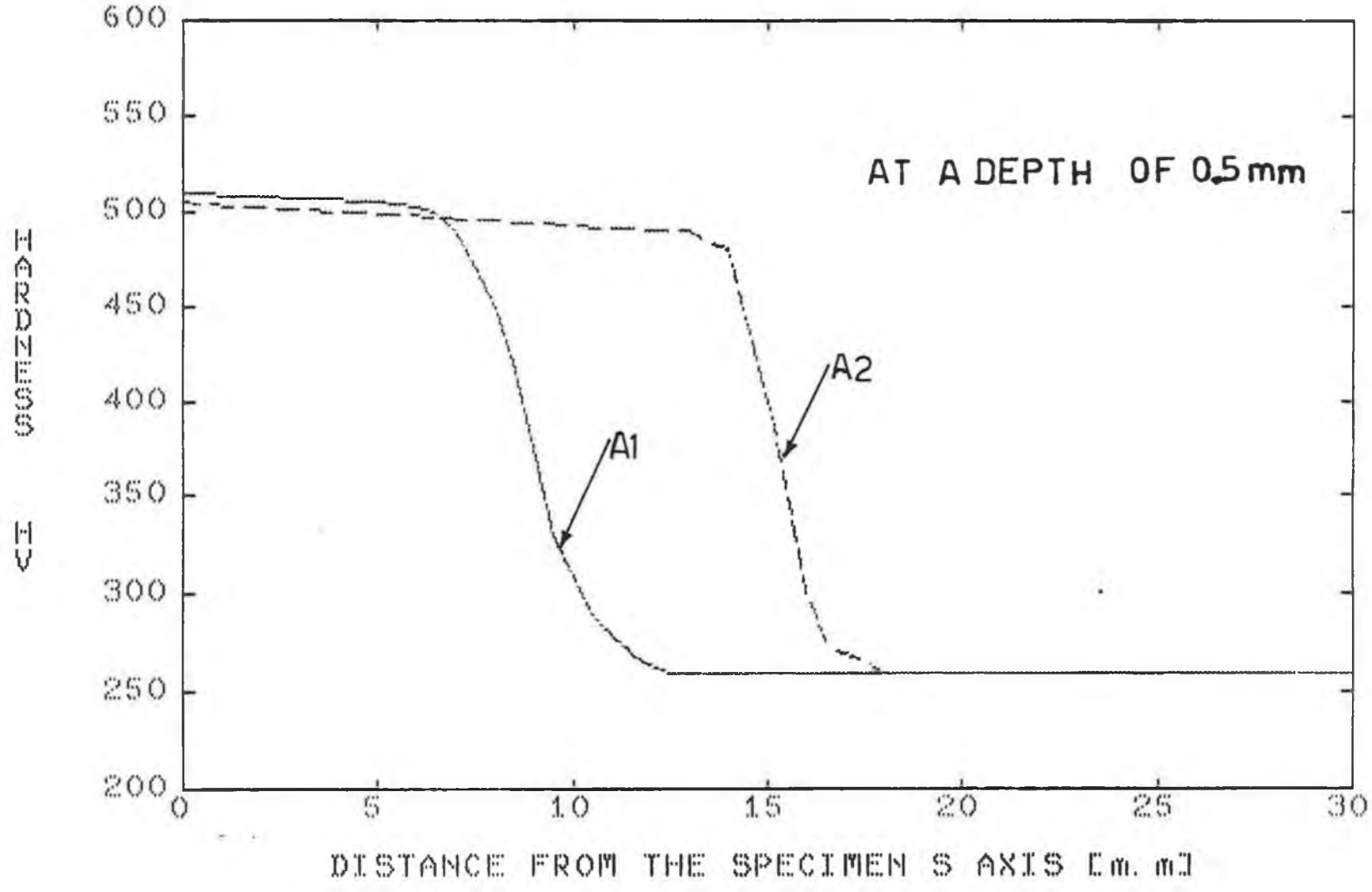

Fig. 75 Comparison between the hardness variation for specimens A1 and A2 which have different bead width.

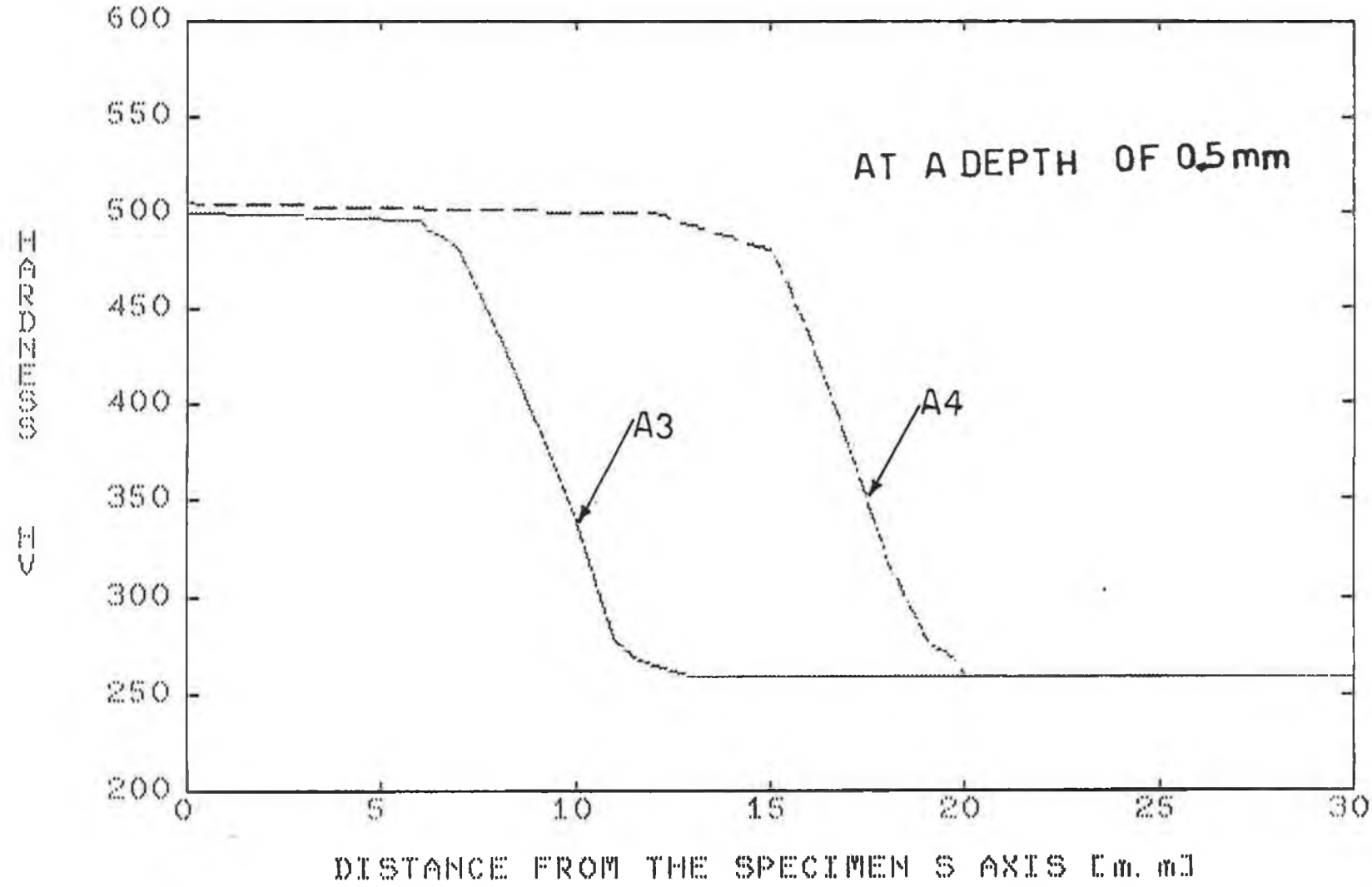

Fig. 76 Comparison between the hardness variation for specimens A3 and A4 which have different bead width.

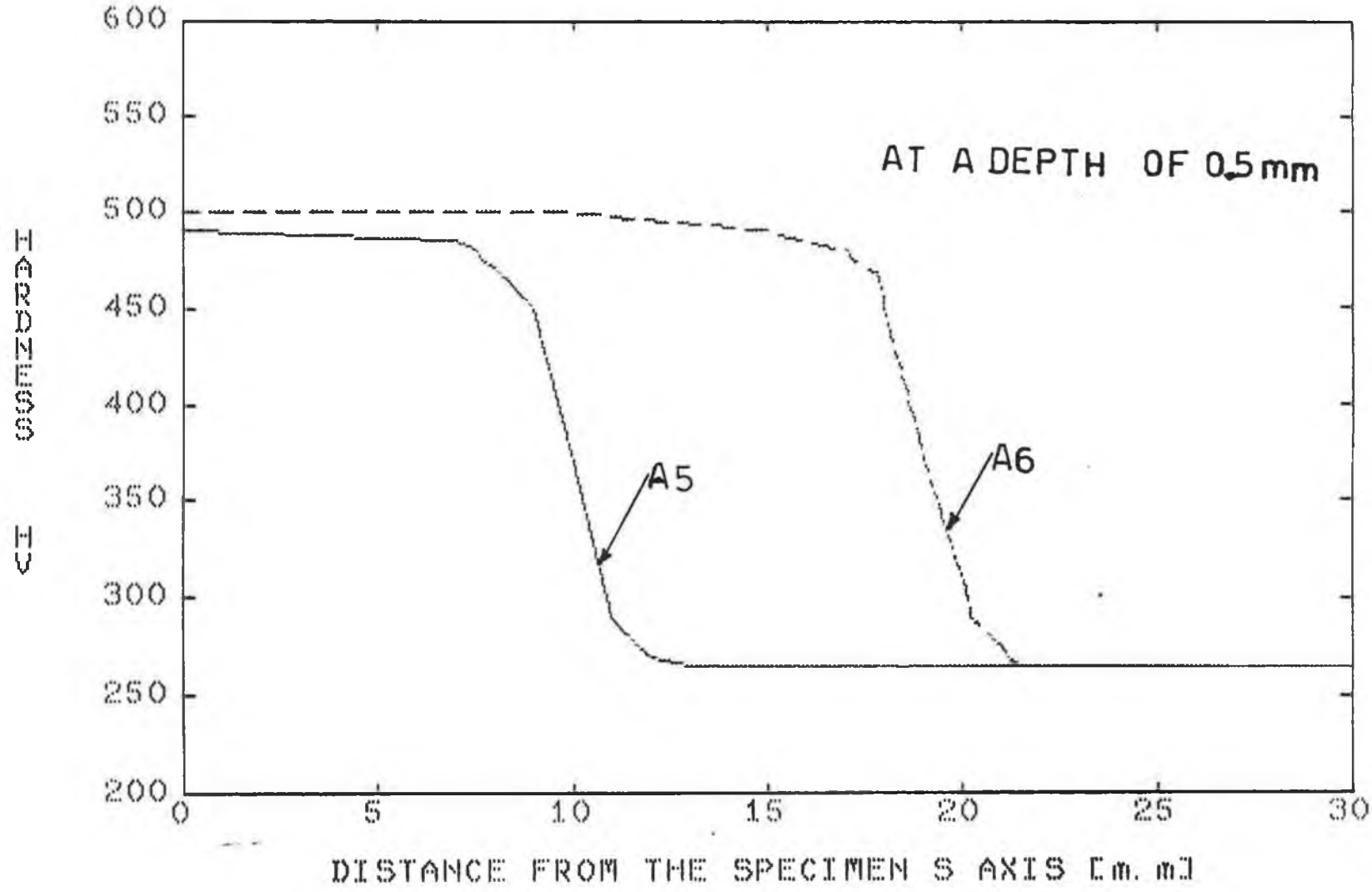

Fig. 77 Comparison between the hardness variation for specimens A5 and A6 which have different bead width.

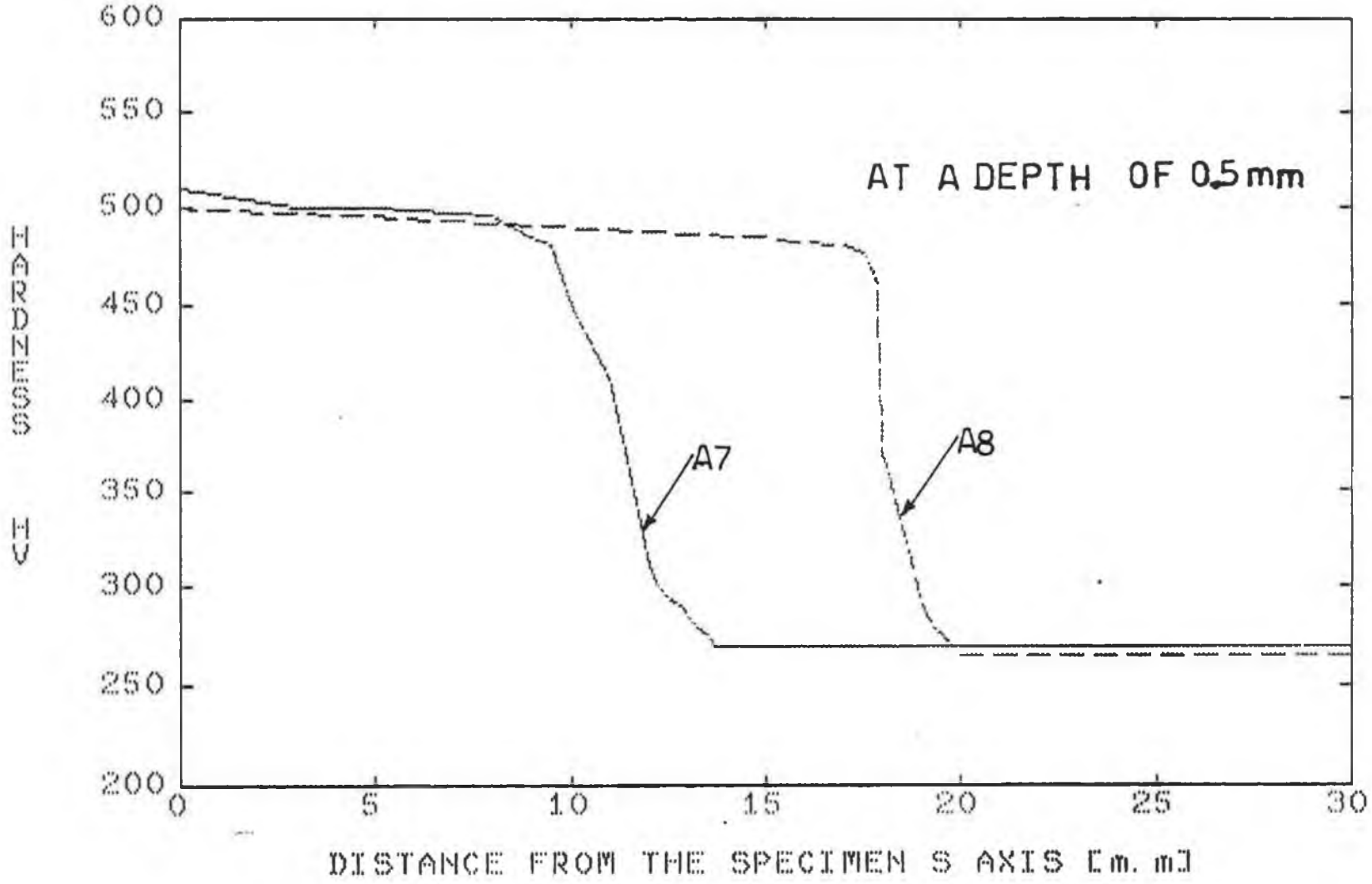

Fig. 78 Comparison between the hardness variation for specimens A7 and A8 which have different bead width.

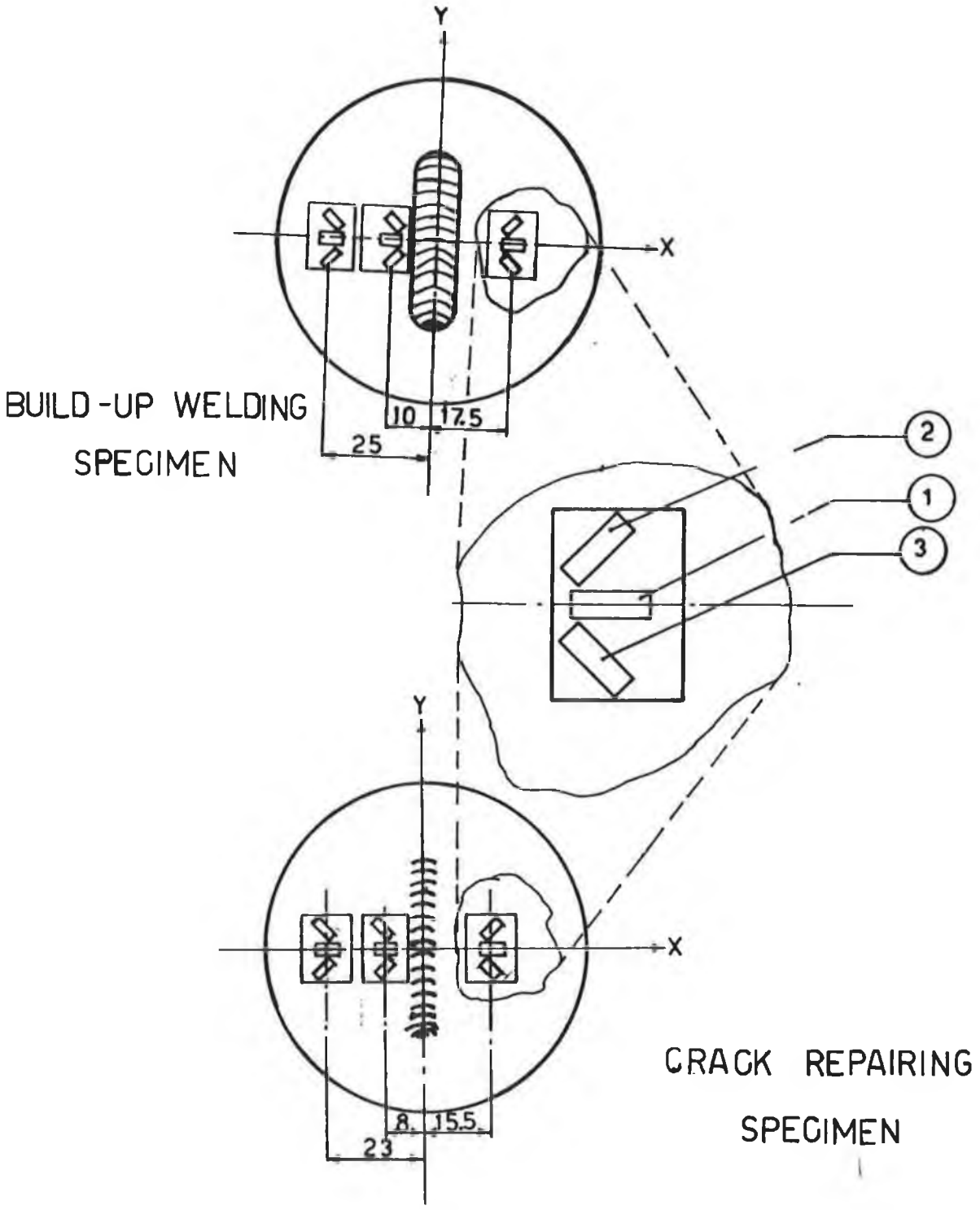

Fig. 79 Illustration sketch for strain gauges positions on the specimen's surface.

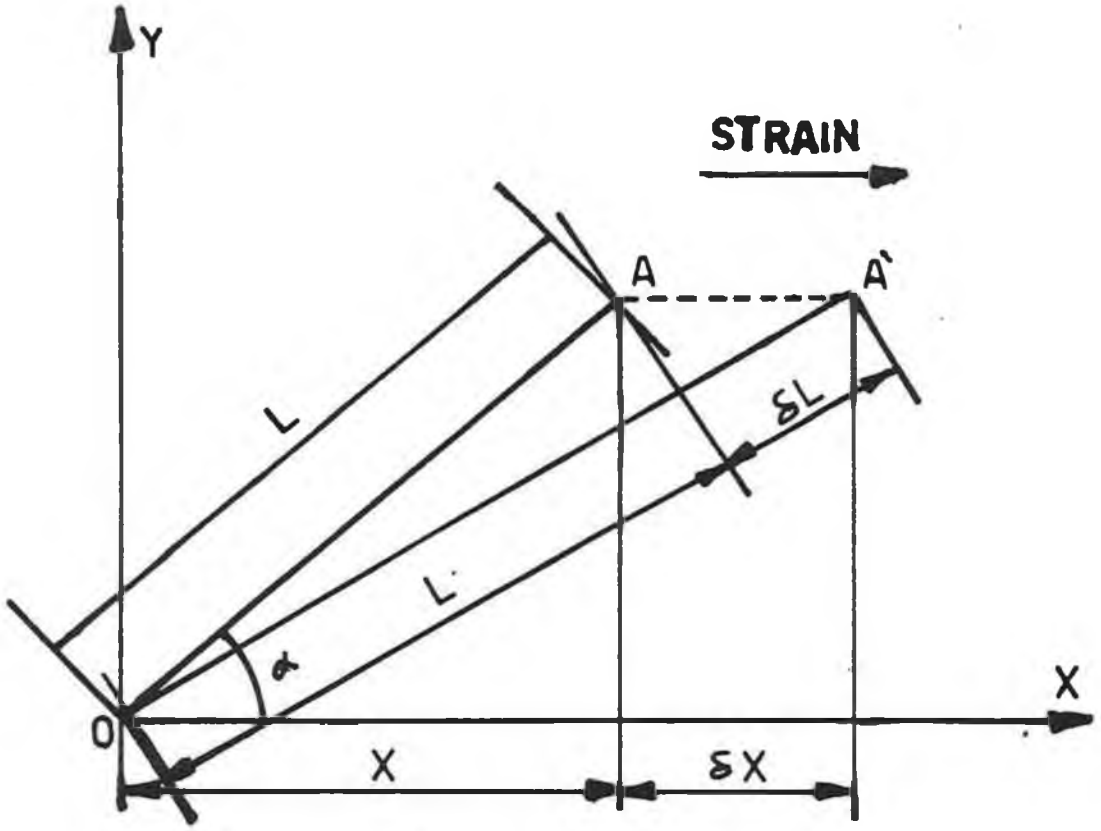

Fig. 80 Illustration sketch to show the strain in x direction.

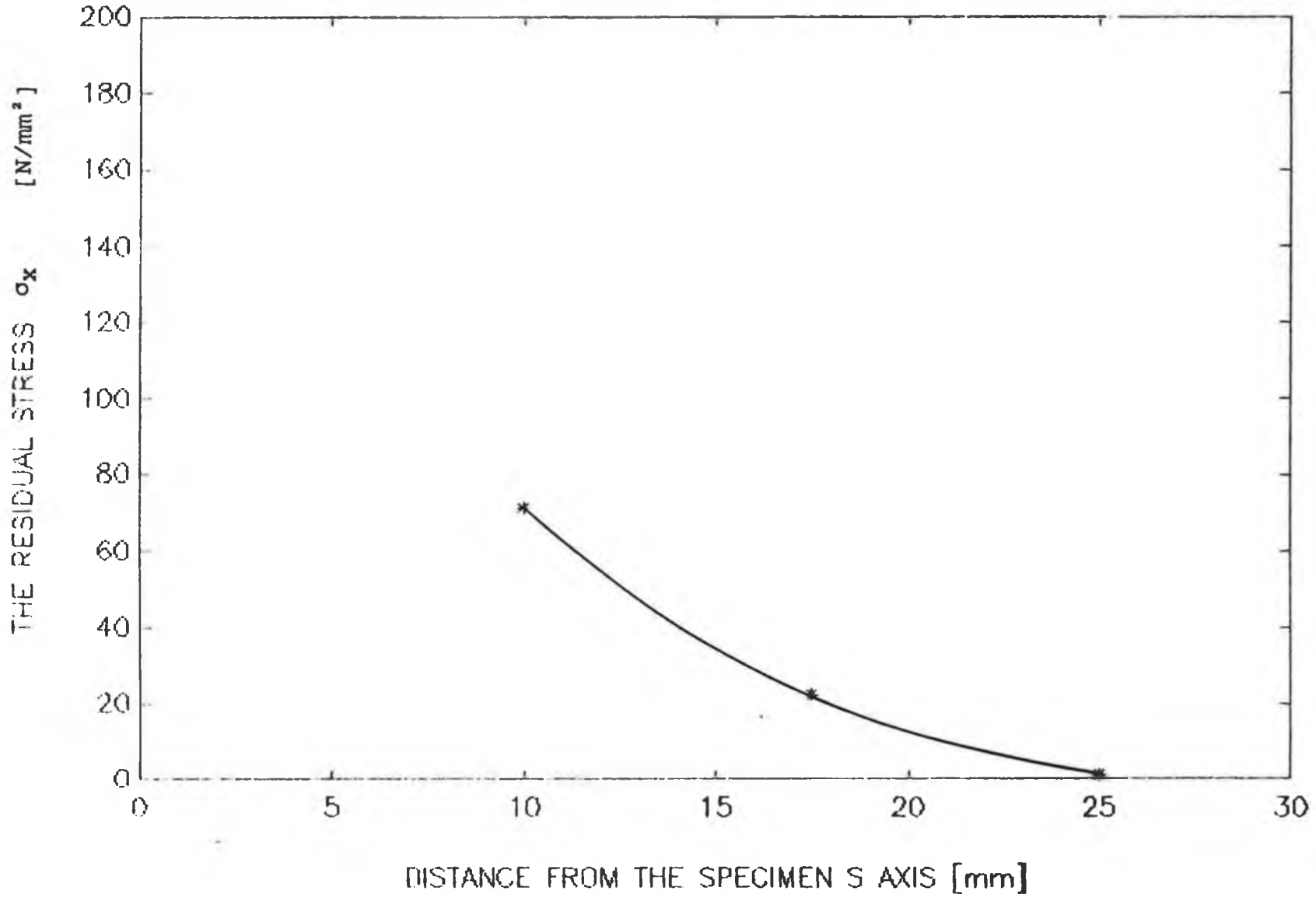

Fig. 81 The distribution of the residual stress σ_x along X axis, for specimen A3.

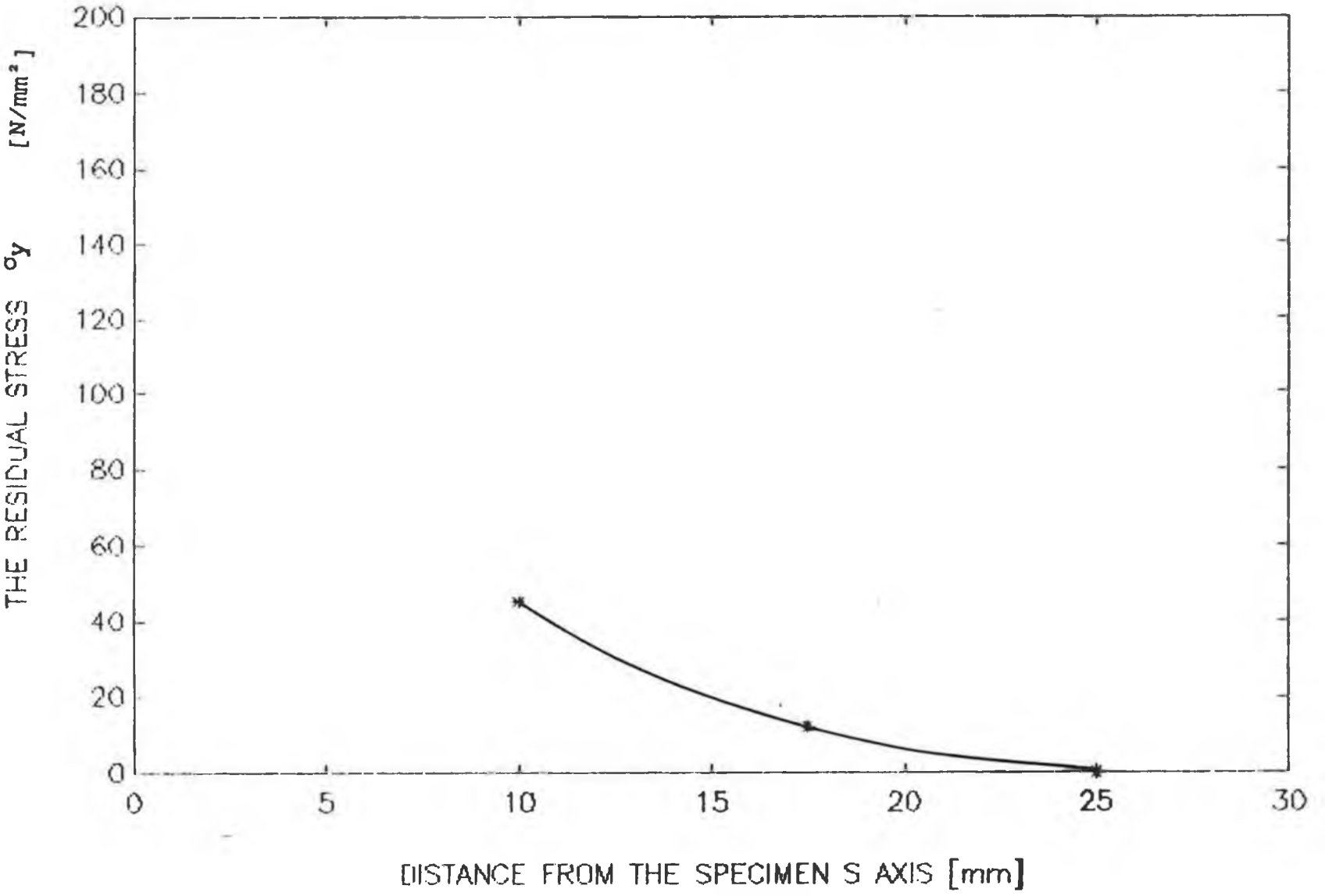

Fig. 82 **The distribution of the residual stress σ_y along X axis, for specimen A3.**

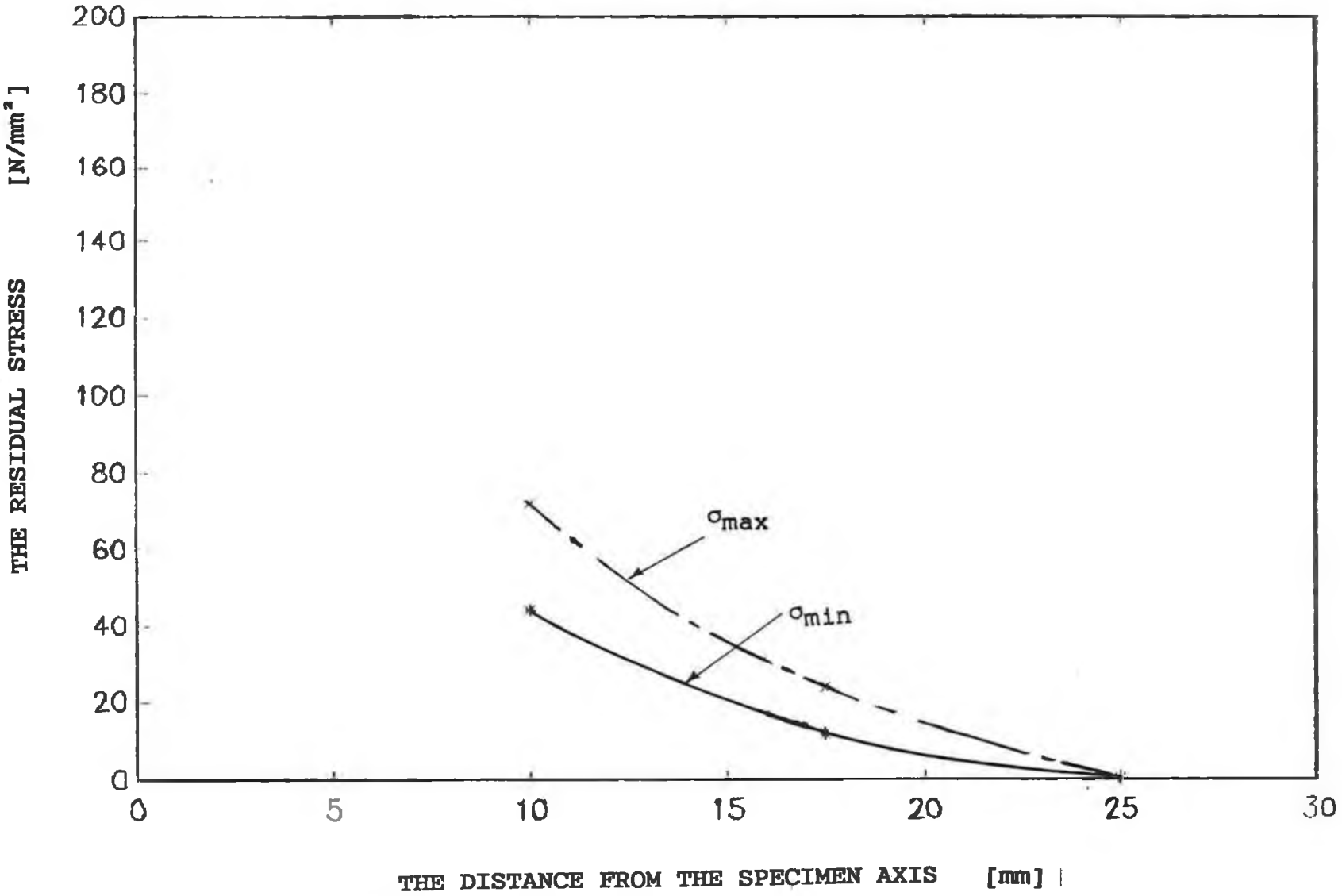

Fig. 83 The distribution of the principal residual stresses along X axis, for specimen A3.

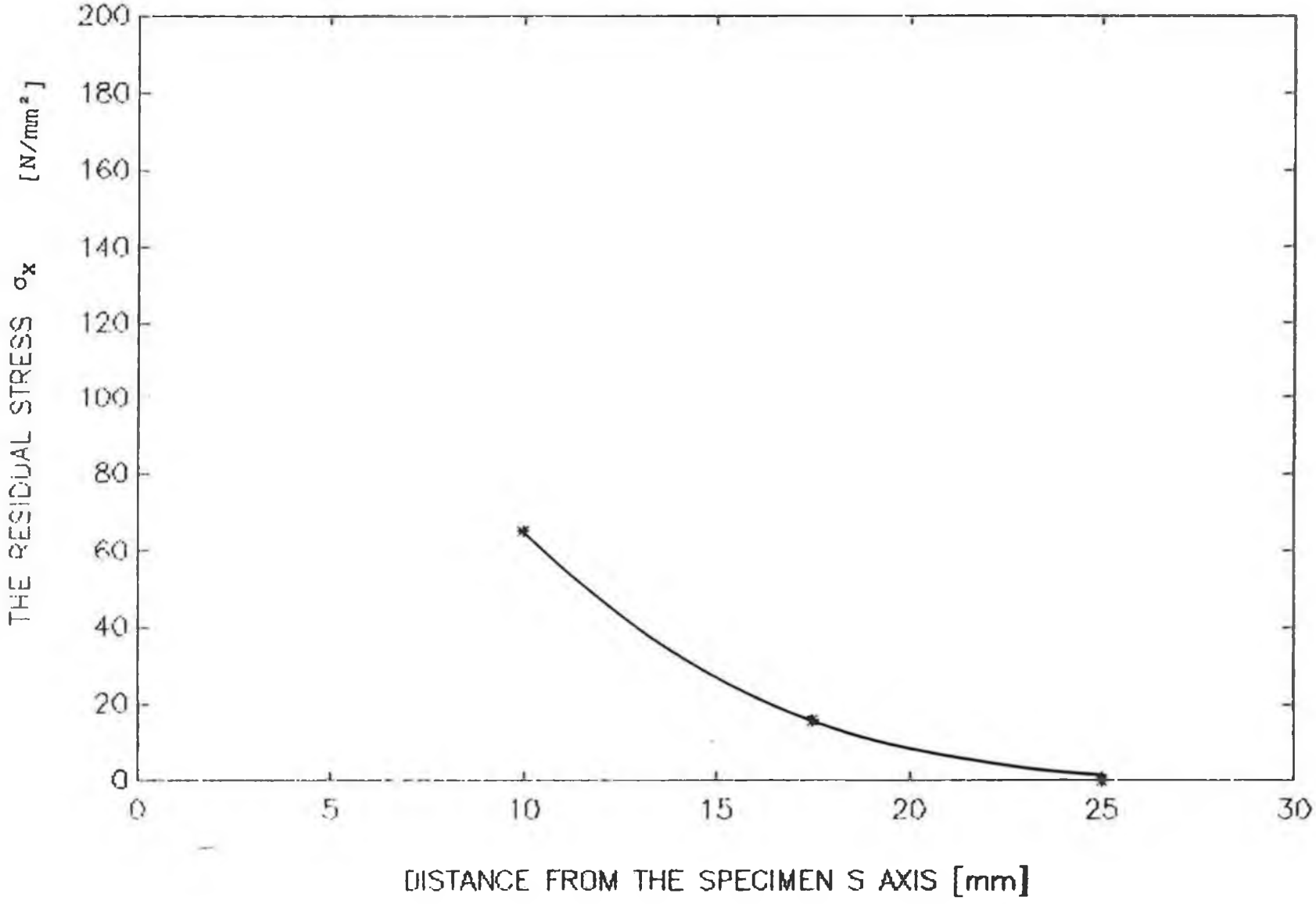

Fig. 84 The distribution of the residual stress σ_x along X axis, for specimen B1.

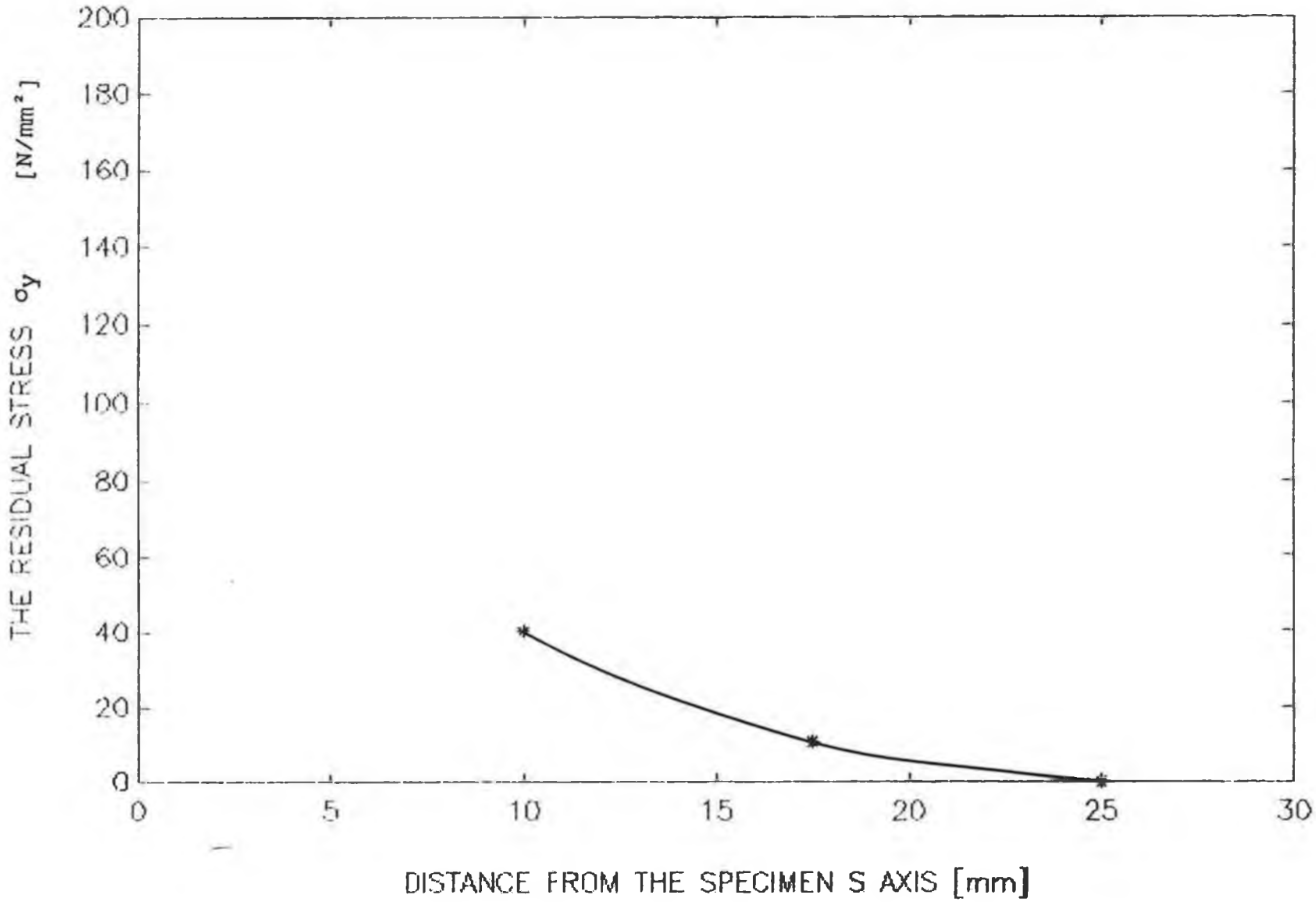

Fig. 8 5 The distribution of the residual stress σ_y along X axis, for specimen B1.

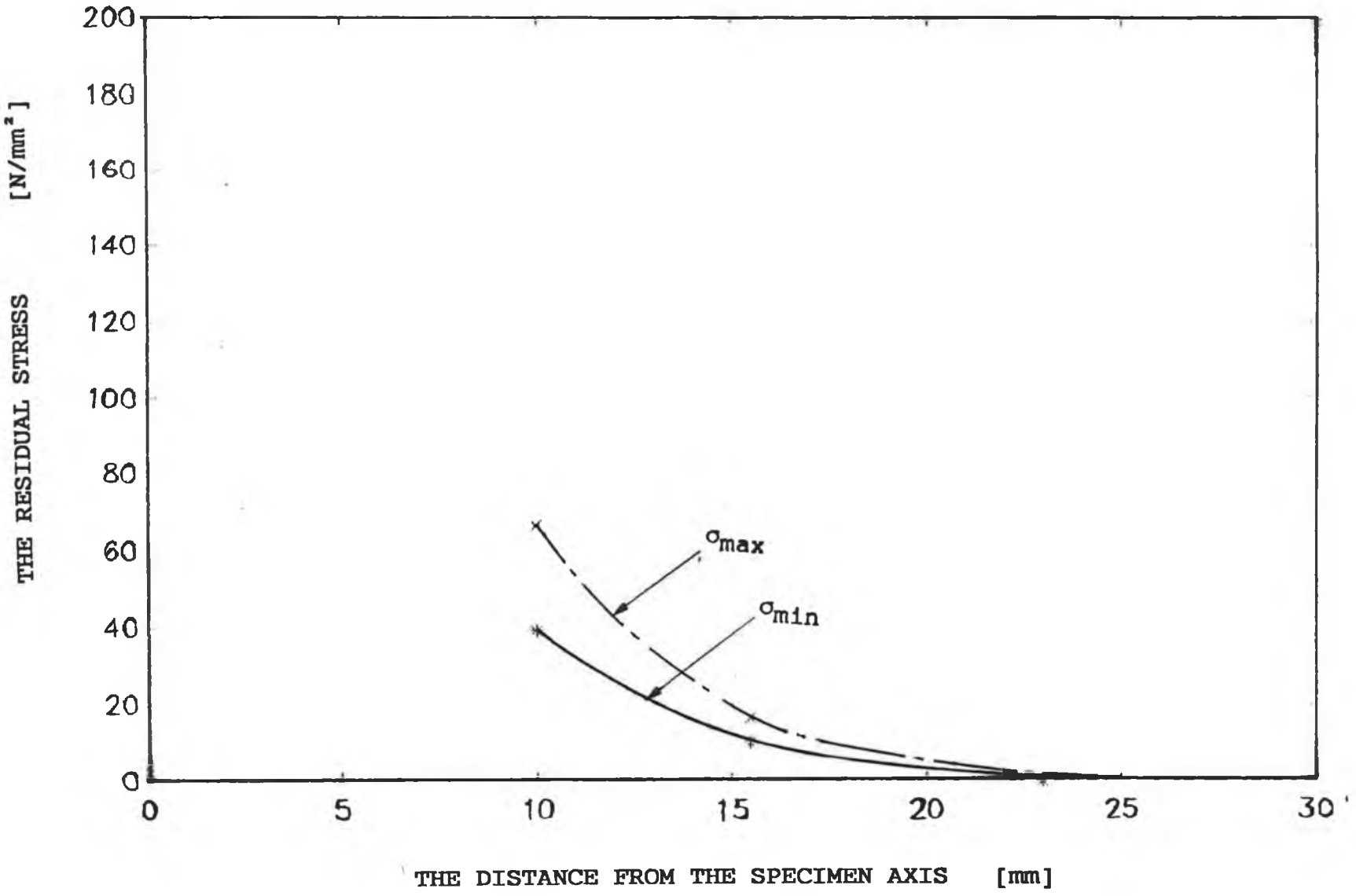

Fig. 86 The distribution of the principal residual stresses along X axis, for specimen B1.

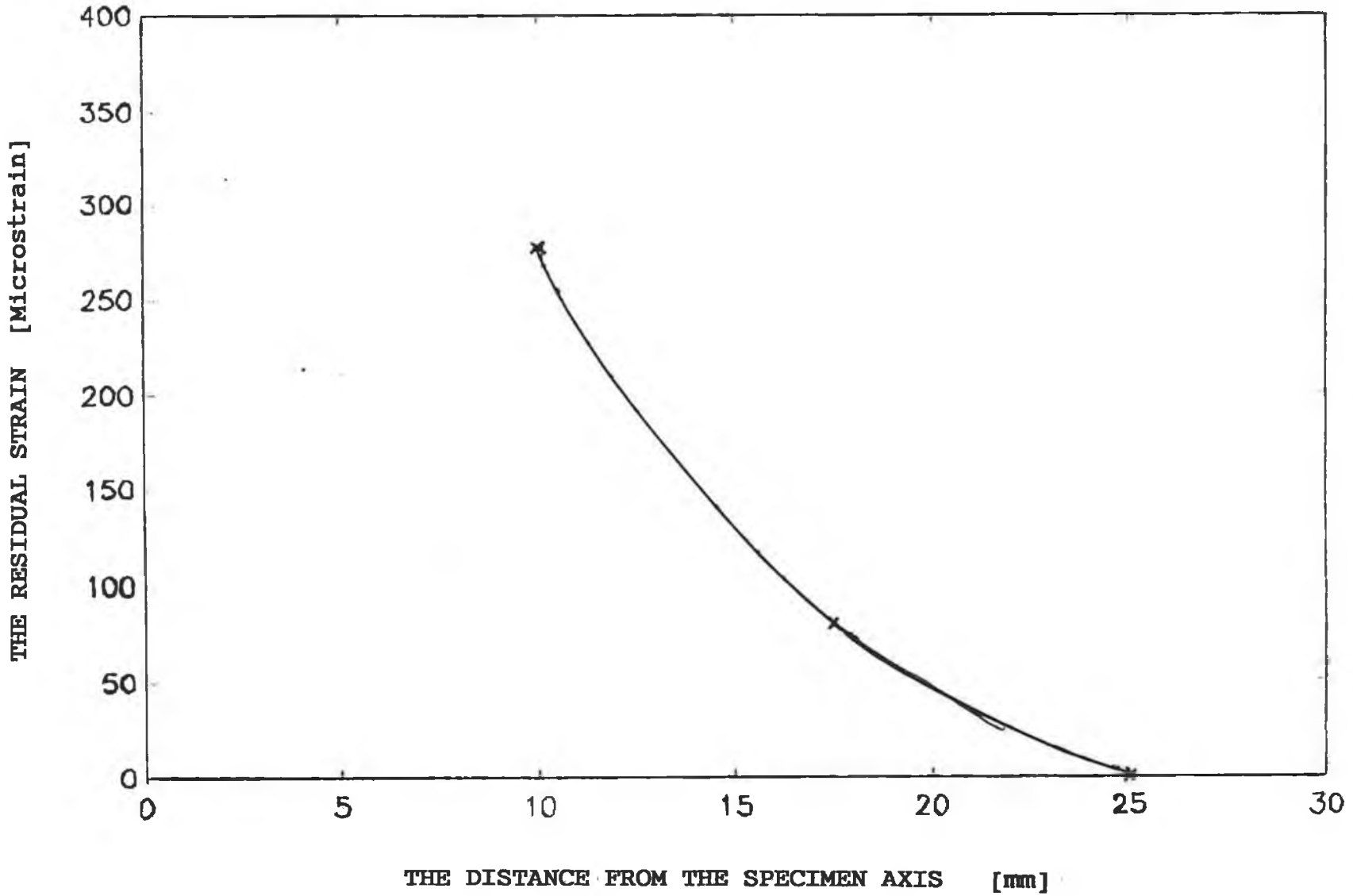

Fig. 87 The distribution of the residual strain along X axis, for specimen A1.

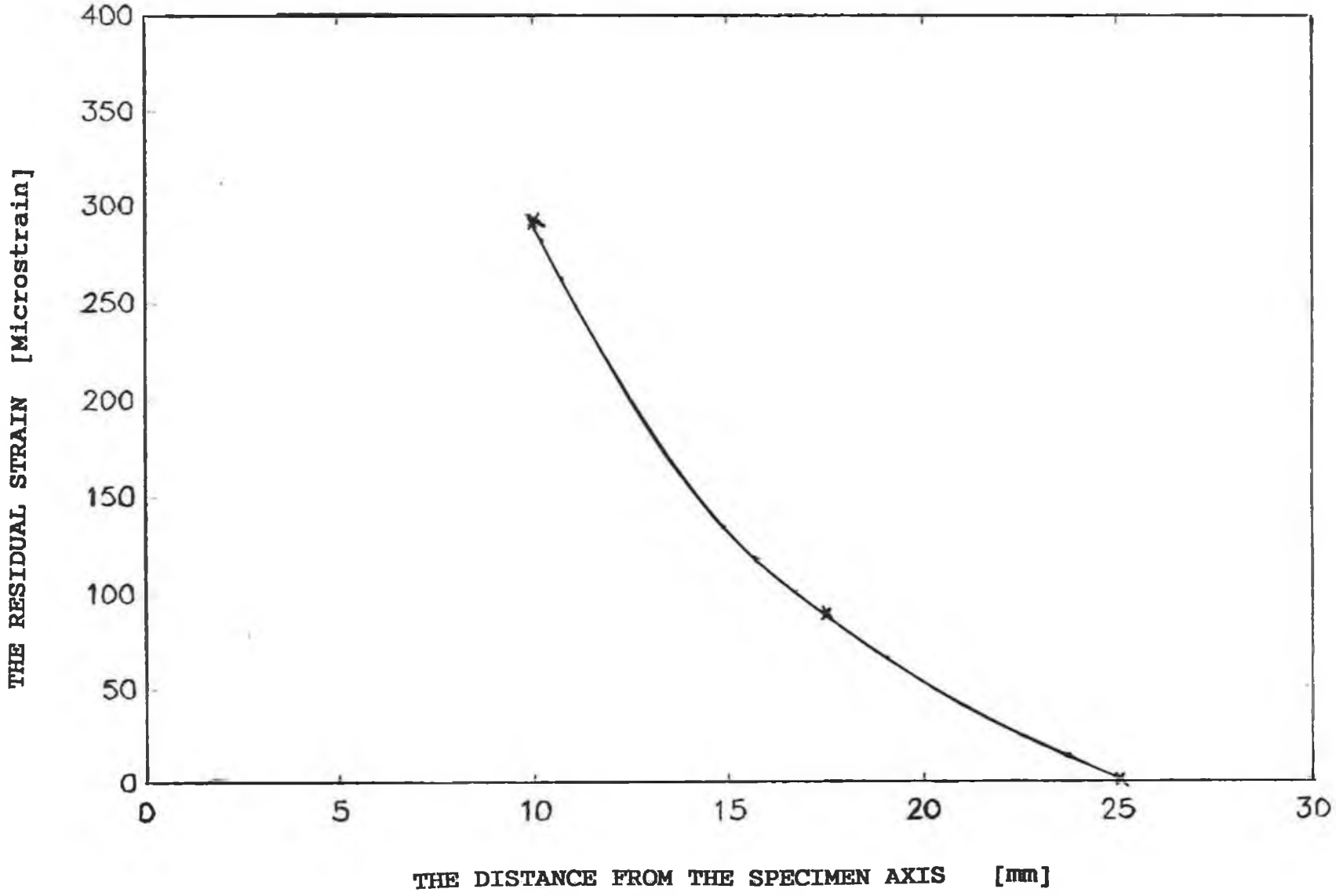

Fig. 88 The distribution of the residual strain along x axis, for specimen A3.

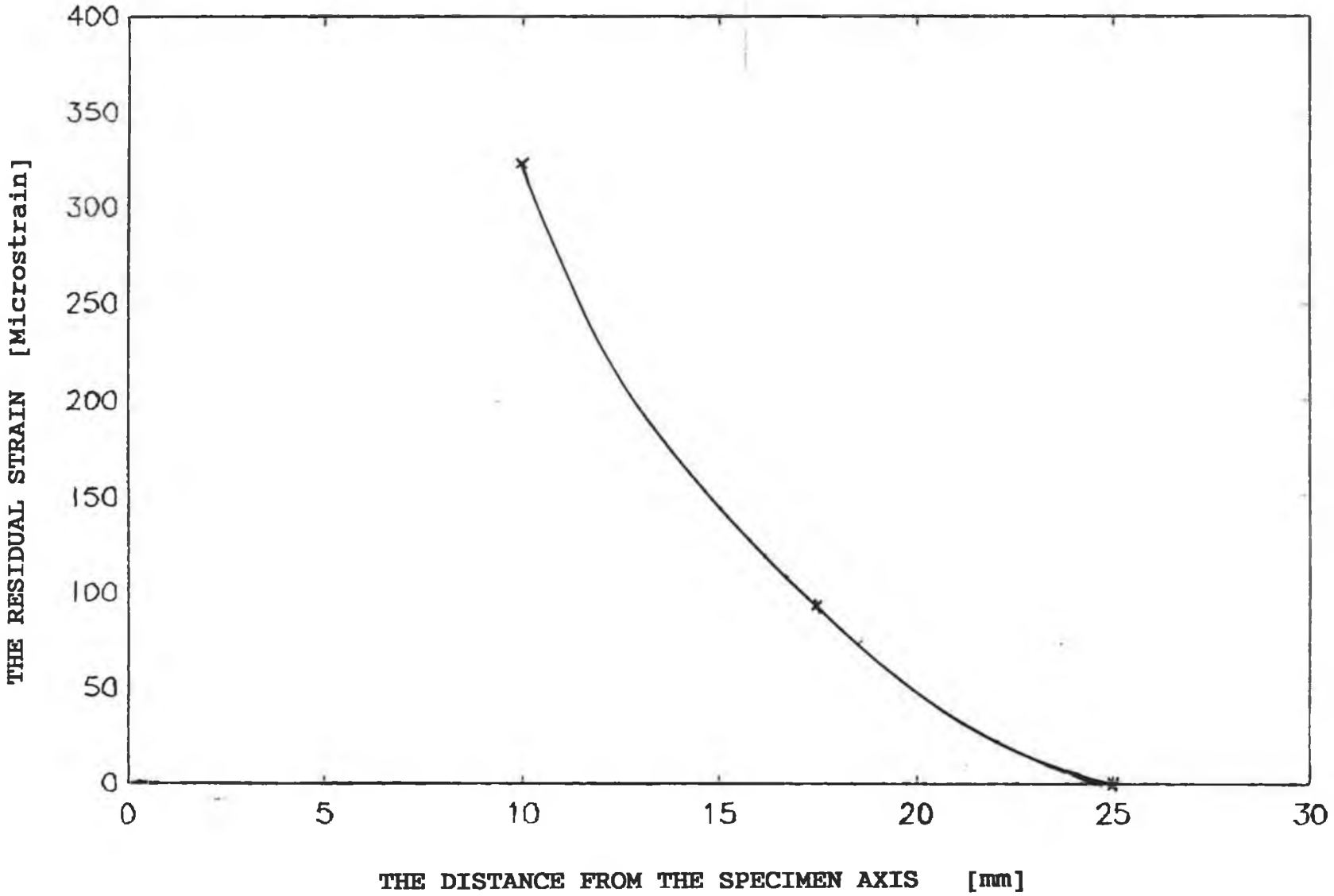

Fig. 89 The distribution of the residual strain along X axis, for specimen A5.

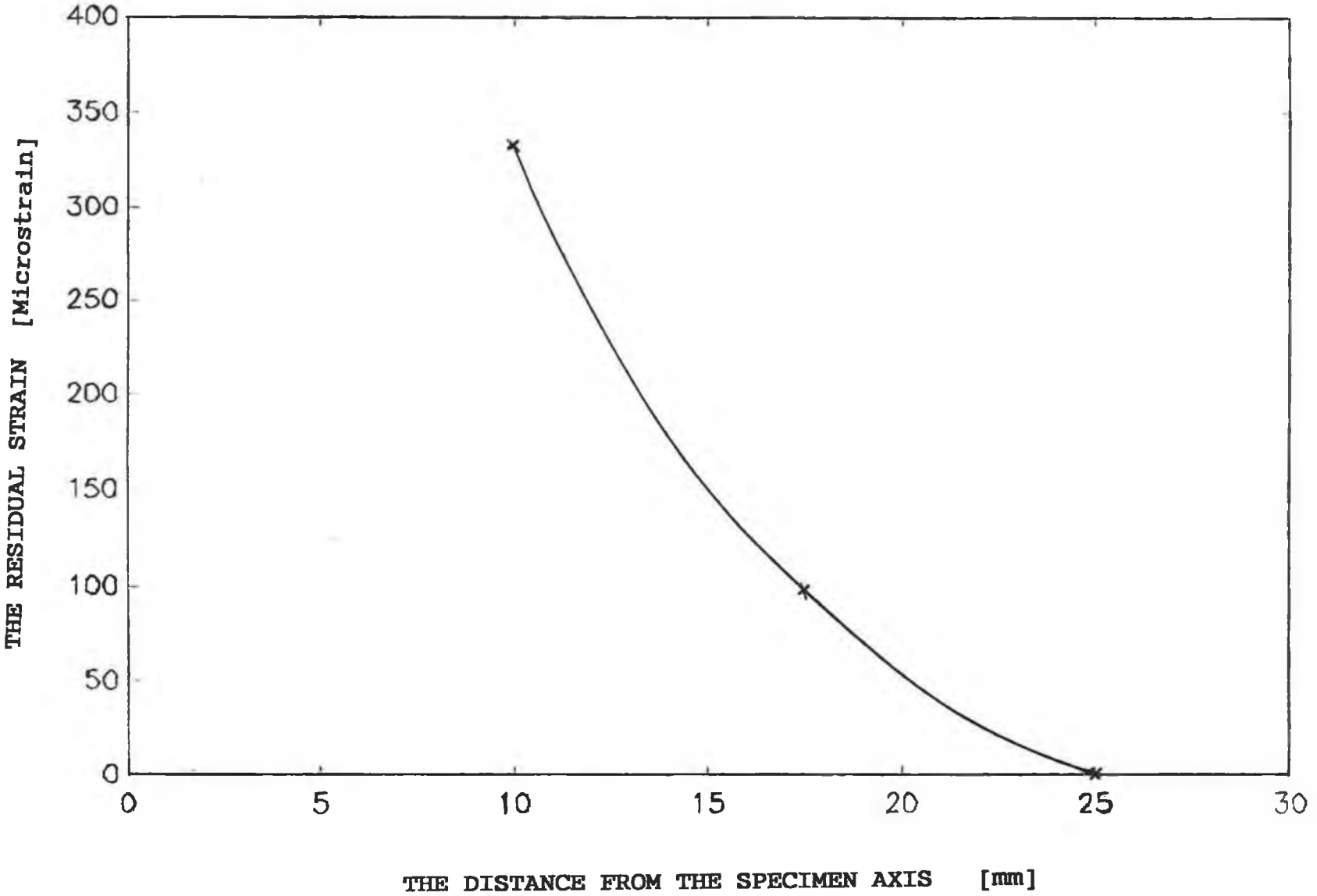

Fig. 90 The distribution of the residual strain along X axis, for specimen A7.

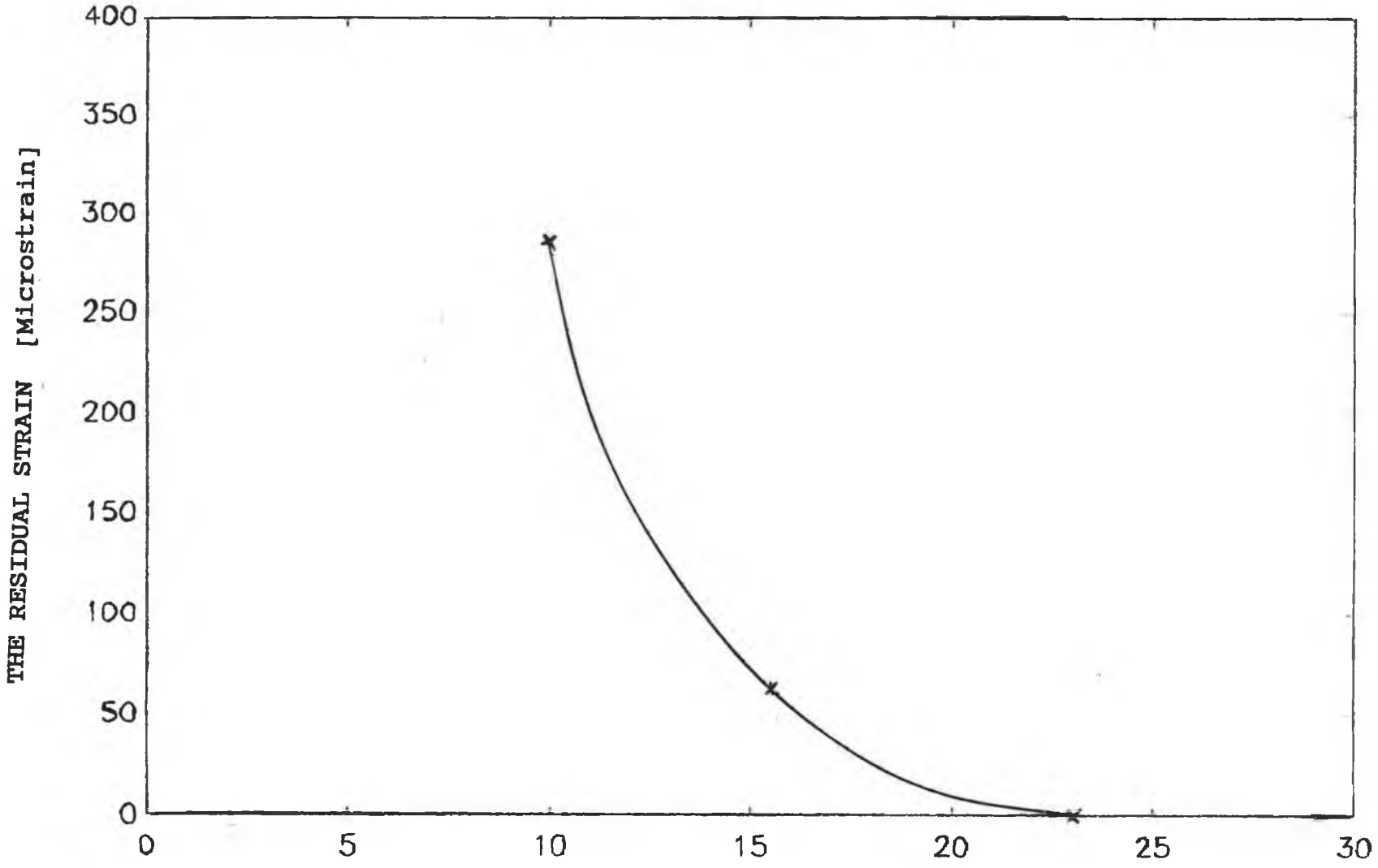

Fig. 91 The distribution of the residual strain along X axis, for specimen B1.

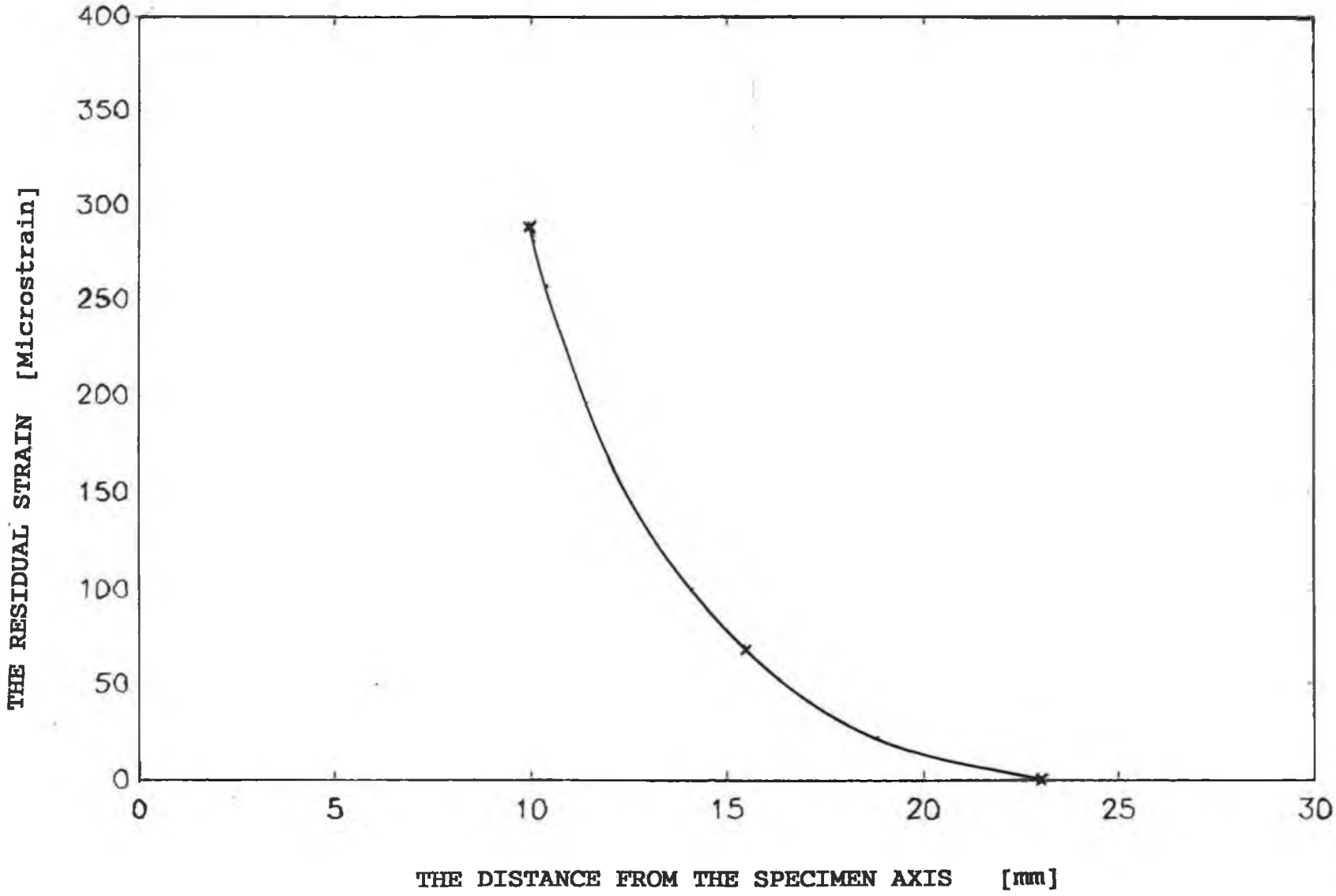

Fig. 92 The distribution of the residual strain along X axis, for specimen B2.

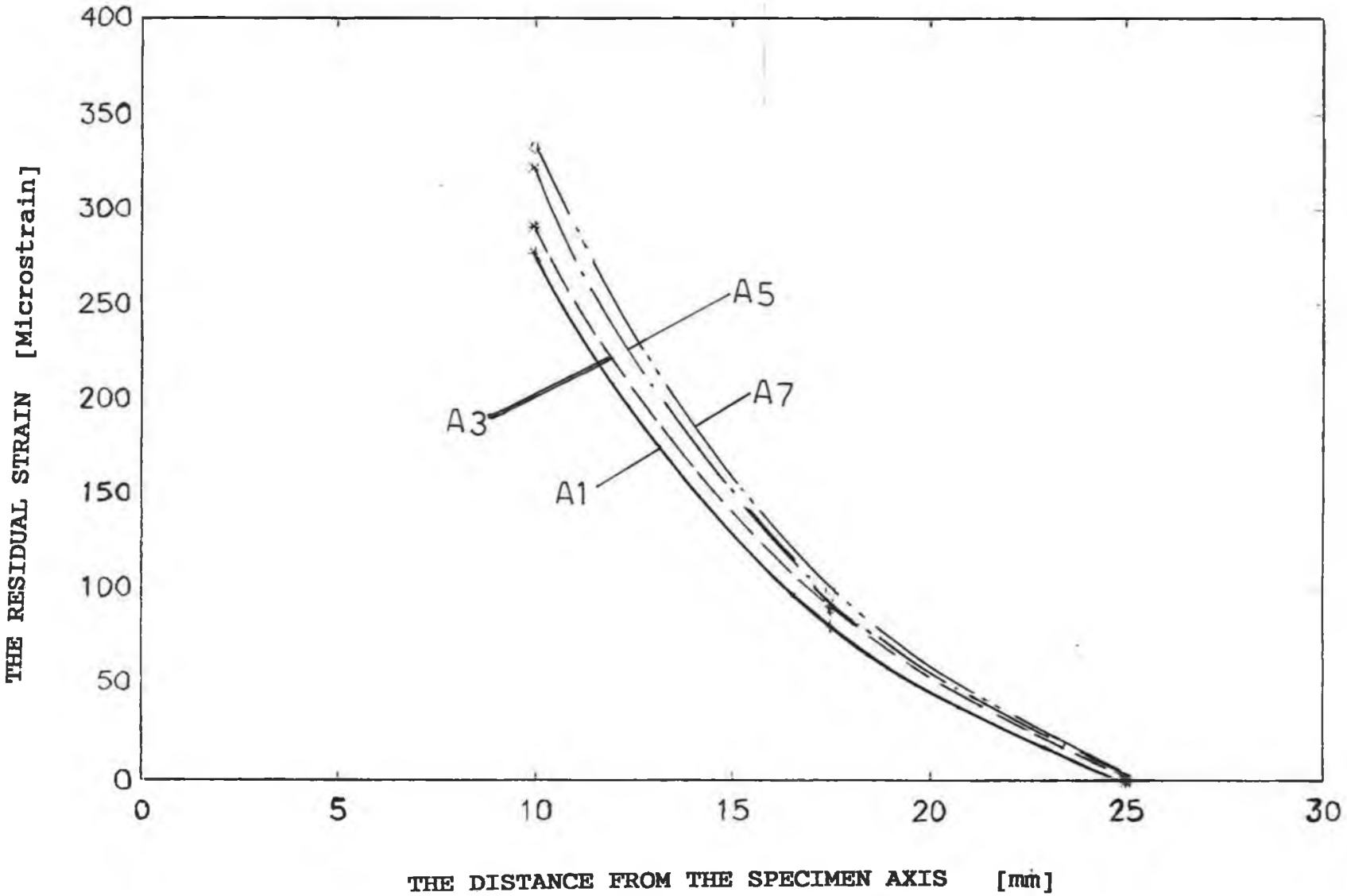

Fig. 93 The distribution of the residual strain along X axis, for specimens A1, A3, A5, and A7.

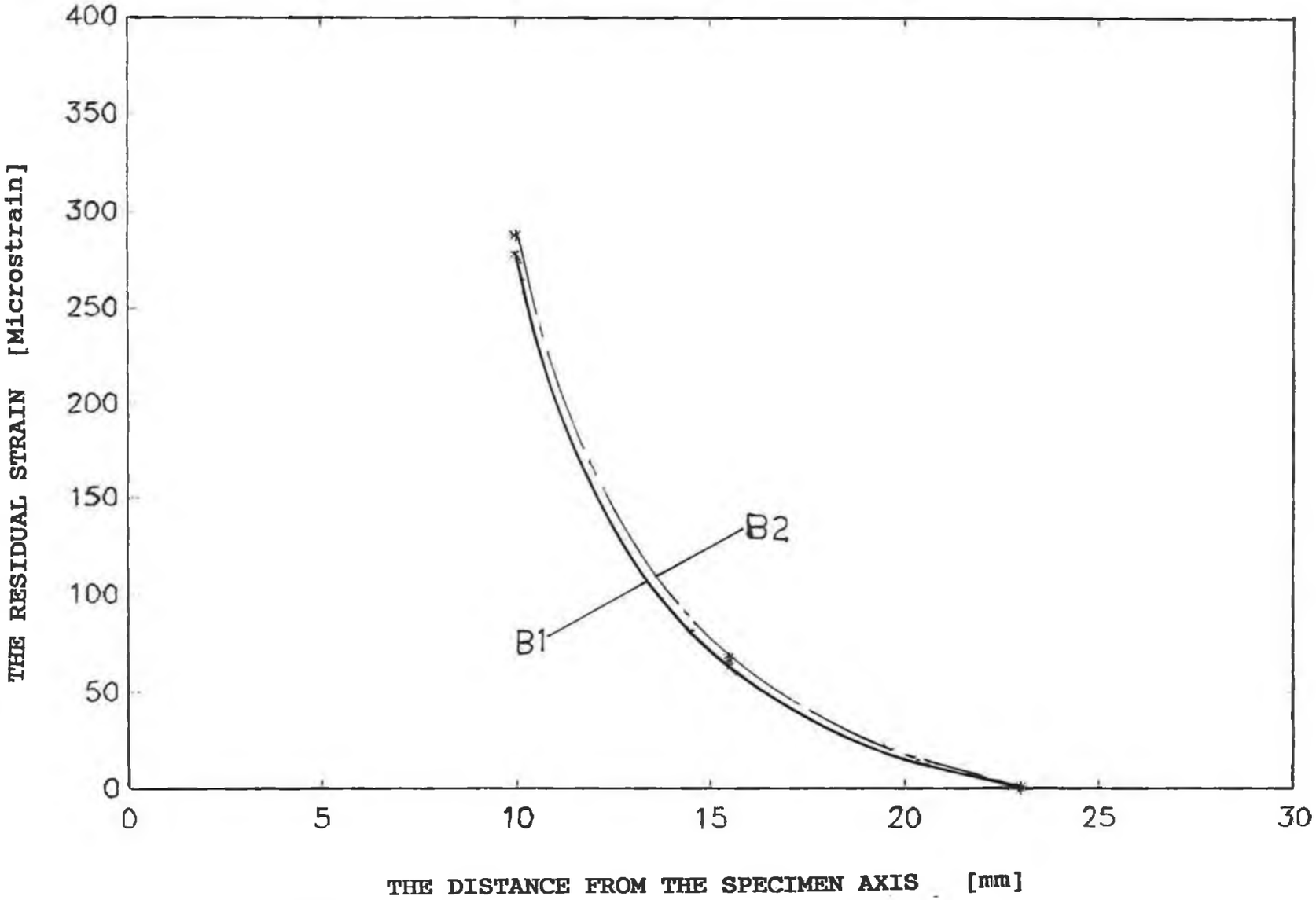

Fig. 94 The distribution of the residual strain along X axis, for specimens B1 and B2.

CHAPTER 4

DISCUSSIONS

4.1 METALS MICROSTRUCTURE

The metal microstructure has been inspected in the welding zone for three different conditions [before and after heat treatment (1) and (2)].

In the first condition, after welding and before applying any kind of heat treatment, the metal microstructure is completely martensite. Which means, that after welding has been completed, the specimen has been cooled at room temperature and martensite has been formed due to the fast cooling speed.

After heat treatment (1), the metal microstructure becomes tempered martensite with low percentage of feritte due to this type of heat treatment. The very slow cooling rate leads to transformation of the martensite and the metal microstructure becomes completely tempered martensite with low percentage of feritte.

After heat treatment (2), the metal microstructure consists of tempered martensite, ferrite, and precipitated carbide. This inspection demonstrates that high temperature in heat treatment (2) and the very slow cooling rate, leads to this type of metal microstructure. This slow cooling rate has given chance to separate the carbide and produce ferrite and precipitated carbide, in addition to the tempered martensite.

These above results prove that the formation of tempered martensite after heat treatment (1) has improved the tensile strength and reduced the hardness in the welding zone by about 15 % when compared with the hardness under as welded condition. The most significant observation was the existence of the precipitated carbide after heat treatment (2), which would result in deterioration of toughness [43]. However, the results show an evidence that the formation of the precipitated carbide after heat treatment (2) has great effect on reducing the hardness in the welding zone by about 40 % when compared with the hardness for as welded condition. The resulting hardness is only marginally greater than the hardness in the parent metal. However, this formation decreased the

tensile strength by about 10 % when compared with the tensile strength of the specimen under as welded condition.

4.2 HARDNESS TESTING

The hardness variation across the specimen axis has been measured for all different types of specimens, at different depths from the specimen surface and for all three conditions [before applying any kind of heat treatment and after heat treatment (1) and (2)].

The results of this testing show that after welding has been completed, a hard area has been produced in and near the welding zone. This hard area which has been measured from the axis of the welding pass will be referred to as area (1), and the next area where the hardness has started decreasing to the edge of the specimen will be referred to as area (2).

Experimental results show that after welding the hardness is increased to about 500 HV in area (1), which extends between 8 and 10 mm for specimens A1, A3,

A5, and A7; between 15 and 19 mm for specimens A2, A4, A6, and A8; and between 3 to 5 mm for specimens B1 and B2.

After heat treatment (1), the hardness is decreased to about 440 HV, and the width of this area [area (1)] is diminished by about 1 to 2 mm.

After heat treatment (2), the hardness is reduced to about 300 HV, and the width of this harder area [area (1)] is diminished to about 3 to 5 mm.

Experimental results show that the hardness in area (2) is between 265 - 270 HV before applying any heat treatment, and about 260 HV after heat treatment (1), and between 250 - 255 HV after heat treatment (2). These results demonstrate that there is no significant change in the hardness in this area of the welded component for all three conditions (before and after heat treatment). This observation would apply to the results shown in Figs. 22, 23, 25, 26, 28, 29, 31, 32, 34, 35, 36, 38, 39, 40, 42, 43, 44, 46, 47, 48, 50, 51, 53, 54.

The results prove that after heat treatment (1) the hardness in the welding zone is reduced by about 15% than that compared to the as welded condition. This reduction is not as great as that obtained by heat treatment (2). These results coincide with the results from the micro-structural tests which showed that tempered martensite has been formed. Meanwhile, the results emphasize that the large reduction in the hardness after heat treatment (2) is in the welding zone where the resulting hardness is only slightly greater than that of the parent metal and the hardness gradually reduced from area (1) to area (2). The results of heat treatment (2) show the possibility of obtaining a welded component with no significant variation in hardness in the specimen.

The results of the hardness variation along the specimen axis, reveal that the hardness variation for all different specimens is between 490 - 510 HV before applying any kind of heat treatment. And it is decreased to the range of 435 - 465 HV after heat treatment (1). Likewise, after heat treatment (2), the hardness is

reduced to become between 290 - 320 HV. These results are shown in Figs. 24, 27, 30, 33, 37, 41, 45, 49, 52, 55.

These results show that the hardness is about uniform along the specimen axis with a reduction of about 15% in the hardness after applying heat treatment (1) and about 40% after heat treatment (2) comparing with the hardness for the same type of specimen before applying any kind of heat treatment.

The variation in the hardness has been measured at different depths from the specimen surface. These measurements have been made at two depths, 0.5 and 2 mm, for specimens A1, A2, A3, and A4. The results show that the hardness is about the same in both situations, but the width of that hard area [area (1)] becomes smaller by about 1 to 2 mm at depth of 2 mm. The results of these measurements are shown in Figs. 56 to 59. Each of these figures compare the hardness variation at depth of 0.5 and 2 mm for the same type of specimen.

In specimens A5, A6, A7, and A8 the hardness variation has been measured at three different depths from the specimen surface, at 0.5, 2.5, and 4.5 mm.

The results show that the hardness is about the same at all three different depths, but that the width of the hard zone [area (1)] reduces by about 1 to 3 mm at depths of 2.5 and 4.5 mm. Also there is no significant change between the hardness variation at depths of 2.5 and 4.5 mm. These results can be seen in Figs. 60 to 63.

In specimen B1, the hardness variation has been measured for two different depths, 0.5 and 1.5 mm. The results show that there is no significant change in the hardness variation at these two depths. Fig. 64 shows a comparison between these results.

In specimen B2 the hardness variation has been measured for two different depths, 0.5 and 2.5 mm the results show that the hardness is about the same but the width of the hard zone [area (1)] decreases by about 1 mm in the depth of 2.5 mm. Fig. 65 shows a comparison between these results.

These above results point out that the hardness magnitudes are about the same at different depths, but that the width of the hard zone [area (1)] is greater

near the surface (at a depth of 0.5 mm than at depths 1.5 mm or more) due to the greater cooling rate at the top of the welded component.

Figs. 66 to 70 have been plotted to study the effect of the thickness of the specimen on the hardness variation. In these figures comparison is made between similar specimens which differ only in the thickness. The results show that the hardness is about the same but area (1) becomes greater in the relatively thicker specimens (A5, A6, A7, A8, and B2).

In terms of studying the effect of the bead width on the hardness variation, comparison between similar specimens which differ only in the bead width has been carried out. In this comparison the difference between the bead width were 5 mm from the specimen axis. The results show that there is no difference in hardness in all these specimens, but area (1) extends by 2 to 4 mm for the specimens (A2, A4, A6, and A8) which have greater bead widths. The above results are shown in Figs. 75 to 78.

Finally, to study the effect of the bead length on the hardness variation, comparison between similar specimens which differ only in the bead length have been made. The results show that the hardness is about the same but the width of the hard zone [area (1)] increases by upto 1 mm in the specimens which have greater bead lengths (A3, A4, A7, and A8). Figs. 71 to 74 show these results.

In these comparisons for the effect of different parameters (thickness, bead width and length), the results prove that there is no significant difference in hardness variation and that there is only light difference in the width of the hard zone.

4.3 TENSILE TESTING

Tensile testing has been carried out on different specimens, for three different conditions [before and after heat treatment (1) and (2)].

Tables 3 and 4 show the tensile testing results for both types of specimens (build-up welding and crack repair specimens). The results reveal that after

applying heat treatment (1), the tensile strength is improved in most of these specimens when compared to the strengths of the specimens without any kind of heat treatment. These results point out that heat treatment (1) has a good affect in improving the tensile strength, which coincide with the results from the micro-structural test and the formation of the tempered martensite has a good effect in improving the tensile strength.

However, the results show that the tensile strength is reduced after applying heat treatment (2) in all different types of specimens. These results are also substantiated by the metallurgy test and the formation of the precipitated carbide has a deterioration effect on reducing the tensile strength. Comparison has been made of the tensile strength of the build-up welding specimens, A1 and A5, A2 and A6, A3 and A7, A4 and A8, which differ only in the thickness and the volume of the deposit metal. The results show that the tensile strength is greater in the thicker specimens (A5, A6, A7, and A8).

The results also show that the tensile strength is slightly greater in specimens which have bigger bead widths (A2, A4, A6, and A8).

Similarly, the tensile strength is slightly greater in specimens which have larger bead lengths (A3, A4, A7, and A8).

Comparison between crack repair specimens B1 and B2 which differ only in the thickness, shows that there is no significant difference in the tensile strength between them. The tensile strength is only marginally greater in specimen B1 than in specimen B2.

4.4 THE RESIDUAL STRESSES

As mentioned in the previous chapter, the residual stresses have been measured along the X axis (see Fig. 79) at three different points, the results show that the greatest value of the residual stress in this direction is about 72 N/mm^2 at a point near the welding zone for specimen A3, and about 65 N/mm^2 for

specimen B1. The residual stresses were not determined in the welding zone itself, which is expected to contain the greatest stress [42].

Figs. 81 to 86 show the distribution of σ_x and σ_y and the principal residual stress σ_{max} and σ_{min} along the X axis for two specimens A3 and B1, which reveal that the residual stresses existed as tensile stress, and the residual stresses decrease as the distance from the welding zone increases.

The results of the above experiments show that the residual stress becomes negligible at the third point along the X axis (near the edge of the specimen).

The above results show that the greatest value of the residual stress is about 72 N/mm², which is considered to be small compared to the yield strength of this type of metal which is about 350 N/mm². However, in fatigue loading such magnitude may be significant.

In order to indirectly compare the relative magnitude and distribution of the residual stresses for different specimens residual strains have been measured by using a single strain gauge.

Different diagrams [Figs. 87 to 92] have been plotted to define the magnitude and distribution of the residual strains for these different specimens (A1, A3, A5, A7, B1, and B2). The results show that the greatest value for the residual strain is near the welding zone, and the residual strains decrease as the distance from the welding zone increases.

Comparisons between these different results have been made to demonstrate the effect of different variables of the specimens on the residual strains. The results reveal that the residual strains are higher in the thicker specimens (A5, A7, and B2). Likewise, the results show that the residual strains are higher in the specimens which have greater bead length (A3, and A5). Figs. 93 and 94 show these results.

These above comparisons prove that there is no significant difference in the residual strain between these different specimens which have different thicknesses and bead lengths.

CHAPTER 5

CONCLUSION
&
RECOMMENDATION

5.1 CONCLUSION AND RECOMMENDATION

This project gave a good idea about the metal microstructure of the welding zone of AISI 410 metal in all different conditions. The results also illustrated the variation in the hardness and magnitude of tensile strength for all different specimens, in all different conditions.

On the basis of these results it is apparent that the heat treatment (1) is more acceptable if the mechanical strength is a critical parameter. However, the relatively higher hardness in the welding zone may not be desirable as this may result in non-uniform stress distribution in repaired zone. The criticality of this variation in hardness may depend on the size and location of the repair in the component and also the type of loading the component is designed for. If the mechanical strength is not critical then the heat treatment (2) appears to be more desirable.

Before, however, any final recommendation can be suggested further investigation is necessary. For example, the relative impact resilience of as welded and heat treated specimens need to be determined in order to suggest the appropriateness of any heat treatment procedure and also whether such heat treatment could be unnecessary for any size of weld repair.

On the present investigation the residual stress distribution was determined only in a limited manner using stress relaxation technique. Such limited results gave only an indication of the magnitude of stress near the welding zone at locations transverse to the weld line. The stress variation around the weld line needs to be determined in order to build a complete picture and to properly assess the effect of any constraint around the welded zone. A better and accurate technique is to be use hole drilling method. The apparatus for this technique was not available for the work reported in this thesis. However, the apparatus has recently been procured and is ready for use now.

The following may be concluded from this investigation:

1 - The metal microstructure in the welding zone before applying any kind of heat treatment is completely martensite.

2 - The metal microstructure becomes completely tempered martensite after heat treatment (1).

3 - After heat treatment (2), the metal microstructure consists of tempered martensite, ferrite, and precipitated carbide.

4 - Harder zone exists in and near the welding zone, where the hardness is about 500 HV.

5 - The hardness is reduced to about 440 HV in and near the welding zone as a result of heat treatment (1).

6 - The hardness is decreased to about 300 HV in and near the welding zone after applying heat treatment (2).

7 - There is no significant change in the hardness in area (2) after applying heat treatments (1) and (2).

8 - There is no difference in the pattern of hardness variation at different depths, but the harder region is wider near the specimen surface.

9 - There is no significant change in the pattern of hardness variation in different specimens, but that harder region is wider for the thicker specimens, and in those specimens which have greater bead widths and lengths.

10 - There is an improvement in the tensile strength after heat treatment (1).

11 - The tensile strength has been decreased after applying heat treatment (2).

12 - When the specimens have been tested for fracture in tensile testing, the fracture was outside area (1) in all different specimens, for all different conditions.

13 - The results demonstrate that there is a tensile residual stress near the welding, which decreases as the distance from the welding zone increases.

14 - The highest value for the residual stress which has been recorded near the welding zone is about 72 N/mm^2.

15- In all the experiments, the results emphasize that the stress value is about zero in the third point (25 mm from the axis of the welding pass).

5.2 FURTHER WORK

In the next work the following points have to be carried out :

1 - Impact test should be carried out on as welded and heat treated specimens.

2 - Residual stresses should be mapped around the welded zone using more accurate hole drilling technique.

3 - Effect of repeated heat treatment should be evaluated.

4 - Effect of variation in heating / cooling rate should be determined.

5 - Effect of the variation in the duration of heat treatment.

6 - Effectiveness of localised heat treatment.

7 - Effect of weld size to specimen size ratio on the residual stress.

REFERENCES

1 - A.C.Davies.
[The science and practice of welding (Volume 1)].
ISBN 0 521 36145 1

2 - A.C.Davies.
[The science and practice of welding (Volume 2)].
ISBN 0 521 36146 X

3 - Andrew D. Althouse; Carl H. Turnquist; William A. Bowditch; Kevin E. Bowditch.
[Modern welding] ISBN 0 87006 668 4.

4 - Howard B. Cary
[Modern welding technology]
ISBN 0 13 599290 7

5 - Anon [Relieving stress without heat].
Tooling and Production, v44, n9, Dec 1978, P 62 _ 63.

6 - Olenin,E.P.; Averin,A.S.; Dobrotina,E.V.; Alekseev, O.K.;

[Reducing the residual stresses in welded components by vibrational treatment].
Welding Production, v30, n5, May 1983, P 19 _ 21.

7 - Hebel,Thomas.
[Better way to relief stress].
Am Mach Autom Manuf, v130, n12, Dec 1986, P 70 _ 72.

8 - Keller,D.S.
[Ultrasonic stress relieving].
Metal Treating, v21, n2, Apr_May 1970, P 14 _15.

9 - Merrin,B.V.; Olenin,E.P.
[Reducing the residual welding stresses by the electrohydraulic treatment of welded joint].
Welding Production, v28, n1, Jun 1981, P 1 _ 2.

10 - Candeland,P.
[Site heat treatment of weldments].
Production Eng & Metal, v11, n3, Mar 1971, P 29 _ 39.

11 - Ankirski,B.M.
[Effect of vibration and heat treatment on the

mechanical properties of the metal and welded joints in 20K steel].
Welding Production, v32, n3, Mar 1985, P 26 _ 28.

12 - Burget, Wolfgang; Blauel, Johann.
[Comparison of procedure qualification test welds and welded joints in plates and pipes for offshore constructionin COD tests].
Schweissen & Schneiden, v40, n4, Apr 1988, P E56 _ E59.

13 - Kameda,Jun; Takahashi,Hideek; Suzuki,Masahiko.
[Residual stress relief and local embrittlement in a A533B reactor pressure vessel weldment].
International Journal Of Pressure Vessels And Piping, v6, n4, Jul 1978, P 245 _ 274.

14 - Adoyan,g.a.; Aldoshin,Yu,S.; Gerchikov,A.M.; Shevchuk,S.A.
[Specimen for evaluating the distortion of metal under the effect of residual welding stresses].
Welding Production, v31, n3, Mar 1984,

15 - Lundin,C.D.; Henning,J.A.; Menon,R.
[Post weld heat treatment (stress relief) cracking in Cr_Mo steels].
Abstracts of papers presented at 67th AWS annual meeting. Miami; USA, 1986, P 154 _ 156.

16 - Anon [Post weld treatments of steel pressure vessels _ state of the art review].
Indian Welding Journal, v17, n3, 1985, P 61 _ 66.

17 - Bosansky,J.; Porter,D.A.; Astrom,H.; Easterling,K.E.
[Effect of stress annealing treatment on the structure of high heat _ input welds containing Nb and Mo].
Scandinavian Journal Of Metallurgy, v6, n3, 1977, P 125 _ 131.

18 - Zubchenko,A.S.; Suslove,E.A.
[Hardening and stress relaxation in reheating welded joints in 15Kh2MFA and 15Kh2NMFA steels]
Weld Production, v33, n1, Jan 1986, P 30 _ 33.

19 - Mesini,Nedeljko.

[Heat treatment of the welded specimens of N_A_XTRA 70 steel].
Zavarivanje (Zagreb), v28, n5, Oct 1985, P 267 _ 275.

20 - Mesini,Nedeljko.
[Heat treatment of the welded specimens of Ni oval steel 47].
Zavarivanje (Zagreb), v28, n4, Jul _ Aug 1985, P 197 _ 204.

21 - Frassoni,G.F.; Somigli,A.; Fedreghini,R.
[Conditions and operating modes for heat treatments of pressure vessels].
Rivista Italiana della Saldatura v35, n2, Mar _ Apr 1983, P 75 _ 85.

22 - Evans,G.M.
[Effects of Sulphur and Phosphorus on microstructure and properties of C_Mn all welded metal deposits].
Metal Construction, v18, n10, Oct 1986, P 631R _ 636R.

23 - Evans,G.M.
[Effects of Silicon on the microstructure and properties of C_Mn all welded metal deposits].
Metal Construction, v18, n7, 1986, P 438R _ 444R.

24 - Evans,G.M.
[Effect of stress relieving on the microstructure and properties of C_Mn all welded metal deposits].
Welding Journal, v65, n12, Dec 1986, P 326S _ 334S.

25 - Glover,A.G.; Jones,W.K.C.; Price,A.T.
[Assessment of resistance of low alloy steels to reheat cracking using Vinckier test].
Metals Technology, V4, Pt6, Jun 1977, P 326 _ 332.

26 - Lieurade,H.P.
[Effect of residual stresses and stress ratio on the fatigue strength of welded components].
Welding in the world, v26, n7_8, 1988, P158 _187.

27 - Mateffy,V.K.; Mikan,J.M.; Abel,A.
[Fatigue of welded joints _ the effect of stress relieving].
Ninth Australian conference on the mechanics of structure and materials, Sydney, 1984, P 106 _ 110.

28 - Fukazawa,M.; Natori,T.; Terada,H.; Akashi,S.
[Effect of stress relief on fatigue strength of high

strength steel corner joint with blowhole].
Proceedings of Japan society of civil engineers, n356/ 1 _ 3 Apr 1985, P 153 _ 161.

29 - Pilous,Vaclav.; Sinal,Jozef.; Stransky,Karel.
[Structure and mechanical properties of thermally loaded welded joints between ferritic and austenitic steels].
Metalic Materials, v24, n2, 1986, P 80 _ 89.

30 - Lamb,W.; West,D.R.F.; Steen,W.M.
[Residual stresses in two laser surface melted stainless steels].
Materials Science and Technology, v2, n9, Sep 1986, P 974 _ 980.

31 - Higushi,M.; Sakamoto,H.; Tamioka,S.
[Study on welded repair through half bead method].
Engineering Review, v13, n2, Apr 1980, P 14 _ 19.

32 - Karjalainen,L.P.; Moilanen,M.; Rautioaho,R.
[Evaluating the residual stresses in welding from Barkhausen Noise Measurements].
Material Pruefung, v22, n5, May 1980, P 196 _ 200.

33 - De,Debabrata.; Bhattacharyya,M.
[On resistance Butt _ welded steel specimen].
Journal of the association of engineers, India, v52, n2, Apr _ Jun 1977, P 87 _ 93.

34 - Watkins,M.; Vonrosenberg,E.L.
[Sulfide stress cracking resistance of welded repairs in welded alloys].
Materials Performance, v22, n12, Dec 1983, P 30 _ 33.

35 - Iwasaki,T.; Nagao,M.
[Residual stress relieving in reclaimed and built_up welding of steel castings by hammer peening].
Hitachi Review, v20, n6, 1971, P 224 _ 232.

36 - Fik,J.I.J.; Rogerson,J.H.
[Root toughness of multipass submerged arc welds in microalloyed steels].
Metal Construction, v12, n9, Sep 1980, P 450 _ 452.

37 - Farrar,R.A.; Taylor,L.G.; Harrison,E.M.
[Effect of stress relieving on fracture properties of submerged arc welds of C_Mn steels].
Metals Technology, v6, Pt10, Oct 1979, P 380 _ 389.

38 - Nath,B.
[Creep behaviour of dissimilar metal welds on stress relieving].
Schweissen in der Kerntechnik, Vortraege des 4th internationalen Kolloquiums, 1982, P 52 _ 56.

39 - DIN, Welding 1, Handbook 8.
DIN 50120, part 1, page 305 - 310.
Published by DIN, 1983.
ISBN 3-410-11584-6.

40 - C.E.Jackson; Len Griffing; S.D.Reynolds; S.Weiss; R.T.Telford; I.G.Betz.
[Welding Handbook (Metals And Their Weldability)].
Volume 4, page 64.34 - 64.35.
ISBN 0-87171-218-0.

41 - John Vaughan.
[Strain Measurements].
Published by Bruel and Kjar.
ISBN 87-87355-08-6.

42 - Koichi Masubichi.
[Analysis Of Welded Structures].
Published by Pergamon Press, 1980.
ISBN 0-08-022714-7.

43 - Braid,J.E.M and Gianetto,J.A.
[The effects of PWHT on the toughness of shielded metal arc weld metals for use in Canadian offshore structure fabrication].
Proceedings of the International Conference on Welding for Chalenging Environments, Tronoto, Ontario, Canada, 1985.
Published by Pergamon Press.
ISBN 0-08-031866-5.